Founded 1909

STABILISATION OF AN EXCAVATION BY AN EMBEDDED IMPROVED SOIL LAYER

BY

GOH TEIK LIM
BEng (Hons)

A THESIS SUBMITTED
FOR THE DEGREE OF DOCTOR OF PHILOSOPHY

NATIONAL UNIVERSITY OF SINGAPORE
2003

Dedicated to my dearest wife, ***Soo Khean***

And my cute son, ***Chan Herng***

Constantly loving

Always understanding

ACKNOWLEDGEMENTS

I would like to express my deepest gratitude to my supervisors, Professor Yong Kwet Yew and Associate Professor Tan Thiam Soon for their constant guidance and encouragement throughout this research programme. Through regular meetings and discussions, I was equipped technically and was trained to be more critical minded. Associate Professor Tan Thiam Soon deserves a special mention here in shaping the final form of this thesis besides providing dedicated assistance and ideas throughout the course of investigation. I am also grateful to Assistant Professor Chew Soon Hoe for his support and financial advice throughout the course of my postgraduate study.

My special thanks are extended to:

(a) Mr. Wong Chew Yuen for his vast experience and critical comments in developing the in-flight excavator besides rendering a helpful hand in operating the centrifuge.

(b) Mr. Foo Hee Ann for his help in fabricating laboratory models and modifying the experimental set-up.

(c) Mdm. Joyce Ang, Mdm. Jamilah and Mr. Loo Leong Huat for their help in sending out quotation forms and ordering equipment and transducers.

(d) Dr. Robinson for his critics during my thesis writing, which has helped to strengthen my idea.

(e) Fellow research engineers and scholars for their assistance and friendship, whom have made the laboratory my second home.

This project has been made possible by the National University of Singapore and National Science and Technology Board (NSTB), for providing the research grant RP940658 and research scholarship (April 1999 to June 2000). Without this funding, this research programme will not be materialised.

TABLE OF CONTENTS

SUMMARY

In deep excavation in soft ground, the maximum deflection of retaining wall usually occurs below the final excavation level where it is impossible to install struts. To limit the wall deflection at this level, one effective solution is to improve a layer of soft soil below the base prior to an excavation. A common approach is to improve the entire soil layer within the excavation zone so as to provide full contact between retaining walls. Nevertheless, carrying out grouting works especially close to the retaining wall is difficult and this often leads to a small region of untreated soil between the retaining wall and improved soil layer. Often, this is overlooked and ignored in design. In the case of a wide excavation, the use of an embedded improved soil berm is usually considered because improving the entire area may not be economically viable.

This research covers the experimental and numerical studies of the behaviour of three different configurations of embedded improved soil layer; namely an improved soil strut, an improved soil strut with a small gap next to the retaining wall and an improved soil berm. The initial scope of the study is to understand the material properties of Singapore marine clays improved by cement mixing. A series of samples with different mix proportions was prepared and tested in the laboratory. This is followed by a series of 100G centrifuge model excavation tests, prepared using different configurations of soil improvement so as to understand the behaviour of a monolithic improved soil layer. All the excavation tests were carried out using the new in-flight excavator (Mark II), which was developed for this study. Numerical analyses using the finite element program (CRISP) were finally carried out to complement the results obtained from centrifuge tests.

The centrifuge results show that the effectiveness of an embedded improved soil strut is very much dependent on its stiffness. The test results confirm that when a stiffer

improved soil layer is used, though it provides a higher passive resistance to the retaining wall, it also induces a much higher bending moment in the wall. This finding becomes substantially important because the Young's modulus (E) of improved soil observed during the material study could be anticipated to be much higher. Results from a parametric study using the FE analyses show that there is a considerable increase in the wall bending moment (15-20%) when a stiffer improved soil layer is used. However, when the E value of improved soil strut approaches 1000MPa, the increase of wall bending moment becomes nominal. It is also shown that there exists a threshold range of between 100-200MPa, below which the improved soil strut will be ineffective, and above which the increased effectiveness is marginal.

In the case when the soil improvement has a gap of untreated soil in between the retaining wall and improved soil layer, the overall composite stiffness of the improved soil layer drops significantly. Besides demonstrating that a larger gap will lead to a lower composite stiffness (E_c), the results also show the detrimental effect of reducing the confining pressure due to excavation. As the excavation proceeds, the stiffness of the untreated soil (E_{gap}) changes from a constrained modulus under 1-D condition at shallower excavation to a tangential stiffness of an unconfined axial compression test at deeper excavation, thus greatly affecting the composite stiffness of such improved soil system.

In the case of a wide excavation, the use of embedded improved soil berm is more economical and proves to be as effective as an embedded improved soil strut in the early stage of excavation. The passive resistance is provided mainly through the contact area of the shear resistance and end bearing. It is also shown that the stiffness of improved soil berm does not have a significant effect on the performance of the excavation.

Keywords: Excavation, soft soil, improved soil, untreated soil gap, berm, centrifuge

NOMENCLATURE

G	Earth gravity
ϕ	Angle of internal friction
γ_{bulk}	Bulk unit weight of soil
C_c	Compression Index
C_s	Swelling Index
λ	Slope of normal compression line
κ	Slope of swelling line
NC	Normally consolidated clay
OC	Over consolidated clay
ν	Poisson's ratio
M	Slope of critical state line in q-p' space
σ_h	Total horizontal stress
σ_v	Total vertical stress
σ_v'	Effective vertical stress
ε	Strain
C	Cement dry weight
W	Water weight
S	Soil dry weight
A_w	Cement content
w	Water content
t	Curing time
c_u	Undrained shear strength
q_u	Unconfined compressive strength
E	Young's modulus
E_{sec50}	Secant Young's modulus at 50% of ultimate strength
EH_{sec}	Secant Young's modulus using Hall's effect transducer
E_c	Young's modulus of composite improved soil
E_{gap}	Young's modulus of untreated soil gap
E_{imp}	Young's modulus of improved soil
L_{gap}	Gap width of untreated soil
L_{imp}	Length of improved soil

LIST OF TABLES

LIST OF FIGURES

LIST OF PLATES

Chapter 1

INTRODUCTION

1.1 Background on Deep Excavation

To optimise high land cost in urban development, underground space is commonly exploited, both to reduce the load acting on the ground and to increase the space available. Many deep excavation works have been carried out to construct various types of underground infrastructures such as deep basements, subways and services tunnel [Tan et al. (1995), Yong et al. (1998)]. Often, the execution of these deep excavation works requires the use of appropriate retaining wall and bracing systems. An inadequate support system has always been a major concern, as any excessive ground movement induced during excavation could cause damage to neighbouring structures, resulting in delays, disputes and cost overrun.

Most of the prime land areas in major world cities are located around river mouth and coastal regions where there usually exists a thick marine clay stratum. Depending on the sedimentary deposition, the thickness of this clay layer could vary from few meters to great depths exceeding 50m. Very often, this clay layer is soft in nature. In such poor soil condition, large ground movements are expected during deep excavation. To mitigate such movement, the common solution is to use a stiff retaining wall system. Nonetheless, this provision might not be sufficient since the maximum wall deflection could occur below the final excavation level where it is impossible to install struts or anchors.

1.2 Stabilisation of Deep Excavation using Soil Improvement Techniques

To ensure that the wall movement is controlled, it is important to restrain the

wall by some form of support system that could be embedded below the final excavation level. One effective solution is to improve the soft soil at this particular depth into a stiff composite improved soil layer by using one of the grouting techniques. As a result of this provision, the wall deflection, surface settlement and base heave are significantly reduced [Figure 1.1]. The effectiveness of such improved soil technique in stabilizing a deep excavation has been proven in several successful projects worldwide [Lee and Yong (1991), Tanaka (1993), Liao and Tsai (1993) and Takada et al. (1998)].

A more recent grouting techniques used to stabilise deep excavation works is the Deep Cement Mixing (DCM) Method. Though jet grouting is still the preferred approach in Singapore, the DCM Method is fast becoming popular among local contractors and its usage is set to increase in the near future. Being part of the Deep Mixing Method (DMM) family, the DCM Method performs mixing of soil with injected cement grout by using a set of mechanical cutting blades. This is unlike jet grouting which requires a high-pressure of water jet to perform cutting and mixing. Considering the way mixing is performed, the DCM Method has always the edge over jet grouting because it does not produce excessive waste nor cause uncontrolled displacement. Both aspects are critical in the context of Singapore owing to the fact that the cost of disposing this waste is extremely expensive and the local requirement on the allowance of ground movement nearby critical structures is very stringent.

When the DCM Method was first developed by the Port and Harbour Research Institute (PHRI), Japan in the late 1960s [Okumura and Terashi (1975)], its usage was limited to improve the bearing capacity of port structures built on soft seabed. Development over the years has broadened its usage where it has now been applied in many substructure works. Among its numerous applications, the use of this method to

stabilise deep excavation works has been only a very recent development. In fact, the DCM method was only introduced in Singapore in the early 1990s [Figure 1.2] after its first successful execution in a deep excavation project in Japan a few years earlier [Mihashi et al. (1987)].

Though the DCM Method has now been used in a number of deep excavation projects, the design concept is still highly empirical and depends on the “know-how” experience [Okumura (1996)]. In view of such uncertainty, its application cost is relatively high and less competitive [Kitazume et al. (1996)]. Considering the high potential of DCM Method to be used in stabilisation of deep excavations, the immediate challenge will be to look into ways to lower its implementation cost, by means of optimising the design. This involves resolving important issues pertaining to the use of DCM Method in deep excavation, which would require a fundamental understanding of the mechanics involved for such soil improvement technique.

1.3 Issues Related to the Use of DCM Method in Deep Excavation

Due to the short history of DCM Method in Singapore, there is very limited data on the properties of such improved soil for local marine clays. Most of the adopted design parameters were based on published results derived mainly from works carried out on Japanese clays. As the clay mineralogy and climatic condition in both countries are different, there is concern regarding the properties assumed. Often, numerous field trials have to be carried out to justify its applicability to local condition, which essentially involves a trial and error approach instead of a proper design methodology. Therefore, it is important to establish the properties of local marine clays improved by the cement mixing technique.

Considering the fact that the DCM Method was initially introduced to improve

the bearing capacity of a weak foundation, it would be expected that most of the published data to-date were based on its mobilized shear strength. This is justifiable simply because the primary concern for such application is stability. However, when the improved soil layer is used as a strut below the final excavation level, it is clear that the main focus is to control the movement and thus, the evaluation of stiffness becomes crucial. Unfortunately, very little study has been done focusing on this and it has affected the way that the stiffness value is typically chosen in design.

A smaller stiffness value is often used in design if calculations indicate that the movement is well controlled. Assigning a smaller stiffness value may not be a conservative assumption, bearing in mind that the overlapping of improved soil columns to form a composite layer in the field may not be perfect. It is deemed to be a safer approach as a smaller stiffness will mean that the movement predicted will be larger than anticipated. However, with a stiffer improved soil layer, the bending moment in the retaining wall may increase. This is somewhat contradictory to the earlier intention and the wall may run the risk of being overstressed. To establish a more rational design, it is therefore important to understand the influence of this stiffness property on the performance of the improved soil layer to the overall behaviour of a stabilised excavation.

Carrying out grouting works especially close to the retaining wall is tedious owing to the fact that the retaining wall itself is not always perfectly even and free from obstruction. Incomplete grouting usually causes gap of untreated soil in between the retaining wall and improved soil layer to form. Although in most cases this gap can be avoided with the use of thorough jet grouting, it is unfortunately not the case in DCM Method, which uses rotating blades of a pre-defined diameter. Depending on the skill of the machine operator, this gap may vary from few to tens of centimetres. If the

gap is large, jet grouting is usually used to fill the gap. However, when the gap is small, it is often overlooked and ignored in design. Such small gap might have an enormous effect on the overall performance of improved soil layer since its intended function is to restrain the wall. To shed away the scepticism on whether the soil gap is critical or not, it is therefore important to assess its detrimental effect on the overall behaviour of an excavation.

In the case of a large excavated area, improving the entire soil layer within the excavation side often proves to be economically not viable. A cost-effective solution is to improve only a portion of soil in front of the retaining wall, allowing an improved soil berm to be formed. This form of improvement is treated as being equivalent to providing a full-improved soil layer with the implicit assumption that if the improved soil berm is sufficiently long, it will still behave effectively like a strut. At present, no clear rationale is available on the design of such improved soil berm though most analyses will treat it similar to improving the entire layer by assigning an equivalent composite value [Borin (1997)]. This is clearly not a rational approach unless a mechanistic study is undertaken to understand its behaviour during an excavation.

1.4 Difficulty in Modelling an Excavation Problem

The number of studies undertaken to understand the fundamental behaviour of deep excavation has been rising rapidly in the past two decades. Knowledge in this field is particularly important when an excavation has to be carried out under a poor ground condition. Often, geotechnical engineers have problems predicting the movement, evaluating the mechanism involved and assessing the potential failure caused by the excavation. Studies that were undertaken to model the excavation behaviour could be summarized into 3 main categories, depending on how the

simulation of excavation had been carried out. They are findings interpreted from analyses of field-instrumented excavation [Hsi and Small (1992), Tanaka (1993, 1994)], finite element method [Bolton et al. (1989), Whittle (1997)] and physical modelling in centrifuge [Bolton and Powrie (1988), Kimura et al. (1993)].

Analysis from field-instrumented excavation has been commonly used to examine the mechanics of an excavated ground despite the fact that the process of excavation in the field is highly complicated. Besides the complexity and variability of the in-situ soil strata, the fact that the characteristics of soil, the groundwater condition, the construction sequence and the configuration of support system differ from site to site often leads to a low degree of repeatability. Furthermore, it is particularly acute in the present study as there is no way at this stage to know what is the true mobilised stiffness of the composite improved soil layer. Therefore, the interpretation of field-instrumented results remains difficult and speculative.

Alternatively, the finite element method (FEM) has been used and thus is a comprehensive tool for analysing the multiple facets of an excavation problem. In recent years, the FEM has gained widespread acceptance through their capability to model complex construction sequences involving various detailed site-specific properties of the structural system and surrounding soils. However, the ability to perform a class-A prediction has not been proven convincingly, as most of the reported comparisons are based on back analysis rather than real prediction. Back-analyses carried out without a clear understanding of the mechanics involved can be very dangerous as it may produce erroneous correlation. Hence, the FEM method requires very careful calibration so as to capture the right behaviour observed in the field.

As explained earlier, due to the complexity involved in interpreting the results obtained from field-instrumented excavations, they will not be used in this study to

understand the underlying mechanics in play. One solution is to perform a correctly scaled physical model in centrifuge where an artificial acceleration field can be created to simulate the prototype behaviour of an excavation. The usage of centrifuge has been well known worldwide and numerous works done on modelling of excavations [Bolton et al. (1989), Kimura et al. (1993)] has shown satisfactory comparisons between the model and prototype behaviour. However, due to the difficulties involved in sample preparation and setting up of equipment for the excavation test, very limited experiments could be conducted during the period of this study. This was where the FEM analysis had been adopted to complement the experimental investigation. It can be used to verify and interpret certain behaviour observed from the centrifuge tests but can also be used to obtain further in-sight to better understand the different mechanisms in play through a detailed parametric study.

In order to have a realistic excavation technique to simulate the removal of soil in-flight in high gravitational field, a robotic miniature in-flight excavator is necessary. As the development works involved substantial amount of resources (e.g. time and manpower) in fabricating such an advanced machine, at the moment, only two geotechnical centrifuge research centres in the world have this sophisticated in-flight excavator. The first in-flight excavator was developed in the Tokyo Institute of Technology (TIT), Japan [Kimura et al. (1993)]. The second and third excavators were developed in the National University of Singapore (NUS); the former, which was a 3D in-flight excavator, was developed by a previous doctoral student [Loh et al (1998)] while the latter was developed by the author for the current study.

1.5 Objectives and Scope of Study

The objectives of this study are as follows: -

- To gain a basic understanding of the strength and stiffness properties of Singapore marine clays improved by mixing with cement.
- To establish the key parameters controlling the performance and behaviour of fully improved soil layer in an excavation.
- To investigate the detrimental effects of having a gap of untreated soil in between the retaining wall and improved soil layer.
- To distinguish the difference in mechanism of an embedded improved soil berm.
- To carry out numerical analyses to re-affirm the different underlying mechanisms involved and conduct further parametric studies to identify the optimal condition.

Knowledge of the properties, especially the stiffness of cement treated clays is crucial as it has a predominant effect on the overall pre-failure deformation behaviour of a stabilised excavation. Therefore, the first part of the study is aimed at understanding the material properties of Singapore marine clays improved by cement mixing. A series of samples with different mix proportions was tested systematically in the laboratory. Unconfined compression tests were carried out for 3 types of clay taken from different parts of Singapore. The strength and stiffness of cement treated clays were evaluated and simple prediction formulae and important relationships between them were established.

In the second part of the study, the behaviour of an embedded improved soil layer in a stabilised excavation was studied by means of both physical and numerical modelling. The physical modelling was carried out in the NUS Geotechnical Centrifuge using the in-flight excavator developed in this study. Numerous model excavation tests with various arrangements of soil improvement were conducted.

Results from these centrifuge tests would form the basis to gain an understanding of the behaviour of improved soil layer in an excavation. Subsequently, numerical simulations of these excavations were carried out using the finite element program known as CRISP (**CRI**tical **S**tate **P**rogram). Finally, the results from the centrifuge experiments and numerical analyses were collated so as to derive a clear conclusion on the underlying mechanics of an embedded improved soil layer in an excavation.

1.6 Scope of Study

The thesis contains seven chapters. Chapter 1 is the introductory chapter and it describes the objectives and scope of works. Chapter 2 is the literature review in which some pertinent deep excavation research works with different soil improvement techniques are discussed. The chapter demonstrates that very limited data has been published on the properties of Singapore marine clays improved by cement mixing. In addition, not many results are available pertaining to the behaviour of an excavation stabilised by an embedded improved soil layer. Chapter 3 presents the fundamental studies on the strength and stiffness properties of Singapore marine clays improved by cement mixing. It is crucial to carry out such material study before investigating further into the underlying mechanics of an embedded improved soil layer. Chapter 4 demonstrates the set up of the excavation test, which involves the development of an in-flight excavator and preparation procedures required to conduct an in-flight excavation test in the centrifuge. In Chapter 5, the experimental results were evaluated to distinguish different behaviours on various configurations of the embedded improved soil layer system. Chapter 6 discusses the important findings in this study. Numerical analyses were presented to complement the findings from the experiments and collaterally, they would provide a coherent view into understanding the mechanics

of an embedded improved soil layer in an excavation. Finally, the main conclusions drawn from this study are presented in the last chapter – Chapter 7.

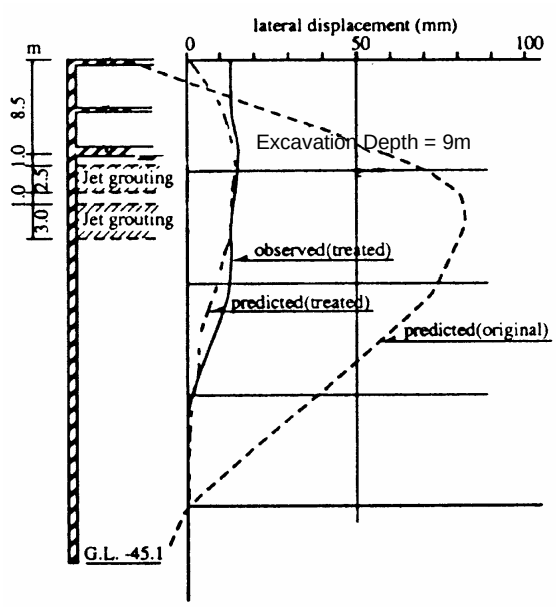

Figure 1.1 Effect of soil improvement works in Bugis Junction project, Singapore [after Sugawara et al. (1996)]

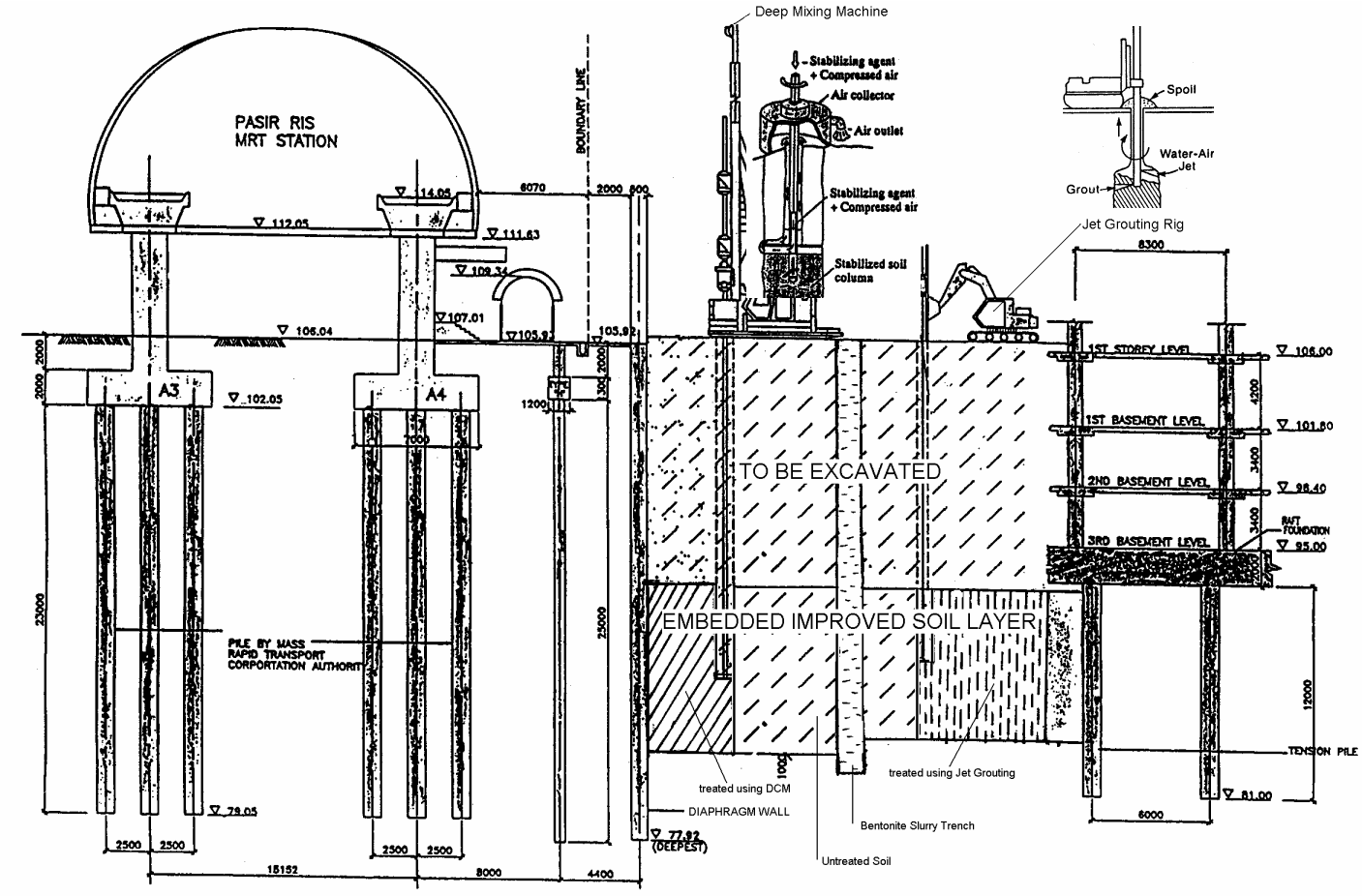

Figure 1.2 Soil improvement works for a deep excavation project nearby a railway station in Singapore

Chapter 2

LITERATURE REVIEW

2.1 Introduction

Deep Mixing Method (DMM) is a ground improvement technique, in which chemical admixtures (e.g. lime or cement) are mixed with soft soils deep inside the ground using a set of rotating blades. After mixing, chemical reactions will take place between the chemical admixtures and soil particles, allowing columns with much higher strength and stiffness than the original soil to form in the field. These improved soil columns, when being overlapped and arranged systematically, will form stiff composite mass of various configurations to spread the load within the rigid system. As such, wide applications of this soil improvement technique have been found. Among these applications, the use of DMM in stabilizing deep excavation works has been a very recent advancement.

After its first application in the mid 1970's in Japan and Sweden, extensive investigations have been carried out to assess the properties of improved soil using various chemical admixtures in many kinds of soft soils. Most of the published properties found in the literature were carried out on Japanese soils [Terashi et al. (1979), Kawasaki et al. (1981)]. There was barely any research work outside Japan in the 1980s, except some from the Scandinavian countries [Assarson et al. (1974)]. However, in the late 1990s, such characteristic studies started to gain momentum in other countries as well [Uddin et al. (1995), Goh et al. (1999)], driven by the fact that the use of the correlations developed in Japan may not be accurate for other type of clays and likely to be affected by the differences in clay mineralogy and climatic conditions.

The examination of published properties in the literature showed that most of the studies focussed mainly on strength. This was expected since the initial usage of DMM was to improve the stability of foundation, where the strength is the governing parameter in design. However, with the recent application of DMM to stabilise deep excavation, the evaluation of stiffness becomes important. Very little research work has been reported on this. Besides such limited information, the fact that the entire treated ground consists of multiple overlapped improved soil columns with specific configuration makes the evaluation of composite stiffness even more complicated. It is almost impossible at the current state for anyone to know the true mobilised improved soil stiffness in the field. The design for such soil improvement works is still very premature and most designers would assign some ambiguous composite stiffness to the improved soil based on simplistic assumptions from mixture theory. This is clearly not a rational approach but based mainly on experience.

In addition, the behaviour of embedded improved soil layer in deep excavation is complicated and cannot be explained by just considering its stiffness. Other factors such as the existence of gap and the use of improved soil berm in a large excavated area could also influence the performance of excavation and thus, they may change the way in which the improved soil layer behaves. Since no clear rationale is available for design, most engineers would treat any form of soil improvement in front of retaining wall to behave in a similar manner like an improved soil strut and assign a composite stiffness to this entire layer [Borin (1997)]. Such implicit approach, though straightforward, may lead to an erroneous solution. Before a more rational and cost-effective design could be developed, it is important to fully understand the underlying mechanics involved.

Even though there were several papers published in this area, very little works

dealt in-depth into the underlying mechanics involved and therefore, the understanding of the behaviour of improved soil layer remain rudimentary. Review of literature showed that most of the reported studies were based mainly on numerical works using the finite element method. The accuracy of such studies is strongly influenced by the input properties and selected soil models. It was also observed that most of these works were only focusing on sensitivity analyses to obtain an economical design. There were some works based on field-instrumented excavations that compared the performance of the excavation with and without the improved soil layer. Although these findings were important, there was very little attempt to understand the mechanisms involved.

In this chapter, the literature review begins with the general design considerations to control ground movements based on conventional support system. Subsequently, attention was paid to evaluate the effectiveness of having an embedded improved soil layer to control associated movements during excavation works in soft ground. The central idea is to evaluate the fundamental behaviour of an embedded improved soil layer. Therefore, most of the previous research works of significance to this research studies were reviewed. Critical comments are given in the review, which are of importance to this study.

2.2 Design Considerations in Deep Excavation

In Singapore and major cities around the world, excavation works for urban development and civil engineering works are often carried out close to property boundary. Ground movements are expected to occur as a result of changing stresses in the surrounding soil during excavation. To ensure that the excavation is safe, adequate support system in the form of retaining wall and bracing members are employed.

To ensure stability of an excavation, the following design checks are usually carried out: -

- provide sufficient embedment depth of wall to prevent overturning or toe-kick-out
- ensure that the lateral wall supports do not buckle or overstressed
- limit the base heave at the formation level

Beside stability requirements, a more critical problem involving excavation in densely built-up area is the serviceability consideration. To ensure that the ground movements do not cause potential damaging effects to the nearby structures, the following design checks are recommended: -

- control excessive surface settlement at nearby buildings and infrastructures
- control excavation induced wall deformation and base heave

2.3 Limitations of Conventional Excavation Support System

To avoid excessive ground movements, it is important that the excavation support system is effective in providing lateral restrain to the retaining wall. It is therefore necessary to examine the wall deformation and ground settlement pattern associated with deep excavation before one can better understand the effectiveness of a particular excavation support system. Yong et al. (1990) presented the time behaviour of excavation support system by comparing the results of consolidation analyses with data from an instrumented excavation project. From the lateral deformations of the sheet pile wall shown in Figure 2.1, it is obvious that the maximum wall movements occur around the final formation level.

Wong and Patron (1993) presented the excavation induced ground movement patterns for 8 deep excavation sites in Taipei area with geological profile consisting of

alternating layers of grey silty fine sand and grey silty clay. Inclinometers' measurements from these deep excavation cases were obtained and analysed. As shown in Figure 2.2, again, the maximum wall deflection occurred around the final excavation level, when soil at the excavation base was not improved. Kusakabe (1996) had also reported similar behaviour in the case of an excavation in a very soft alluvial clay near Tokyo. This indicates that the soft soil has inadequate strength and stiffness to provide sufficient passive resistance to restrain the wall.

When the wall deforms at such level, it would not be practical that the induced movement could be controlled using the conventional bracing system. Though the common solution is to use a much stiffer retaining wall system, in this case, the expected reduction of wall movement will be limited because the wall is not propped at the most critical level. One alternative is to bring down the lowest strut to the utmost bottom level. This is not always favourable because it obstructs the base slab construction.

2.4 Stabilisation of Deep Excavation by Improved Soil Techniques

The presence of the embedded improved soil layer prior to excavation has significantly improved the performance of excavation. This is contrary to conventional excavation support system where strut, tieback or anchor can only be installed after an excavation to the underside of the strut level is done when the wall is acting as a cantilever in the initial stage. The provision of an earlier embedded strut will greatly limit the wall movement.

The success of improved soil techniques to reduce the wall deflection has been reported in many completed excavation projects [Tanaka (1993), Yong and Lee (1995), Okumura (1996), Wong et al. (1999)]. In Singapore, such soil improvement

techniques had been successfully used during the construction of Singapore Mass Rapid Transit (MRT) System in the 1980s. Jet grouting was used at the Dhoby Ghaut MRT Station [Tornaghi and Perelli Cippo (1985)] and Newton Circus Station [Gaba (1990)] while Deep Lime Mixing (DLM) Method was used at the Bugis and Lavender stations [Hume et al. (1989)]. The use of jet grouting was reported again at the Esplanade Theatres by Wong et al. (1999). More recently, the Deep Lime Mixing (DLM) Method was also used in the construction of the proposed HDB Centre next to Toa Payoh MRT Station [Tan et al. (2001)].

The above trend indicates that the use of this method is increasing. Nevertheless, most of the reported case histories are mainly success stories, justifying the necessity of such improved soil techniques in deep excavations. Though its use is becoming more extensive, unfortunately, no studies are focussed to unveil the underlying mechanics involved on how the improved soil layer behaves. The present state of design concept is still highly empirical, consisting of many implicit assumptions which may be very conservative resulting in high construction cost.

2.5 Previous Works on Properties of DCM Improved Soil by Cement Mixing

The investigation of the engineering properties of DMM improved clays started in Sweden and Japan in the late 1960s where the method was first developed. The Swedish Geotechnical Institute together with Linden-Alimak AB have done extensive works on the use of lime column technique to improve the foundation of embankments on soft clays [Assarson et al. (1974)]. In Japan, the research work started at the Port and Harbour Research Institute (PHRI) in 1967 [Okumura et al. (1972)], initially using granular quick lime as the hardening agent and later, using cement slurry and powder. A variety of Japanese marine clays were first collected and tested in the laboratory to

check its effectiveness. Subsequently, field trial tests were performed to confirm its degree of improvement at different sites [Terashi et al. (1979)].

In Singapore, the first major application of deep mixing was in the 1980s when it was used to improve the bearing capacity of a reclaimed land [Kado et al. (1987)]. In the early stage, the method used lime as the hardening agent. As the cost of cement is lower and some problems have been encountered in storing unslaked lime in the hot and humid climate in Singapore [Broms (1984)], Ordinary Portland Cement (OPC) was introduced later to suit the local environment. Currently, there are limited reported results on local marine clays improved by cement mixing. Therefore, the design approach has to rely on the published results obtained mainly from Japanese improved clays. This is obviously not a good practice unless an independent study on such improved properties for local marine clays is carried out.

2.5.1 Unconfined Compressive Strength (q_u)

As the original intention of DMM is to improve the bearing capacity of foundation works in soft ground, the principal objective is to transfer the structural load vertically down to a firm stratum. To achieve the safety factor for such design, the stability against shear failure has to be considered and therefore, the mobilised shear strength of the improved soil is important. According to Kawasaki et al. (1984), the shear strength (τ_f) of improved soil can be estimated from the unconfined compression strength (q_u) where τ_f is approximately $q_u/2$ if the value of q_u is less than 1000 kN/m^2. When q_u becomes larger, the τ_f has to be estimated at a value lower than $q_u/2$ depending on its corresponding compressive strength [Figure 2.3].

In the laboratory, the unconfined compressive strength (q_u) of a stiff material can be easily determined. q_u represents the highest stress that the material can sustain

in an unconfined compression before shear failure occurs. Due to the simplicity of stress measurement, the unconfined compression test is commonly carried out to evaluate the degree of improvement for a particular improved soil. Hence, many researchers [Saitoh et al. (1985)] used the unconfined compressive strength (q_u) to represent the strength results.

2.5.2 Modulus of Elasticity (E)

The control of wall deformation and ground movement normally governs the success of a support system in deep excavation in an urban area. An excavation is considered a failure when the allowable limit of ground movement is exceeded even though there is no sign of stability failure. When the improved soil layer is used as a strut, the safety factor for such design shall be treated differently as the loading conditions and failure criterion are not the same as those for the foundation problem. Since the serviceability criterion are more crucial in this case, it is therefore important to evaluate the stiffness of improved soil in addition to its strength. Nonetheless, very limited studies on the stiffness property of improved soil are available in the literature.

Unlike the evaluation of q_u, the determination of stiffness requires careful measurement of the strain. Often, the evaluation of strain is tedious and sensitive to how the measurements are made. The modulus of elasticity can be determined using the unconfined compression test by assessing the gradient from the stress-strain curve. Many researchers prefer to use E_{50}, which represents the secant modulus at 50% of the ultimate strength. This is only a rough indicator and is based on the assumption that the cement mixed clay is behaving roughly like a linear elastic material.

However, Saitoh et al. (1996) found that the initial elastic modulus (E_i) of cement treated clay is much higher, which is 10-20% greater than E_{50}. This also

indicates that the behaviour at small strain of cement treated clay may be non-linear. The significance of such non-linear behaviour for hard soils, soft rock and cement treated clays has been widely recognised [Tatsuoka et al. (1996)]. According to Burland (1989), strains in the ground near structures in stiff soils are generally in the small strain region, reflecting the importance of considering the non-linearity behaviour of a stiff material such as the improved soil at small strain.

To determine the strain reading during the unconfined compression test, differential displacement gauges are commonly placed between the top and bottom of loading caps. Recently, this conventional approach has been seriously criticised for hard soil testing [Tatsuoka et al. (1996)]. Due to the effect of bedding error, this external method of strain measurement has led to an underestimation of stiffness [Kohata et al. (1996)]. According to Tatsuoka and Shibuya (1992) [Figure 2.4], the bedding error at the top and bottom ends of the specimen may be due to: -

a) a loose layer formed at both ends of specimen during preparation,
b) the imperfect contact between specimen and rigid cap and pedestal, and
c) the compression of lubrication layer when it is in use.

To overcome such inaccuracy in strain measurements, Burland (1989) has suggested using local axial gauges for measuring the deformation of the specimen at the centre of the sample. Subsequently, different types of local axial gauge have been developed and some of those that are commercially available include the Hall's effect gauge, the local displacement transducer (LDT), the inclinometer gauge, etc.

As the evaluation of strain is tedious, prone to error and very much depended on the strain measurement methods, the process of the stiffness determination is often difficult. Therefore, it is more convenient in practice to relate the stiffness (E) with the unconfined compression strength (q_u), enabling the E of the improved soil to be

estimated from its corresponding q_u. Some correlations obtained from the Japanese cement mixed clays are listed in Table 2.1 and shown in Figures 2.5 and 2.6.

Besides having difficulties in evaluating the individual stiffness of an improved soil sample in the laboratory, it is also noted that the evaluation of the true mobilised stiffness of the entire improved soil mass in the field will be even harder. The complexity in understanding the composite interaction between treated soil columns and surrounding clays has made the accurate assessment of stiffness for design very difficult. Sometimes, a smaller value is being assigned in design, which will be considered conservative as decreasing the stiffness means that the movement induced is expected to be even larger. This is valid, provided only the movement is considered. No study has been undertaken to investigate the implication of such approach on the retaining wall system in an excavation.

2.5.3 Factors Influencing the Degree of Improvement

As the changes in the strength will finally affect the stiffness as well, it is therefore important that the factors affecting the strength development of the cement treated clays are studied together. Various controlling factors of strength over different types of soft soil have been reported [Kawasaki (1984), Gotoh (1996)]. Based on the results of research work done in Japan over the last ten years, Babasaki et al. (1996) has categorised the relationships of various factors on the improved soil [Table 2.2].

To proceed with this kind of soil improvement technique, predictions on the strength and stiffness of improved soil are important. The prediction would include the factors influencing the degree of improvement, which are normally a function of strength as shown below: -

$$q_{ul} = \text{function } (S, A, C/W_t, O_c, F_c, T_c) \quad (2.1)$$

$$q_{uf} = \text{function } (q_{ul}, T_c, \theta, M, H) \quad (2.2)$$

where q_{ul} = laboratory strength under thorough mixing and constant curing conditions

q_{uf} = field strength under different mixing and curing conditions according to site and equipment used

S = characteristics of the soil

A = type and content of hardening agent

C/W_t = ratio of weight of hardening agent and total water (including mixing water)

O_c = organic matter content (pH or lg. loss may be substituted)

F_c = fine's content (soluble silica, alumina may be substituted)

T_c = curing time

θ = curing temperature

M = degree of mixing

H = humidity and manufacturing conditions.

Though there are a number of prediction formulae available [Nagaraj et al. (1996), Gotoh (1996)] to estimate the strength of cement treated clays, the prediction is normally derived from only a particular site, which could not be used in general in other areas. Most of these predictions are made by carrying tests on samples prepared in the laboratory and then, estimating the field strength on the basis of past experience. Consequently, most predictions made are not accurate for local clays and often, they have to be re-confirmed by field trials.

An accurate prediction of the properties of improved soil is important. If the required properties are under-predicted during construction, time and cost will be wasted unnecessarily as rectification works have to be carried out later. To avoid this, contractors will normally ensure that the properties of improved soil are much higher than required by over-estimating it from the prediction. This approach is conservative but it may cause other negative impact such as increased bending moment in the

retaining wall, which needs to be evaluated more carefully.

2.6 Previous Works on Improved Soil Techniques in Deep Excavation

The first few successful applications of this soil improvement technique for excavation works in soft ground have been reported in the late 1980s by Mihashi et al. (1987) and Furuya et al. (1988). Most of the soil improvement works were performed inside the excavation below the final formation level. Although, the effectiveness of this soil improvement technique in deep excavation has been recognised in many countries, the analysis method and design concept are still highly empirical, and an explicit design methodology has not been fully developed. The underlying mechanics on how the embedded improved soil layer behaves in deep excavation has not been thoroughly investigated. Studies undertaken to-date by several other researchers are as follows: -

2.6.1 Studies by Gaba (1990)

Gaba (1990) reported the use of a 3.5m thick jet grouted raft immediately below the final excavation level, spanning between the diaphragm walls for a 15m top-down excavation in Singapore marine clay [Figure 2.7]. At this formation level, there existed a soft marine clay stratum, which was subsequently improved into a stiff improved soil layer. The author presented records of wall inclinometer, which showed the benefits of the improved soil layer in reducing the lateral wall deformation. This is solely to prove the effectiveness in providing an embedded improved soil layer to mitigate the wall movement.

2.6.2 Studies by Lee and Yong (1991)

Lee and Yong (1991) reported the use of jet grouting to improve the soil beneath formation level for two case studies of deep excavations in soft Singapore marine clay. The improvement of the soil stiffness at critical depths below the formation level helped to reduce the wall and ground movements as shown in Figures 2.8 (a) and 2.8 (b). The schemes used were in the form of single (2m thick) or double layer jet grouted rafts installed at critical sections along the excavation to control wall deformations. The grouted rafts acted as 'base struts', which transferred the excavation-induced forces to the retaining walls. The rationale behind the schemes used was to install the grouted rafts at the point of maximum deformation as ascertained from analyses without grouted rafts. The authors proposed the two layers grouting scheme to take advantage of the residual effects of an increase in stiffness of the soil sandwiched between the grouted layers.

2.6.3 Studies by Tanaka (1993)

Tanaka (1993) drew attention to an interesting aspect of stabilising a braced excavation with the retaining wall not reaching a hard stratum, allowing the wall to be floated in soft ground [Figure 2.9 (a)]. The thickness of the clay layer is over 50m at some sections and due the high stiffness of the stabilised soil layer, existing design approach allowed the retaining wall to be terminated at a much shallower depth. The soil stabilisation scheme was in the form of a layer of overlapping DCM columns spanning across the excavation. The field measurements of wall deformation are shown in Figure 2.9 (b). Observing the large basal heave as shown in Figure 2.9 (c), the author reported that the ground stabilised by DCM has offered only a very low resistance against lateral forces [Figure 2.9 (d)].

2.6.4 Studies by Liao and Tsai (1993)

Liao and Tsai (1993) studied the passive resistance of partially improved soft soil through two types of reinforcement patterns, namely the column and buttress types [Figure 2.10]. A horizontal-moving wall was used to load the reinforced soil specimens to failure and the deformation of the wall was being monitored throughout the entire loading period. From a series of tests with different reinforcement patterns, the column-reinforced soil tends to yield a higher passive resistance against the retaining wall movement than the buttress type reinforcement. For the buttress type soil reinforcement, the double "L" pattern showed a higher passive resistance than the box shape and the panel patterns due to its greater ability to mobilise the end bearing resistance and the side friction of the buttress effectively.

2.6.5 Studies by Ou and Wu (1996)

Ou and Wu (1996) reported the study of grouted column (soilcrete pile) type soil improvement for deep excavations at Kon-Her Building in Taipei. The authors employed 2-D and 3-D finite element analyses in their study and verified them using field-instrumented results. The primary objective proposed by the study was to formulate a method to evaluate the composite material properties of the treated soil mass whereby the treated area of soil could be replaced by a single material in the FE analysis instead of explicitly representing finite elements of appropriate geometry [Figure 2.11]. This method could eliminate the need for a very fine 3-D FE mesh, which would demand substantial computational resources such as enormous computer storage and computation time.

2.6.6 Studies by Uchiyama and Kamon (1998)

Uchimaya and Kamon (1998) presented field excavation results on the movement of DMM buttress walls. The buttress wall type was installed by using a double mixing wing machine, which makes overlapping soil cement columns of 1m in diameter. The buttress walls were 2m thick with two rows of columns, arranged with different spacing and depth [Figure 2.12]. Field measurements showed that the buttress-wall type was successful in reducing lateral deformations of retaining walls during excavation. From a series of buttress wall configurations carried out, it was found that the wall deformation reduces as the buttress walls are spaced closer, which apparently formed a composite ground. This study pointed to the effectiveness of stabilised composite ground to control movement in an excavation but no underlying mechanics was discussed.

2.6.7 Studies by Yong et al. (1998)

Yong et al. (1998) studied the effectiveness of grouted layer in an excavation analysed using 2-D and 3-D finite element method. The configuration of grouted layer used in this parametric study was a whole block with thickness 3m installed across the entire excavated area [Figure 2.13]. The presence of the grouted layer below the final formation level had altered the wall deformation magnitude significantly.

2.6.8 Studies by Wong et al. (1998)

Wong et al. (1998) carried out sensitivity analyses to study the optimal condition of jet grout configuration for braced excavation in soft clay based entirely on finite element analyses. A series of simulation were performed with different jet grout configurations where the wall deflection and bending moment were compared. The

excavation is based on 52m wide and 13m deep with three levels of strut while the retaining wall consisted of a 42.5m length of 600mm thick diaphragm wall, being keyed into the hard stratum. A 1.5m thick layer of jet grout was used just below the formation level [Figure 2.14]. The presence of a 1.5m layer of jet grout greatly enhanced the performance of the braced excavation with a reduction of 20-30% in strut forces, bending moment, wall deflection and ground settlement. Though the study resulted in an optimum condition in providing the improved soil layer to control the ground movement and lateral wall deformation, there was no specific mention on the behaviour of the improved soil layer.

2.7 Model Tests in Geotechnical Engineering

To obtain reliable and controlled data that is essential to better understand the behaviour of embedded improved soil layer during the process of excavation, the simulation should be realistic and reproducible. Though the field-instrumented excavation is the most straightforward and effective method, the major obstacle of using field test results for mechanistic study is the low degree of repeatability. The soil condition and construction sequence are different from one site to the other, often making correlation and comparison difficult. More so, it is almost impossible to know the true mobilised stiffness of the composite ground consisting of multiple overlapped improved soil columns. However, field measurements remain important and should be used as a means of calibration and verification of physical and numerical models.

The most cost-effective method to analyse the soil-structure interaction problem is to use the finite element method. It has been proven to be a very powerful tool to model complex construction sequences and detailed site-specific properties of the structural system. However, the ability to predict ground movements reliably is

strongly related to input material properties. Sensitivity analysis will provide the optimum condition but it is unlikely to be effective in furnishing the kind of database needed for mechanistic studies unless the results is collated with other type of modelling results.

As an alternative method to simulate the prototype behaviour of an excavation, small-scale centrifuge model has been used. A centrifuge is used to create an artificial acceleration field to simulate the gravitational stress needed to ensure correct scaling in a small model. Centrifuge modelling provides a correctly scaled physical model to enable the simulation of the prototype behaviour of excavation so that it could effectively be used to investigate the importance of various mechanisms at work when soil layers are improved. Nevertheless, it recognizes the sophistication in model ground preparation and difficulty in carrying out in-flight excavation. The beauty of this method is that the test can always be repeated and the excavation test can be tested until failure stage, which will be abnormal to happen in the field. Even most finite element programmes will not be executable to such failure stage. Due to these facts, physical modelling in centrifuge has gained acceptance worldwide and it is therefore chosen as the main physical modelling tool for this study.

2.7.1 Current Methods Used to Perform An In-flight Excavation

To model an excavation in a centrifuge, a method of simulating the soil removal has to be carried out in-flight. Currently, the following four methods are used to model an in-flight excavation in the centrifuge: -

a) Increasing centrifugal acceleration till failure [Lyndon and Schofield (1970)].

b) Draining of a heavy fluid [Kusakabe (1982), Powrie (1986)].

c) Removal of a bag of material from the excavation area [Azevedo (1983)].

d) An in-flight excavator [Kimura et al. (1993), Loh et al. (1998)].

In the first method, soil in the excavation area is initially removed in 1G environment before being subjected to an increasing centrifugal acceleration until failure. Although the overall total stress of model ground could be re-produced, the characteristics of the soil would have changed correspondingly to the increased G-level. This method is only suitable for modelling excavation in sand but not in clayey soil. For sandy material, the effective stress can develop almost instantaneously with the increased in G-level, as the dissipation of excess pore water pressure occurs almost immediately. However, for clayey material with a much lower permeability, the consolidation process requires a much longer period for the dissipation of excess pore water pressure. Nevertheless, this method is the simplest and it can only be used to provide a quick preliminary result on the potential failure pattern of an immediate and undrained excavation for a clayey material.

In the second method employed, the key idea is to replace the soil to be excavated by a fluid of identical density. The excavation process was simulated by draining the heavy fluid [Figure 2.15]. This method was employed by a number of researchers [Kusakabe (1982), Powrie (1986)] working on excavation in heavily consolidated clay. The main setback of this method is that for a fluid, the coefficient of lateral stress is always 1. For a heavily over-consolidated soil, the K_o is also expected to approach 1 and thus, this method is considered a reasonable approximation to the excavation in such a soil. However, K_o value of 1 is not typical for normally consolidated clays, which falls within the range of 0.55 to 0.65 [Kimura et al. (1993)]. Even then, it is recognised that during the excavation, the K_o on the passive side still remains as 1, which is not consistent with what happen in the field where the K_o value will approach K_p.

In the third method, soil bags were placed at the zone to be excavated and were removed during the excavation process. This method has the advantage over the first two methods, as the modelling of stress history of the soil model is more straightforward. Since the soil used in the bags is similar to the soil model, the coefficient of lateral stresses is consistent. Nevertheless, the interaction behaviour between the interface of soil bags with both the retaining wall and improved soil layer is difficult to be quantified.

Therefore, the first three methods cannot satisfactorily model a proper excavation in a clayey material in the centrifuge. This is because the actual excavation has not been carried out and the process of removing soil is not simulated in each case. In view of the above problems, researchers at Tokyo Institute of Technology, Japan (TIT) and National University of Singapore (NUS) have developed the fourth method, which uses a small-scale robotic excavator to remove the soil in-flight in the centrifuge.

2.7.2 The In-flight Excavator

The first in-flight excavator was reported by Kimura et al. (1993). This excavator consists of a movable table, a cutting blade and a soil retaining gate as shown schematically in Figure 2.16. The movable table sits on a pair of linear rails. The thrust is provided by a stepping motor through a timing belt and a pair of screw rods to the table. The vertical movement of the cutting blade and soil retaining gate is conducted by worm gears built into the stepping motors. The three stepping motors used in the excavator are small 5 phase stepping motors (UPD544HGI-NA, Oriental Motor), which make the accurate position of control possible. The excavator is finally mounted on a steel-made strong box with 500mm in length, 360mm in depth and

150mm in width.

Loh et al. (1998) reported the second in-flight excavator, which was designed to perform a 3-D excavation in the centrifuge. This excavator consists of a detachable lift-shaft and a centrifuge container as shown schematically in Figure 2.17. The centrifuge container has a width and length of 435mm, and a depth of 550mm. The stepper motor 1 (N43HCHL, Pacific Scientific Motor) is mounted on the top of the centrifuge container. Inside the detachable lift-shaft, a scrapper platform is mounted on the wall, and a cutting blade and soil-retaining gate are then rested on it. The horizontal movement of the cutting blade is powered by an intermediate size stepping motor (M22NSXB, Pacific Scientific Motor). Commands are sent via personal computers located in the remote control room through a pair of on-board indexers/drivers to control the motors.

To simulate an excavation using either of the above in-flight excavators, the cutting blade is first pushed down into the clay near to the wall and then pulled backward, skimming off a layer of clay and subsequently dumping it into the open space at the bottom. This cycle is repeated until the excavation reaches the required depth. The soil-retaining gate is allowed to move up and down corresponding to the cutting blade movements. When the cutting blade is lowered into the clay to perform an excavation, the gate is also lowered so that the top of gate comes just a little lower than the level of the blade edge.

The development of both in-flight excavators has unveiled a new chapter in centrifuge modelling of deep excavation problems in soft ground. Taking into consideration that only two groups have such facility to conduct scaled down centrifuge modelling, it is expected that the quantum of research studies carried out on deep excavation related works in the centrifuge are still limited. Even though several

research works on deep excavation were carried out in TIT, no work has been reported on the behaviour of an excavation stabilised by an embedded improved soil layer.

2.8 Concluding Remarks

Ground improvement techniques in the form of deep mixing and jet grouting have been the main focus at the Second International Conference on Ground Improvement Geosystem (IS-Tokyo'96), reflecting the growing importance of these new soil improvement methods for solving various geotechnical problems in soft ground. Among these numerous applications, the use of DCM Method in controlling ground movement in deep excavation works in different types of underground infrastructures has been a recent discovery. Its application in deep excavation looks set to increase due to fact that there is no better solution available to restrain the maximum deflection occurring at the bottom or just below the final excavation level other than to provide an embedded improved soil layer.

As the DCM Method was first introduced to improve the bearing capacity of soft ground to support structures, most research to-date concentrated on the strength properties. Nevertheless, very little study has focussed on evaluation of its stiffness property, which is of primary concern when the improved soil is used as an embedded soil strut. Taking into consideration the complexity in evaluating the composite stiffness of treated columns with surrounding untreated soil, it is expected that the determination of mobilized stiffness of the entire embedded improved soil layer in actual field is almost impossible. Furthermore, the strain measurements from the field instrumentation is often tedious and inaccurate, and hence, the composite stiffness assigned to the improved soil layer is basically a guessing work.

More importantly, the current design guideline of embedded improved soil

layer in deep excavation has been found to be inadequate. Though there are a number of reported field studies and numerical simulations on such soil improvement method in deep excavation, the understanding of the fundamental mechanics of the embedded improved soil layer is far from adequate. Postulations presented by different researchers to explain the behaviour are at times contradicting or not supported by experimental evidence. In addition, many studies have been performed merely to obtain economical configurations of improved soil without understanding in depth how the improved soil layer works in an excavation.

Due to the absence of data to describe the behaviour of the improved soil layer, the current design is based on 'know-how' experiences. Not many well-instrumented sites are available, and if there is any, the difficulties to interpret the interaction between the improved soil layer, the untreated soil and the excavation support system in the field further complicate the investigation. The finite element method has proven to be a very powerful tool for estimating the amount of ground settlement due to excavation but the accuracy of analysis is questionable due to the lack of proper calibration. Furthermore, other factors such as construction sequence, site control, local perturbation and variation in soil stratification further complicate the investigation.

The most accepted alternative to overcome the above problems is through model testing in a geotechnical centrifuge [Taylor (1995)]. The increasing use of centrifuge in geotechnical modelling is evident by the number of papers presented in international centrifuge conferences namely Centrifuge '88, Centrifuge '91, Centrifuge '94 and Centrifuge '98. This is simply because the small-scale model can be instrumented intensively, more reliably monitored and less expensive. More importantly, the stiffness properties of the improved soil layer could be determined

realistically.

In retrospect, some of the main points that could be extracted from the previous case studies are summarised as follows. Detailed investigation needs to be carried out for each case to further understand the behaviour of such improved layer in an excavation in soft ground.

(a) The embedded improved soil layer has been used to increase the passive resistance on the retaining wall. Consequently, the wall deflection and ground movements were significantly reduced, which very much depended on the stiffness of the improved soil. Nevertheless, the underlying mechanics behind such improvement for retaining wall has not been well investigated especially when the wall is floating in soft ground. Due to this uncertainty, some engineers would still insist to have the retaining wall keyed into a hard stratum even if the hard stratum is very deep.

(b) The existence of gap of untreated soil in between the stabilised ground and retaining wall could not be avoided during the installation process of the DMM [Tanaka (1993)]. Due to conservative thoughts, some contractors have already taken measure to improve this untreated soil portion by a high pressure jet grouting. Others may just ignore the existence of the gap or some even do not realise that such gap could exist. The necessity of such additional rectification work was not verified, as not even a single attempt has been carried out to investigate its effect to the overall behaviour of the support system in an excavation.

(c) The 'berm' improvement scheme is becoming popular among contractors in a large excavation project. Nevertheless, the selection of the pattern of improved soil berm is still highly empirical and at times, very conservative. Previous works have only

reported a comparison study on several patterns but no work has been done to understand how such improved soil berm works and no one has attempted to investigate the mechanism involved.

It is obvious that the knowledge on the behaviour of the improved soil layer in deep excavation has not been satisfactorily understood. To address these issues, detailed experimental programmes and numerical analyses were planned and described in the subsequent chapters.

Table 2.1 Relationships between E and q_u from different references

References	Relationship
Kawasaki et al. (1982) (refer to Figure 2.3)	E_{50} ~ 350 to 1000 q_u
Asano et al. (1996) (refer to Figure 2.4)	E_{50} ~ 150 to 400 q_u
Futaki et al. (1996)	E_{50} ~ 150 to 200 q_u
Tatsuoka et al. (1996)	E_{max} ~ 1000 q_u

Table 2.2 Factors affecting improvement effect [after Babasaki et al. (1996)]

Category I: Characteristics of cement	1. Type 2. Quality 3. Mixing water and additives
Category II: Characteristics and condition of soils	1. Individual characteristics of soil 2. Organic content 3. pH value of pore water
Category III: Mixing conditions	1. Water cement ratio 2. Degree of mixing 3. Period of mixing / re-mixing
Category IV: Curing conditions	1. Quantity of cement 2. Temperature 3. Curing time

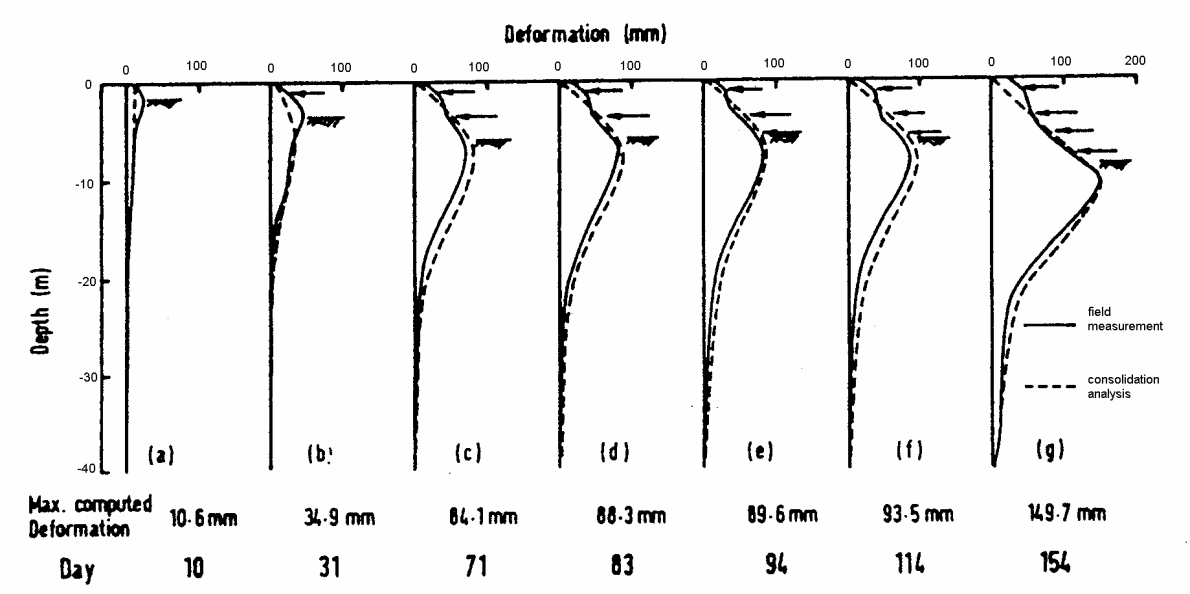

Figure 2.1 Lateral deformation of sheet pile wall [after Yong et al. (1990)]

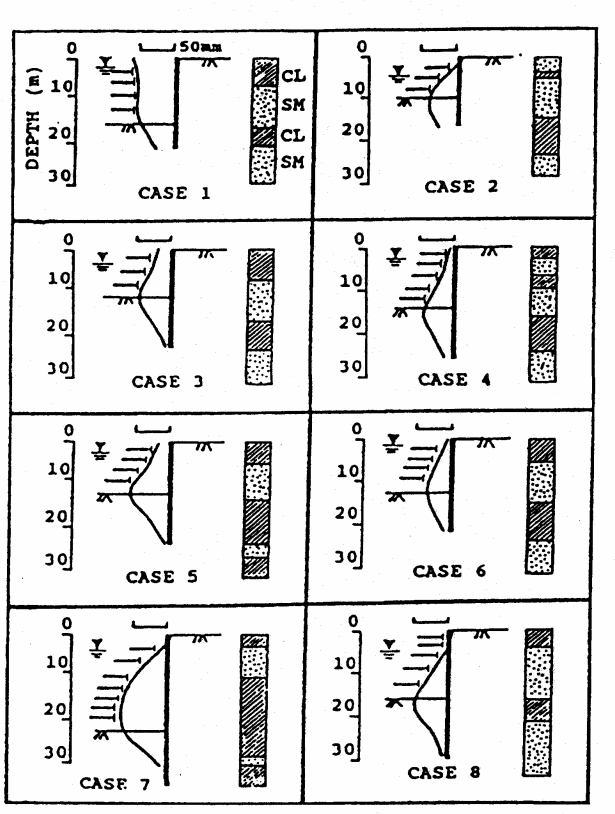

Figure 2.2 Lateral movement of diaphragm walls [after Wong and Patron (1993)]

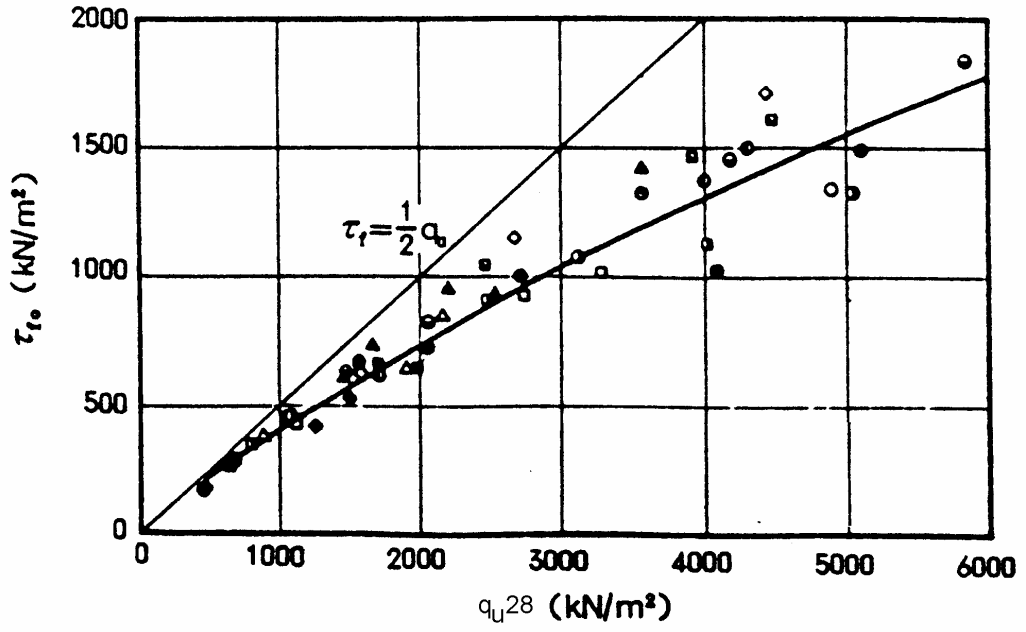

Figure 2.3 Relationship between shear strength (τ) and unconfined compressive strength (q_u) [after Kawasaki et al. (1984)]

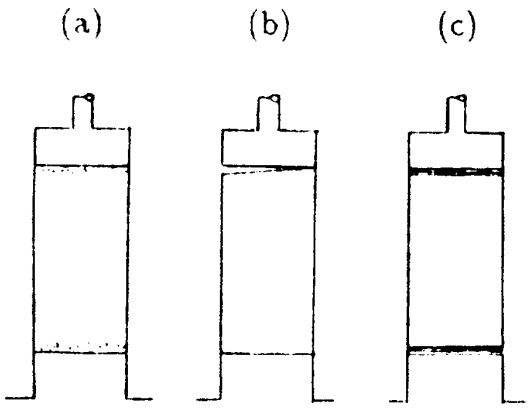

(a) a loose layer formed at both ends of specimen during preparation
(b) imperfect contact between specimen and rigid cap and pedestral
(c) compression of lubrication layer when it is in use

Figure 2.4 Factors of bedding error [after Tatsuoka and Shibuya (1992)]

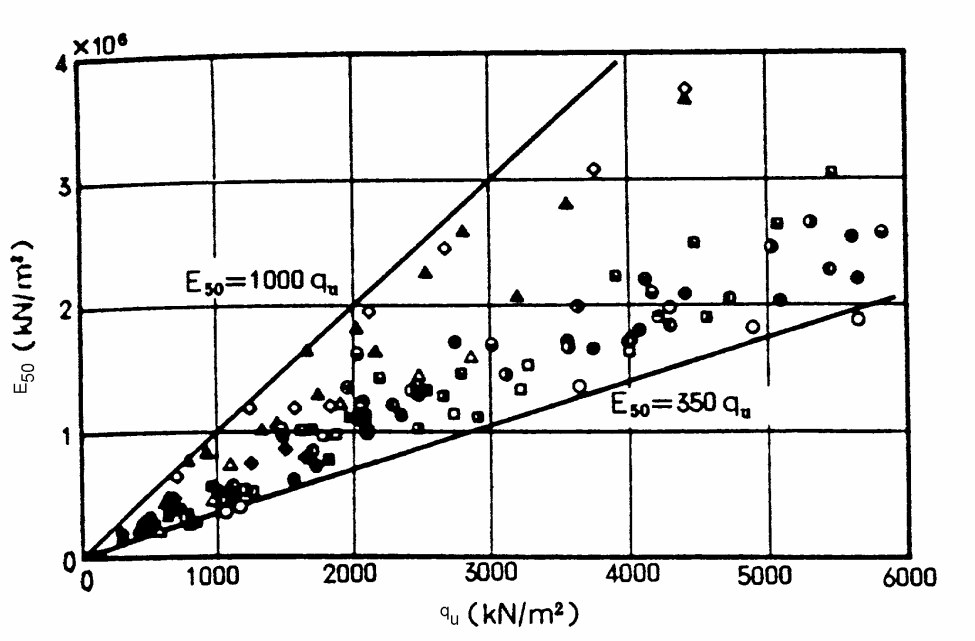

Figure 2.5 Relationship between unconfined compressive strength (q_u) and elastic modulus (E_{50}) for improved soil [after Kawasaki et al. (1984)]

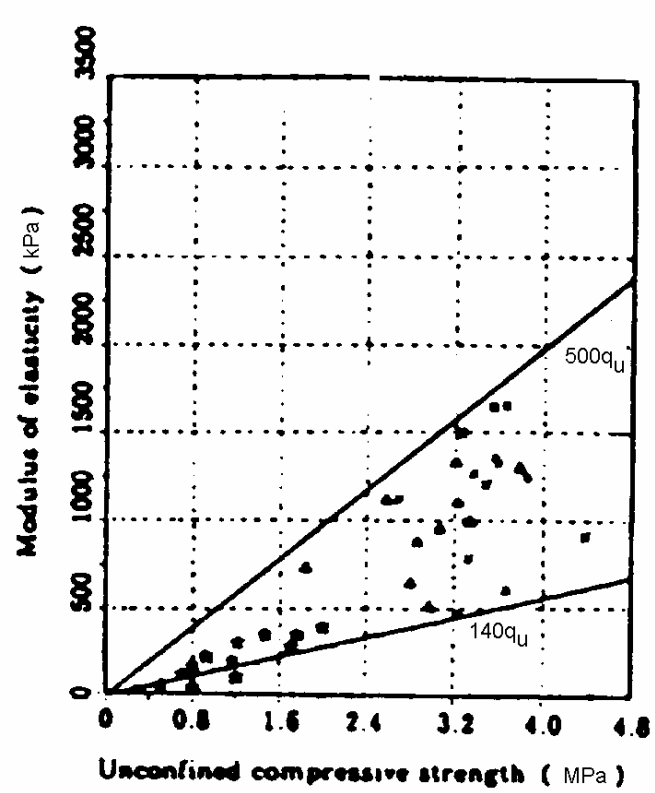

Figure 2.6 Relationship between unconfined compressive strength (q_u) and elastic modulus (E_{50}) for improved soil [after Asano et al. (1996)]

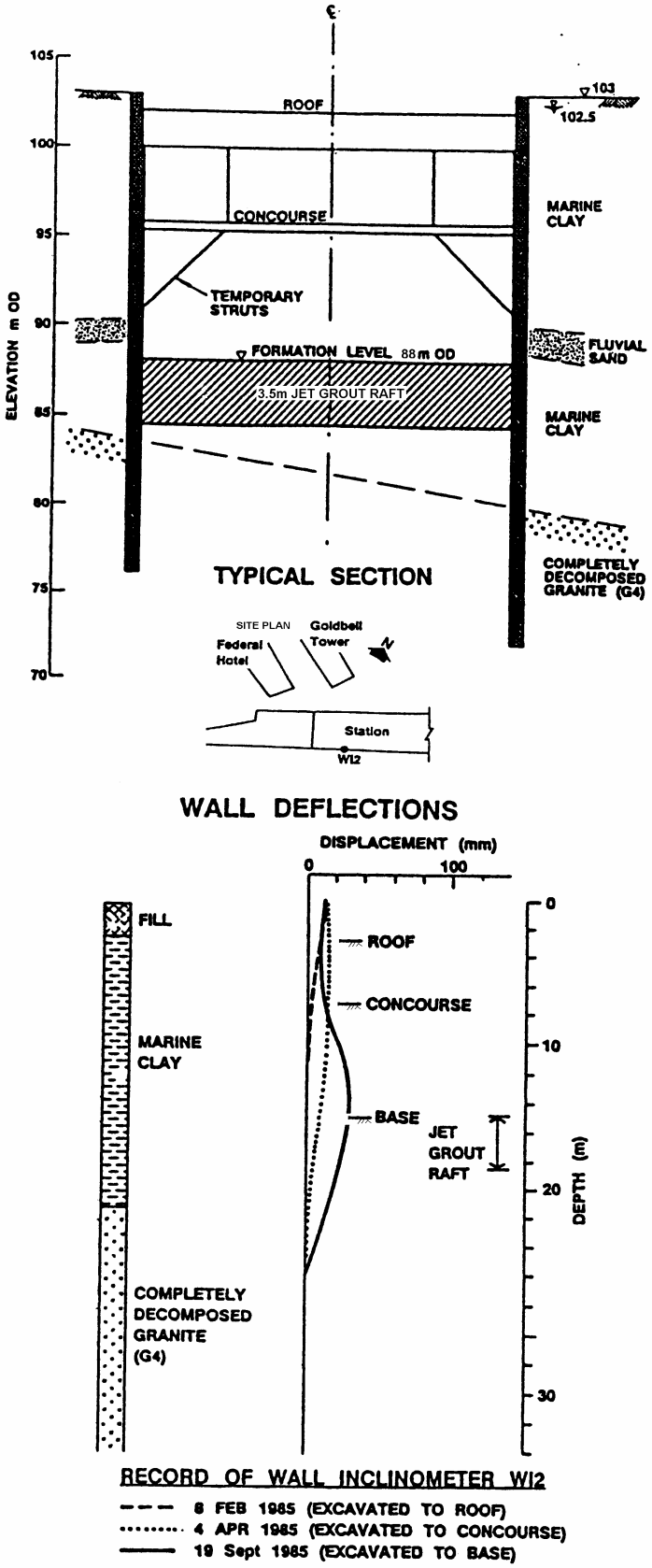

Figure 2.7 Base stabilisation of top-down excavation in Singapore marine clay [after Gaba (1990)]

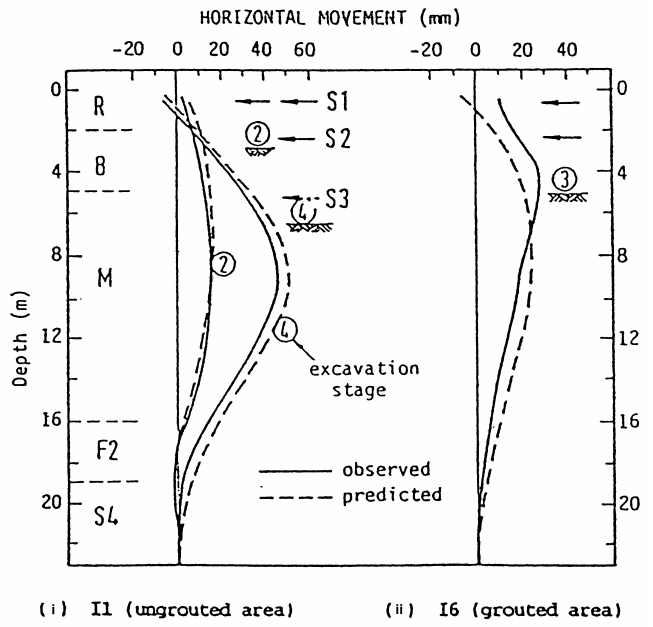

Figure 2.8 (a) Base stabilisation with one layer of jet-grouted soil scheme [after Lee and Yong (1991)]

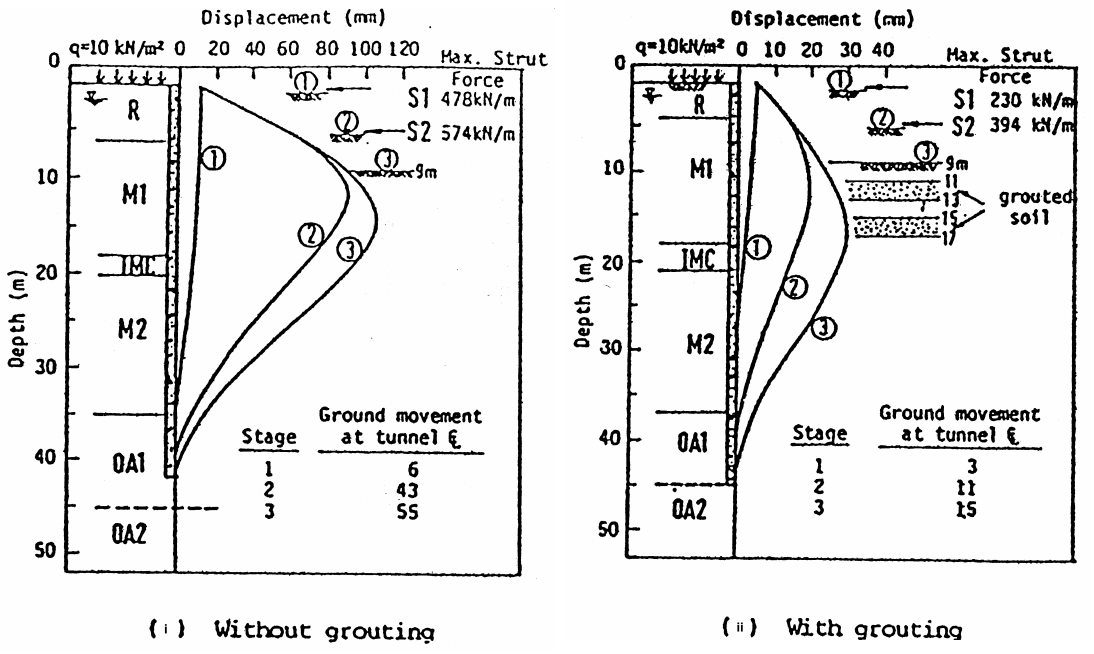

Figure 2.8 (b) Base stabilisation with two layers of jet-grouted soil scheme [after Lee and Yong (1991)]

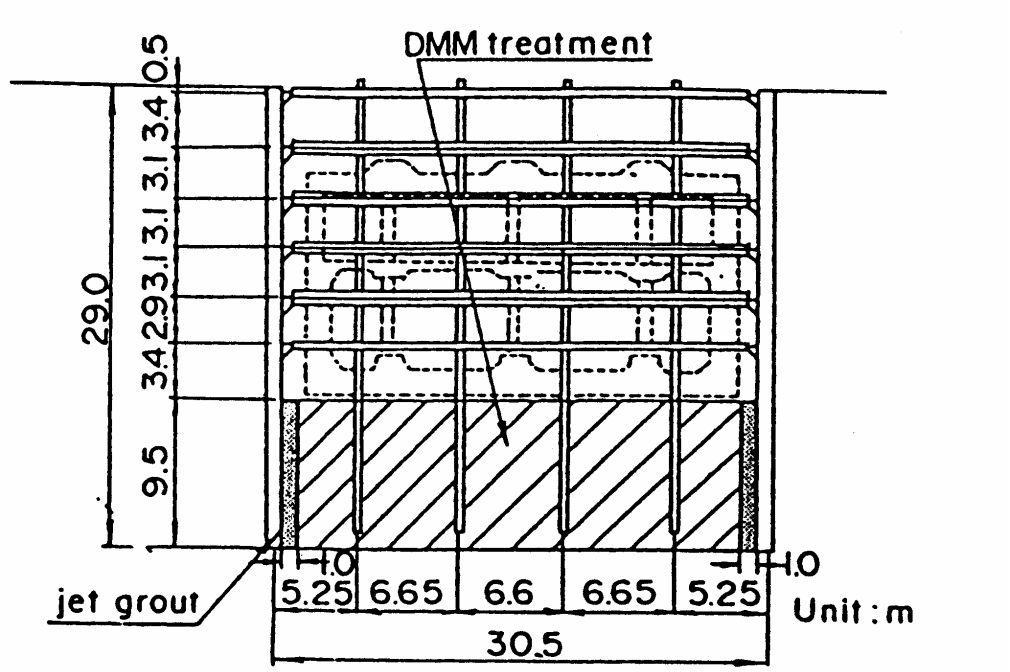

Figure 2.9 (a) Section of braced excavation with soil improvement work [after Tanaka (1993)]

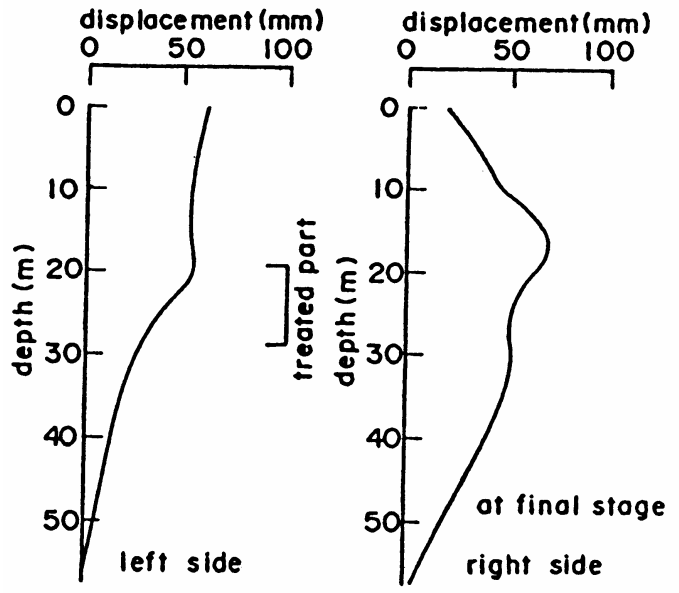

Figure 2.9 (b) Wall deformation from field measurements [after Tanaka (1993)]

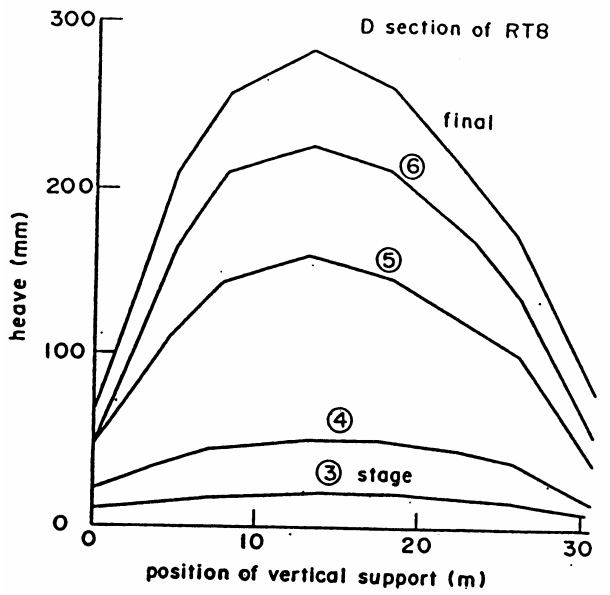

Figure 2.9 (c) Large heave of vertical supports due to basal heave [after Tanaka (1993)]

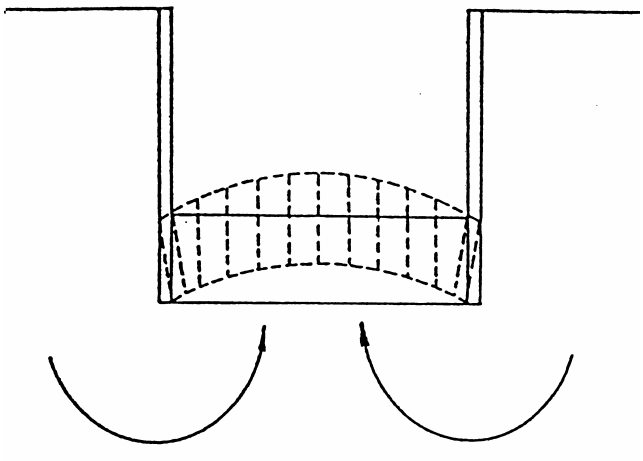

Figure 2.9 (d) Predicted deformed shape of the treated soil [after Tanaka (1993)]

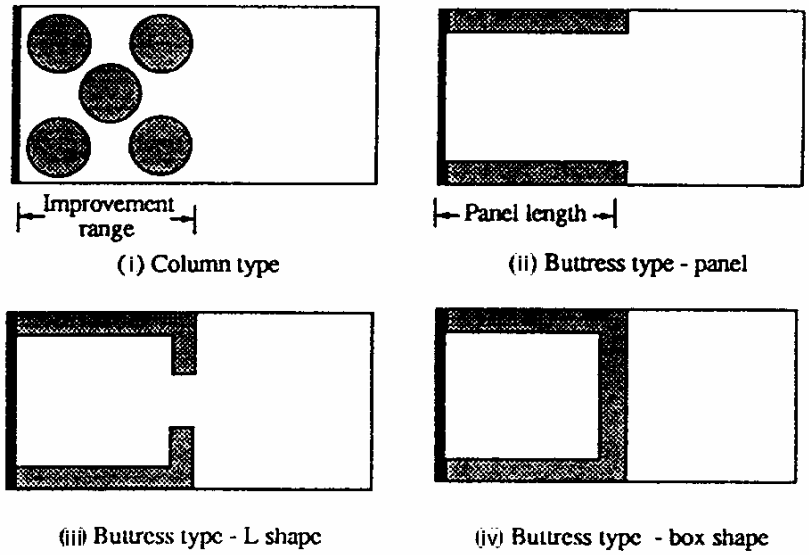

Figure 2.10 (a) Layout patterns for reinforced soil specimens [after Liao and Tsai (1993)]

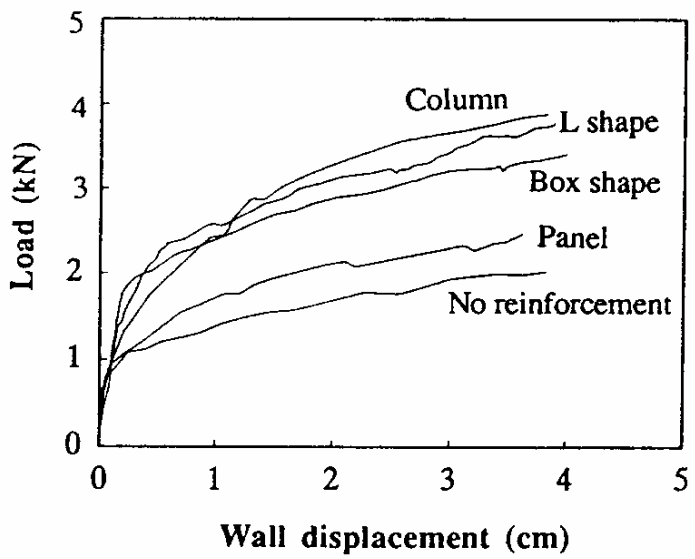

Figure 2.10 (b) Load deformation relationship for specimens reinforced with different layout patterns [after Liao and Tsai (1993)]

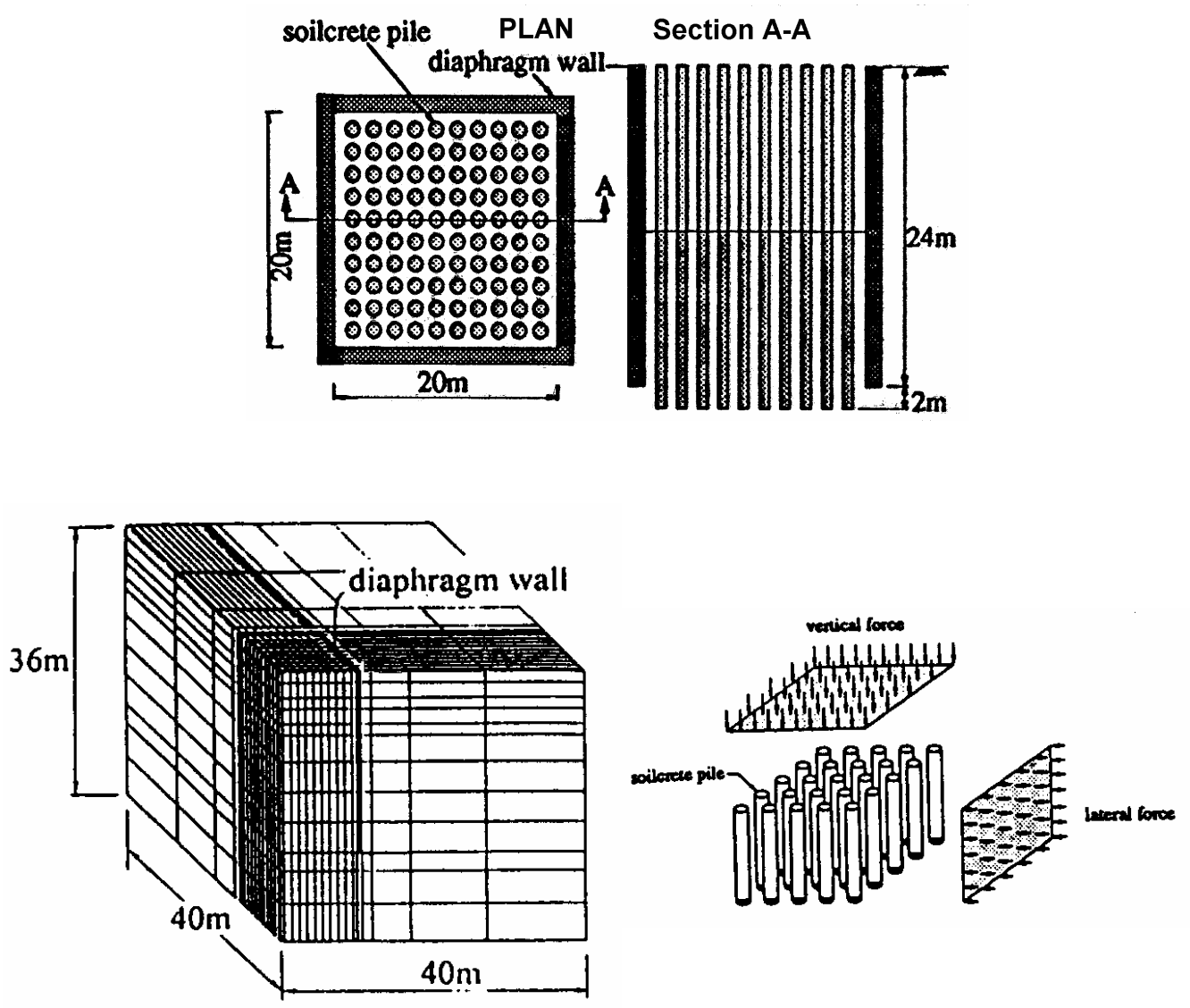

Figure 2.11 Column type of ground improvement in hypothetical excavation [after Ou and Wu (1996)]

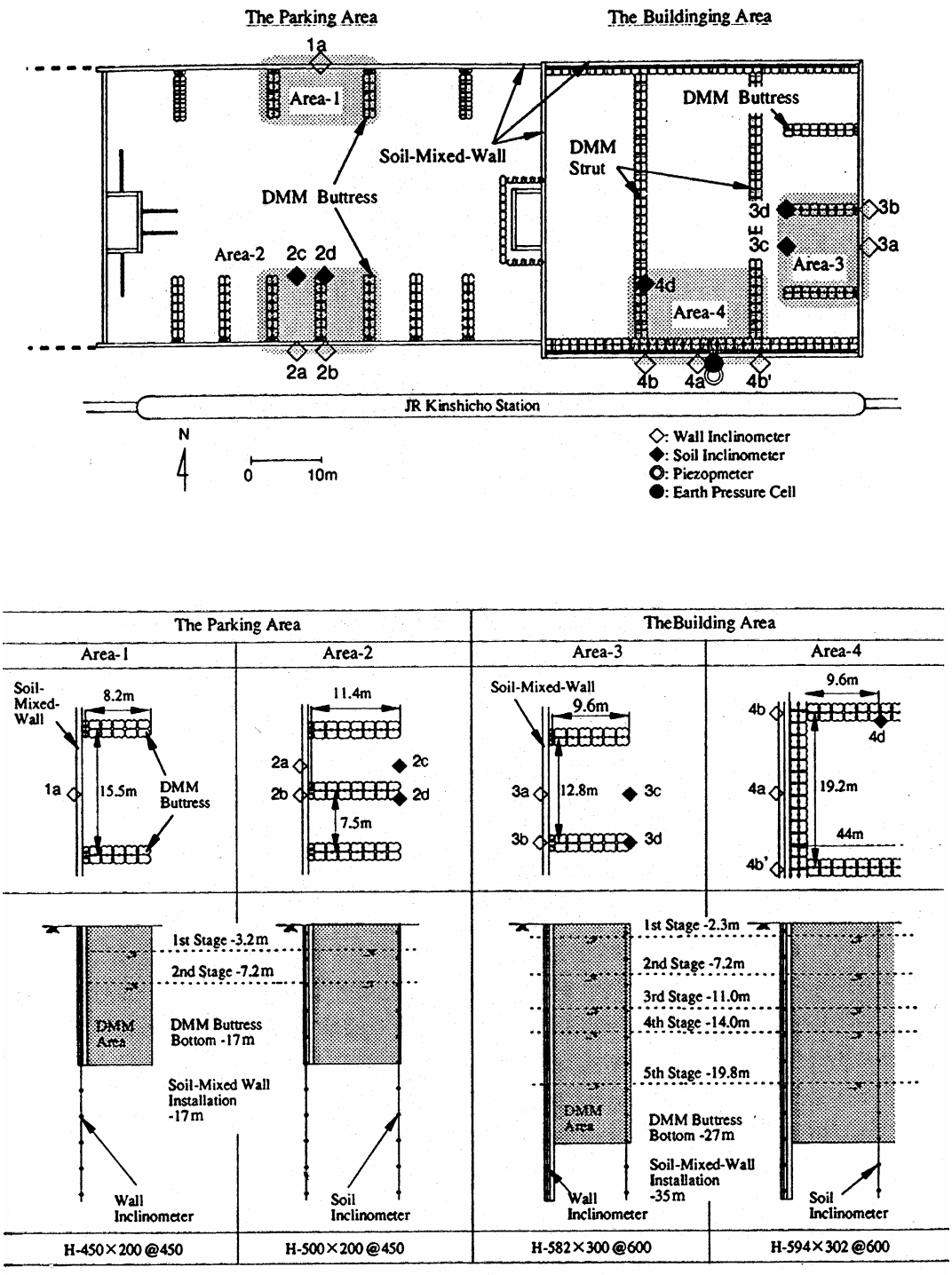

Figure 2.12 The shapes of DMM buttress showing the improvement and excavation stages [after Uchiyama and Kamon (1998)]

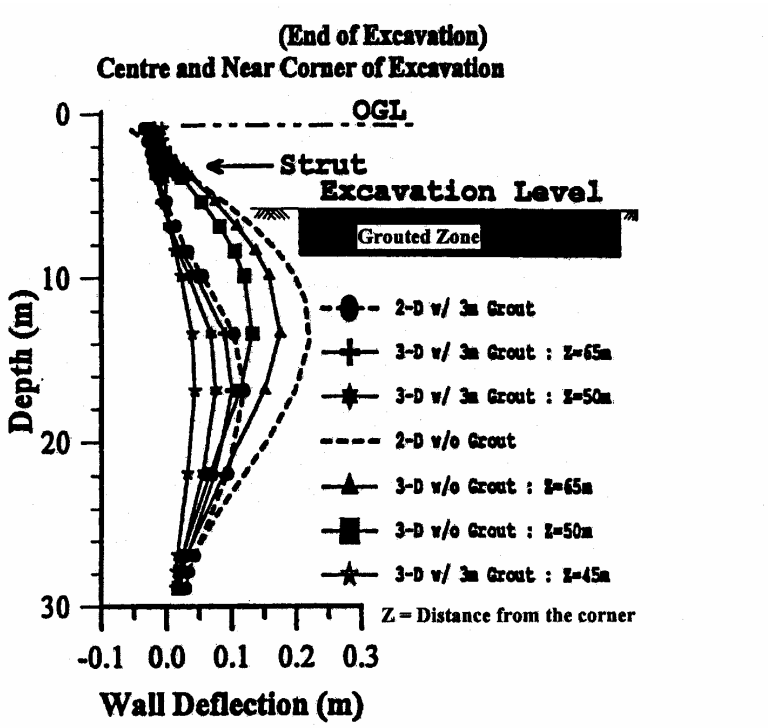

Figure 2.13 Wall deflection profiles with and without grouted layer [after Yong et al. (1998)]

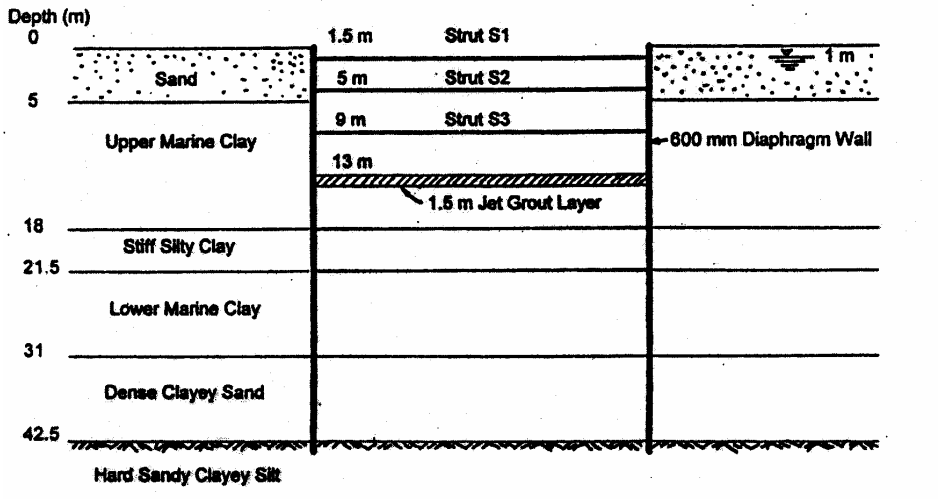

Case	Description	Strut force (kN)			Max wall bending moment (kNm/m)	Max wall Deflection (mm)
		1st strut	2nd strut	3rd strut		
1	No jet grout	262	835	893	1300	197
2	1.5m jet grout layer	187	585	696	1020	139

Figure 2.14 Effect of jet grouting layer in excavation [after Wong et al. (1998)]

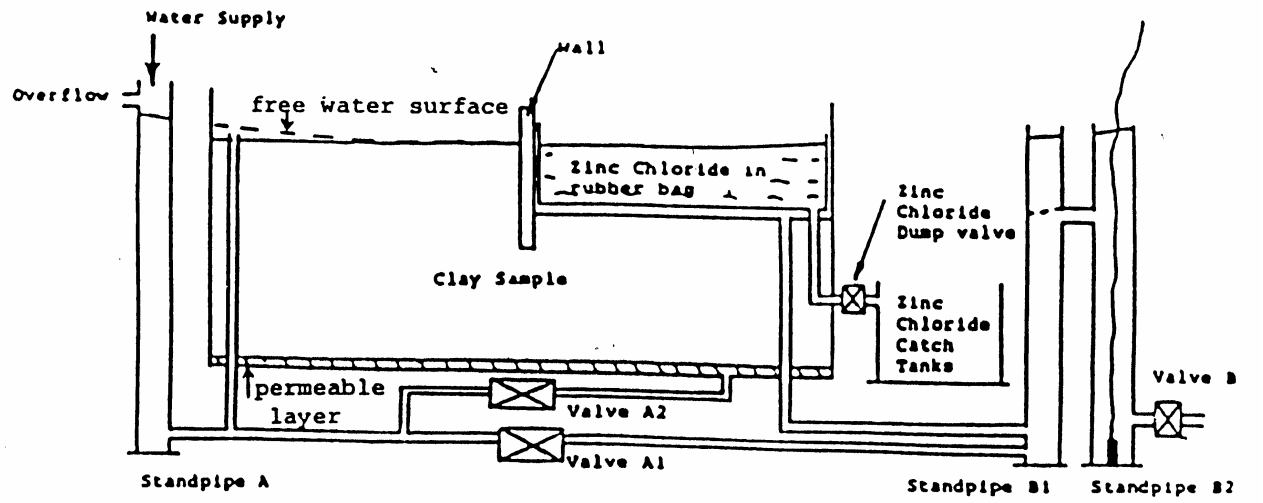

Figure 2.15 Draining a heavy liquid to simulate an in-flight excavation [after Bolton et al. (1989)]

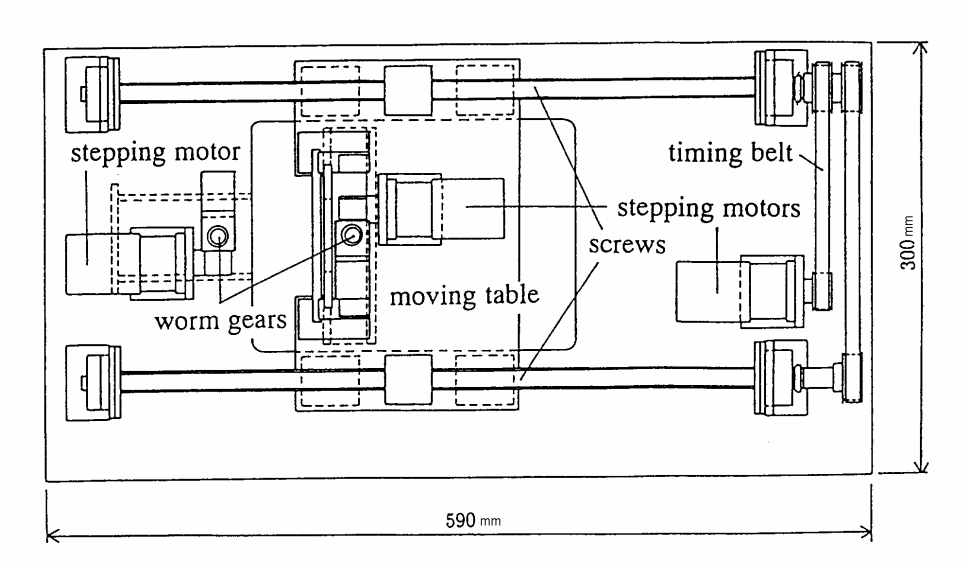

PLAN VIEW

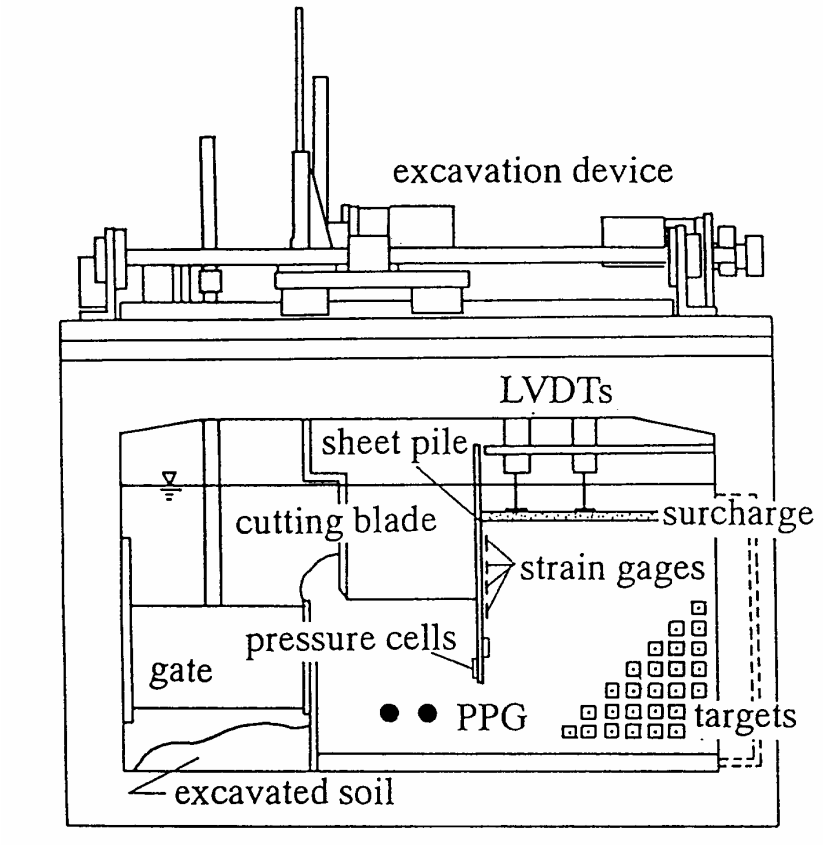

FRONT VIEW

Figure 2.16 In-flight Excavator at TIT [after Kimura et al. (1993)]

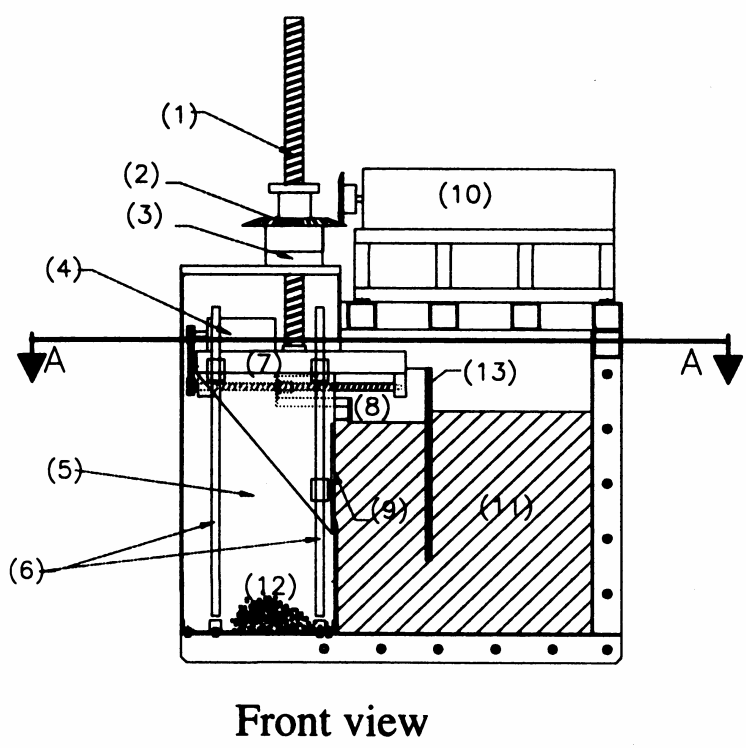

(1) Precision ball screw
(2) Bevel gear
(3) Trust bearing
(4) Stepper motor 2
(5) Detachable lift shaft
(6) Linear rail
(7) Scraper platform
(8) Scraper
(9) Soil-retaining gate
(10) Stepper motor 1
(11) Soil sample
(12) Excavated soil
(13) Retaining wall
(14) Perspex window

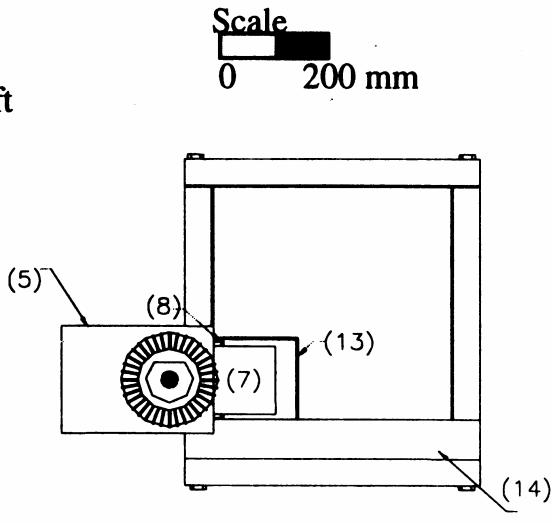

Figure 2.17 In-flight Excavator (MARK I) at NUS [after Loh et al. (1998)]

Chapter 3

PROPERTIES OF SINGAPORE MARINE CLAYS IMPROVED BY CEMENT MIXING

3.1 Introduction

To control movement in an excavation in soft ground, soil improvement technique is often needed to improve the strength and stiffness of the ground. In-situ stabilisation technique by feeding cementing agents into soft ground is one such approach and has become increasingly popular. In this technique, chemical reactions among the stabilising agent, clay minerals and water are allowed to take place deep below the ground to produce a high strength product rapidly and which will continue to strengthen with time. Several such techniques are presently used in Singapore, including jet grouting, deep cement mixing and lime column methods.

The Deep Mixing Method (DMM), a mechanical mixing method, nowadays is considered as an alternative to jet grouting which is still the more popular choice in Singapore. In DMM, a blade is pushed into the ground and mixes the soil while cement grout or dry cement is injected into the mix. In jet grouting, air and water are first used to cut the soil and mix it while grout is injected, and all these are carried out under fairly high pressure. As a result, DMM causes little expansion to the surrounding soil during installation and thus minimises uncontrolled movement in adjacent ground. Furthermore, as it mixes the soil at the in-situ water content, it does not produce any slime. In contrast, the jet grouting method produces a large amount of slime, which is an industrial waste and must be properly disposed. From the perspective of improved property, the principal difference between a jet grouted soil and deep mixed soil is the range of water content of the soil mixed; this is usually much higher in a jet-grouted soil.

In the early days of DMM application, lime was used as the hardening agent, but later, Ordinary Portland Cement (OPC) was introduced due to problems encountered in storing unslaked lime in a hot and humid country like Singapore [Broms (1984)]. The method is now known as the Deep Cement Mixing (DCM) Method.

Research and development of this method was initiated in Japan in the late 1960s [Okumura and Terashi (1975)]. Stimulated by the successful applications of this technology in Japan in the 1970s, many related studies on the engineering properties improved soils have been carried out [Terashi et al. (1979), Kawasaki et al. (1981)]. The first major application of DMM in Singapore was in the 1980s when it was used to improve the bearing capacity of a reclaimed land located southeast of the island [Kado et al. (1987)]. This method was used again in subsequent years to improve the foundations of various Mass Rapid Transit stations [Kado et al. (1987)], which are founded in soft clay. In a recent project in Singapore, this method was adopted to stabilise a deep excavation located next to a Mass Rapid Transit's station in the eastern part of Singapore. The consultants in that project were concerned about the strength and stiffness of local improved clays, and also the effect of continual increase in stiffness of the improved soil on the design of the diaphragm wall. Thus far, only limited data, mainly from contractors' records, are available on such improved properties in Singapore.

As the clay mineralogy and climatic conditions in various countries are different, often, there is concern about using correlations from elsewhere for local application. This study is carried out to establish the characteristics of improved Singapore marine clays, but more importantly, also to investigate the possibility of using a normalised approach to ensure greater applicability of results. In this study, the interaction among various constituents and their impact on improvement with time will be evaluated.

Measurements with local strain transducer indicated significantly higher stiffness values compared to the conventional approach. Though this point is well understood in the testing of solid material, it is not so in the testing of soil. As an improved soil is very much like stiff clay, most studies continued to use conventional soil testing approach. Therefore, there is a need to carry out independent study using the more advanced local strain measurement transducer.

3.2 Properties of Clays and Cement Used

The majority of marine clays found on Singapore Island are composed of a sedimentary deposit known locally as the Kallang Formation. This deposit is widely distributed and covers nearly 25% of the total land surface of the island [Yong and Karunaratne (1983)]. This formation usually consists of Upper Marine Clay and Lower Marine Clay separated by a stiff desiccated intermediate layer [Chong et al. (1998)]. Common properties of Singapore marine clay around the Singapore Island have been extensively reported [Yong and Karunaratne (1983), Tan (1983) and Chong et al. (1998)]. The Upper Marine Clay is highly plastic with the liquid and plastic limits typically ranging from 76 to 101 and 45 to 69 respectively. The average bulk unit weight is 16.3 ± 0.5 kN/m^3 and the natural moisture content is about 60% to 92%. The Lower Marine Clay is highly plastic with the liquid and plastic limits typically ranging from 65 to 85 and 38 to 55 respectively. The average bulk unit weight is 15.2 ± 0.6 kN/m^3 and the natural moisture content is about 50% to 69%. Typically, the organic content for both clay members is around 3% with moderate contents of kaolinite, illite, chloride and smectite.

In this study, three clays from the Kallang Formation were used [Figure 3.1]. Clays collected from Eunos and City Hall sites are from the Upper Marine Clay, while

the clay from the Singapore Art Centre (SAC) site is from the Lower Marine Clay. Prior to cement treatment, the physical and chemical properties of these marine clays and their pore fluids were determined and the results are summarised in Table 3.1. The cement used in the test was Ordinary Portland Cement. To ensure that the cement used throughout the study has consistent physical properties and chemical compositions, cement from the same batch of production had been used. Table 3.2 shows the physical properties and chemical compositions of the cement used.

3.3 Sample Preparation and Testing

Besides the three main constituents of mixture (clay, water and cement), other factors such as the mixing time, kind of blades, rotational speed of blades, curing temperature and humidity also have an effect on the properties of the cement treated clay [Babasaki et al. (1996)]. Thus, to investigate only the effect of the constituent materials on the strength of improved clay, it is necessary to adopt a standard procedure for preparing the sample.

After the water content of each batch of clay was determined, water was added to fix the water content at 90%, 120% and 150%. Subsequently, a specified weight of dry cement powder was added into the clay to fix the cement content at 10%, 20% and 30%, this is defined as the ratio of mass of cement, C to the mass of dry soil, S. The water and cement contents considered in the study are within the practical ranges encountered in the Deep Cement Mixing (DCM) Method. The sequence of mixing was also standardised; first the soil is mixed with water and then with cement, as the sequence will also influence the strength of the cement clay mix [Fam and Santamarina (1996)]. The hydrated clay and cement powder was mixed thoroughly by a ‘Hobart’ mixer for exactly 10 minutes with a rotational speed of 48 revolutions per minute.

After mixing, the cement clay paste was placed into a cylindrical mould with an inside diameter of 70mm and length of 140mm. To reduce the trapping of air bubbles, the paste was compacted in three layers by slowly tamping the mould on the ground. Compaction by vibrating and ramming were tried but was unable to provide sufficient densification due to the high viscosity and low workability of the cement clay paste. Hence, all the samples were compacted by the tamping method to a percentage of air voids below 1.5%. This is important in order to produce samples with almost identical compaction effort.

The presence of air voids has an adverse effect on strength development of the cement treated clay. To illustrate this, several samples were compacted using different amount of tamping effort and consequently have different percentage of air voids in them. These samples were then cured for 3 days and after that, the strength of each sample was determined. Figure 3.2 shows that the strength reduces linearly with an increase in air voids, the reduction is about 5% for every 1% increase in air voids for the range evaluated in this study. It is therefore important to control the amount of air voids in the sample, and for the study, the percentage of air voids is kept within 1.5%, allowing the strength to only vary within a very small range.

After compaction, samples were left overnight and de-moulded on the following day. Each sample was then sealed inside a polyethylene bag and covered with wet textile to preserve the humidity during curing at a controlled temperature of 26^{o}C. Unconfined compression tests were performed on the cement mixed samples to evaluate its strength and elastic modulus. The test was conducted in accordance to BS 1377: Part 7: 1990. All the tests conducted in this study are summarised in Table 3.3. Two methods were used to measure the axial displacement of the specimen [Plate 3.1]. The first method, a conventional approach, measures the external displacement between the two end platens

using a set of Linear Variable Displacement Transducers (LVDTs). The method of measurement does not have to be corrected for apparatus compliance as the LVDTs are directly placed between the platens. The second method uses a Hall's effect strain transducer placed at the centre part of a sample to measure the displacement [Clayton et al. (1989)].

For testing of solid materials such as concrete and steel, the issue of bedding errors is well understood and measuring displacement between end plates is rarely done. Usually, strain gauges are attached directly to the specimen to measure the deformation. However, in soil testing, this issue is only recognised more recently. As the clay-cement mix is more like very stiff clay, engineers have continued to use conventional soil testing apparatus for such measurement. A second relevant issue is that for materials like concrete and steel, it is generally accepted that the behaviour is linearly elastic at small strain. However, for soil, at strain level between 0.001% and 0.1%, the behaviour is generally recognized to be non-linear elastic. It is therefore important to establish whether this also holds for the clay-cement mix. To date, only Tatsuoka et al. (1996) have specifically investigated this aspect on Japanese clays.

3.4 Results and Discussions

3.4.1 Typical Stress Strain Curves

For each mix proportion, two samples were tested and to ensure reliability of the result, a third sample would be used if the first two did not show good agreement. Figure 3.3(a) shows a set of typical stress strain curves for two samples of cement mixed clay with the same cement content (30%) and water content (90%) tested after 7 days of curing. The stress strain curves for the two samples using the Hall's effect transducer for strain measurement are virtually identical, indicating that the results are consistent and

repeatable. However, for external measurements, the strain measured is considerably larger, and there is significant difference between the two samples tested. Closer examination indicates that the initial movement measured by the LVDT for Sample 2 is unusually large, clearly showing that bedding error due to imperfect end-restraints in this case is more substantial than in Sample 1. This set of results reinforces the reliability of using local strain transducers.

Figure 3.3(b) shows the comparison of stress strain curves for the untreated and cement treated clays, which are plotted for different cement contents after 28 days of curing. The stress strain curves of cement treated clays were found to increase sharply up to a peak strength, and then suddenly decreased to a low residual value upon further straining. It is observed that the cement treated clays have changed into a more brittle material, which fails at a much smaller strain. It is also noted that with increasing cement content, there is a corresponding increase in the strength, as well as in the stiffness of the cement treated clay.

3.4.2 Strength Results

The unconfined compression test is frequently used to evaluate the degree of improvement of treated soil. Many factors affect the unconfined compressive strength, q_u, of a cement-mixed clay, but the more important factors are the type of clay, cement content, water content and curing time. Therefore, an investigation was carried out on how each of these factors would influence the strength of the improved clays.

(a) Effect of Clay Type

Figure 3.4(a) shows the stress strain curves of the clay-cement mix of the three clays after 7 days of curing, and where the cement content is 20% and the water content is 90%. This shows that the unconfined compressive strength, q_u, varies considerably

according to the type of clay even though these clays come from the same sedimentary deposit. Figure 3.4(b) shows the correlation of the unconfined compressive strength of improved City Hall Clay and SAC clay versus that of Eunos marine clay under similar mix proportion and testing conditions. This shows that the improved Eunos clay attains the highest strength, followed by City Hall clay, which achieves only 85% of that for Eunos clay and the SAC clay achieves only 70% of that for Eunos clay. A more pertinent and interesting observation from Figure 3.4(b) is the fact that the shear strengths of the different improved clays show nearly linear correlation with each other. This observation provides the motivation for a normalised approach to be discussed next.

Every type of clay has its own mineralogy with different physical and chemical properties, and each of these properties may affect the strength improvement [Gotoh (1996)]. Although no X-ray diffraction was carried out on the 3 samples used in this study, the difference in mineralogy may explain the results in Figure 3.4. To derive a strength relation that incorporates all relevant factors, especially at a fundamental level, is ideal and desirable, but is extremely complicated and difficult. However, if the improved strengths of different clays under the same conditions show a consistent pattern, then an effective alternative is to explore if a normalised strength shows the same consistent pattern. This is motivated by the linear correlations observed in Figure 3.4(b) for the three clays studied.

In this study, it is proposed that the strength of any improved soil, q_u, is normalised against a reference unconfined compressive strength of the same clay improved at a specified cement content (A_w), water content (w) and curing age (t), q_u (A_w.w.t) as follows: -

$$\text{Normalised strength of improved soil} = \frac{q_u}{q_u(A_w.w.t)} \qquad (3.1)$$

First, it is important to establish whether this approach works only for a special case where the strength has to be normalised against a specific reference value determined through trial and error, in which the case, the usefulness is limited. However, if the reference value is general, and the normalised behaviour shows consistent pattern, then this is a powerful approach. To evaluate this, the normalised strengths for improved City Hall clay and SAC clay, following the definition in Equation 3.1, are plotted against that for improved Eunos clay, as shown in Figures 3.5(a) to (d) for four widely different reference values.

As an example, Figures 3.5(a) shows the normalised strength of improved City Hall and SAC marine clays compared against those from Eunos marine clay, where the reference strength for normalisation is the unconfined compressive strength for a clay improved with cement content, A_w of 10%, water content, w of 90% and curing age, t of 1 day, q_u(10.90.1). This figure indicates that a very good correlation between the normalised strengths of the improved clays. Figures 3.5(b), (c) and (d) show the results when the reference unconfined compressive strengths are set for conditions of (20.90.14), (30.120.7) and (30.150.28) respectively, and again very good correlations are obtained. This is an important result, and leads to the conclusion that though different clays were used, the normalised strengths for these clays are consistent with each other. Based on this observation, a generalised relationship between the normalised strength of improved soil for the three different marine clays studied can be proposed as follows: -

$$\frac{q_{u\,Eunos}}{q_{u\,Eunos}(A_w.w.t)} = \frac{q_{u\,CityHall}}{q_{u\,CityHall}(A_w.w.t)} = \frac{q_{u\,SAC}}{q_{u\,SAC}(A_w.w.t)} \qquad (3.2)$$

However, if this relation is applicable only to the three clays studied here, again the usefulness is limited. Thus, this idea is extended to the normalised improved strength

of two Japanese clays, namely Tokyo-4 and Kanagawa-2; inferred from the results presented by Kawasaki et al. (1984). These Japanese clays have water content of approximately 90%. In this case, the reference unconfined compressive strength used is that for clays improved with cement content of 30%, water content of 90% and cured for 28 days. Earlier, Figure 3.5 showed that the actual reference mix proportion used is not critical, as long as it is from the same clay. The results of Figure 3.5 also mean that the choice for cross-referencing is not critical; any clay could have been chosen. Figure 3.6 shows the normalised results using the strength of Eunos Clay for cross-referencing, and again a very good correlation is obtained, though very different clays are now used. This suggests that Equation (3.2) is quite universal and can be used for different types of clay. This is an important point, as this approach means that cross-referencing of results from literature on different clays can now be done. To use this with confidence, a detailed statistical study is needed but this is beyond the scope of the present study.

(b) Effect of Water Content (w) and Cement Content (A_w)

In the field, using the DCM technique, the only parameter that can be controlled is the cement content. However, the cement content to be added is influenced very much by the in-situ water content of the clay. In this section, these two factors will be investigated. First the influence of water content on the strength of improved soils is studied. For this, it is necessary to fix the cement content and the curing age of the sample. Three water contents were used in the study, namely 90%, 120% and 150%. All three clays were tested, and their results normalised with the respective q_u (30.90.28). As pointed out in the previous section, the precise choice of this particular set of reference parameters is not a critical issue.

Figure 3.7(a) shows the effect of water content on the normalised strength for the three local clays, tested after 28 days of curing. Though different clays were used, the

normalised results show a consistent trend confirming the usefulness of this approach. As expected, the lower the water content of the clay, the greater is the strength improvement and this inverse relationship was also reported in the literature [Kawasaki et al. (1984), Babasaki et al. (1996)]. Because of this, to boost the strength improvement, a dryer mix proportion is often desired. This is one reason why dry cement powder has been introduced and proved to be successful in the Dry Jet Mixing Method, which is a new technique in DMM. However, mixing the clay in a dryer condition creates problems of homogeneity and workability that affect the degree and efficiency of mixing, and therefore the improvement.

Figure 3.7(b) shows the variation of normalised strength with cement content for samples at three different water contents and cured for 28 days. The normalised strength for different clays at a fixed water content is seen to increase nearly linearly with the cement content. Though the increase is expected, the nearly linear increase is not, and has important practical implications. But due to the limited number of tests used in this study, it is not possible to explore this further. Another point to note is that the rate of increase of strength with increasing cement content is also increasing with reducing water content of samples. As many factors influence the strength improvement, it is equally important to look at the relative proportion of the constituents in the mix.

(c) Effect of Water-to-Cement (W/C) Ratio

To illustrate the influence of water-to-cement (W/C) ratio on the strength, the normalised soil strength at 28 days is plotted against W/C ratio, for different cement content [Figure 3.7(c)] and different water content [Figure 3.7(d)]. As shown in these two figures, the greater the W/C ratio, the lower is the strength. This inverse relationship of strength with W/C ratio has also been reported in the studies of concrete and is

referred to as Abrams' rule [Neville (1995)].

However, Figure 3.7(c) also shows an intuitively not obvious trend. When W/C ratio is kept constant (say, W/C = 6), the improved strength at 20% cement content is higher than at 30% cement content, suggesting that a decrease in cement content will result in an increase in the strength, an apparently counter-intuitive observation. To make sense of this requires an evaluation of the interactions among the parameters. Table 3.4 provides a summary of these interactions, and shows that an increase in q_u under condition (1) and (2) is intuitively expected but not for condition (3). In condition (1), if the amount of water (W) and soil (S) are kept constant and the amount of cement (C) is increased, W/C ratio will reduce while C/S ratio will increase, and both cause an increase in q_u. In condition (2), if C and S are kept constant and W is reduced, W/S and W/C ratios will reduce, and both cause an increase in q_u. In condition (3), if W and C are kept constant and the amount of soil treated, S, is increased, W/S and C/S ratios will both decrease, but a reduction in W/S will cause an increase in q_u, whereas a reduction in C/S will cause a reduction in q_u. Therefore, the trend of q_u depends on whether the effect of decreasing the W/S ratio or C/S ratio is more dominant for a particular mix proportion.

In the range of water and cement contents used in this study, decreasing the water content seems to be more effective than reducing the cement content, which results in an increase in the compressive strength even though the C/S ratio has reduced, as the results of Figure 3.7(c) suggest. This understanding is important for the field application of DCM stabilisation whereby the W/C ratio is often kept constant [Yoshizawa et al. (1996)] while determining the proportion of mix design. Hence, the accurate determination of water content, including the natural water content of clay, is important before a decision to fix the W/C ratio can be made.

(d) Effect of time (t)

The ability to estimate the strength development of the improved clay at various construction stages is an important consideration in giving an early indication of whether the particular mix proportion can achieve the desired strength at 28 days, the usual benchmark for determination of strength. To be able to estimate the future expected strength from early tests, empirical relationships have to be established to relate the strength of the stabilised clays at various periods of curing time. These relationships are summarised from all the experimental results conducted in this study. By co-relating the normalised strength at 28 days to the normalised strength at 1, 3, 7 and 14 days, as shown in Figure 3.8(a), reasonably linear relationships can be obtained from the data. The following empirical linear relations can thus be established: -

$$q_u28 \approx 2.9 \times q_u1$$

$$q_u28 \approx 2.1 \times q_u3$$

$$q_u28 \approx 1.6 \times q_u7$$

$$q_u28 \approx 1.2 \times q_u14 \qquad (3.3)$$

Figure 3.8(b) shows the increase in strength development of Singapore cement treated clays normalised to the strength at 28 days. It is obvious that the hardening of cement treated clays is a time dependent process. The rate of strength development is exponential initially, whereby the greatest rate of strength gain occurs within the first 14 days. Thereafter, the improved clays continue to strengthen even after 28 days.

3.4.3 Stiffness Results

Most of the previously reported results were on the strength of improved clays, which is important in stability design. However, if ground movement is the key design consideration, then the stress-strain relation is more important. For soils, it is now

recognised that even at very small strain, the stress-strain behaviour is highly non-linear, but thus far, only Tatsuoka et al.'s study (1996) has specifically focused on this for an improved soil. The variation of stiffness with strain is vital as it can affect the design of the improved clays considerably.

Accurate determination of stiffness is never easy. Tatsuoka et al. (1996) had pointed out that measurement of deformation between end-platens, frequently used for soils and also improved soils usually underestimated the stiffness considerably. Clearly, the way strain is measured has an important bearing on the correlation of stiffness with the unconfined compressive strength, q_u. Published literatures yield an extremely wide range of values as summarised in Table 3.5.

(a) Non-linear Stress-strain Behaviour

In order to investigate the non-linear behaviour of cement treated clays, the sample is first loaded and unloaded in compression to about 30% of the ultimate strength. As shown in Figure 3.9, the cement treated clay is actually a non-linear and non-elastic material. A permanent deformation exists after removal of load. This behaviour has made the determination of stiffness complicated. For such case, two methods for stiffness determination are proposed and given as

$$\text{Tangent stiffness, } E_{tan} = \frac{\delta\sigma}{\delta\varepsilon} \tag{3.4}$$

$$\text{Secant stiffness, } E_{sec} = \frac{\Delta\sigma}{\Delta\varepsilon} \tag{3.5}$$

Like concrete, the cement treated clays behave as elastic material to a certain degree. The non-linearity in cement treated clays is mainly due to creep; consequently, the demarcation between the elastic and creep strain is difficult [Neville (1996)]. According to Neville, an arbitrary distinction can be made for practical purposes; the

deformation resulting from application of the design stress is considered elastic and the subsequent increase in strain under sustained loading is regarded as creep. In this way, the material can be defined as an elastic material, having stiffness based on the secant modulus, E_{sec}. This stiffness is normally measured at 50% of the ultimate strength and is notated as E_{sec50}.

(b) Stiffness at small strain

The variation of stiffness with strain for SAC clay is shown in Figure 3.10 by plotting the results in terms of E_{sec}/q_u versus log ε, where the strain (ε) was measured using the Hall's effect strain transducer. E_{sec} is the secant Young's modulus, while q_u is the unconfined compressive strength. The behaviour of the cement treated clay is clearly non-linear, with E_{sec}/q_u decreasing from about 1400 at 0.005% strain to less than 100 at 1% strain for improved clay with 30% of cement. The same behaviour is also observed for samples with lower cement content. It is therefore important to consider such non-linearity for the improved clays as in practical excavation, the strain induced in this layer is expected to be very small. However, it must be noted that the behaviour is more brittle and will fail at a smaller strain.

(c) Comparative stiffness between external and local strain measurement methods

Nowadays, it is recognised that the conventional method of measuring axial strain, derived from external displacement between loading piston or the specimen cap can cause serious errors due to bedding and other related errors involved [Tatsuoka and Shibuya (1992)]. This has resulted in the stiffness of soil measured in the laboratory to be much lower than that of the actual value. A comparison between the externally and locally measured strains is shown in Figure 3.3(a). The stiffness results using both

methods of strain measurements are correlated in Figure 3.11. From this plot, the external strain measurement was found to underestimate the stiffness by approximately 2.3 times.

(d) Effect of time (t)

The effect of time has been studied before, but the primary concern to structural engineers is the change in stiffness with time and the effect of this on the design bending moment of the diaphragm wall. Figure 3.12 shows the increase in stiffness normalised at 28 days. It is obvious that the improved clays continue to stiffen even after 28 days. This is an important observation, as excavation works usually will take many months, and often the more critical work is carried out at the later stages.

(e) Relationship between E_{sec50} and q_u

It is common practice to relate the Young's modulus (E) with the unconfined compression strength (q_u), so as to establish a correlation between the two parameters. The relation between E_{sec50} and q_u, based on conventional method of strain measurement, for the three improved Singapore marine clays is shown in Figure 3.13(a), where E_{sec50} is the secant Young's modulus at 50% of the ultimate strength. This shows that the all the data fall within the range of E_{sec50}=150 to 400q_u, similar to those reported by Asano et al. (1996) and Futaki et al. (1996). Figure 3.13(b) shows the relation between E_{sec50} and q_u, using local strain measurement by a Hall's effect transducer. The results now fall within the range of EH_{sec50}=300 to 800q_u, much higher than that from using the external strain measurements, and more in line with that observed by Kawasaki et al. (1984) and Tatsuoka et al. (1996), who used a similar method of measurement. These comparisons were presented previously in Table 3.5.

3.5 Concluding Remarks

The study reported in this chapter was carried out to establish the properties of cement mixed clays for a range of mixed proportion commonly associated with the Deep Cement Mixing (DCM) Method. More importantly, it forms the initial part of the study into understanding the behaviour of embedded improved soil layer in an excavation. Based on the experimental results, the following conclusions can be drawn:

-

a) When different marine clays are improved using cement mixing, the degree of improvement for each type of clay is different. Many physical and chemical factors contribute to this and it is difficult to isolate the effect of each factor. However, the results of this study show that using a normalisation approach, as given in Equation (3.2), the behaviour of these different improved clays gives a unified behaviour.
b) There are three key constituents in cement mixed soils, namely water, cement and soil. It is important to recognise that the interactions among these constituents do not always produce an obvious trend about the way the soil will improve. For example, when the water to cement ratio is fixed, decreasing the cement content gives rise to an increase in strength, an observation that is not intuitively obvious. The interactions among these constituents and their impact on strength improvement are summarised in Table 3.4.
c) Hardening of cement mixed clay is a time dependent process. Some empirical relationships have been proposed to relate the strength at 28 days with that at 1, 7 and 14 days.
d) The cement mixed clays are seen to behave non-linearly at very small strain, just like most of the soils. Thus, it is important to ensure that the correct strain measurement is made. Due to bedding errors, external strain measurement method (LVDT)

generally shows a softer behaviour as compared to local strain measurement method (Hall's effect transducer). This is known in testing of solid, but less so in soil testing, including stiff soil.

e) Correlation between stiffness and unconfined compression strength has been obtained, but this relationship is very much dependent on how the strain measurement is taken as concluded earlier. If the conventional method is used to measure the strain, the E_{sec50} falls within a range of 150 to $400q_u$. However, if the Hall's effect transducer is used, the EH_{sec50} falls within a range of 300 to $800q_u$, representing approximately an increase of 2.3 times.

Table 3.1 Properties of the Eunos, City Hall and Singapore Art Centre marine clays

Properties	Eunos	City Hall	Singapore Art Centre (SAC)
Specific Gravity	2.61	2.61	2.62
Natural Water Content (%)	66.23	61.52	57.62
Liquid Limit (%)	71.89	65.12	72.63
Plastic Limit (%)	31.89	30.03	30.82
Organic Content (%)	2.09	1.66	1.37
Chloride Content (%)	0.38	0.30	1.10
Sulphate Content (%)	1.70	1.60	0.92
PH	7.4	7.4	6.5

Table 3.2 Physical properties and chemical compositions of Portland Cement

Physical Properties	Value
Density	3140 ± 3 kg/m^3
Fineness	327 ± 2 m^2/kg
Chemical Composition	**Unit (% w/w)**
Silica, SiO_2	21.3 ± 0.2
Alumina, Al_2O_3	4.7 ± 0.2
Ferric Oxide, Fe_2O_3	3.1 ± 0.1
Calcium Oxide, CaO	64.4 ± 0.3
Magnesia, MgO	2.3 ± 0.1
Sulphur as SO_3	2.3 ± 0.1
Sodium as Na_2O	0.47 ± 0.1
Potassium as K_2O	0.63 ± 0.1
Loss at Ignition	0.7 ± 0.1
Insoluble Residue	0.1 ± 0.1

Table 3.3 Mix proportions and curing period prepared for testing of different clay types

Type of clays	Cement content (%)	Water content (%)	Curing (days)									
			1	3	7	14	28	70	77	140	154	161
Eunos	10	90	●	●	●	●	●	●		●	●	
	20	90	●	●	●	●	●	●			●	
	30	90	●	●	●	●	●	●			●	
	10	120			●	●	●					●
	20	120			●	●	●	⇨	**Eunos (20.120.28)**			●
	30	120			●	●	●					●
	10	150			●	●	●				●	
	20	150			●	●	●				●	
	30	150			●	●	●				●	
City Hall	10	90	●	●	●	●	●		●	●		
	20	90	●	●	●	●	●	●				
	30	90	●	●	●	●	●	●				
SAC	10	90	●		●	●	●			●		
	20	90	●		●	●	●					
	30	90	●		●	●	●					
	30	120	●		●	●	●					
	30	150	●		●	●	●					

Table 3.4 Influence of the three main constituents of mixture

Condition			W/S (water content)	W/C (water to cement	C/S (cement content)		q_u	Comments
(1)	S constant W constant	C↑	•	↓	↑	=	↑	Obvious
(2)	S constant C constant	W↓	↓	↓	•	=	↑	Obvious
(3)	W constant C constant	S↑	↓	•	↓	=	↑	Not obvious

• denotes value that is constant

Table 3.5 Relationships between E and q_u from different references

Reference	Relationship
Kawasaki et al. (1984)	EH_{sec50} ~ 350 to $1000q_u$
Tatsuoka et al. (1996)	EH_{max} ~ $1000q_u$
Futaki et al. (1996)	E_{sec50} ~ 100 to $250q_u$
Asano et al. (1996)	E_{sec50} ~ 140 to $500q_u$
Present Study - External Strain Transducer - Local Strain Transducer	E_{sec50} ~ 150 to $400q_u$ EH_{sec50} ~ 300 to $800q_u$

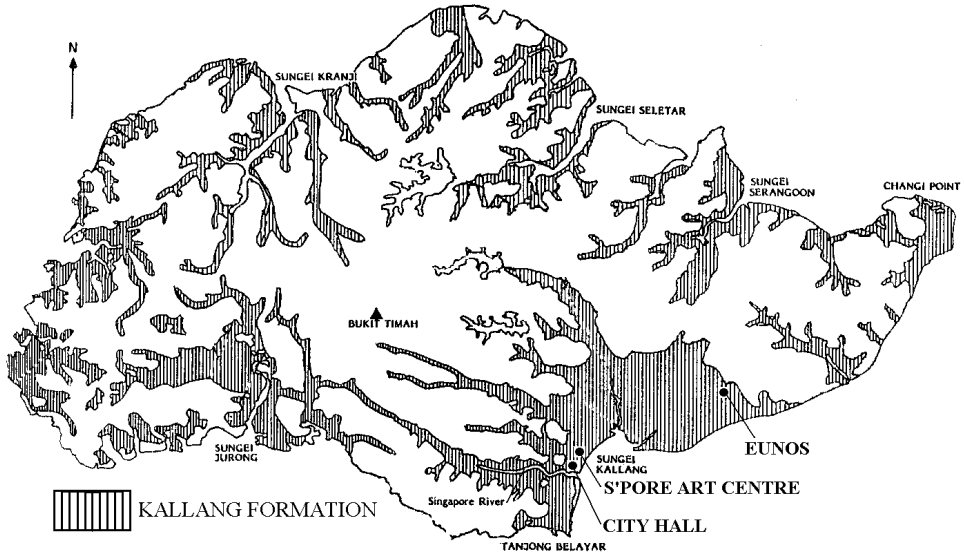

Figure 3.1 Kallang Formation of Singapore Island

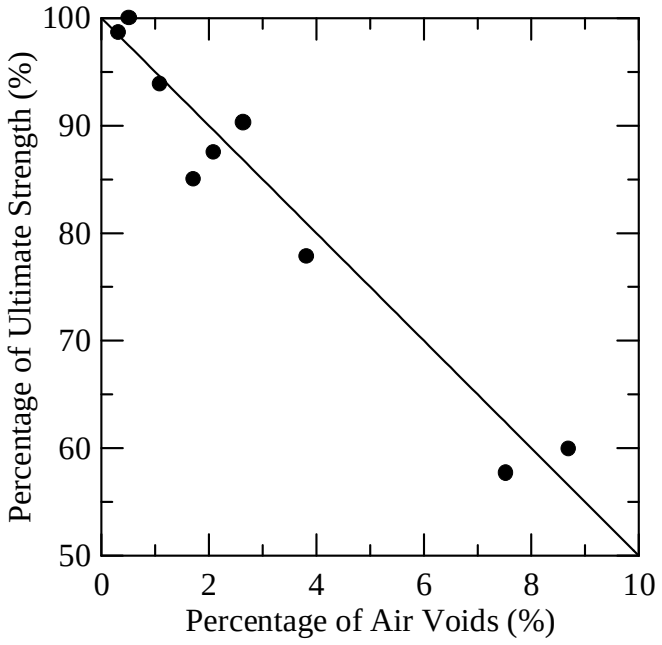

Figure 3.2 Effect of air voids on the strength of cement treated clay

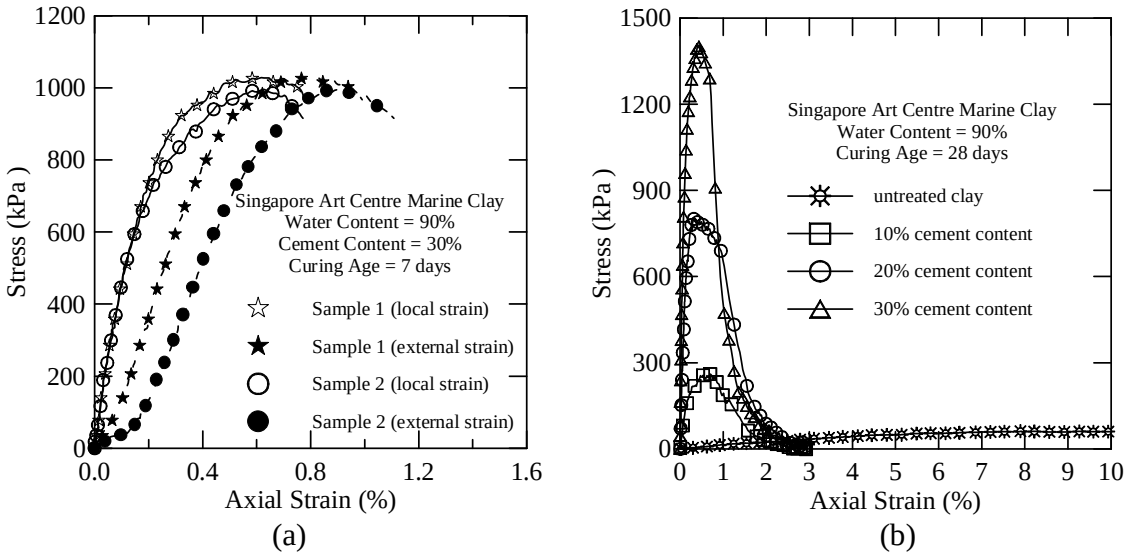

Figure 3.3 Typical stress strain curves of unconfined compression test

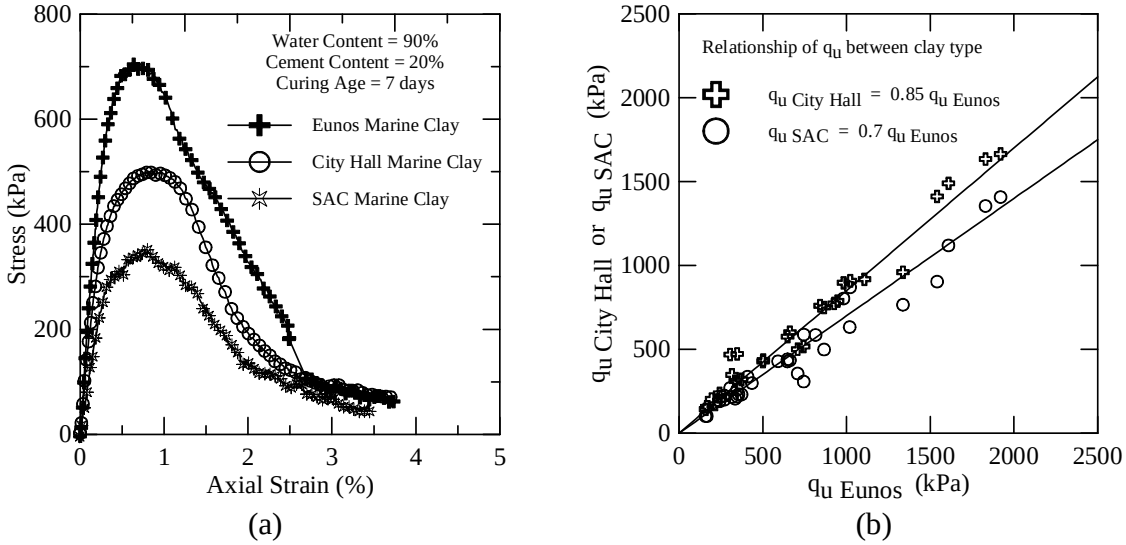

Figure 3.4 Effect of different types of Singapore marine clay improved by cement mixing

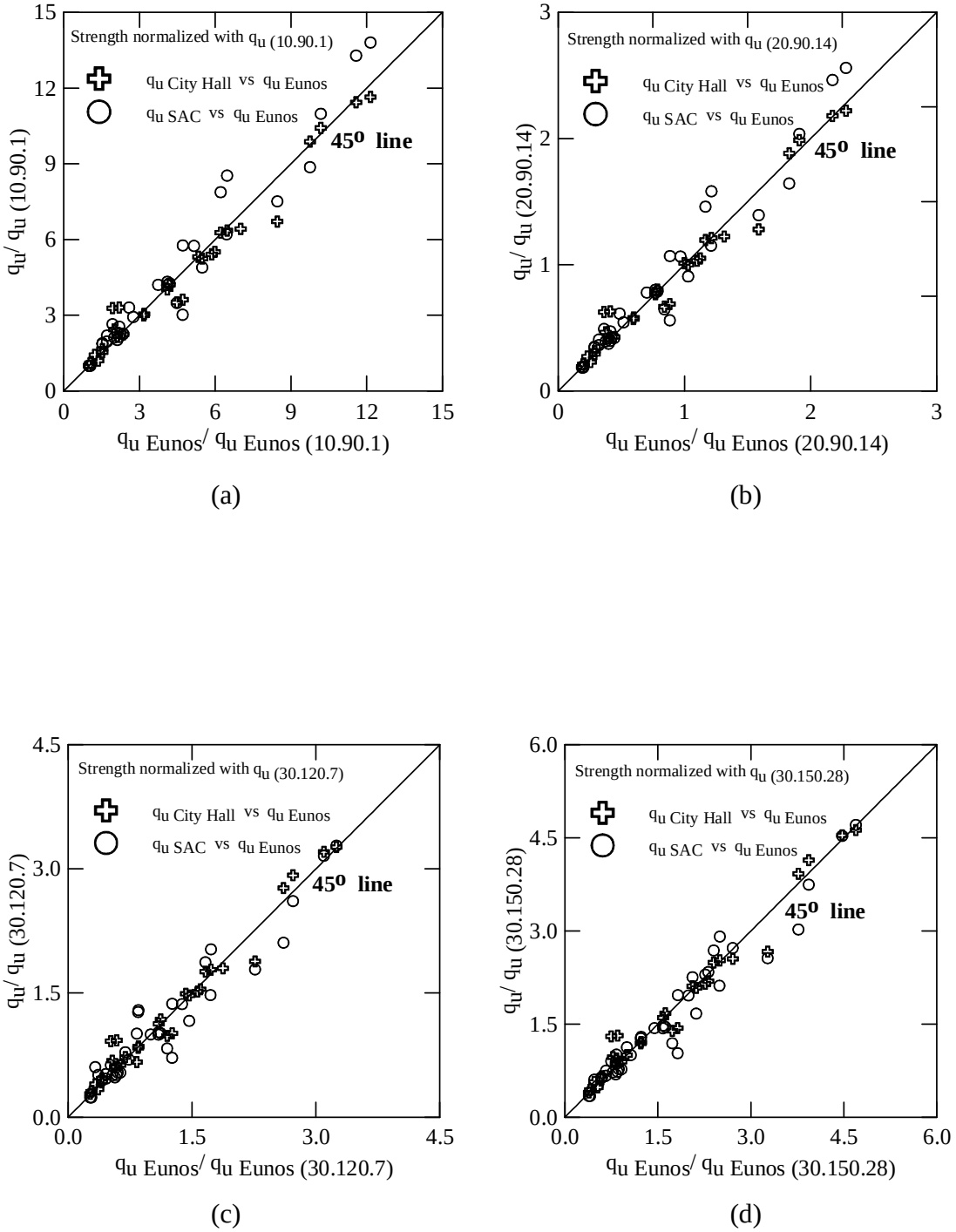

Figure 3.5 Relationship between normalised strength of Eunos, City Hall and SAC marine clay mixed with cement, normalised with
(a) q_u(10.90.1) (b) q_u(20.90.14) (c) q_u(30.120.7) (d) q_u(30.150.28)

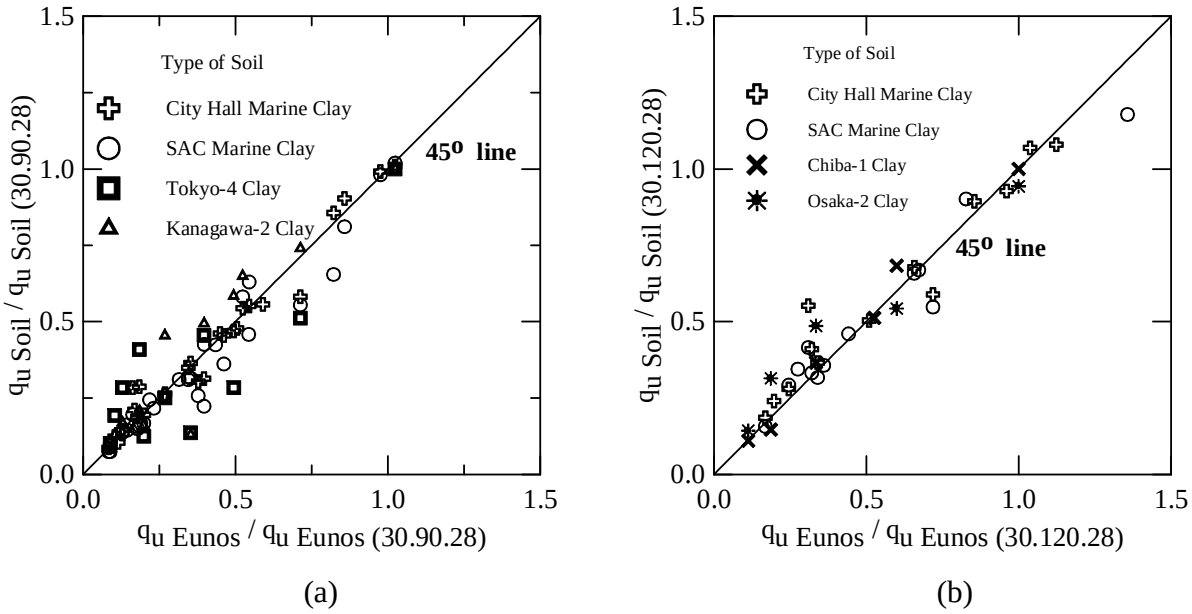

Figure 3.6 Relationship between normalised strength of Singapore and Japanese improved clays normalised with
(a) q_u(30.90.28) (b) q_u(30.120.28)

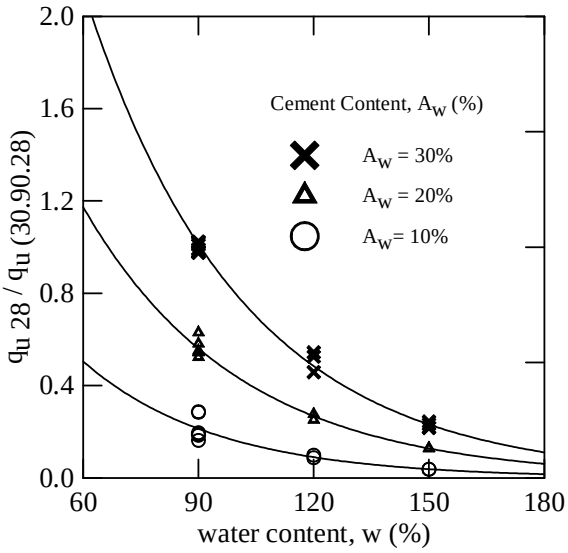

(a) Effect of water content

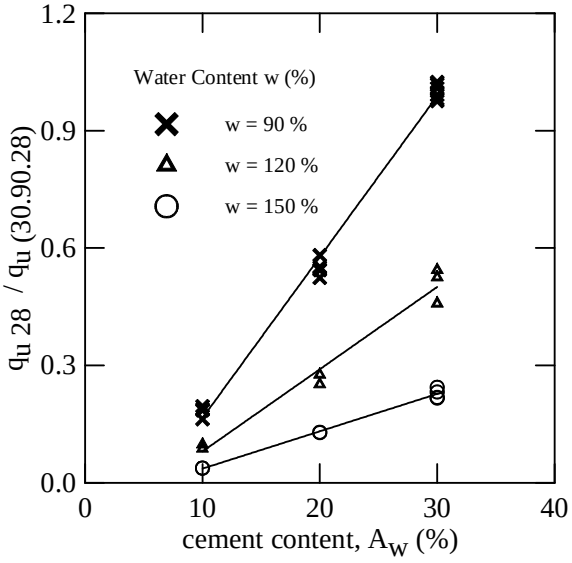

(b) Effect of cement content

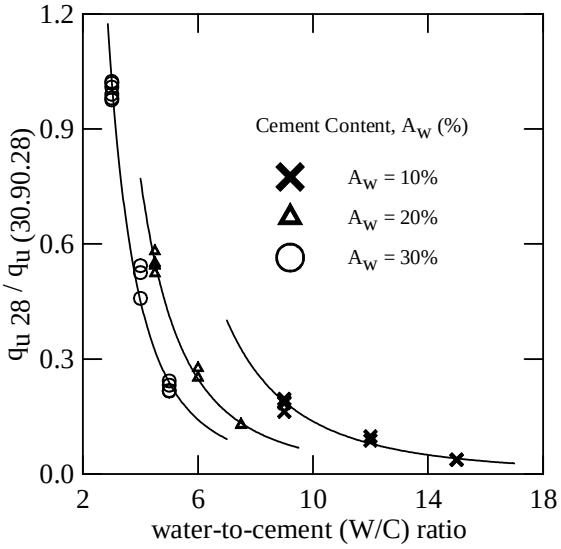

(c) Effect of water-cement-ratio, differentiated by cement content

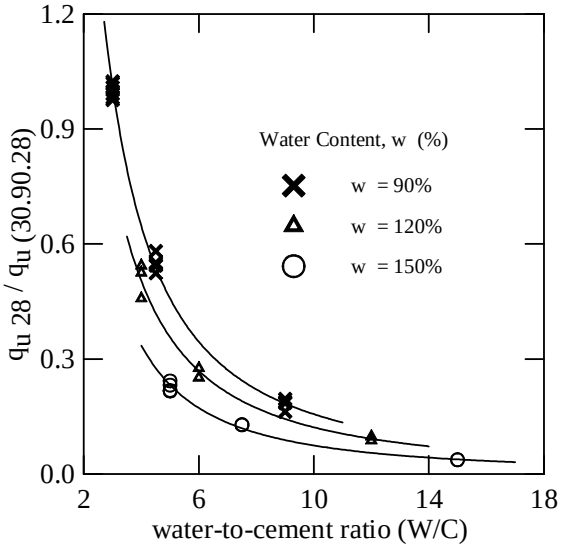

(d) Effect of water-cement-ratio, differentiated by water content

Figure 3.7 Effect of water and cement contents on the normalised strength of Singapore improved clays

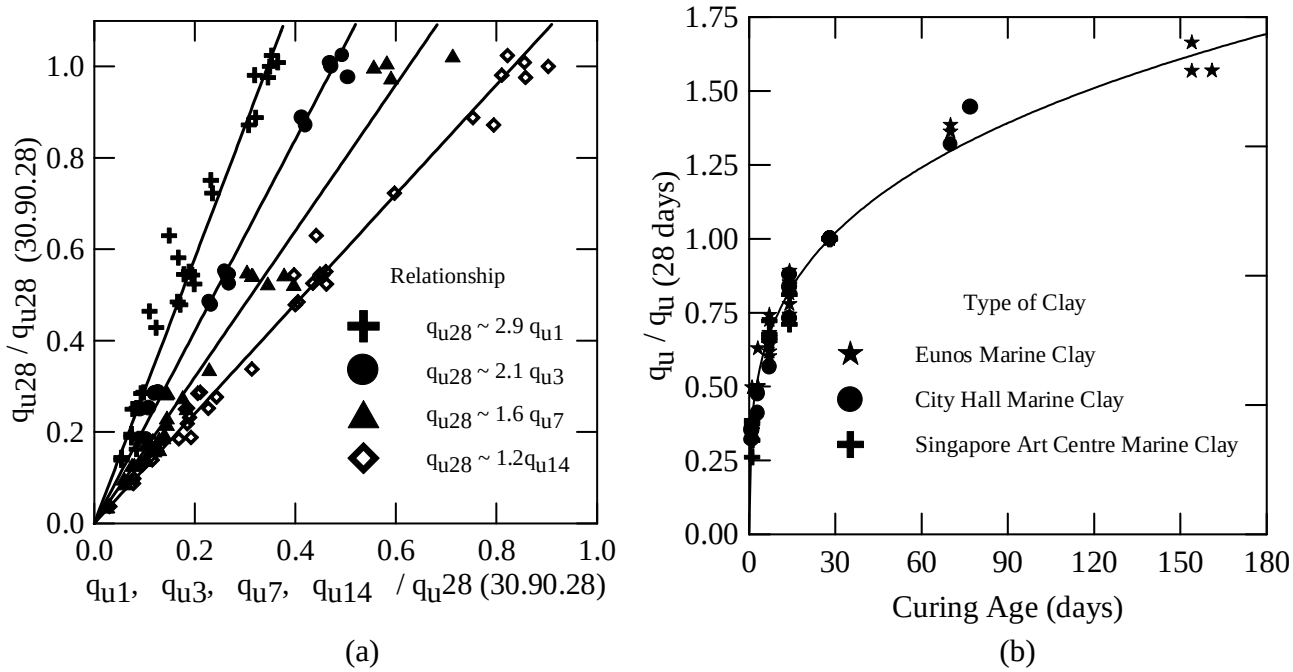

Figure 3.8 Strength relationship of Singapore improved clays

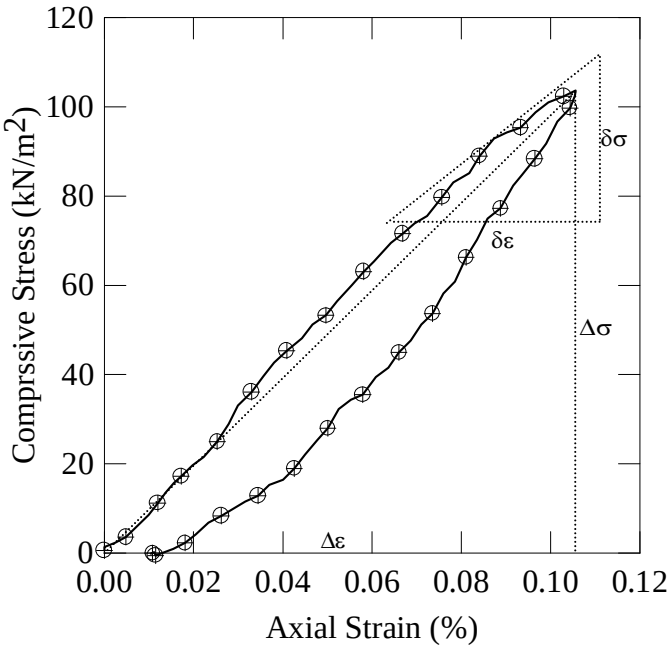

Figure 3.9 Non-linear and non-elastic stress strain behaviours of cement treated clay

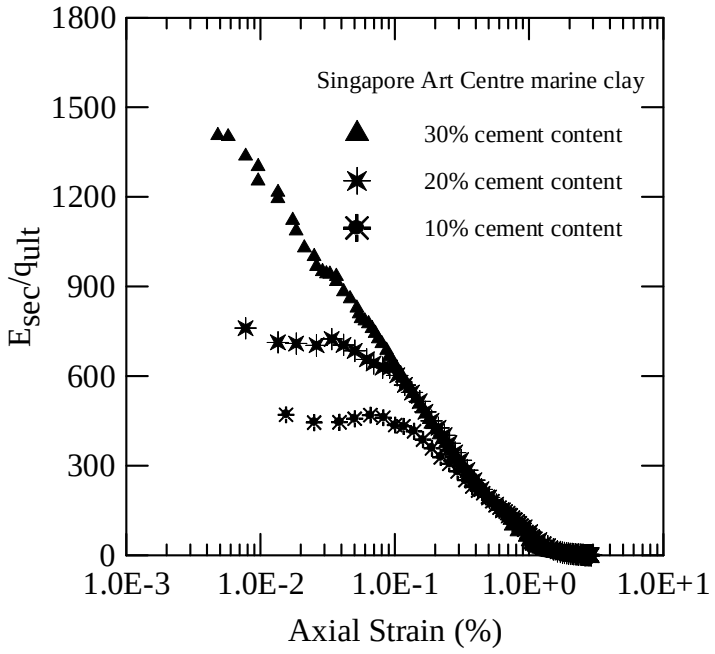

Figure 3.10 Variation of stiffness with strain

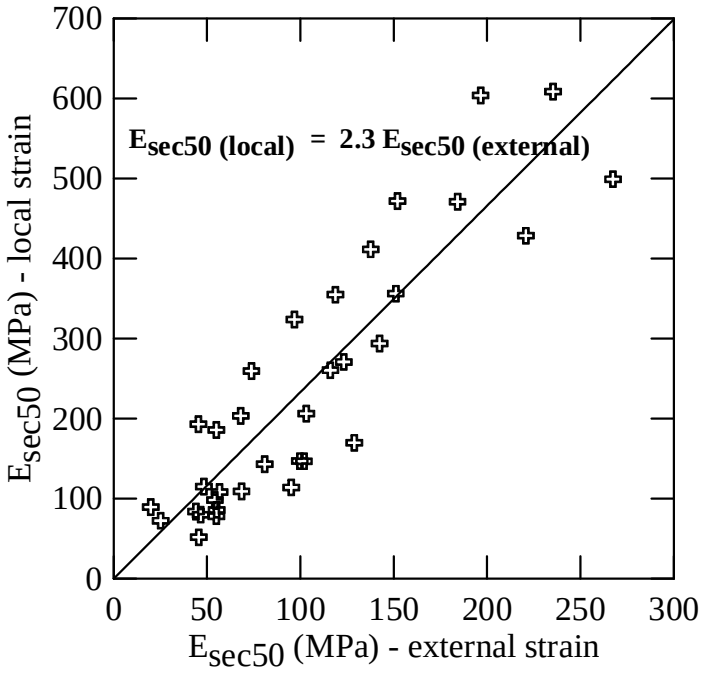

Figure 3.11 Comparative stiffness between external and local strain measurements

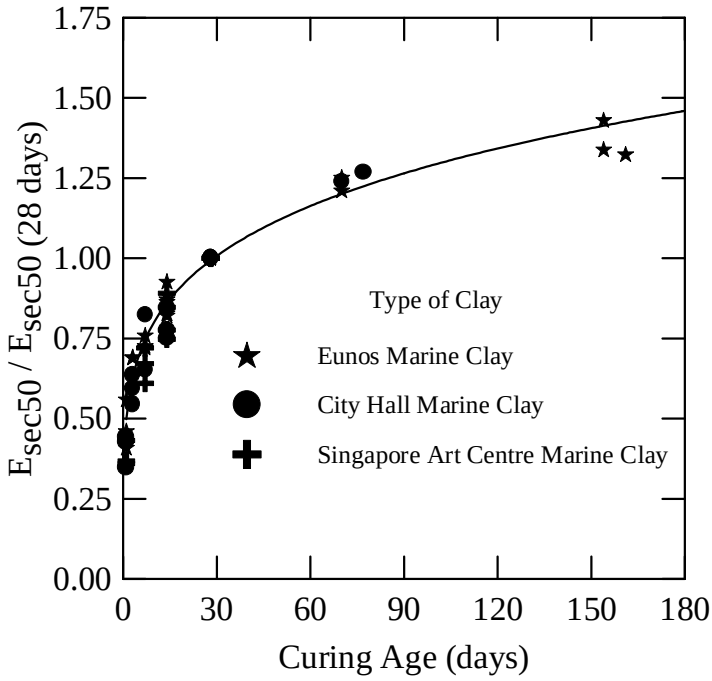

Figure 3.12 Stiffness development of Singapore cement treated clays

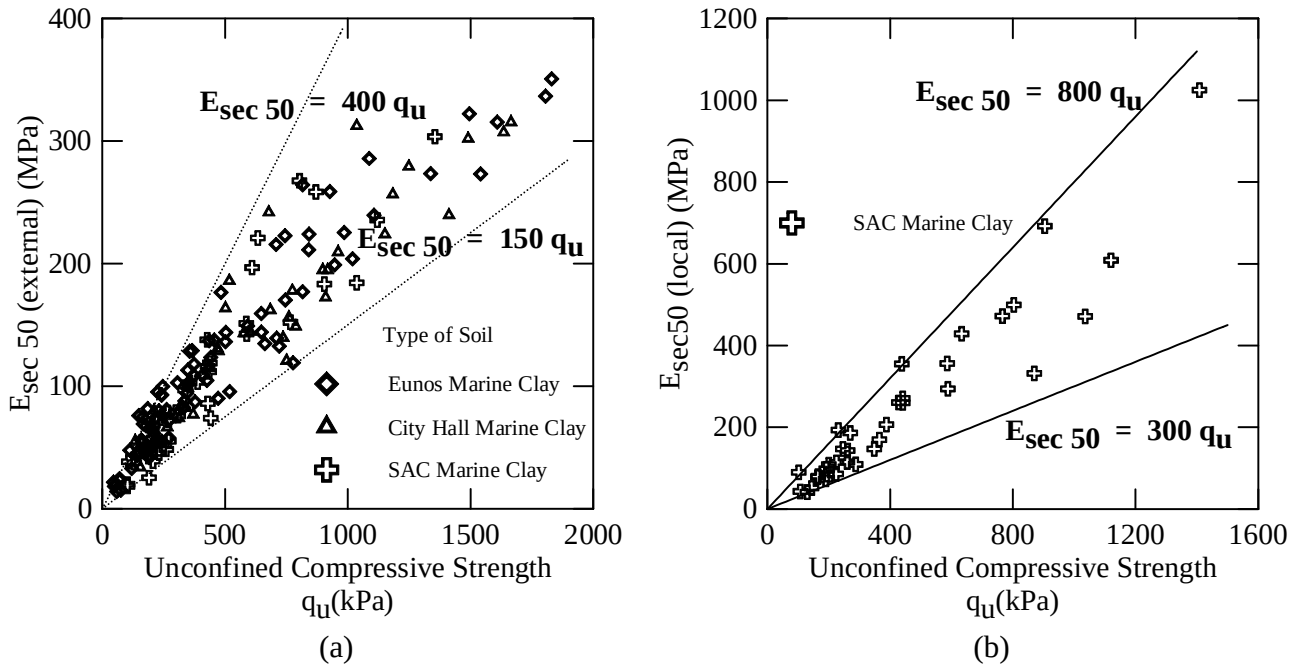

Figure 3.13 Correlation between E_{sec50} and q_u, derived using
(a) external strain measurement method
(b) local strain measurement method

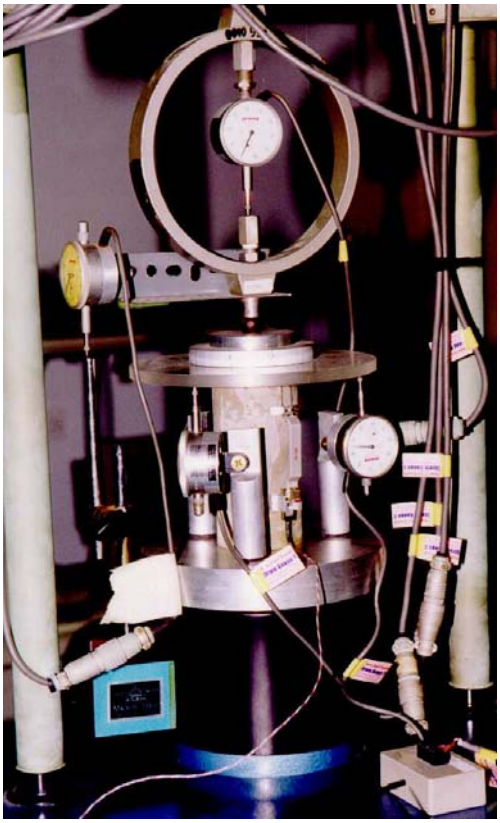

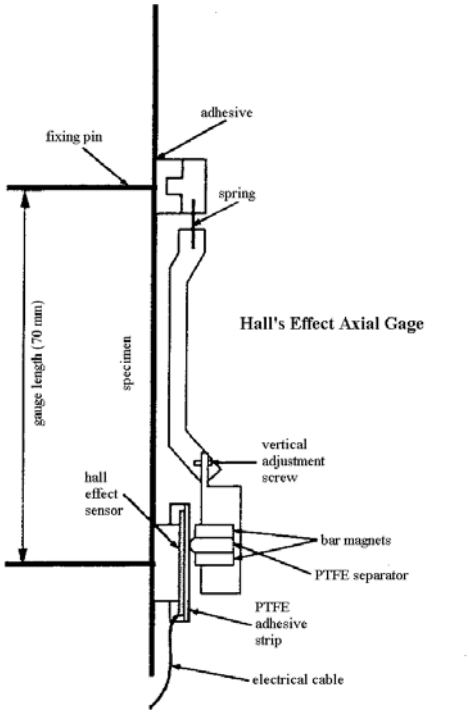

Plate 3.1 Apparatus for unconfined compression test with Hall's effect axial gage

Chapter 4

CENTRIFUGE MODEL TESTING

4.1 Introduction

Soil is a highly non-linear and stress dependent material. These characteristics have made it almost impossible for a small-scaled geotechnical model tested under 1-g condition to simulate the behaviour of a prototype. However, by subjecting the model to an appropriate gravity field, prototype stress levels can be simulated at geometrically similar points throughout the model and thus, prototype soil behaviours can be reproduced in the model. In other words, if a prototype is simulated by a $1/N^{th}$-scaled-model, the prototype soil behaviour can be replicated in a small-scaled model if the test is carried out under a gravitational field of N times the earth gravity.

The usage of centrifuge model testing has been rapidly increasing since 1970 [Schofield (1980), Craig et al. (1981), Craig (1984), Corte (1988), Ko and McLean (1991), Leung et al. (1994) and Kimura et al. (1998)]. The acceptance of its usefulness has contributed to the steady growth in the number of application, necessitating more development of centrifuge facilities to be carried out. The increase in its utilisation is mainly due to its practicality in setting out certain critical parameters such as the geological profile and material properties, which is unlikely to occur at two different locations in the field. Recent developments in data acquisition and signal processing technology have further improved the data processing technique, resulting in higher quality of centrifuge test results.

However, the major obstacle of using centrifuge is the unavailability of ready tools to simulate a particular geotechnical problem. Often, the development of specified equipment would take several years before the first successful centrifuge test results

could come in. The centrifuge technique applied in this present study is very much advanced which necessitated the fabrication of a sophisticated miniature in-flight excavator. This robotic in-flight excavator was designed to simulate the excavation process at 100G and moreover, it also allows the retaining wall to be propped at one specified level. This is an important advancement in centrifuge technology, as it would enable a supported excavation to be correctly modelled in the centrifuge environment. In particular, this improved in-flight excavator was developed in this study so that model excavation tests could be carried out to understand the behaviour of an excavation stabilised by an embedded improved soil layer. This modelling technique is believed to be the optimal way in making use of centrifuge technology in establishing a coherent understanding of the behaviour of the embedded improved soil layer during an excavation.

In this chapter, the development of the in-flight excavator, which involves the design and fabrication works are initially presented. Subsequently, procedures used to prepare the soil model with specific stress-state condition are described. Other supporting facilities such as the data acquisition system, the image processing, the instrumentation and monitoring are shown. It is the central focus to ensure that the simulation of an excavation is properly done in order to obtain consistent test results throughout the study. Critical comments are given during the reporting, which are of importance in this study.

4.2 The Development of An In-flight Excavator

4.2.1 The Importance of A New In-flight Excavator

Simplified methods to model an excavation process in centrifuge test which often involve artificial simulation techniques such as the “draining of a heavy liquid”

method have been found to be inadequate [Kimura et al. (1993), Loh et al. (1998)] for inappropriate soil condition especially in the normally consolidated clays. In order to have a proper simulation of an excavation that can generally be applicable to all soil conditions, the modelling of excavation in centrifuge must reflect the actual process of soil removal in the field. This has led to the development of a miniature in-flight excavator, which could perform an excavation during centrifuging, similarly like a prototype excavator in the field.

The first in-flight excavator has been developed at the Tokyo Institute of Technology, Japan [Kimura et al. (1993)]. Though the excavator has been successfully used to model different excavation tests, it was reported to be operating smoothly only until 50G, whereas, the original design was to provide the excavator with the ability to carry out excavation up to 100G [Kimura et al. (1993)]. The performance is reduced significantly by 50% from the initial design due to the drop in efficiency caused by the friction of worm gears and the resistance between soil retaining gate and wall of the model container. Stepping motors with higher capacity could not be used, as the set-up is very tight and does not have space for modification.

The major setback of that set-up is that the movement of cutting blade, which protruded from the moving table above, could not be extended very close to the retaining wall once the wall starts to incline inwards during excavation [Figure 2.17]. Hence, part of the soil in front of wall could not be excavated and this non-excavated soil would impose some additional passive resistance onto the retaining wall. Furthermore, this excavator could not physically accommodate a strut device since any propping device in the horizontal direction would obstruct the movement of the cutting blade. To simulate a braced excavation using such excavator, a 'tieback wall' system is used instead [Kimura et al. (1993)]. This could be done by having ties attached to the

back of retaining wall with load-measuring cells on them. Although this type of bracing is extremely useful, the system is only an approximation to the actual propping in field.

The methodology in propping a retaining wall has been developed earlier in the Cambridge University [Powrie et al. (1994)]. In this study, two struts were performed and each strut was supported with linear bearings at two locations through a Bosch pneumatic locking device outside the strongbox. This method of propping is extremely effective, but the level of propping has to be fixed at a stationary location. The conventional technique of "draining of a heavy liquid" method was used instead of an in-flight excavator due to the space constraint. This is acceptable since the excavation tests have performed in heavily over-consolidated clay. However, this method would not be acceptable if the excavation test was performed in normally consolidated clay due to the difference of K_o condition simulated by a heavy fluid as explained earlier.

Due to the above limitations, it is therefore necessary to develop a new in-flight excavator that could model a proper in-flight excavation and allows propping to be performed concurrently during centrifuging. The special features being incorporated into the new in-flight excavator are as follows: -

a) it could work easily under 100G-environment,
b) it could control scrapping of the soil at an accurate speed, and
c) it allows propping of retaining wall by introducing a strut device.

4.2.2 Outlines of the In-flight Excavator (Mark II) at NUS

The new in-flight excavator (MARK II) developed in this study is an extended version of the existing excavator (MARK I) [Loh et al. (1998)] at the National University of Singapore. Limitations have been identified from the existing excavator (MARK I) and substantial modifications were made to increase its overall capability.

Similar to the existing excavator [Figure 2.18], this new excavator set-up consists of a detachable lift-shaft and a strongbox container [Figure 4.1]. The strongbox container has a width of 150mm, length of 400mm and a depth of 480mm. The detachable lift-shaft has been dimensioned to allow for plane strain model container but larger container such as the one used for 3D-excavation test [Loh et al. (1998)] can also be fitted. This lift-shaft will be replaced by a detachable side-wall during the initial stage of consolidation.

Instead of having only two motors in MARK 1, an additional motor was installed in MARK II to facilitate the movement of strut. Dimensions of these motors were reduced significantly in order to create more space to house additional mechanical parts. An intermediate size servomotor (Motor 3) was mounted on top of the lift-shaft, which has a maximum torque capacity of 0.95Nm (S22HMNA, Pacific Scientific Motor). This servomotor was specially chosen as it has the capability to drive the shaft to a very high speed exceeding 10,000 rpm. This is about two times faster than the stepper motor used in the existing MARK I. More importantly, the torque reduction for this servomotor during high rotational speed (about 20% reduction at 5000 rpm) is less than that of a stepper-motor (about 80% torque reduction at similar speed). To further increase the torque capacity, a special harmonic drive with a gear ratio of 1:160 was mounted in front of the servomotor.

Two platforms (one for scrapping of soil, called the 'Scrapper Platform' and the other for propping of retaining wall, called the 'Strut Platform') were mounted inside the lift-shaft wall by 2 pairs of identical linear rail. The Scrapper Platform holds the cutting blade and a soil-retaining gate while a movable propping tool is rested on the Strut Platform. Each platform was specially machined to form a continuous solid section with many hollow blocks in it in order to reduce its self-weight and overall thickness. The

vertical movement of the cutting blade and soil-retaining gate has been synchronised in such a way that the top of the gate is always 1mm lower than the bottom edge of the cutting blade. In order to reduce the large holding torque caused by the weight of platforms on the servomotor (Motor 3), a counter weight system has been introduced [Figure 4.2]. With this system, approximately 80% of the weight could be countered and this has therefore significantly reduced the working torque required.

The horizontal movement of the cutting blade and strutting tool are each controlled by an intermediate size stepping motor with a maximum torque capacity of 5.68Nm (K31HRFH, Pacific Scientific Motor). To move the cutting blade, the stepper motor drives a ball-screw through timing belt. To move the strut device, a spear gear is connected to the motor shaft and another ball-screw. Commands to control the motors are sent via personal computers located in the remote control room through a pair of on-board drivers. Since the first day after full commissioning, this in-flight excavator has been operating smoothly at 100-G with its performance shown in Table 4.1.

4.3 The NUS Geotechnical Centrifuge

The NUS Geotechnical Centrifuge has been used throughout the physical modelling exercise carried out in this study [Plate 4.1]. This machine is a beam type centrifuge with a radius of 2m and a capacity of 40g-ton. The working area of the swinging platform measures 750mm x 700mm and the maximum allowable height of the package is 1187mm. Detailed description of the NUS Geotechnical Centrifuge are given in Lee et al. (1991) and Lee (1992).

4.4 Centrifuge Scaling Relations

The scaling relations between a small-scale model in the centrifuge and its

full-scale prototype can be derived either by dimensional analysis or consideration of the governing equations and system mechanics. A list of commonly used scaling relations is shown in Table 4.2 [Leung et al. (1991)]. The centrifuge model test results in the present study will be extrapolated to their prototype scale by appropriate scale factors shown in this table.

4.5 Experimental Set-up

4.5.1 Preparation Procedure of Soil Model

Preparation of soil model is one of the very basic but most important aspects in physical modelling in the centrifuge. Test results from centrifuge modelling are difficult to interpret unless the soil condition is carefully established. Therefore, utmost attention was taken during the preparation stage so that the initial soil condition is simulated correctly. The following shows the standard procedure used to obtain the soft ground condition of soil used for this study.

The preparation of model ground adopted here is to a large extent, similar to those of Kimura et al. (1993) and Loh et al. (1998). Kaolin clay is chosen instead of marine clay, principally due to the greater consistency achieved in the model ground and because of its high permeability ($k = 2 \times 10^{-8}$m/s), which allows a shorter consolidation time. This was decided after having several preliminary failures using marine clay after spinning continuously for 72 hours in achieving the degree of consolidation required.

The physical properties of kaolin used are shown in Table 4.3. Figure 4.3 illustrates its compressibility behaviour obtained from the oedometer tests. Before the soil model is prepared inside a centrifuge container, the clay was first soaked in de-aired water overnight, and then mixed uniformly in a rotating mixer with water content of approximately 1.5 times of its liquid limit. Subsequently, the clay slurry was de-aired in

a vacuum chamber for 1 day to evacuate air bubbles and to ensure that an almost saturated soil sample slurry is achieved [Plate 4.2]. Mixing of clay at greater water content was not performed due to the restriction of container height. However, de-airing of the soil sample slurry will ensure the consistency of the model ground prepared in each test.

Prior to pouring of slurry into the container, coarse sand was rained down into the container bottom and then compacted to form a 20mm thick of bottom drainage layer. Two layers of thin polyethylene sheets with a coating of grease in between the sheets were then wrapped around the walls. Khoo et al. (1994) has shown that this lubrication method is able to minimise the friction between concrete-sand, steel-sand and perspex-sand interfaces in 100G-centrifuge testing.

During the placement of clay slurry into the container, attention was paid to prevent the trapping of air pockets. The air pockets can be minimised if the clay slurry is transferred under a layer of water. A trowel was then used to level the surface of clay slurry, providing an even surface to ensure uniform loading. The clay was then loaded to a pressure of 20kPa at 1G-environment by a pneumatic compression machine. The consolidation load was applied stepwise to ensure that the clay slurry did not squeeze through the gap between the loading plate and container. A load cell was placed below the pneumatic piston to measure the load and to ensure that an accurate pressure was applied to the soil model at all time. The initial loading was applied by the self-weight of loading plate (1.7 kN/m^2), followed by pneumatic loading (3, 6, 10 and 20 kN/m^2). The clay was allowed to consolidate until at least 90% degree of consolidation is achieved at the final loading stage. Eventually, a normally consolidated soil with uniform consolidation pressure of 20kN/m^2 throughout the depth is obtained.

The model ground container was then transferred onto the centrifuge's swing platform for self-weight consolidation at 100G for several hours until more than 90% degree of consolidation was achieved. The model ground was spun down to 1G condition to allow the insertion of model retaining wall and improved soil layer, the installation of instruments and finally, attaching the in-flight excavator to the model container. Subsequently, the model was re-consolidated in the centrifuge again until more than 90% degree of consolidation has been achieved. This will ensure that an almost equilibrium stress state of soil model is obtained prior to excavation test.

To monitor the level of self-weight consolidation, several pore pressure transducers were inserted into the model ground besides having settlement transducers placed on the surface. Typical surface settlement reading and pore pressure responses during the first stage of consolidation and second stage of re-consolidation in centrifuge are shown in Figures 4.4 (a) and 4.4 (b) respectively. As shown in both figures, the degree of consolidation exceeded 90% for the two consolidation stages. Calculation of the degree of consolidation was based on the Hyperbolic method [Tan et al. (1971)] and being confirmed using the Asaoka procedure [Asaoka, (1974)].

4.5.2 Stress History of Model Ground

In this study, the intention was to prepare a soil model consisting of a normally consolidated (NC) soil with increasing strength profile and having a thin layer of over-consolidated (OC) layer on the top surface [Figure 4.5 (a)]. This type of ground profile is quite common in Singapore [Chang (1991)]. Confirmation tests have to be carried out initially to validate the actual characteristic of the soil model. Such related tests have to be performed at 1G-environment after completing the process of self-weight consolidation, as at the time of testing, in-flight profiling devices were not

available. These tests were carried out immediately after spin down from high G since the clay can swell with time, which will then change its properties [Mair (1979), Kimura and Saitoh (1982)].

The vane shear test was used to check the strength profile of the model ground [Plate 4.3]. As shown in Figure 4.5(b), it is obvious that the undrained shear strength of a typical model ground increased with depth, varying from 10 to 30 kN/m^2. The stress profile in the model ground is re-confirmed by checking the water content along its depth [Plate 4.4]. Water contents were then compared with those estimated based on oedometer test results [Figure 4.5 (c)]. It is obvious that both results have shown good agreement.

To further assess the quality of model preparation, an in-flight in-situ soil investigation tests were later undertaken by another doctoral student who is also using identical soil model for his test [Thanadol (2003)]. The in-flight miniature T-bar, developed by Stewart and Randolph (1991) was used to check the strength profile of the soil model in the 100G after the completion of consolidation. The undrained shear strength profile of the model ground obtained was compared using the SHANSEP (**S**tress **H**istory **A**nd **Normalise**d **S**oil **E**ngineering **P**roperties) method (Ladd and Foott, 1974). Thanadol (2003) reported in his research study using the same material for the model ground that the correlation obtained to estimate the undrained shear strength in a normally consolidated clay is consistent with that proposed by Ladd and Foott (1974) and Trak et al. (1980), which is given as follows: -

$$\frac{s_u}{\sigma'_v} = 0.22 \qquad (4.1)$$

4.5.3 Modelling of Retaining Wall

The retaining wall was modelled using a 4 mm thick aluminium alloy with an

equivalent stiffness (EI) of 384 x 10^3kNm^2/m in prototype scale [Plate 4.5]. The property of the aluminium alloy used is shown in Table 4.4. This wall stiffness could simulate a concrete diaphragm wall with a thickness of about 0.6m in the field. This is quite common as the thickness of diaphragm wall typically ranges from 0.6m to 1.2m.

Aluminium alloy is chosen as it is stiff but has a relatively low density. Such a light plate minimises the settling of the wall in soft ground during the self-weight consolidation stage. Rubber wiper with flips was used to prevent water from seeping through edges of the wall on both sides of the strong box [Plate 4.6]. The flips were lavishly greased to ensure that almost free sliding condition with negligible friction is produced. The wall was then installed at a depth of 160mm (equivalent to 16m in prototype scale) into the original ground level. A set of vertical guide was used during the wall insertion to ensure the verticality of the retaining wall.

4.5.4 Modelling of Improved Soil Layer

The improved soil layer was prepared under similar condition as described in Chapter 3. A wooden framework had been used to mould the cement treated clay into the required shape and size. Two additional cylindrical samples were also prepared during the same batch. The samples were then tested to determine its stress strain behaviour. To install the improved soil layer, the soil in front of the excavation side was first removed from the model ground while the retaining wall is held vertical by the guide. The improved soil layer was then installed into the model ground and thereafter, the appropriate block of pre-cut soil was inserted back into the model ground again [Figure 4.6]. The improved soil layer was inserted at 80mm (equivalent to 8m in prototype scale) below the ground level in front of the retaining wall.

4.5.5 Instrumentation and Monitoring

In this study, four different types of miniature transducers were used; namely the potentiometer, strain gage, pore pressure transducer and total stress cell. The locations of these miniature transducers are shown in Figure 4.7. Prior to installation of model retaining wall, miniature total stress cells (Model: Entran – EPL Series) and strain gages (Model: Kyowa – KFG Series) were placed on the wall. Pore pressure transducers (Model: Druck – PCDR81 Series) were then inserted into the model ground around the retaining wall. Finally, several potentiometers (Model: Sakae – FLP Series) were assembled vertically on the ground settlements and horizontally on the wall. The frequency of monitoring of all instruments is set to 1 second per sampling.

4.5.6 Excavation Test Procedure

Since the clay had swelled during the installation process in the 1G-environment, each time, the model was re-consolidated back to the original normally consolidated soil condition. Then, the excavation test was started. The sequence in carrying out an excavation was pre-programmed and controlled from the remote control room. When the excavation stage began, the servomotor at the top was first activated, moving the cutting blade, strutting tool and soil retaining gate downwards. This movement was terminated as soon as the cutting blade penetrated into the soil. Stepper motor 1 at the scrapper platform would then be activated, allowing the cutting blade to pull and scrap a small portion of soil horizontally into the base of lift-shaft, simulating an excavated layer of soil. The scrapper platform was then moved up again till a level slightly higher than the excavated level. Subsequently, the cutting blade was extended out to a point near to the model retaining wall. This sequence is then repeated until the required excavation depth is reached [Figure 4.8].

To allow propping of the strut device, stepper motor 2 at the strut platform was activated to move the propping device horizontally towards the wall. This movement would be terminated once it touched the retaining wall. To model a braced excavation, the sequences of scrapping and propping were synchronised. Initially, the scrapping and propping devices moved together. Once the wall was propped, the propping device was de-coupled from the scrapping device and the sequence of scrapping was allowed to continue until the final excavation depth [Plate 4.7]. For the current test, every sequence of scrapping will remove a 5mm layer of soil at 50 seconds, which is equivalent to the removal of 0.5m thickness of soil in about 6 days in prototype scale, which is quite realistic in the field for large excavation.

4.5.7 Data Acquisition System

All the analogue output signals from the transducers were transmitted by cables via electrical slip rings to the control room. The analogue signals were low-pass filtered and subsequently, amplified for better resolution. These signals were then sent into the acquisition system in which they were converted into a 12-bit digital format by Microstar A/D converter, running under the Dasylab software environment [Plate 4.8]. In this software, the digital signals were smoothened by the block averaging facility. A real time display of the selected incoming signals could be viewed on the computer screen before it was finally stored in the hard disk. Conversion to the engineering unit according to the respective calibration factor was done after each test.

4.5.8 Image Processing

Bits and grid lines were placed on the surface of the ground in front of the perspex plate prior to excavation test. Close circuit TV (CCTV) camera, which was also

mounted in front of the perspex plate captured the deformation of the model ground by dictating the movement of the bits and gridlines during the excavation test. Plate 4.9 shows the bits and gridlines of a model ground prior to excavation. A video cassette recorder (VCR) was used to record the entire excavation process [Plate 4.10]. The images were then played back from the recorded tape and digitised by a frame grabber board installed on the computer. The image processing software, Global Lab was used to sharpen the images before the vectors of movement were analysed. This software has facilities such as image enhancement, morphological filtering, intensity analysis and other operations, which produces a better image. The movement of each point on the surface of the model ground can be detected by superimposing the images at different stages of the excavation test. The distance travelled between two points can be calculated from the vectors of the movement based on the calibrated pixels.

4.6 Excavation Tests Programme

The entire centrifuge model excavation tests that have been performed for this study are summarised in Figure 4.9. All the model excavation tests were conducted at 100 G, corresponding to a linear scale factor of N = 100.

4.6.1 Preliminary Model Excavation Tests

In the initial stage, preliminary model excavation tests were carried out by using the “draining of a heavy liquid” method to simulate the excavation process since an in-flight excavator was unavailable to the author. For the first model excavation test, the soil used was marine clay. As this marine clay has a low permeability of 2×10^{-10} m/s, the process of consolidation is extremely long. For the preparation of a normally consolidated soil model with increasing strength profile, approximately 5-6 days of

continuing self-weight centrifuging is needed. Hence, it was found unrealistic to prepare this kind of soil model in order to achieve a high degree of consolidation in the centrifuge.

A normally consolidated soil model with constant strength profile was prepared in the laboratory floor instead. To prepare the model ground with such stress history, the soil was initially compressed by a pneumatic jack to a pressure of 80kPa until at least 90% degree of consolidation has taken place. Upon releasing the load, part of the soil in front of the retaining wall was quickly cut and replaced with a rubber bag. This bag was subsequently filled with a liquid (zinc chloride) of identical unit weight of the excavated soil. The soil model was spun quickly to 100g and the simulation of excavation was performed immediately. Nevertheless, this model test failed to provide realistic results due to the following reasons: -

(a) The swelling effect of soil occurred immediately after the release of load. Though the swelling of marine clay was low, the effect became important when the time for the preparation of model ground was long. As the swelling effect altered the stresses in the soil, it became extremely difficult to know the true soil condition.

(b) The effect of self–weight consolidation during the swinging up process to 100 G could not be neglected. As the whole process of swinging up, which includes the time required for performing the excavation test could take more than an hour to complete, the effect of self-weight consolidation of soil could not be ignored. This caused further confusion to the stress state of soil.

As the effect of swelling and self-weight consolidation occurred simultaneously, the soil model could not reach the state of equilibrium before the excavation test begun. Therefore, this preliminary model test was discarded to avoid inconsistent data and wrong interpretation. The marine clay was then replaced with kaolin clay, which has a

higher permeability (2 x 10^{-8} m/s). Normally consolidated clay with increasing strength profile was prepared and the process of self-weight consolidation could be accomplished within a shorter duration of about 8-10 hours.

Nevertheless, several problems were encountered when using the "draining of a heavy liquid" method to simulate the excavation process of a normally consolidated soil model. Besides the K_o deficiency, which causes the wall to move backward during centrifuging, other problems encountered are: -

(a) the original level of ground surface could not coincide with the level of heavy liquid. This is simply because the heavy liquid does not behave like a clay undergoing consolidation.

(b) the interaction between the improved soil and surrounding soil could not be simulated accurately. When the rubber bag replaced the pre-excavated soil, the friction property between the improved soil layer and surrounding soil is significantly altered. This is crucial, as the effectiveness of improved soil is much dependent on the interaction between the improved soil layer and soil above it.

Although both preliminary model tests have not produced realistic results for this study, they have assisted in the design of the final experimental set-up used in this study. As described in the above evaluation, the "draining of a heavy liquid" method is not suitable for normally consolidated clay. Therefore, excavations in subsequent tests were carried out by the in-flight excavator, which was available later, and this was described earlier in section 4.2.

4.6.2 Model Excavation Tests

The excavation tests programme is subdivided into 4 distinct categories, depending on the configuration of soil treatment and they are generally referred to as

'NTreat', 'FTreat', 'Gap' and 'Berm' [Figure 4.10]. All these model excavation tests were prepared in accordance to the procedure described earlier and hence, all the soil models, retaining walls and improved soils would have identical properties (unless otherwise stated) to allow direct comparison to be made.

The first model excavation test was 'NTreat', which was carried out initially to evaluate the behaviour of an unsupported excavation in soft ground. No soil improvement was done and this untreated model excavation test is a benchmark test for comparison with other model excavation tests involving soil improvements, which were subsequently carried out.

The second model excavation test was 'FTreat-7d', which was to investigate the effect of fully improved soil layer in an excavation. The entire soil layer in front of the retaining wall at 80mm (equivalent to 8m in prototype) below the ground level was replaced by a 20mm block (equivalent to 2m in prototype) of $SAC_{30.90.7}$ improved soil (please refer to Chapter 3 on the properties of $SAC_{30.90.7}$ improved soil). Both ends of the improved soil layer were in contact with the retaining wall in front and the wall gate of excavator's lift-shaft behind. To evaluate the behaviour of the improved soil layer in a braced excavation condition, the excavation test was then repeated with allowance for one strut to be installed at the ground level after 3m of excavation. This test was called 'FTreat-7d-Strut'. The subsequent test, referred to as 'FTreat-28d', would involve investigating the effect of stiffness increase in the improved soil layer due to a longer curing age.

Taking into consideration on the effectiveness of full-improved soil layer behaving like a strut, subsequent model excavation tests would involve the study on the effect of having a small gap of untreated soil in between the improved soil layer and the wall. Two model excavation tests with varying widths of gap were conducted;

‘Gap-800-7d’ with 8mm gap (equivalent to 800mm gap in prototype) and ‘Gap-400-7d’ with 4mm gap. Both improved soil layers have identical properties of the $SAC_{30.90.7}$, which had been previously used in Test ‘FTreat-7d’. The geometry and arrangement of the improved soil layer in both model tests were almost similar to model excavation test ‘FTreat-7d’, except for the fact that the front edge has a gap via untreated soil in between the improved soil layer and retaining wall.

Model excavation test involving improved soil berm was finally performed. This is to evaluate the effectiveness of improved soil berm in an excavation where only a part of the soil in front of the retaining wall was treated. This would further mean that the length of the improved soil layer was shortened and part of the clay behind the improved soil berm was left untreated. However, no gap was left in between the front end of the improved soil and retaining wall. The back edge of the improved soil layer is therefore not restrained by any rigid structure and it is left floated on the surrounding soft clay. To assess the effect of stiffness of improved soil berm, results from two model excavation tests were compared; ‘Berm-7d’ and ‘Berm-6m’ where these excavation tests were carried out with improved soil berms of increase in stiffness due to longer curing age.

Table 4.1 Performance of In-flight Excavator (MARK II) at NUS

Moving Parts Of Excavator	Effective Stroke	Maximum Speed	Minimum Speed	Accuracy Of Disp.	Accel.
Vertical Lift-shaft	150mm	2.0mm/sec	0.1mm/sec	±0.001mm	100g
Cutting Blade	150mm	50mm/sec	0.01mm/sec	±0.1mm	100g
Strutting Tool	30mm	5mm/sec	0.01mm/sec	±0.01mm	100g

Table 4.2 Scaling Relation of Centrifuge Modelling [after Leung et al. (1991)]

Parameter	**Prototype**	**Model at Ng**
Linear dimension	1	1/N
Area	1	$1/N^2$
Volume	1	$1/N^3$
Density	1	1
Mass	1	$1/N^3$
Acceleration	1	1/N
Velocity	1	1
Displacement	1	1/N
Strain	1	1
Energy	1	$1/N^3$
Stress	1	1
Force	1	$1/N^2$
Time (viscous flow)	1	1
Time (dynamics)	1	1/N
Time (seepage)	1	$1/N^2$
Energy density	1	1
Flexural rigidity	1	$1/N^4$
Axial rigidity	1	$1/N^2$
Bending Moment	1	$1/N^3$

Table 4.3 Physical properties of kaolin clay

Properties	**Sample 1**	**Sample 2**
Compression Index (C_c)	0.604	0.520
Swelling Index (C_s)	0.1238	0.1197
Bulk Density (γ_{bulk}), kN/m^3	16.39	
Permeability (k), m/s	2.0 x 10^{-8}	
Specific Gravity (G_s)	2.60	
Liquid Limit (w_L), %	79.8	
Plastic Limit (w_P), %	35.1	

Table 4.4 Properties of the aluminum alloy

Properties	**Value**
Modulus of Elasticity (E_o), kPa	72 x 10^6
Ultimate Strength (C), kPa	275 x 10^3

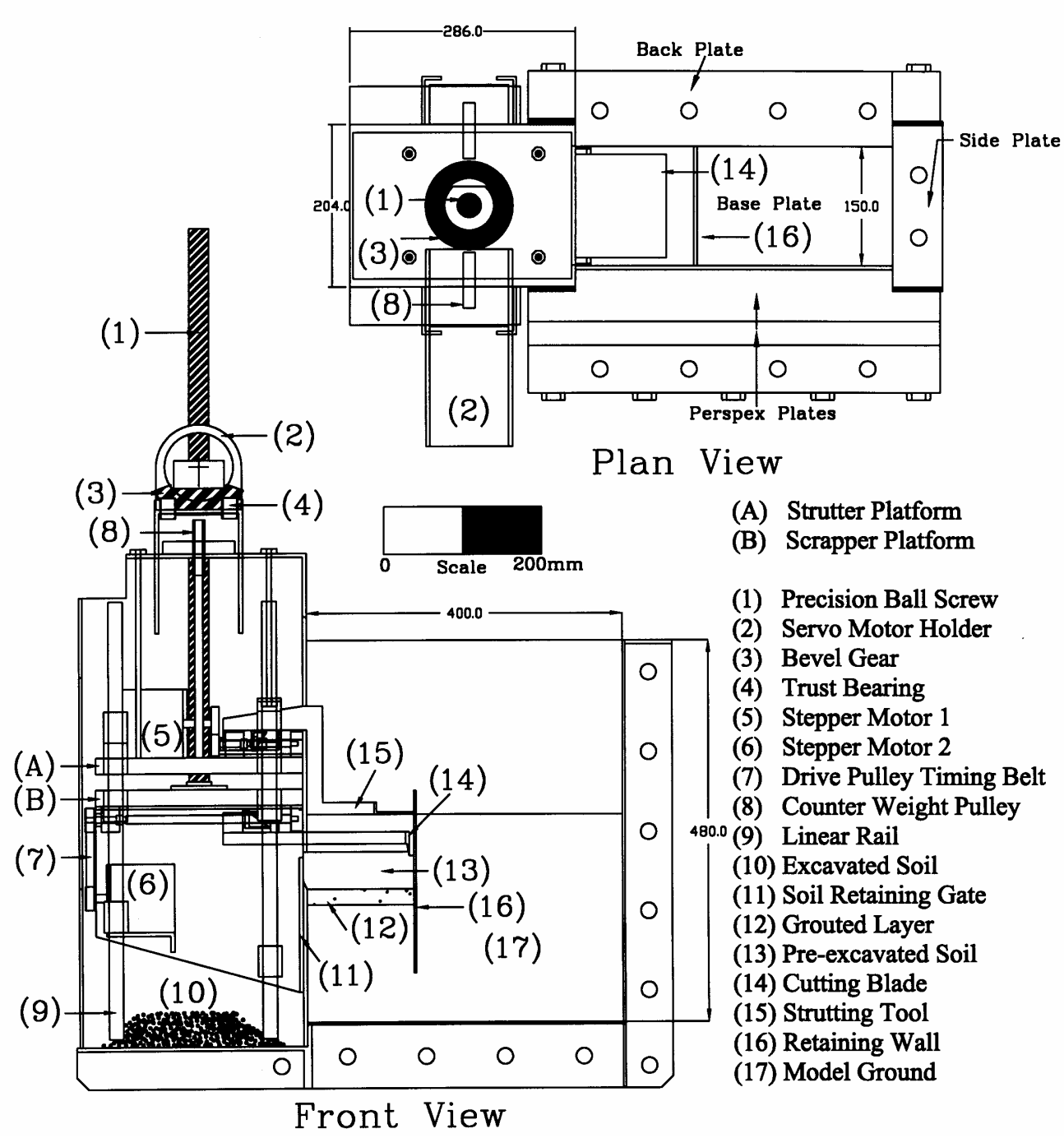

Figure 4.1 In-flight Excavator (MARK II) at NUS

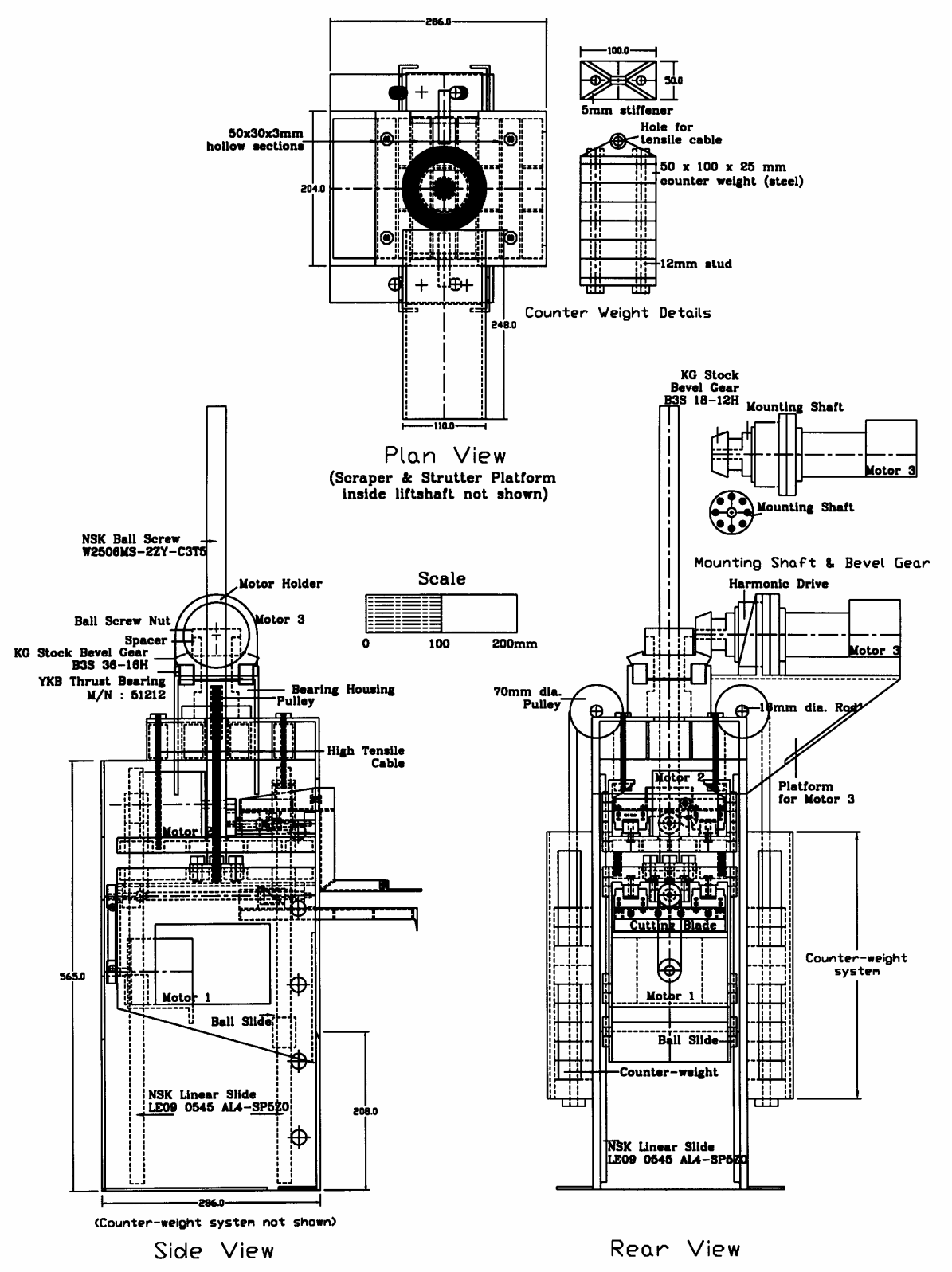

Figure 4.2 Mechanical Details of In-flight Excavator (MARK II) at the NUS

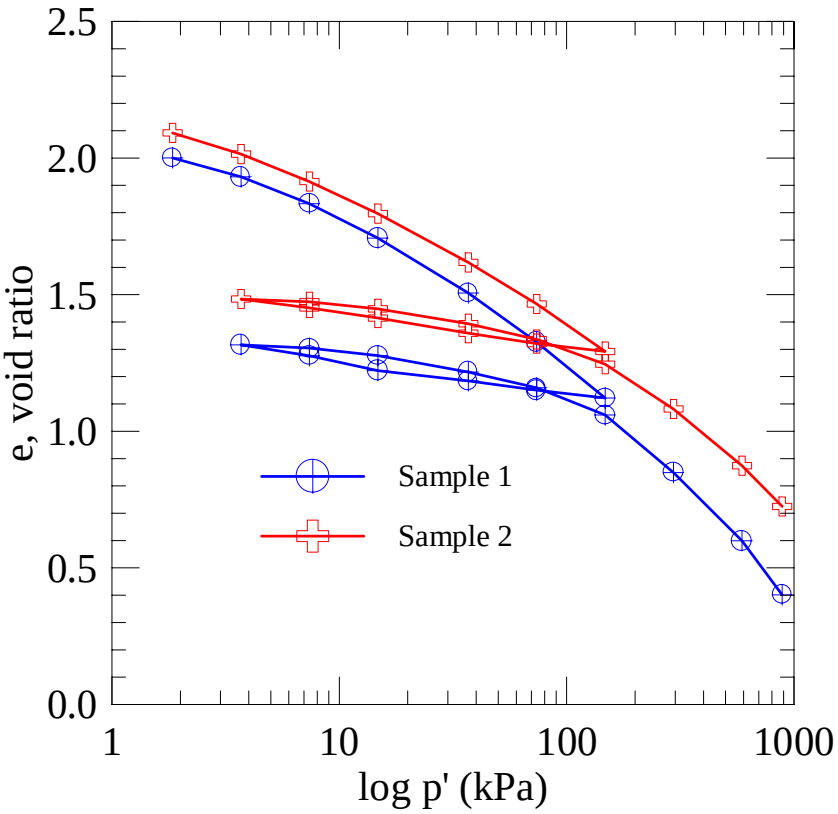

Figure 4.3 e-log p’ of kaolin clay from oedometer test

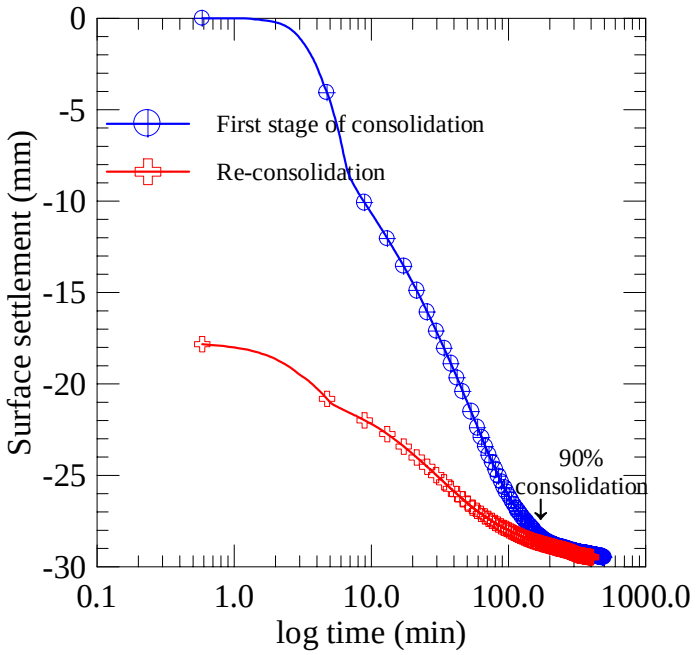

Figure 4.4 (a) Typical settlement results of model ground during consolidation

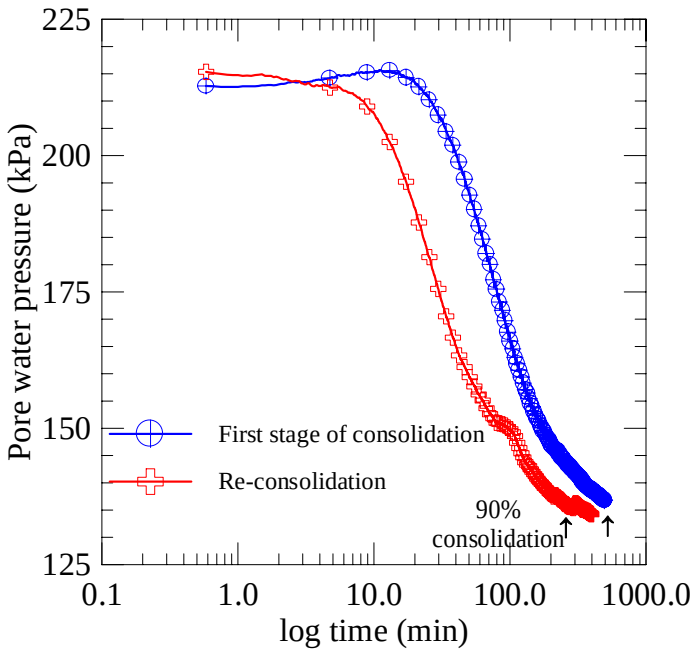

Figure 4.4 (b) Typical pore water pressure results of model ground during consolidation

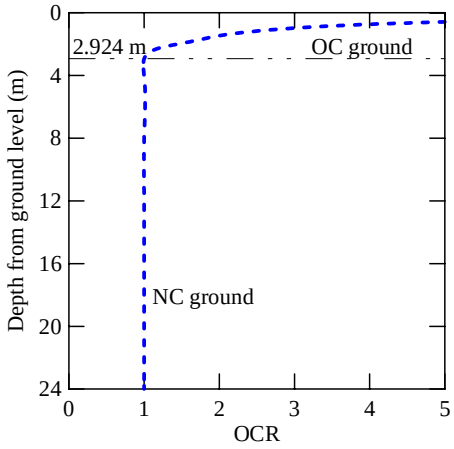

(a)

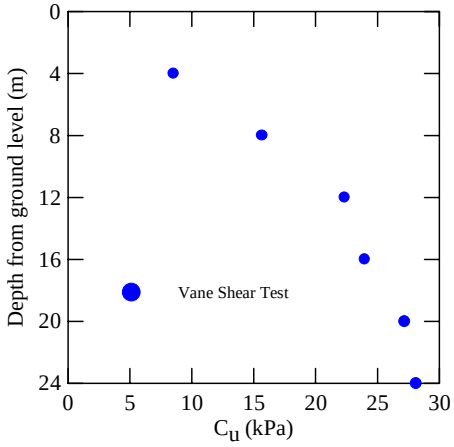

(b)

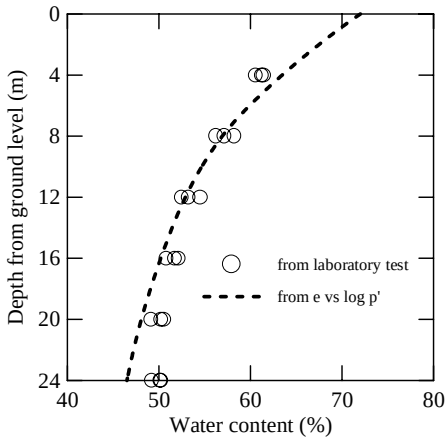

(c)

Figure 4.5 Profiles of OCR, undrained shear strength and water content of model ground

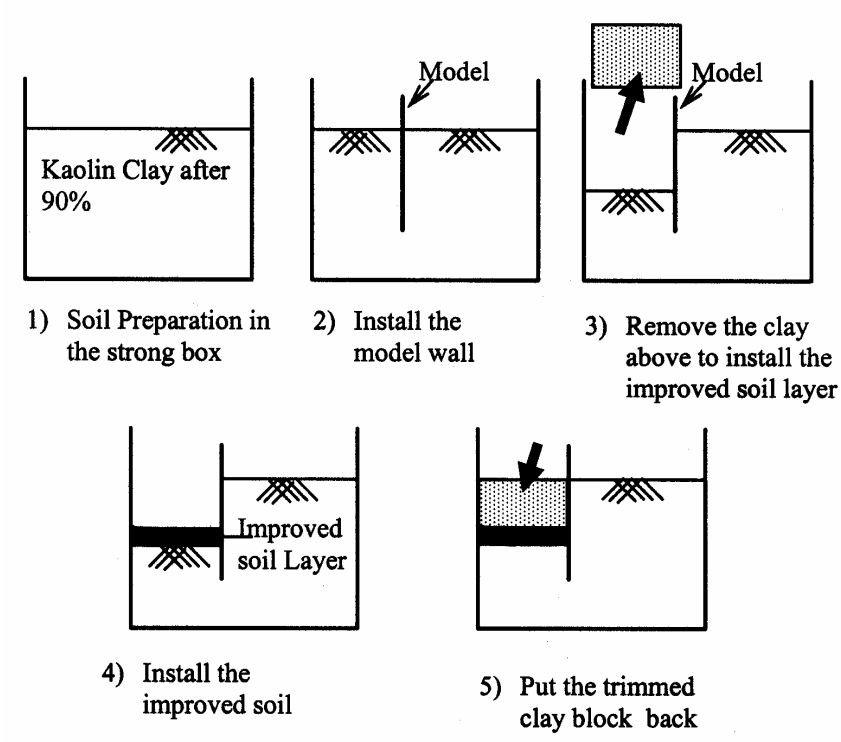

Figure 4.6 Schematic diagram of model preparation

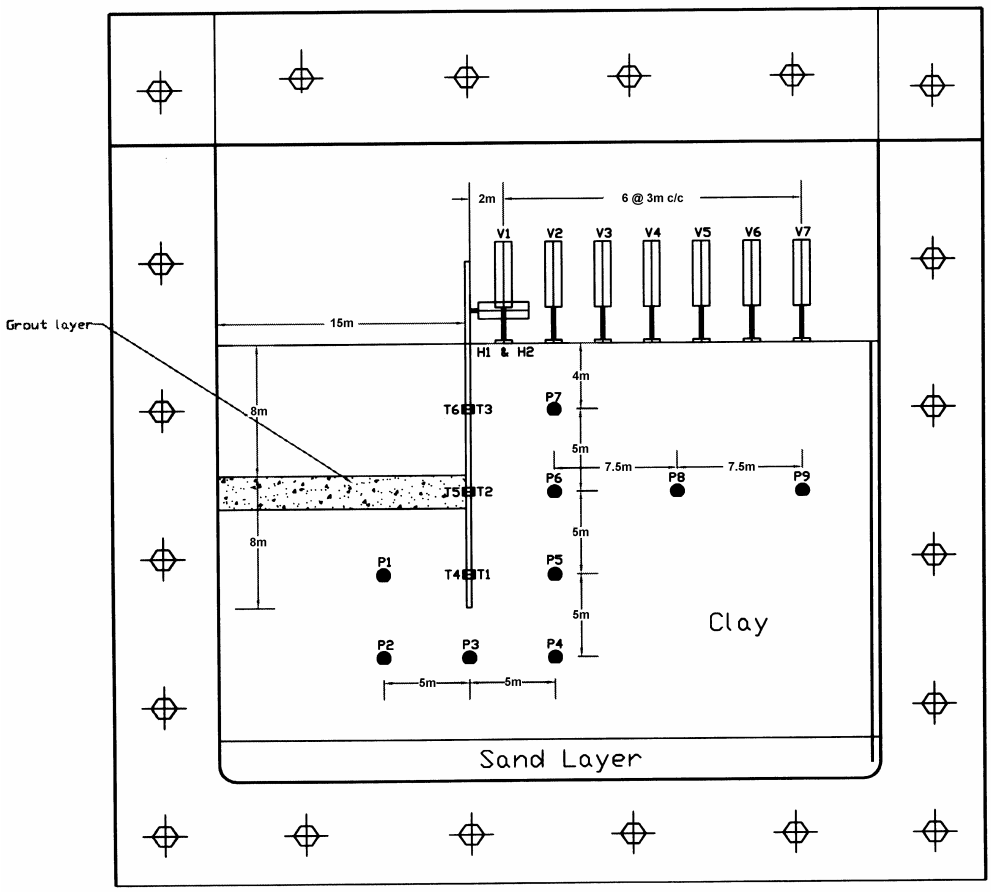

Figure 4.7 Location of various instruments in model ground

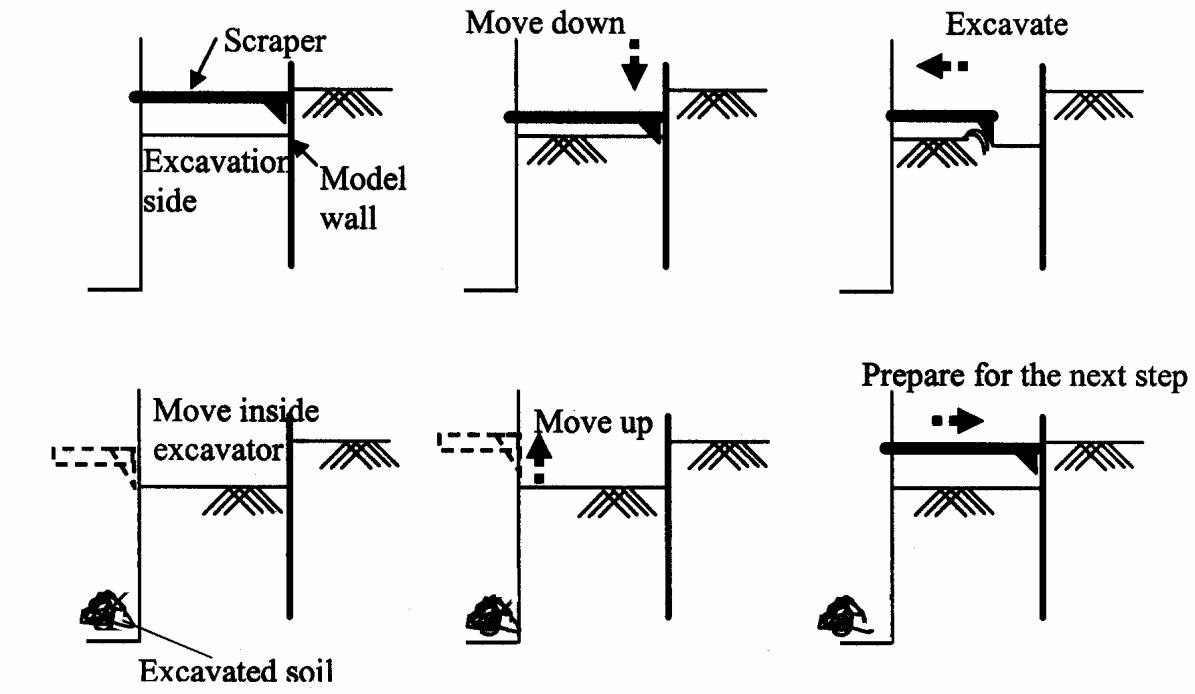

Figure 4.8 Schematic diagram of in-flight excavation sequence

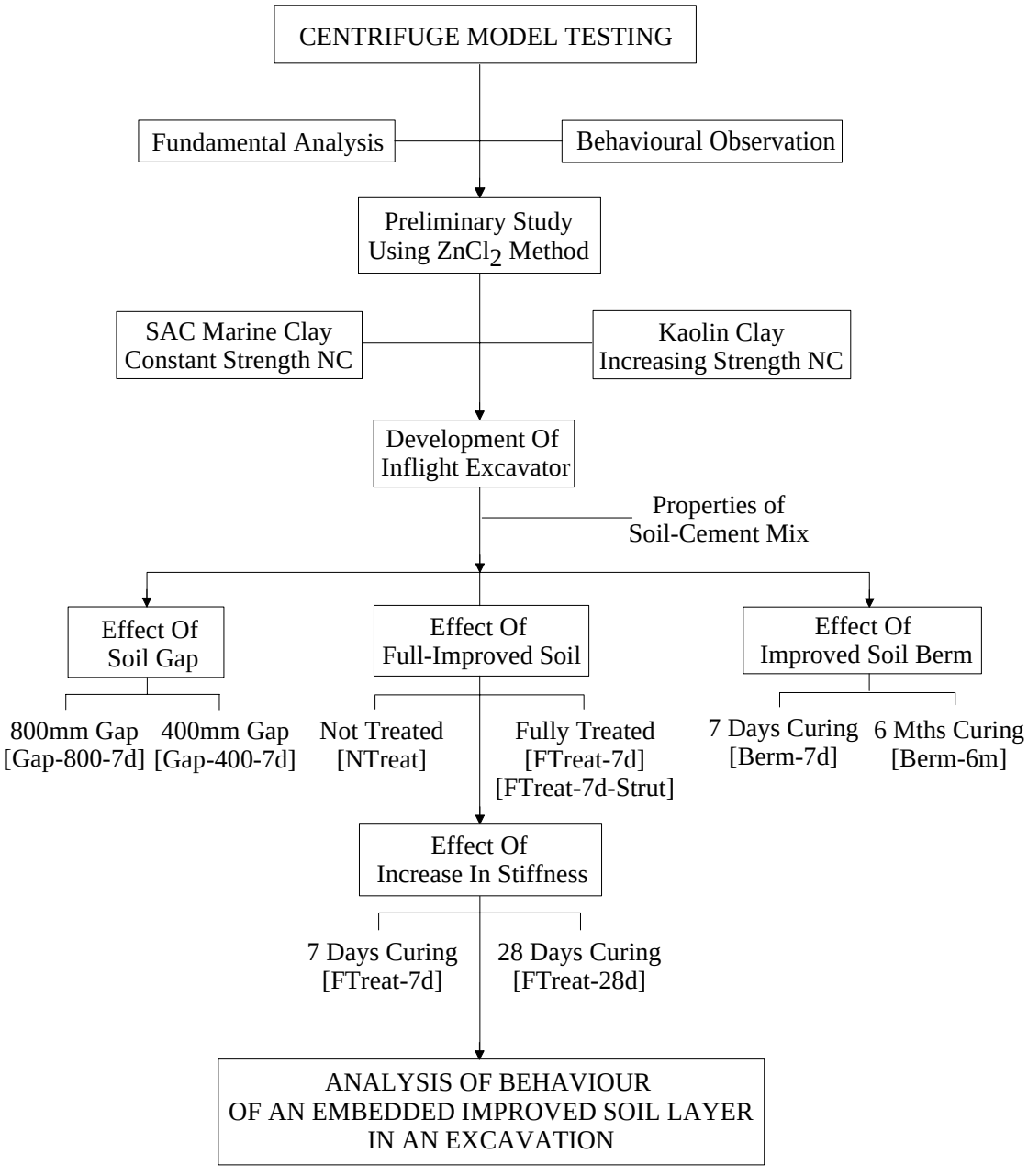

Figure 4.9 Stages of development in centrifuge model tests

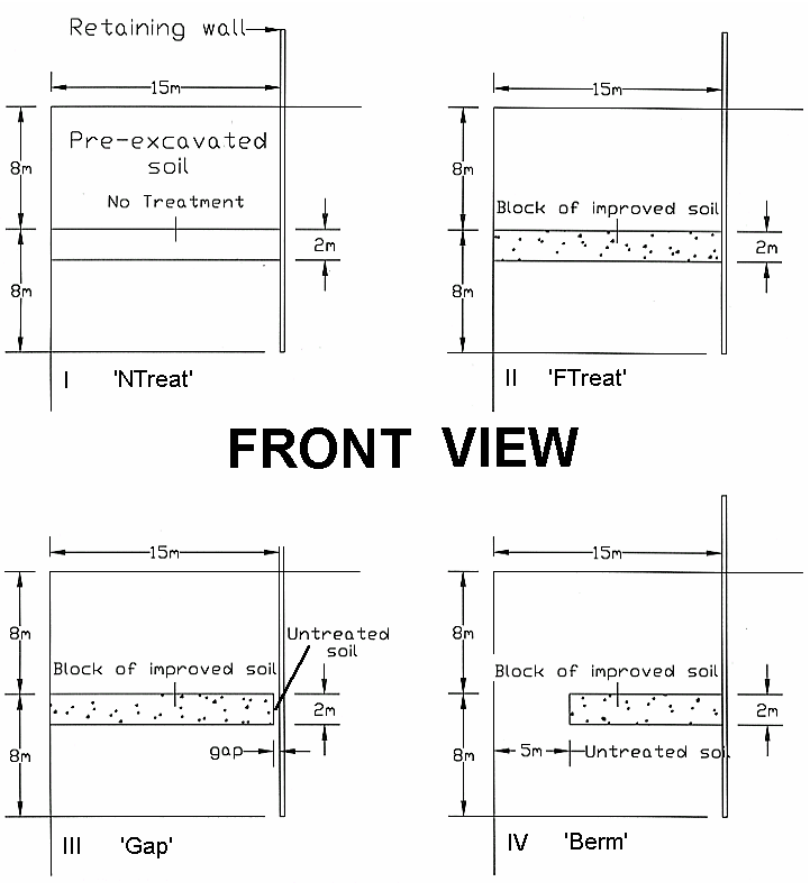

Category	Test ID.	Description
I. NTreat	NTreat	*No soil treatment* No improved soil, unbraced excavation
II. FTreat	FTreat-7d FTreat-7d-Strut FTreat-28d	*Full-improved soil layer* Improved soil cured for 7 days, unbraced excavation Improved soil cured for 7 days, braced excavation Improved soil cured for 28 days, unbraced excavation
III. Gap	Gap-800-7d Gap-400-7d	*Soil gap* Gap width of 800mm, unbraced excavation Gap width of 400mm, unbraced excavation
IV. Berm	Berm-7d Berm-6m	*Improved soil berm* Improved soil cured for 7 days, unbraced excavation Improved soil cured for 6 months, unbraced excavation

Figure 4.10 Schematic diagrams on typical excavation tests

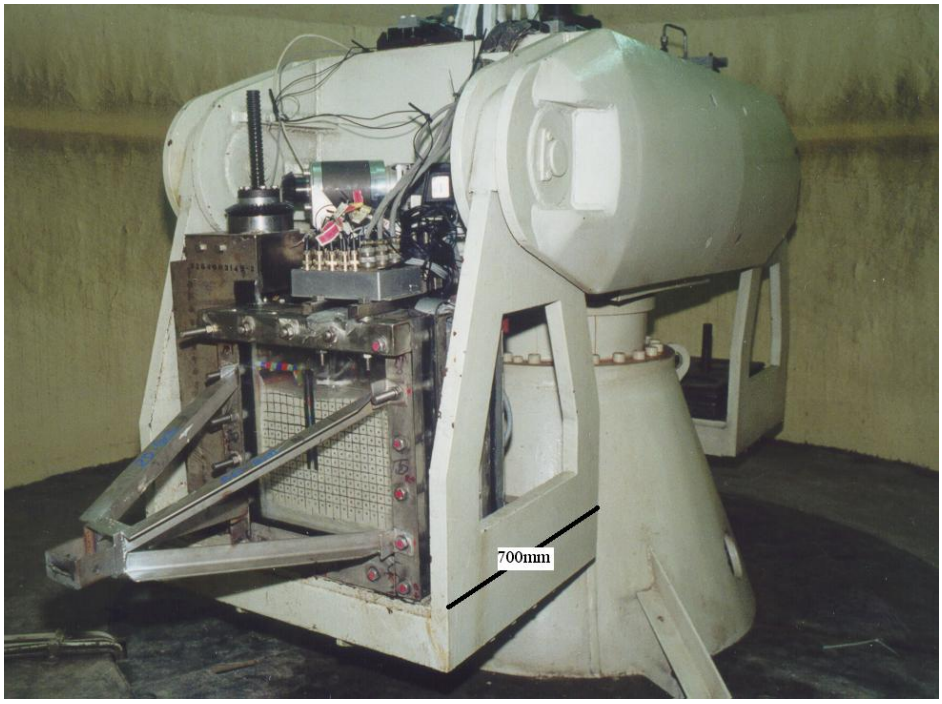

Plate 4.1 Model Set-up on the NUS Geotechnical Centrifuge

Plate 4.2 De-air Chamber

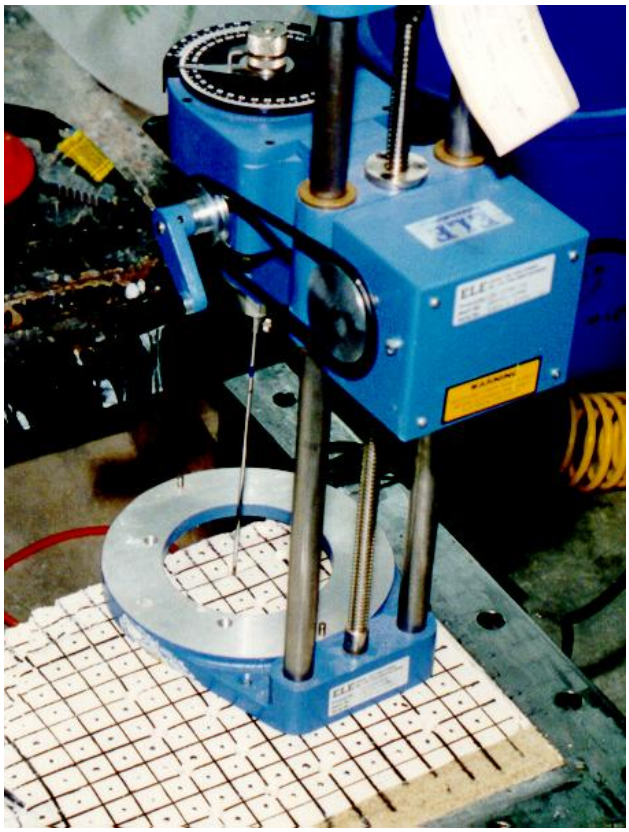

Plate 4.3 Vane Shear Test

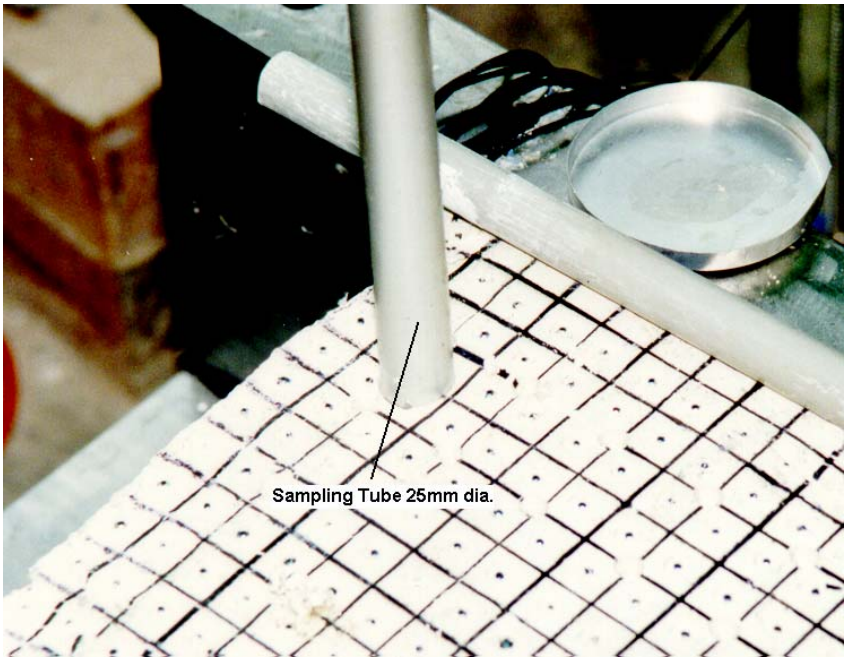

Plate 4.4 Determination of Water Content

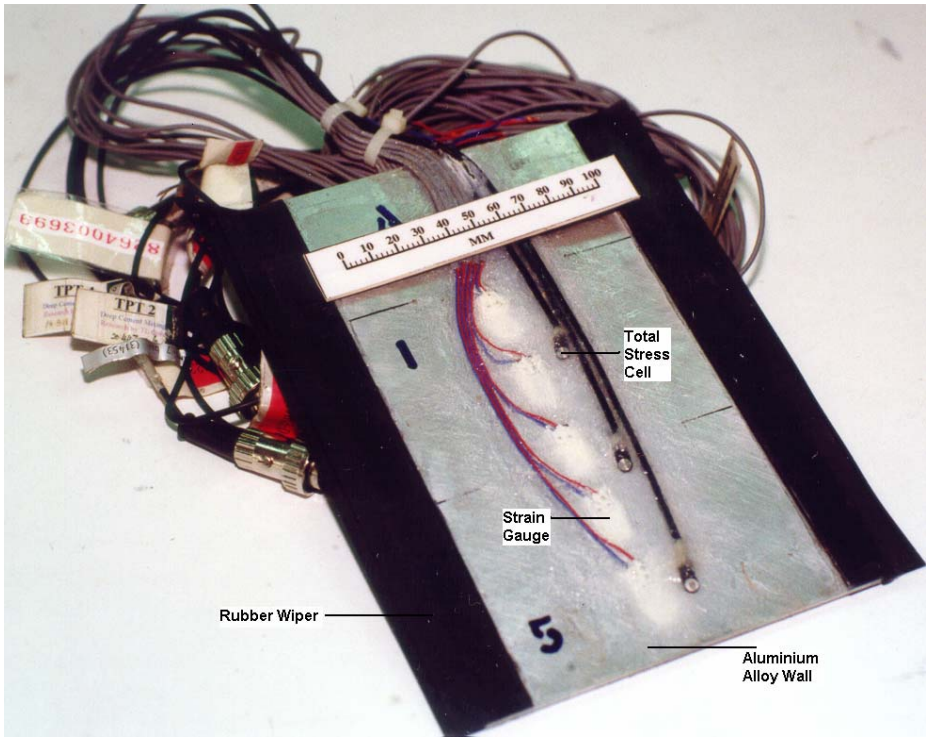

Plate 4.5 Model Retaining Wall

Plate 4.6 Rubber Wiper with flips

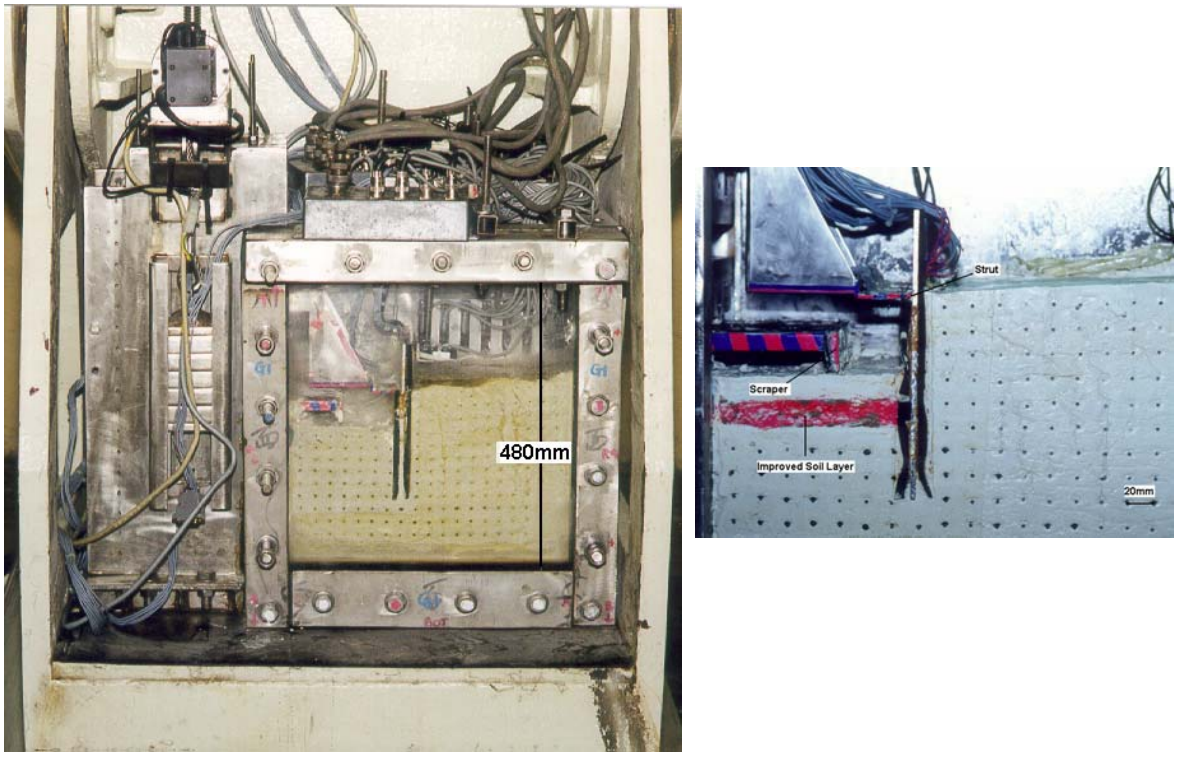

Plate 4.7 Excavation and strutting action on model ground

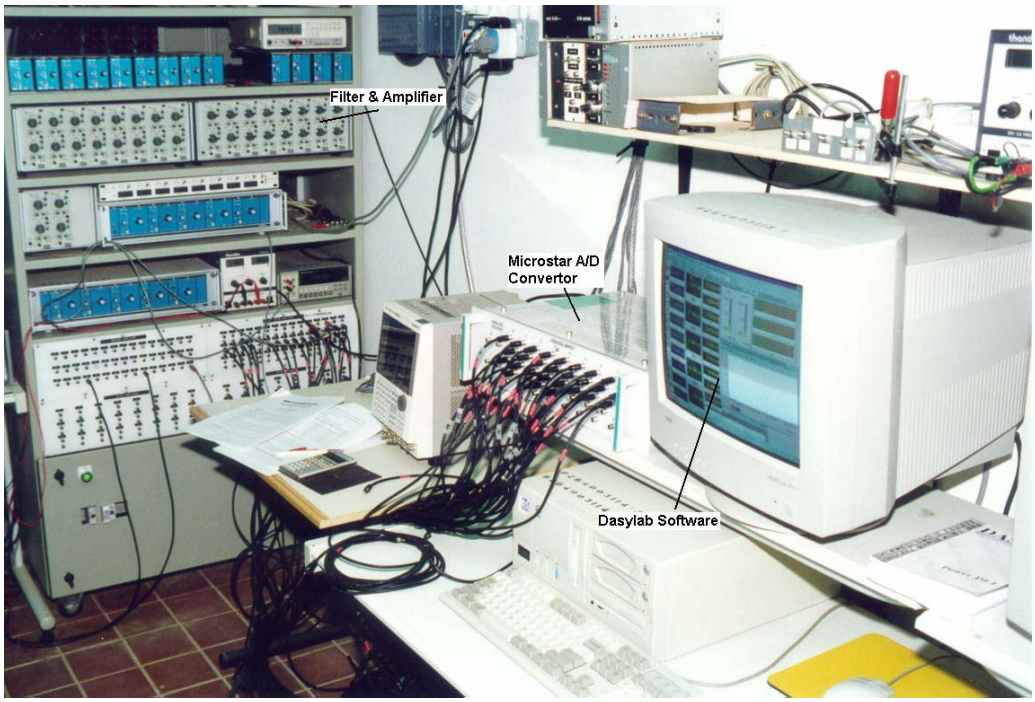

Plate 4.8 Data Acquisition System

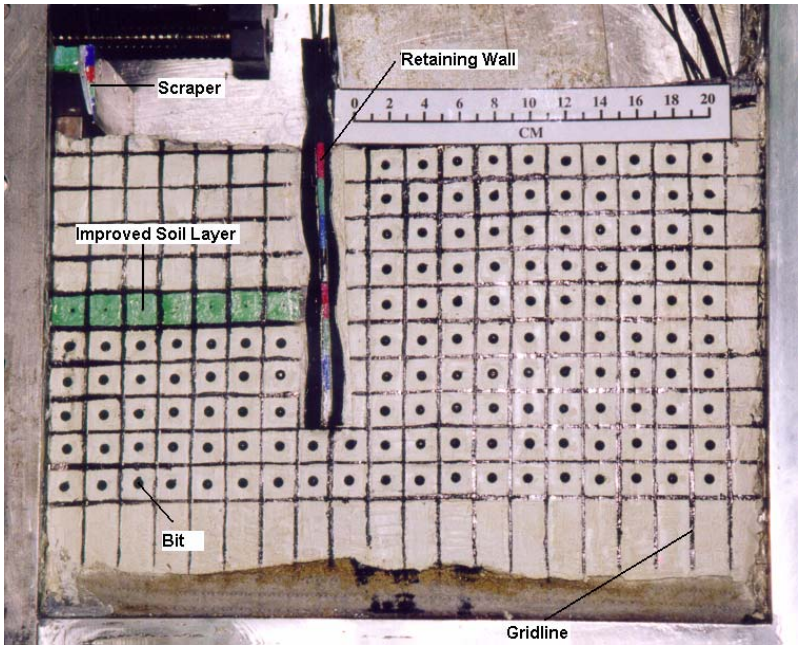

Plate 4.9 Bits and Gridlines on the model ground prior to excavation test

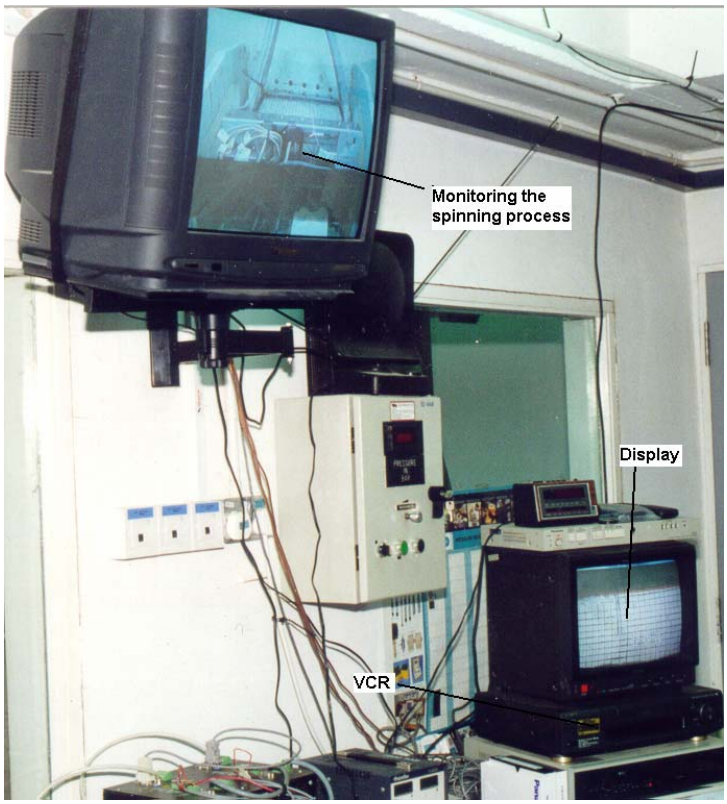

Plate 4.10 Video Recording Process in Control Room

Chapter 5

BEHAVIOUR OF AN EXCAVATION STABILISED BY AN EMBEDDED IMPROVED SOIL LAYER

5.1 Introduction

In deep excavation in thick deposits of soft clay, the maximum wall deflection usually occurs below the final excavation level, even when a stiff retaining wall with an appropriate bracing system is adopted. To limit the wall deflection in such situation, one cost-effective solution is to improve the soft soil around the location where the maximum deflection would occur, prior to excavation. Deep mixing method or jet grouting can be used for that purpose. In either method, soft soil of a particular thickness at a required depth can be improved by in-situ cement mixing, producing multiple overlapped soil-cement columns, which collectively form an embedded stiff composite improved soil layer. The term 'embedded' is used to emphasize the fact that the improved soil layer is located below the final excavation level.

The study presented in this chapter first reviews the function of the embedded improved soil layer, which has been well recognised to behave like a strut [Lee and Yong (1991), Tanaka (1993)]. To function as a strut, the improved soil layer must be able to transmit the lateral force from the retaining wall to another stiff member, usually the opposing wall. Therefore, the stiffness of the improved soil, which will directly affect the composite stiffness of passive ground, will be the key parameter in governing the performance of the excavation. To ensure adequate lateral rigidity in restraining the retaining wall during excavation, ideally, soil improvement works shall be carried out at the required depth on the entire area within the excavation zone so that the layer is in contact from one side of the wall to the other side.

Continuous grouting of a large area requires skill, experience and precision to ensure that the soil-cement columns are properly overlapped to form a homogeneous monolithic composite improved soil layer. Nevertheless, carrying out grouting works especially close to the retaining wall is often difficult, given the fact that the wall itself is not perfectly even. Incomplete grouting will lead to a region of untreated soil in between the retaining wall and improved soil layer. This gap of untreated soil is often quite small and is sometimes ignored in design, as it is considered an issue of workmanship. As the function of an improved soil layer is to provide an effective strut to the retaining wall, it is important to evaluate the detrimental effect of the existence of such an untreated gap on the performance of the excavation system. An important aspect is to establish the threshold value on the gap width, if any, smaller than which, the overall excavation performance might not be significantly affected.

In the case of a large excavated area, improving the entire layer so as to form a strut is usually a very expensive option. One cost-effective solution is to provide an improved soil berm, which only requires soil improvement to be carried out to a certain distance away from the retaining wall. This will imply that one end of the improved soil berm is in contact with the retaining wall while the other end is embedded in soil. In such a condition, the underlying mechanics by which the improved soil berm mobilises its resistance needs to be understood, especially in relation to the behaviour of a strut.

In view of limited experimental and field data on the behaviour of an excavation stabilised by an embedded improved soil layer, the first part of the study focused on a series of model excavation tests in the centrifuge with different configurations of soil improvement. The tests are highly complicated, conducted in 100G-environment using the newly developed miniature robotic in-flight excavator

developed in this study as explained in the previous chapter. Signals from all the instruments were regularly calibrated and carefully converted so that correctly scaled high quality test data could be captured consistently in each test. This is crucial in facilitating a meaningful comparison so as to understand how various forms of soil improvement work.

To evaluate the general behaviour of an excavation stabilised by an improved soil layer, ground displacements, lateral wall movements, surface settlements, lateral stresses and pore water pressures were used to assess the differences and trends developed during the process of excavation. From the initial set of test results, preliminary postulations were made and further excavation tests were then performed to verify these postulations. This ensured that key behaviours were scrutinised in detail before arriving at a firm conclusion. All the model excavation test results have been reported in prototype scale, which makes it convenient for the reader to visualise and compare these results to those measured in the field.

5.2 General Behaviour of An Excavation Stabilised by An Embedded Improved Soil Layer

Four sets of experimental results will be discussed in this section. Though the conditions of all these tests have been elaborated broadly in the previous chapter, it is necessary to re-iterate the specific tests that will be used for the comparison in this section. The first excavation test, referred to as NTreat, was an excavation test without any soil improvement. The second excavation test, called FTreat-7d was for an excavation in which the entire layer of soil in the excavation side was improved so as to act as an improved soil strut. In the third excavation test, referred to as Gap-800-7d, the excavation model is identical to FTreat-7d except that an 800mm width of soft soil

was left untreated in between the retaining wall and improved soil layer. The fourth excavation test, called Berm-7d was performed with only 10m of soil in front of the retaining wall being stabilised. To ensure fair comparison, similar properties of model ground and improved soil were prepared in each test and instruments were also placed at identical locations. Though the new excavator has the ability to install strut at a particular level, all the four excavation tests were carried out unbraced, mainly because of constraint on the amount of channel that can be used to send relevant signals to activate the strutting device. Nevertheless, the main objective of the present comparison study is to evaluate the fundamental difference of various configurations of soil improvement in mobilising its resistance and therefore, it was felt that the excavation procedure should be kept simple initially.

5.2.1 Ground Displacements with and without Treatment

Test NTreat was initially carried out to understand the mechanics of an unbraced excavation without any soil improvement, that is, the only support is the retaining wall. In this test, the excavation was carried out to a depth of 4m. Images captured throughout the excavation process were processed and re-plotted in order to display the ground displacement vectors at the final excavation stage [Figure 5.1]. Large ground movements were observed close to the retaining wall and near to the surface but reduced towards the toe and away from the wall. The direction of the displacement vectors indicates that the wall has translated and rotated towards the excavation side, pivoted around the wall toe. The soil on the excavation side in front of the retaining wall was subjected to substantial lateral compression and some base heave was observed. Preliminary results show that there is insufficient passive resistance provided by the soil below the excavation level to resist the wall movement,

once the excavation exceeds a depth of 4m.

Subsequently, Test FTreat-7d was conducted to investigate the effectiveness of having an improved soil strut below the excavation level in front of the retaining wall. To provide a comparison, images from Test NTreat after 2m and 4m of excavations are juxtaposed with those from Test FTreat-7d [Figure 5.2]. In Test NTreat where no soil improvement was provided, it was observed that the wall had rotated after 2m of excavation and the induced ground movements became even more pronounced when the excavation reached a depth of 4m. In contrast, in Test FTreat-7d, no such large movement was observed even though the excavation had reached a depth of 4m. This clearly demonstrates the effectiveness of providing an embedded improved soil strut to restrain the wall movement. It is especially effective as this is provided prior to excavation, in marked contrast to conventional braced excavation where the struts can only be installed after excavation. Ground displacement vectors were not presented for the rest of the excavation tests involving soil improvement due to the fact that the current image processor was unable to capture accurately the small movement between translating points.

5.2.2 Comparison of Lateral Wall Movement and Surface Settlement

The cumulative lateral wall movement during an excavation is a good indicator to quantify the effectiveness of different configurations of soil improvement and it could also be considered as an indirect measure of the mobilised stiffness of the passive ground. The lateral wall movements measured at a point approximately 3m above the ground level during the process of excavation for all the tests were compared in Figures 5.3. Except for Test NTreat, monitoring was carried out throughout the entire excavation process until a depth of 6m. For Test NTreat, the

excavation was terminated at a much shallower depth of 4m after it was observed that the wall had continued to move after the excavation at this step had been completed, a clear sign of an excavation failure.

From the results of Test NTreat, it was observed that the wall started to move excessively at an early stage of excavation, even before the excavation reached a depth of 1m. This was in contrast with the other three excavation tests involving soil improvement where the wall movement at this point was very much controlled. With an improved soil strut in Test FTreat-7d, the wall moved only about 100mm throughout the entire excavation. In the case of an improved soil strut with a gap of untreated soil (Gap-800-7d), the lateral wall movement increased to about 700mm after reaching the final excavation level. This was almost 7 times larger than that of a stabilised excavation test without any gap of untreated soil (FTreat-7d). This means that the presence of a small layer of untreated soil in between the retaining wall and improved soil strut has greatly affected the overall performance of the stabilised excavation.

As for Test ‘Berm-7d’, it shows that the provision of an embedded improved soil berm is also effective in restraining the lateral wall movement especially during the early stages of excavation. When the excavation was shallow, the behaviour of improved soil berm was almost indistinguishable from that of an improved soil strut (FTreat-7d). However, significant deviation was observed once the excavation exceeded a certain critical depth and thereafter, the lateral wall movement increased rapidly, showing a trend very much like that of an untreated excavation test (NTreat). This showed a dramatic shift in behaviour of an improved soil berm during the process of excavation, denoting that there might be a unique mechanism involved.

To examine further, surface settlement during the process of excavation at a

distance of 2m behind the retaining wall for all the tests were evaluated. The surface settlement is another good indicator to assess the performance of the different configurations of soil improvement, driven by the fact that the composite stiffness on the passive side, which directly influences the wall movement, would affect the surface settlement behind the wall as well. In effect, one of the main objectives in stabilizing an excavation is to reduce the surface settlement behind the wall by first limiting the wall movement during an excavation. As shown in Figure 5.4, the trends of settlement profiles are largely consistent with the mechanics discussed in relation to the profiles of lateral wall movements.

Based on this first series of test data involving three different configurations of soil improvement to stabilise an excavation as presented above, some preliminary observations of the different configurations can be made. In the case of Test FTreat-7d when an entire layer of soil at some depth was improved, as expected, only small lateral wall movement and surface settlement could be observed. This is because the improved layer acts as an embedded strut and provides an effective restraint on the inward movement of the wall, resulting in smaller wall movement and settlement.

In the case of Test Gap-800-7d with a gap of untreated soil, the performance of the improved soil strut was found to deteriorate significantly. From the amount of lateral wall movement and surface settlement induced during the initial stage of excavation, it can be inferred that the untreated soil in between the retaining wall and improved soil strut has undergone significant compression. The impact of such compression would lead directly to larger wall movements and surface settlements even at the early stage of excavation. Nevertheless, it is important to note that these movements are induced gradually even with increasing depth of excavation.

In the case of Test Berm-7d where an improved soil berm was provided, the

initial lateral wall movement and surface settlement were more in line to those from Test FTreat-7d where an improved soil strut was provided. However, its restraining behaviour becomes significantly less effective after excavation exceeds a certain depth and after that, the excavation behaviour is similar to the behaviour of an untreated excavation test (NTreat). It was also noted that in Test Berm-7d, the improvement ratio (66.7%) was smaller than that in Test Gap-800-7d (94.7%) but the performance of an improved soil berm was more superior to an improved soil strut with a gap of untreated soil in the early stages of excavation, though beyond a certain depth, sudden failure occurs. This is only true provided that there is sufficient resistance provided by the improved soil berm. The above case has demonstrated that poor workmanship can have a severe detrimental effect. Clearly, in such design, not only the compression of the improved soil alone needs to be considered, other factors such as the influence of a gap of untreated soil and the arrangement of the improved soil (e.g. improved soil berm) will affect the behaviour of a stabilised excavation.

5.2.3 Comparison of Normalised Surface Settlement

The surface settlement is now normalised with the excavation depth and re-plotted in Figure 5.5 with respect to the distance away from the retaining wall. The surface settlement is from a distance of 2m to 20m behind the retaining wall. Larger surface settlement was observed close to the wall, but this reduced significantly further away from the wall. This trend of normalised surface settlement is consistent with general field measurements observed in most of the excavation projects [Peck (1969)]. As the data points presented by Peck (1969) referred to excavations in braced condition, the magnitude of movement was smaller as compared to the present unbraced excavations, except in Test F-Treat where the improved soil strut is

provided.

With an improved soil strut (FTreat-7d), only a small value of normalised surface settlement was observed, affirming the effectiveness of this technique. As for Tests Gap-800-7d and Berm-7d, the effect of soil improvement is noticeable but they are less effective as compared to that of Test FTreat-7d especially at deeper excavation. However, all three excavations stabilised with improved soil showed a distinct contrast in behaviour when compared to the normalised surface settlement obtained from the untreated excavation test (NTreat). These trends confirm the effectiveness in stabilising a deep excavation using an embedded improved soil layer, the word 'embedded' is used to emphasize that the improvement is carried out below excavation level and usually prior to excavation. The consistency in the four sets of results also provides confidence in the reliability of the centrifuge tests.

5.2.4 Comparison of Lateral Earth Pressure

The response of lateral earth pressure from total stress cells placed on the retaining wall is another interesting parameter to provide a better understanding of the way earth stresses are mobilised during an excavation stabilised by an embedded improved soil layer. In particular, the total stress transducer on the passive side located at the level of the improved soil layer could provide useful information on how the stresses in the improved soil layer developed during the process of excavation. Figures 5.6 and 5.7 show the development of an estimated deviatoric stress (σ_h-σ_v) during the process of excavation. σ_h was measured by the total stress transducer while σ_v, the total vertical stress was estimated from the weight of the remaining soil above the respective transducer.

As shown in Figures 5.6 and 5.7, all deviatoric stresses in the active zone (T1,

T2 and T3) reduce while those on the passive side (T4, T5 and T6) increase during the process of excavation. This is expected, given the fact that during the process of excavation, the lateral earth pressure behind the wall will reduce to the active state while stresses in front of the wall will increase to the passive state. The rate of reduction (or increase) in deviatoric stress at active (or increase at passive) side is much faster in the case of an untreated excavation test (NTreat), as compared to other tests where an embedded improved soil layer has been provided. This means that the movement of the retaining wall is much larger, and the active state is approached more rapidly.

For the total stress transducer T5, which was located in front of the retaining wall where the improved soil layer is located, the total stress in Test FTreat-7d increases at the fastest rate. The lateral stresses at this point develop continually until the end of the excavation. This is due to the fact that the improved soil layer is rigid enough to transmit the lateral force from the retaining wall to the other rigid end, which in this case is the sidewall of the strongbox container, effectively acting as an embedded soil strut. With the restraining effect provided by the improved soil layer, most of the lateral forces from the retaining wall would be attracted to this stiff layer. Consequently, the development of the total stresses at location T6 and T4 is lower as can be seen in Figures 5.7 (a) and 5.7 (c) respectively. The ability of the improved soil layer being able to attract higher lateral stress is a clear indication that the improved soil layer is behaving like a strut.

The rate of increase in deviatoric stresses at T5 in Tests Gap-800-7d and Berm-7d is much lower than that in Test FTreat-7d but they are still higher than that in Test NTreat. In the case of Test Berm-7d, it is noted that the lateral stresses for the improved soil berm have a sudden dip when excavation reaches a depth of about 3.5m.

Such a drop in lateral stress implies that the improved soil berm may have failed. After the excavation test, a closer visual inspection showed that the improved soil berm was still intact with no sign of any compression failure. Therefore, the more likely scenario is that the improved soil berm could have failed by a sliding mechanism similar to the behaviour of a floating pile when it's being overloaded.

The principal difference between an improved soil strut and an improved soil berm is that in the latter, one end is in contact with the wall while the other end is floating in the soft soil matrix. Thus, the improved soil berm cannot fully mobilise its compressive strength, as the end bearing will control the amount of compressive stresses that could be transferred. Clearly, the behaviour of an embedded improved soil berm is much more complex and cannot be explained by just considering the compressive stiffness as in the case of the improved soil strut. As the behaviour of such berm is quite different from that of a strut, the use of a composite layer to represent such berm with an equivalent stiffness, such as in most numerical programs based on sub-grade reaction, has to be re-considered. Clearly, the stiffness of improved soil, which plays a critical role in the case of improved soil strut, needs to be re-assessed for an improved soil berm. This issue will be addressed at a later stage.

5.2.5 Comparison of Pore Water Pressure

The response of pore water pressure on the active side at 5m behind the retaining wall was also monitored and provided another indicator to examine behaviour of the ground due to the excavation. Profiles of negative pore water pressure of these four tests are plotted in Figures 5.8 for 3 stages of excavation, namely 1m, 3m and 5m. After 1m of excavation, in Test NTreat, higher negative excess pore water pressure was registered near to the ground surface (P7), but reduced in magnitude

downwards to the wall toe (P5). However, the negative pore pressure increased again beyond the toe of the wall (P4); clearly indicating that at this location on the active side, the effect of load reduction on the excavation side was felt. This development of negative excess pore water pressure is consistent with the soil movement caused by the wall movement as shown by the displacement vectors in Figure 5.1. For the excavation tests where an improved soil layer is provided, the magnitude of negative pore water pressure is much smaller, clearly indicating less ground movement induced. At this early stage of excavation, the differences among the tests are small though it is also clear that the negative pore water pressure for Test FTreat-7d is smallest, followed by the case with a berm and finally with a gap.

In all the stabilised excavation tests, the initial drop in pore water pressure is small but increases with increasing depth of excavation as seen in Figure 5.8b for an excavation depth of 3m. A larger drop in pore water pressure is now observed when there is a region of untreated soil in between the retaining wall and improved soil layer as in Test Gap-800-7d. This drop is slightly bigger than that of the excavation test with an improved soil berm (Test Berm-7d) at this stage of excavation, indicating that more wall movement have been induced in Test Gap-800-7d. This was expected due to the fact that the region of untreated soil would be compressed with the exertion of lateral force from the retaining wall. In the other two treated excavation tests that do not have such a gap of untreated soil (FTreat-7d and Berm-7d), the wall movement is much smaller at this point of excavation, resulting in smaller negative pore pressure.

However, the drop in pore water pressure in Test Berm-7d became very significant after excavation reached a depth of 5m and in fact exceeded that of the case with a gap. The sudden increase was found at P6 where the improved soil berm was located. This was a clear sign of a failure in the improved soil berm, which then lost its

restraining capability. Due to the fact that only the front portion of soil next to the retaining wall was treated and there existed a large untreated soil behind, the improved soil berm has to transmit the lateral load from the retaining wall to the surrounding soil. Thus, the berm is behaving like a horizontal floating pile, which mobilises its passive resistance mainly through the skin friction and end bearing. At some point in time, the combined skin friction and end bearing is inadequate to resist the inward movement of the retaining wall and as a result, failure occurs. When this happens, its response becomes worse than the case with gap and hence, a much larger negative pore water pressure is developed. Clearly, this confirms that with an improved soil berm, the failure is sudden and thus this fact must be accounted for in design.

The response of pore water pressure located below the wall toe, namely P4 was also examined for all 4 cases and 3 different excavation depths, to understand the behaviour of an excavation with a floating wall system. It was noted that the drop of pore water pressure at this point was always greater than those transducers above it. This is consistent with the fact that the wall toe was floated in soft ground and not keyed into a hard stratum. Though the improved soil layer can act as a screen to reduce the effect of load relief, it also shows that there is a greater potential of base heaving to occur in an excavation if a floating wall system is adopted.

5.2.6 Performance of Composite Ground Resistance on Passive Side

Hitherto, only cumulative effect of various parameters is examined for the different configurations of soil improvement. However, often at a particular stage of excavation, it is difficult to compare the composite stiffness of the system as a result of using different configurations of soil improvement based on these cumulative effects. A more useful parameter is to examine the performance of various parameters due to

the removal of one layer of soil at a fixed depth for the different configurations of soil improvement. Obviously, it is near impossible to obtain such data from field works. This is where correctly scaled physical models can prove to be extremely useful. In the present case, the resulting movement or change in load due to one scrapping operation at a fixed depth is compared for the different tests. This is termed the “incremental movement” and its direct comparison provides a useful benchmark to evaluate the composite stiffness available at that depth for different systems of soil improvement.

An excavation step in the centrifuge test, as mentioned in Chapter 4, referred to the process of removing a soil layer of 0.5m thick using the excavator’s scrapper where this scrapper initially cut the soil next to the retaining wall and dragged it towards the lift-shaft at the other end. Since this is a controlled test with continuous data acquisition, incremental movements arising from each excavation step are being captured accurately. By comparing the behaviour of different incremental parameters, the behaviour of the composite passive ground during the removal of soil at a particular depth can now be studied.

Figures 5.9 show the incremental lateral wall movements due to the removal of another 0.5m of soil at 3 different depths of excavation, namely at 1m, 3m and 5m. For example, if the scrapper is at a depth of 1m, this means the removal of soil from a depth of 1m to a depth of 1.5m. In the case of an untreated excavation Test NTreat, the incremental wall movement increases throughout the entire process of soil removal but at a more rapid rate in the early stage of removal near to the wall. However, this was not the case for Test FTreat-7d where an improved soil strut was provided. Besides having a much smaller movement, the way the incremental wall movement developed was completely different. As shown in Figure 5.9(c)(ii), the movement induced was very small when only 6m of soil layer in front of the retaining wall was removed and

only thereafter, the movement began to pick up. Nevertheless, the overall movement is still much smaller than in the other 3 cases.

Clearly, the relief of overburden pressure during an excavation affects the composite stiffness on the passive side of the excavation as well as increasing the imbalance between the active and passive side. When the removal of soil happened at greater depths, the impact of soil removal would be more substantial, as the initial lateral stress acting against the wall increases with depth. Therefore, a larger incremental movement would be expected as the excavation goes deeper. This effect of stress relief was very significant for an excavation test without an improved soil layer (NTreat) since the soft soil on the passive side could only offer limited resistance to the inward movement of the wall.

In the case of Test FTreat-7d, where an embedded improved soil strut was provided, during the early stage of the scrapping operation, only negligible movement occurred. It was only after some amount of soil had been removed before a more noticeable movement occurred. This is consistent with the behaviour of a strut, whereby only with certain amount of opening would the strut then be allowed to bend and as a result develop movement in the retaining wall. Hence, this incremental movement trend strongly suggests that the improved soil layer is behaving like a strut where the bending of strut will become significant after a certain amount of removal of soil has taken place from the retaining wall. Similarly like a strut, the improved soil layer would then be expected to depend on the stiffness and amount of bending to derive its resistance.

In the case of soil improvement with a gap of untreated soil, the incremental wall movement was induced in the early stage of scrapping and continued to increase throughout the entire operation. This trend is somewhat similar to that of the untreated

excavation test (NTreat) though the magnitude of movement is much smaller. Thus, the presence of the untreated soil has affected the overall behaviour of the composite passive ground, and a significant movement is induced even at the early stage of soil scrapping. As the gap is located next to the retaining wall, the impact of soil removal will be felt directly once the overburden stress above the untreated soil portion is reduced. The reduction of the composite stiffness of the passive ground is seen to occur throughout the process of scrapping at the same depth.

When an improved soil berm was provided, the incremental wall movement occurred mainly during the early stages of scrapping and beyond a certain distance from the retaining wall, further scrapping of soil did not induce additional movement. This trend, qualitatively, is the exact opposite of that observed for FTreat-7d. Despite the similarity shown in earlier comparison, the two behaviours are markedly different. It was found that the incremental movement almost ceased once the excavator's cutting blade passed the edge of the improved soil berm. This is an interesting observation, which means that the incremental movement would only occur when the soil above the berm was removed. The behaviour of an embedded improved soil berm in many ways is similar to the behaviour of a floating pile. Thus, the removal of soil above the berm would reduce the skin friction. This means that the compression of improved soil berm is insignificant and therefore, the passive resistance would not be governed by its stiffness. Like a floating pile, the improved soil berm has to transmit the lateral force from the retaining wall to the surrounding ground through frictional resistance and end bearing. Since the improved soil berm was resting in soft clay, the contribution of end bearing to its composite stiffness of passive ground would not change much and therefore, it is mainly the interfacial shear resistance that is being increasingly mobilised to restrain the inward movement of the retaining wall.

5.2.7 Performance of Improved Soil Layer in A Braced Excavation

In order to understand the behaviour of an embedded improved soil layer in a braced excavation, Test FTreat-7d-Strut was subsequently carried out. Similar to Test FTreat-7d, a 2m thick improved soil layer extending from wall to wall was placed at 8m below the ground level in front of the retaining wall. During the initial stages of excavation, the retaining wall was not braced. When the excavation reached a depth of 3m, the scrapping of soil ceased temporarily in order to allow a strut to be installed at the ground level in front of the retaining wall. After the strut was installed, the excavation proceeded till a depth of 6m.

The profile of bending moment in the wall in Test FTreat-7d-Strut is shown in Figure 5.10. Two distinct sets of bending moment profiles were observed; the first profile was for an unbraced excavation and the other profile was after the wall had been propped. When the excavation was supported by a retaining wall but without bracing above the excavation level, the profile of bending moment was rather straightforward; the maximum bending moment in the wall occurred approximately at the level where the improved soil layer was located. However, the profile of the bending moment changed drastically after the wall was propped at the ground level. The direction of bending moment at the upper part of the retaining wall in between the improved soil layer and strut was reversed. This is consistent with the behaviour of a simply supported wall, which are restrained by two rigid supports: one being the strut device at ground level while the other being the embedded improved soil layer at the mid-level of the retaining wall. Similar trends of wall bending profiles were observed at the lower part of the retaining wall between the improved soil layer and wall toe though the magnitude was much smaller.

The above results demonstrated the impact of having an embedded improved soil layer regardless whether the excavation was braced or not. The observation points out the fact that the presence of an embedded improved soil layer has provided a rigid support to the retaining wall below the excavation level. With such a support, the lateral wall movement is restrained and the wall tends to bend about this level. Thus, the embedded improved soil layer behaves very much like a strut to the retaining wall, albeit this is below the excavation level.

To further understand the stresses induced in the improved soil layer due to the propping action, the lateral stresses in the passive zone at T5 were presented in Figure 5.11. The lateral stresses increased initially at a faster rate when the excavation was not braced but after the wall was propped, the stress development was much slower. Clearly, the strut member installed above the excavation has helped to bear part of the lateral load transmitted by the retaining wall, which were mainly resisted by the improved soil strut alone at the initial stage when the excavation was not braced.

5.3 Effect of Stiffness of Improved Soil Strut

Previous sections have put forth evidences that for a full-improved soil layer to function as a strut, it needs to be stiff enough to transmit lateral forces from the retaining wall to the other rigid end. Intuitively, this implies that the stiffer the improved soil, the more effective the improved soil layer will be in restraining the retaining wall. This is a valid assertion as far as control of movement is concerned. Usually in design, a smaller stiffness value is used in the analyses to provide an upper bound on the expected movement. This is considered to be conservative, as using a more realistic stiffness will mean that the predicted movement will be smaller.

However, with a stiffer improved soil layer, the bending moment of wall will

increase. This is because when a stiffer improved soil strut is introduced, the capability of the wall to retain the soil increases and as a result, more forces would be attracted to the wall. Though this seems logical, to the author's awareness and experience in industry in Singapore, this is rarely considered. To evaluate the extent of this effect, another test was carried out, namely Test FTreat-28d. In this test, the improved soil was cured for 28 days instead of 7 days as used in Test FTreat-7d. As expected, the longer curing time would increase the stiffness of improved soil. Reviewing the results obtained in Chapter 3, elastic modulus of the improved soil in Test FTreat-28d would be about 1.5 times higher than that in Test FTreat-7d. In reality, due to the nature of cement mixing and the way the improved soil layer is formed, the range of elastic modulus can be significantly larger.

Figure 5.12 compares the surface settlement behind the wall in these two tests. The results show that the surface settlement for stiffer improved soil layer is consistently lower at every excavation stage. However, when the profile of bending moment in the wall is plotted in Figure 5.13, Test FTreat-28d, with a stiffer improved soil layer, clearly shows that the retaining wall experiences a much higher bending moment. Figure 5.14 shows that a higher resistance is mobilised in the improved soil layer where the lateral stresses develop at a faster rate for the stiffer improved soil layer. The trends of the incremental wall movements in both tests as shown in Figure 5.15, are very similar, but again, the test with the stiffer improved soil layer proved to perform better in restraining the wall movement.

These results consistently show that the effectiveness of an improved soil layer behaving like a strut is very much dependent on the stiffness of the improved soil layer. While a stiffer improved soil layer provides a higher resistance to the retaining wall, the bending moment in the wall also increases as well. If the curing time is much

longer than what is expected, the increase in wall bending moment will become more significant. This is an important point, and in design, it is recommended that the maximum expected stiffness in the improved soil, which will then produce a higher bending moment to be considered during the design of the retaining wall. On the other hand, in estimating the ground movement in adjacent ground, the lower expected stiffness should be used as per present practice. This is an important consideration that needs to be enforced to ensure a safer design and is currently overlooked by many geotechnical engineers.

5.4 Effect of the Width of Gap of Untreated Soil

The detrimental effect of having a gap via presence of untreated soil in between the retaining wall and improved soil layer had been demonstrated clearly in Test Gap-800-7d. The existence of a gap reduces the overall performance of the improved soil layer tremendously even at the early stage of excavation. As the untreated soil is highly compressed during the lateral load transfer stage, it would be crucial to investigate how the gap could still withstand this force if the width of the soil gap is made smaller.

Therefore, an additional test, namely Gap-400-7d was carried out. In this test, the width of the gap of untreated soil was reduced to 400mm, which was half of the gap width of Test Gap-800-7d. The behaviour of these tests was examined together with Test FTreat-7d where the excavation test was stabilised with an improved soil strut. In actual fact, FTreat-7d could be re-named as Gap-0-7d, as this test was very similar to the other two tests except that it had no gap in between the retaining wall and improved soil layer.

Cumulative wall movement and surface settlement in Tests FTreat-7d, Gap-

400-7d and Gap-800-7d are compared in global as shown Figures 5.16 (a) and 5.17 (a). With the gap width halved, the reduction in wall movement and surface settlement was almost 50%. This shows that the gap width significantly influence the performance of the improved soil layer. A closer examination of the enlarged movements at the early stage [Figures 5.16 (b) and 5.17 (b)] shows that the improved soil layer with a smaller gap has almost similar behaviour to that of an improved soil layer without gap but beyond an excavation of 1m, significant deviation between the two starts to appear. This means that the mechanism of how the gap of untreated soil transfers the high compression load might be crucial in influencing the overall performance of its passive resistance.

The behaviour of deviatoric stress σ_h - σ_v in the improved soil layer for these tests against the lateral wall deflection is shown in Figure 5.18. The way lateral stresses is mobilised in the three tests showed marked contrast. In the case of Test FTreat-7d, the lateral stress increases rapidly and continually all the way until towards the end of excavation. In contrast, for the two excavation tests with gap of untreated soil in between the retaining wall and improved soil layer, the lateral stresses also increase monothically but the rate of increase is significantly smaller. With a smaller gap, the mobilised lateral resistance is higher, but there is still a distinct difference with that in the case where there is no gap.

The incremental lateral wall movements in the two tests, Gap-400-7d and Gap-800-7d are shown in Figure 5.19. The incremental wall deflection in each and every step of soil removal for both tests increased with increasing depth of excavation and most of these movements were induced in the early stage of scrapping. When the gap was smaller, the wall movement ceased much earlier. This implied that the area of influence from the impact of reducing the overburden stress increased with wider gap.

Due to the fact that the presence of untreated soil in between the improved soil and the retaining wall, there is a discontinuity in lateral rigidity of the improved soil layer restraining the retaining wall. As a result, the composite ground resistance of the improved soil layer would be reduced. The net effect is as good as a drop in the stiffness of an equivalent improved soil strut. The presence of a soft untreated soil would mean that very high compression of this portion of soil could occur when the retaining wall exerted a lateral force on it, to be transmitted to the improved soil layer. As such, it is important to be able to have an assessment on how the presence of such untreated soil portion will affect the composite stiffness. This aspect will be dealt later in Chapter 6, which presents the numerical studies, as carrying out centrifuge tests to study this effect is expensive and lengthy. More importantly, a soil smaller than that as in Test Gap-400-7d (which is going to be smaller than 4mm in model scale) would be very difficult to place with any accuracy.

5.5 Effect of the Stiffness of Improved Soil Berm

To justify that the behaviour of improved soil berm is similar to the behaviour of a floating pile and not of an improved soil strut, the results from a test conducted by another student [Thanadol (2003)] is reported, namely Berm-6m. In this test, the length of the improved soil berm was kept the same as in Test Berm-7d, which was measured to be 10m from the retaining wall. Instead of 7 days curing, the improved soil berm in Test Berm-6m was cured for 6 months. From the results in Chapter 3 – Section 3.4.3(d), clearly in this case, the stiffness of improved soil berm would increase significantly with the ratio of elastic modulus for a sample cured for 6 months to be about 2 times higher than that at 7 days.

The cumulative lateral wall movement above the ground level for both tests is

compared in Figure 5.20. The results show that the wall movements in both tests with improved soil berms of significantly different stiffness are pretty much the same. This showed that in the present case, doubling the stiffness of the improved soil berm has virtually no impact on its resistance. Further evaluation using a normalised surface settlement behind the wall showed consistent results [Figure 5.21], which again confirm the fact that increasing the stiffness did not make any difference. Obviously, these results show that the behaviour of using an improved soil berm is not the same as using an improved soil strut.

To understand the behaviour of improved soil berm further, a comparison was made on the mobilised deviatoric stress of these tests as shown in Figure 5.22. The comparison indicated that the mobilised development of deviatoric stress in Test Berm-7d and Berm-6m were practically the same, and they were much lower than that of Test FTreat-7d. This shows a very interesting feature of an improved soil berm, in contrast with an improved soil strut. In an improved soil berm, the results suggest that the end bearing mobilised is virtually the same. This is reasonable for if the improved soil layer is sufficiently stiff, the end bearing will be a function of the location and dimension of the improved soil layer, in particular the thickness. The other resistance would then be mobilised by the interfacial friction between the berm and surrounding soil. In this scenario, as long as the stiffness of the improved soil layer exceeds some threshold, then raising the stiffness beyond that threshold will not improve the overall resistance provided by the berm. This is a complicated issue and has been studied by Thanadol (2003). Therefore, the main purpose to conduct the test with improved soil berm in this study is to understand its difference from an embedded improved soil strut.

As before, the composite ground resistance could also be evaluated in greater

details by studying the incremental wall movement. As shown in Figure 5.23, there is very little difference in the behaviour between Test Berm-7d as compared to Berm-6m. Consistent with the observation made in Test Berm-7d earlier, the bulk of the movement in Test Berm-6m had also occurred when the soil directly above the improved soil berm was removed. Removal of soil beyond the edge of improved soil berm does not further contribute to the incremental wall movement. The results reinforce the postulation that the interfacial shear resistance is playing an important role in providing the resistance force and the end bearing is not as critical.

Clearly, in the case of an embedded improved soil berm, the failure mechanism is, in many ways, similar to the behaviour of a floating pile, in spite of being subjected to a continually reducing confining stress, especially on the upper face. Therefore, the combined interfacial shear resistance and end bearing play a more dominant role than the compression of the improved soil berm itself. As discussed above, increasing the stiffness of the improved soil berm above a threshold value would not provide any improvement in the performance to restrain the retaining wall.

5.6 Summary of Findings

The main objective of conducting the series of excavation tests reported above was to investigate the behaviour of composite ground resistance provided to a retaining wall when different configurations of soil improvement are applied to the soil on the excavated side and below the level of excavation. By comparing the results of these experimental tests, an insight of the different mechanisms involved in mobilising these improved grounds to restrain the retaining wall is gained. Some of these insights have significant implications on the design of excavation with such soil improvement. The key findings established in this chapter are summarized as follows: -

(a) When an excavation is carried out in deep deposits of soft clay without soil improvement, the soil mass on the passive side in front of the wall is subjected to substantial lateral compression and some amount of basal heave. This indicates that insufficient ground resistance has been provided by the soil below the excavation level to restrain the retaining wall, and as result of this, causing large associated ground movements.

(b) When soil of a certain thickness at a particular depth in the passive side is entirely improved, the ground resistance in front of the wall increases, resulting in reduced associated ground movements. This embedded improved soil layer was found to behave like a strut, mobilising its resistance from the compression effect of improved soil in between the two walls to transfer the lateral force from the active side. As a result of such provision, the stiffness of improved soil strut, which directly affects the composite stiffness of passive ground, is the key parameter to be considered in design. Notwithstanding the positive contribution of a stiffer improved strut in restraining the retaining wall, it is also noted that a stiffer improved soil strut would yield a higher bending moment in the retaining wall. This is an important consideration to ensure a safer design.

(c) In the case when the soil improvement has a gap of untreated soil in between the retaining wall and improved soil layer, the performance of the excavation drops significantly with almost 100% increase when the width of gap is doubled. The ground movements were induced even during the initial stage of excavation but it was noted that these movement are gradual even at greater depth of excavation. Though the improved soil layer is still behaving like a strut, the high compressibility of the untreated soil in between the retaining wall and improved soil layer has affected the composite stiffness to a large degree.

(d) For a cost-effective design, an embedded improved soil berm is sometimes used in excavations, especially when the excavation area is large. The 10m berm was found to be almost as effective as a strut. Nevertheless, the way the berm transfers the lateral force from the retaining wall to the surrounding soil, which is by a combination of skin friction and end bearing, is totally different from the behaviour of a strut. Instead of compressive strength, the passive resistance is provided mainly through the contact area of the shear resistance and end bearing. What is also clear in this case is that the stiffness of the berm does not have a significant effect on the performance during excavation. It is important to note that the failure behaviour of a berm is sudden and therefore, adequate provision in design should be allowed to avoid a catastrophic failure.

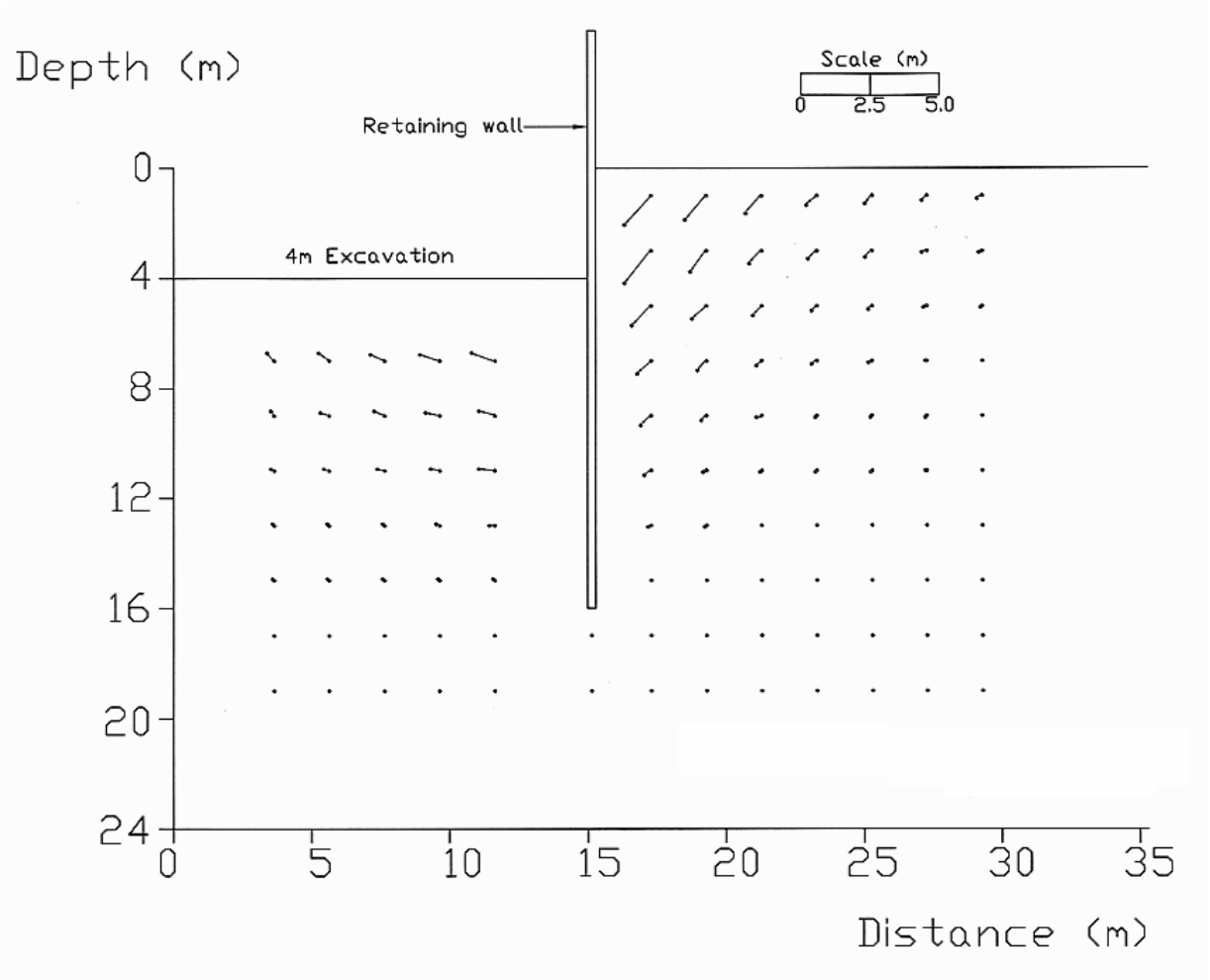

Figure 5.1 Ground displacement vectors in Test NTreat

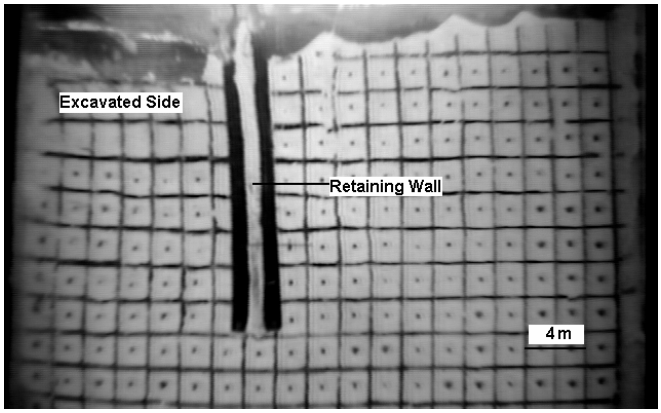

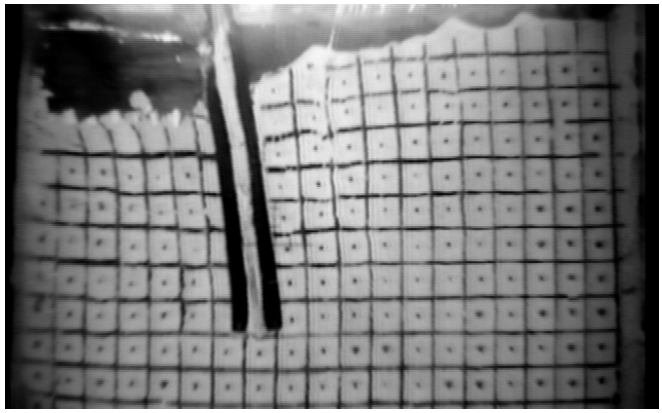

(i) After 2m excavation (ii) After 4m excavation

(a) Images of Test NTreat

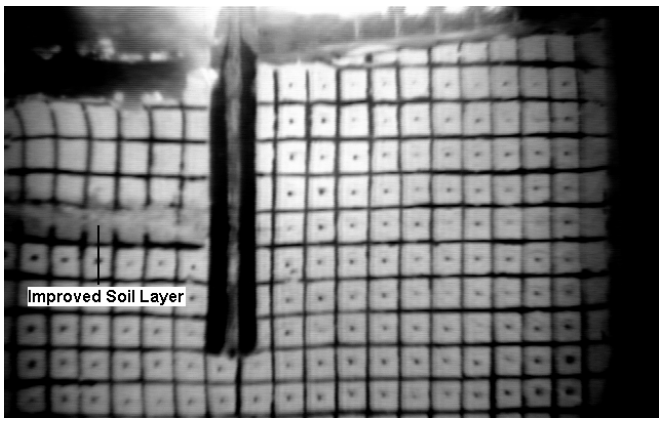

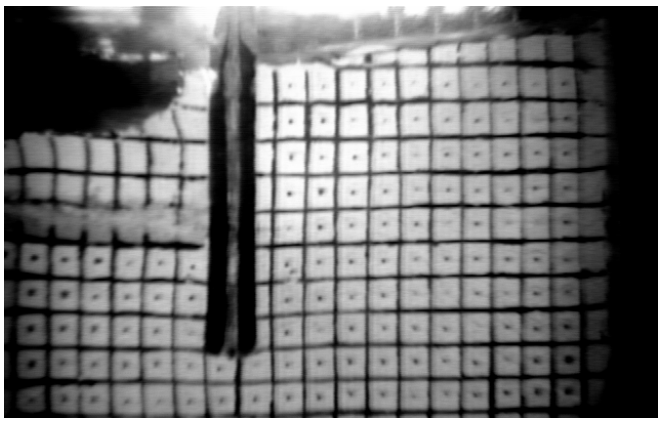

(i) After 2m excavation (ii) After 4m excavation

(b) Images of Test FTreat-7d

Figure 5.2 Images of Tests NTreat & FTreat-7d

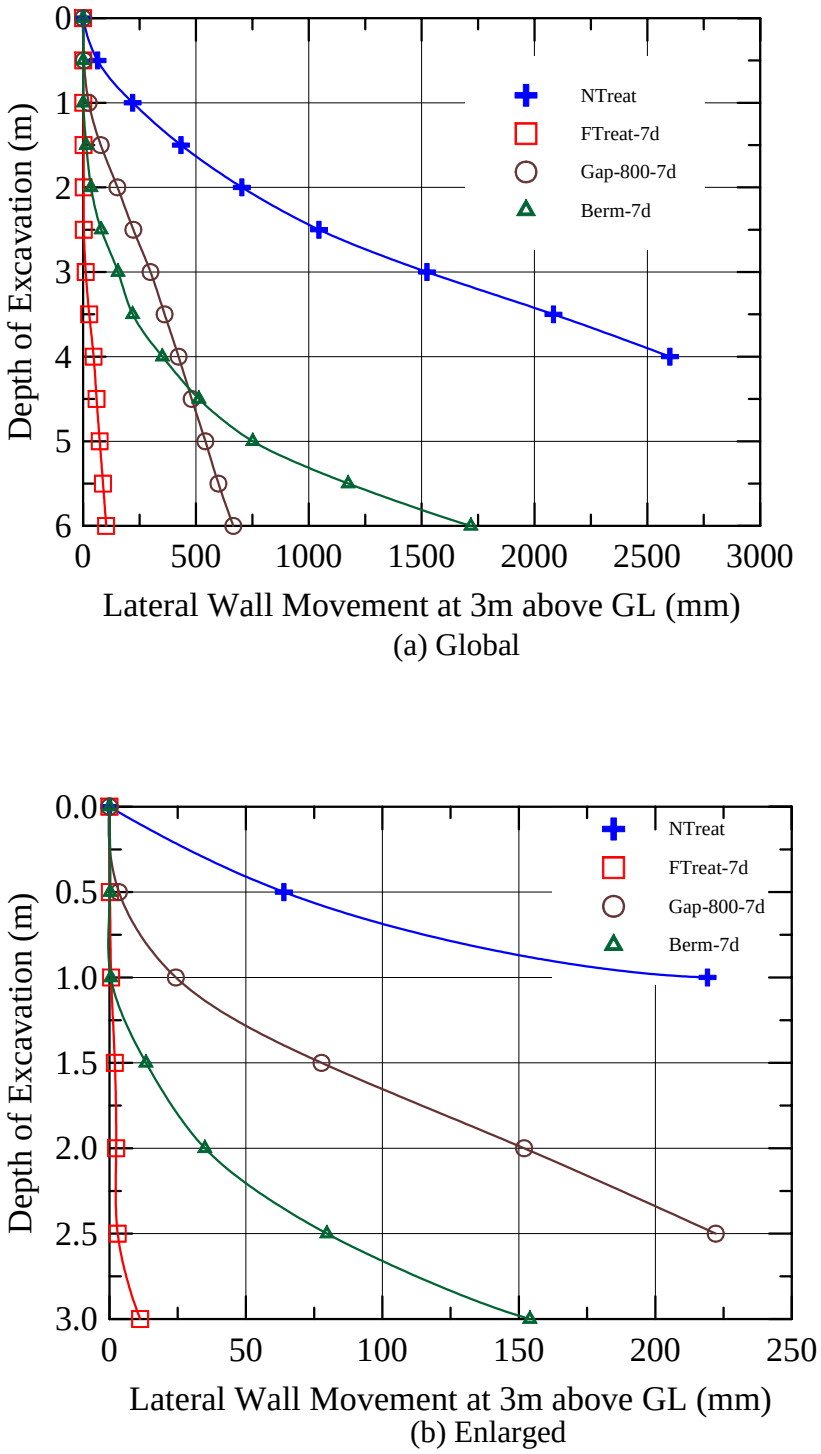

Figure 5.3 Lateral wall movement at 3m above ground level (GL) in Tests NTreat, FTreat-7d, Gap-800-7d and Berm-7d

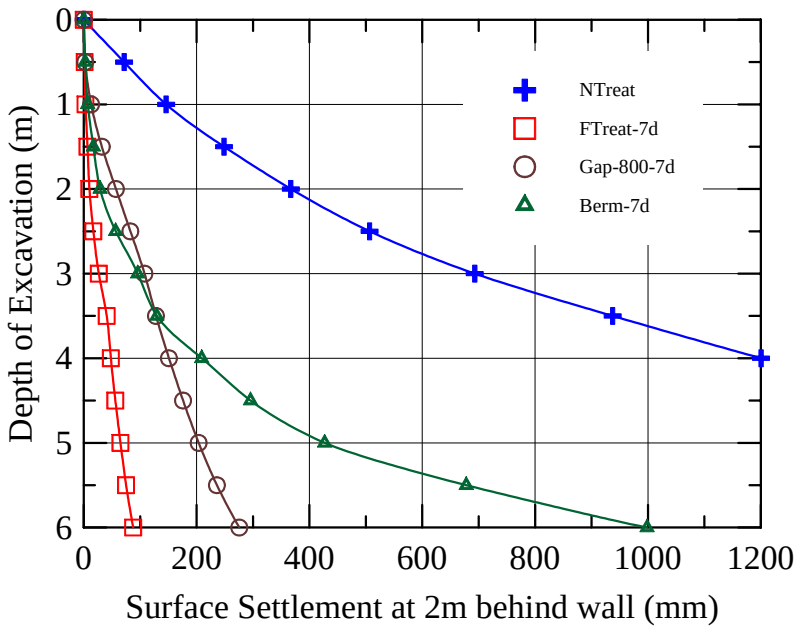

Figure 5.4 Surface settlement at 2m behind wall in Tests NTreat, FTreat-7d, Gap-800-7d and Berm-7d

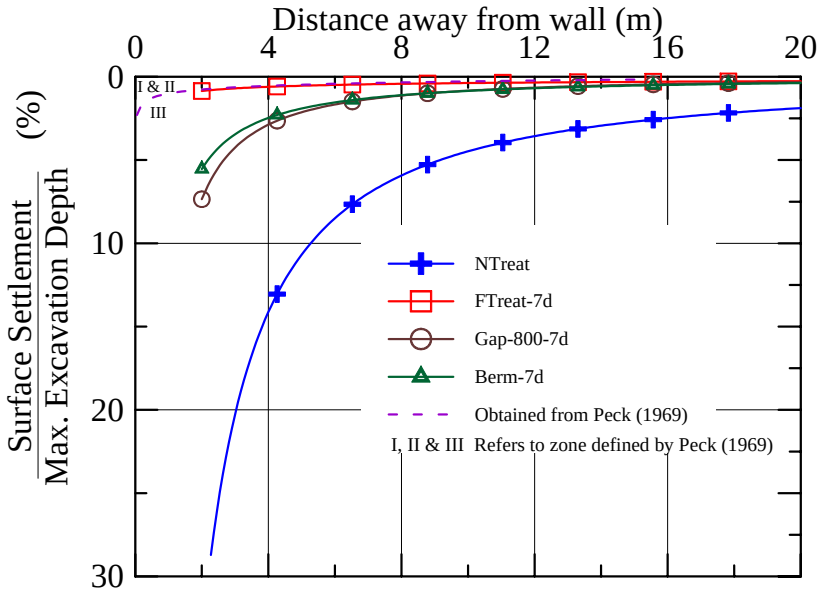

Figure 5.5 Normalised surface settlement behind wall in Tests NTreat, FTreat-7d, Gap-800-7d and Berm-7d

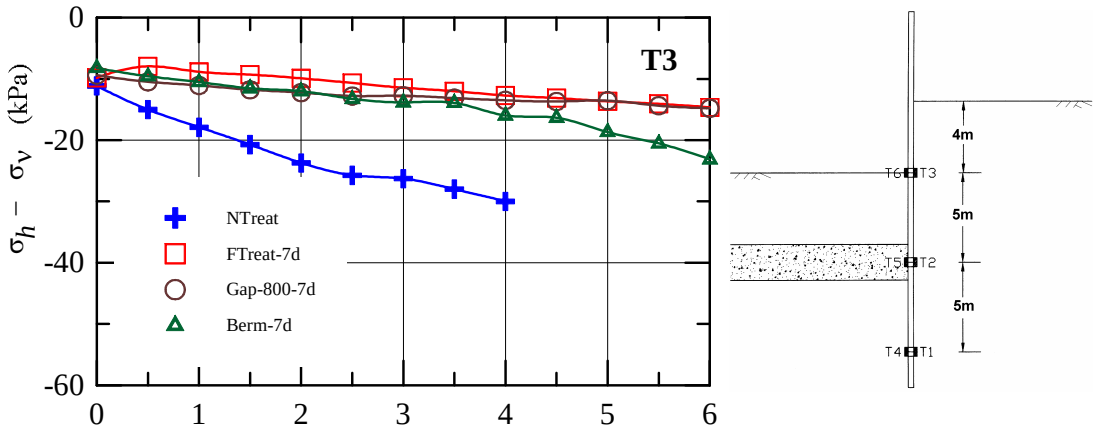

(a) Located at T3

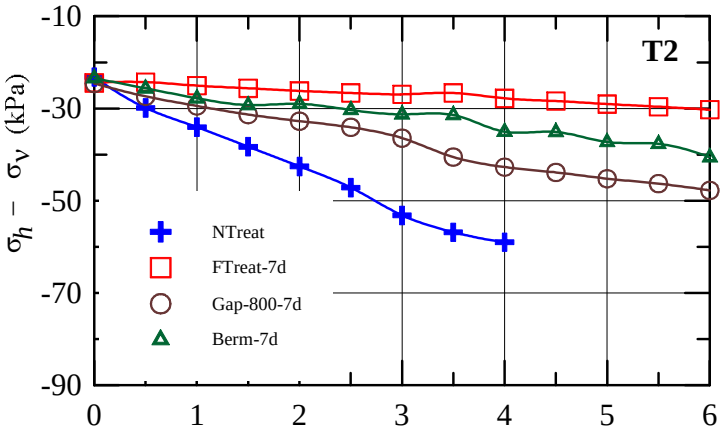

(b) Located at T2

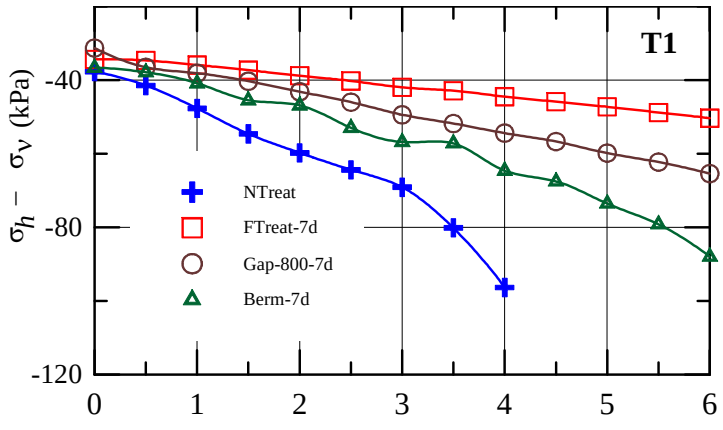

(c) Located at T1

Figure 5.6 Lateral earth pressure response in terms of deviatoric stress (σ_h-σ_v) in active side in Tests NTreat, FTreat-7d, Gap-800-7d and Berm-7d

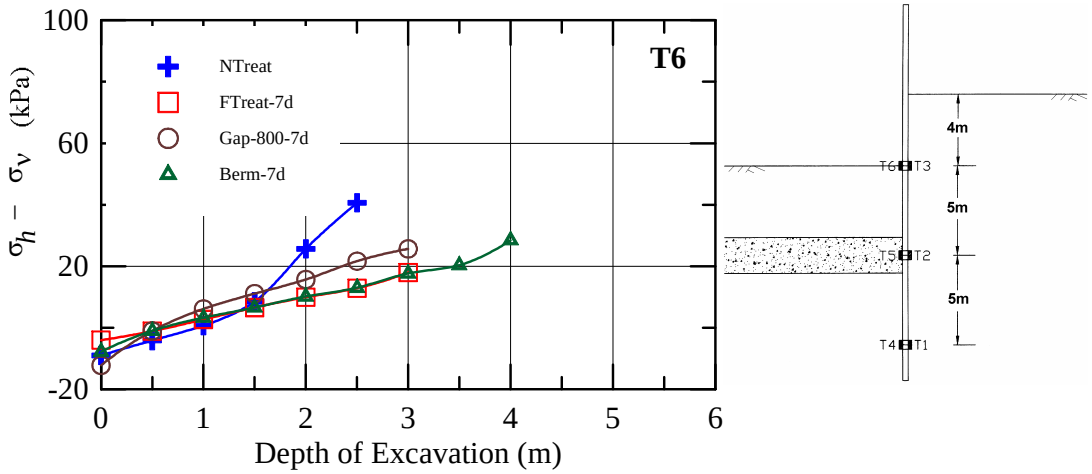

(a) Located at T6

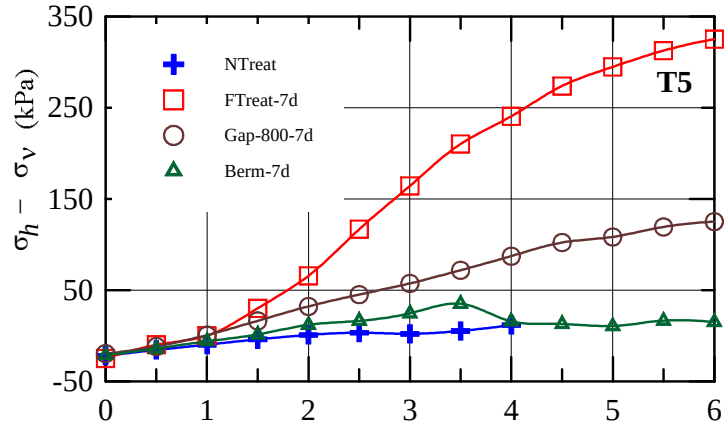

(b) Located at T5

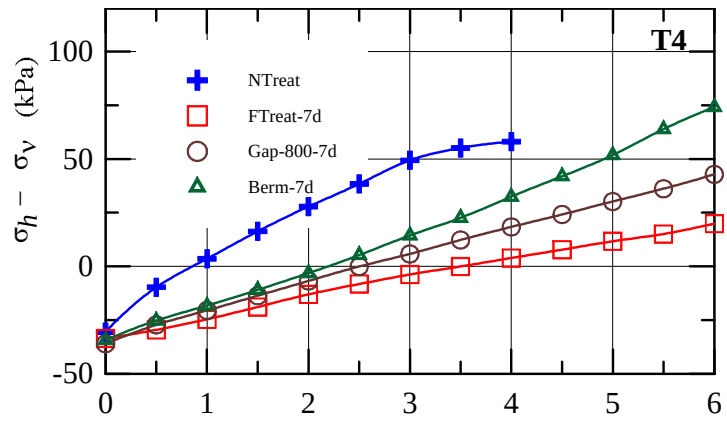

(c) Located at T4

Figure 5.7 Lateral earth pressure response in terms of deviatoric stress (σ_h-σ_v) in passive side in Tests NTreat, FTreat-7d, Gap-800-7d and Berm-7d

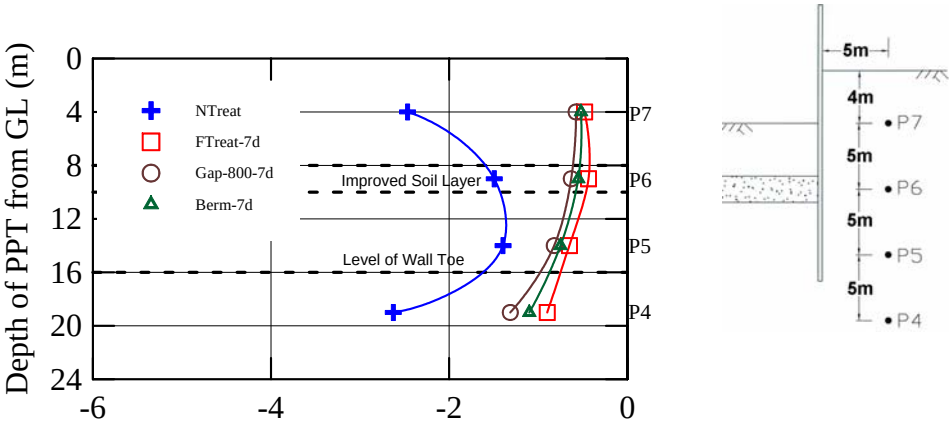

Figure 5.8 Pore water pressure response in Tests NTreat, FTreat-7d, Gap-800-7d and Berm-7d

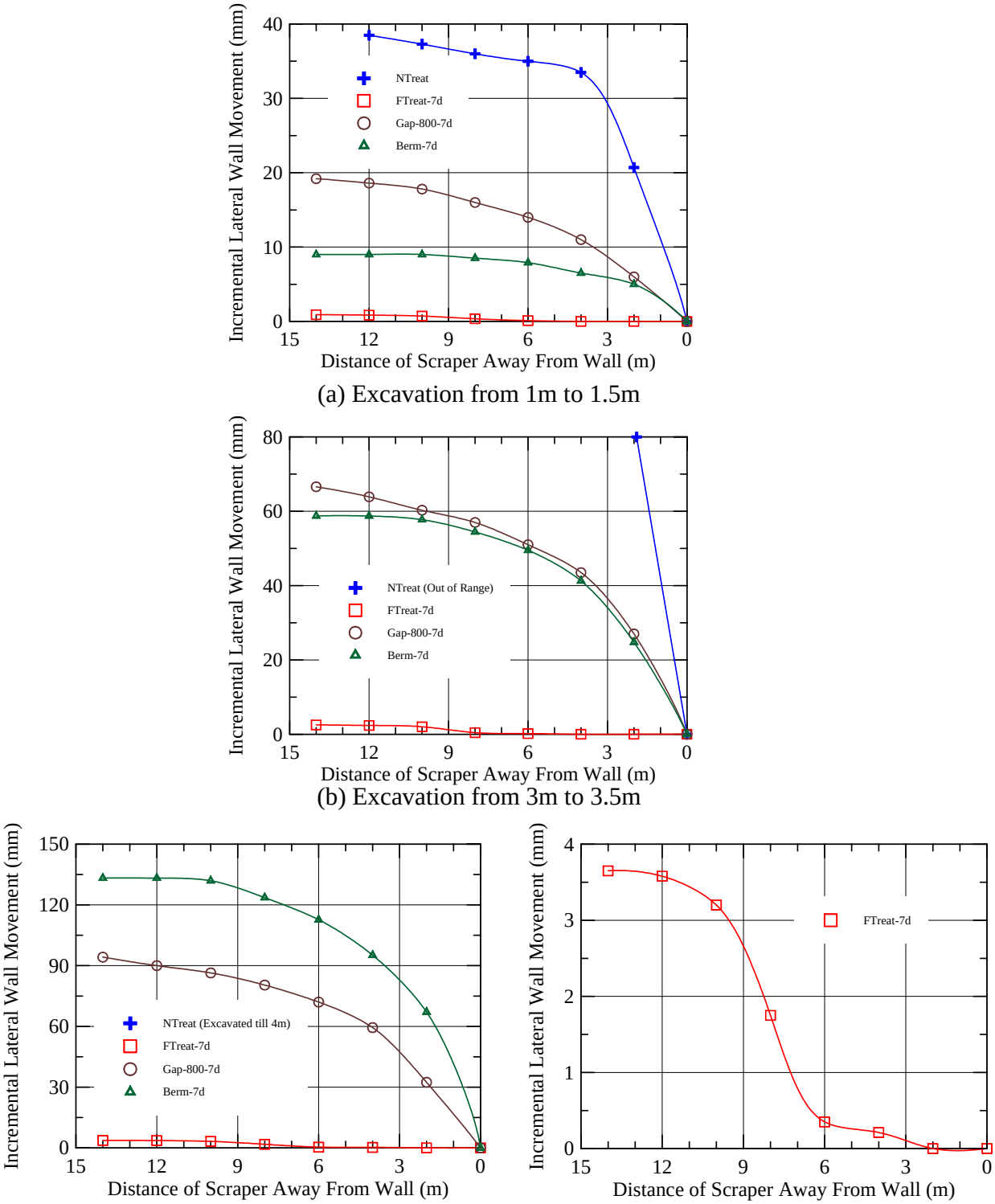

(a) Excavation from 1m to 1.5m

(b) Excavation from 3m to 3.5m

(i) Global (ii) Enlarged

(c) Excavation from 5m to 5.5m

Figure 5.9 Incremental lateral wall movement in Tests NTreat, FTreat-7d, Gap-800-7d and Berm-7d

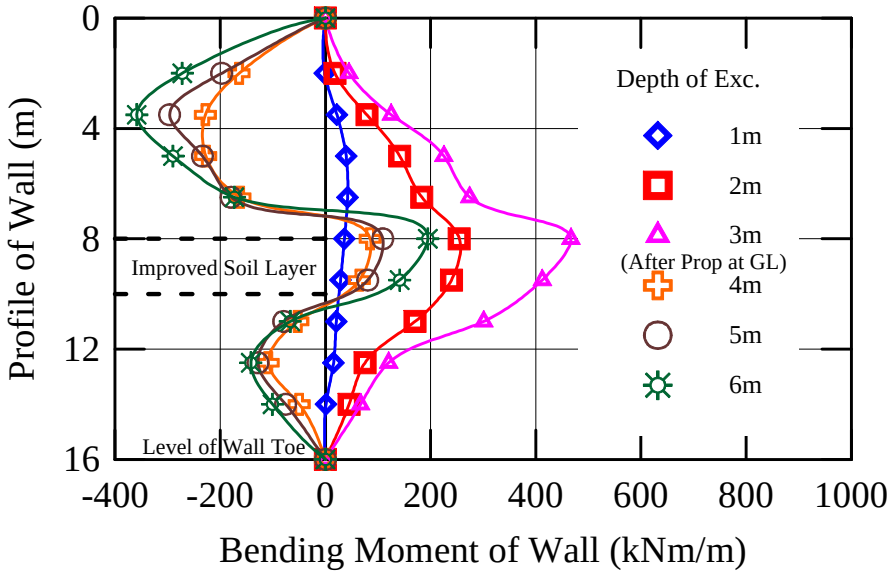

Figure 5.10 Profiles of wall bending moment in Test FTreat-7d-Strut

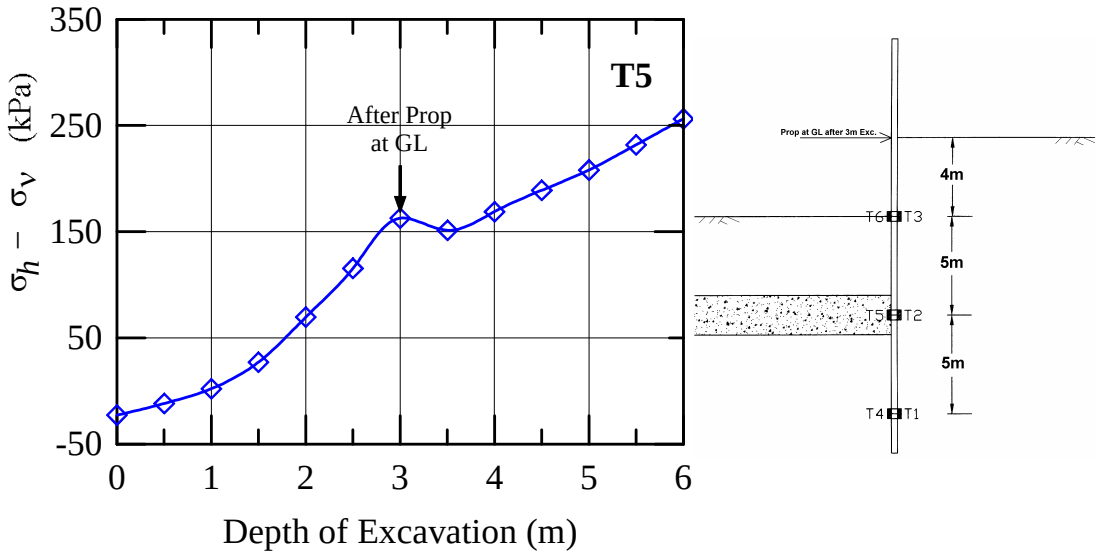

Figure 5.11 Mobilised lateral load resistance in Test FTreat-7d-Strut

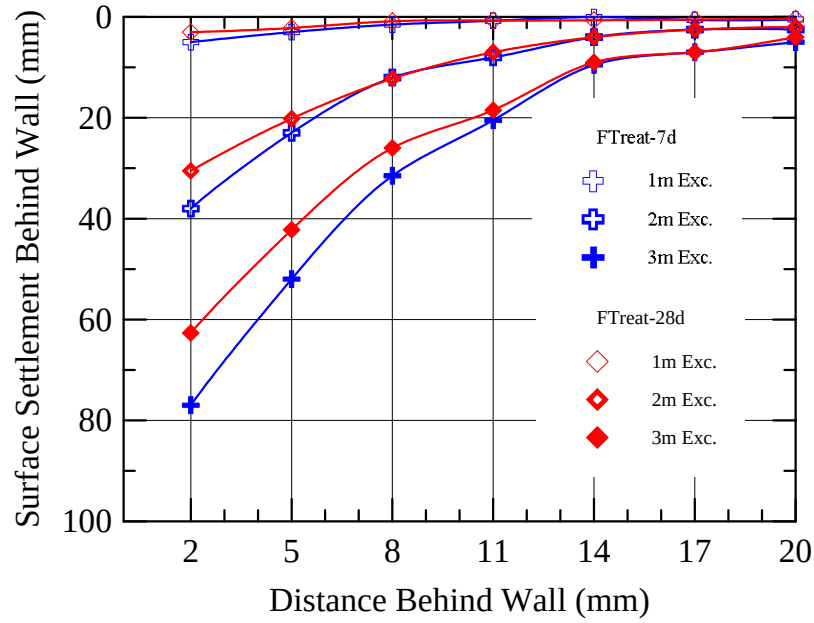

Figure 5.12 Surface settlement behind wall in Tests FTreat-7d and FTreat-28d

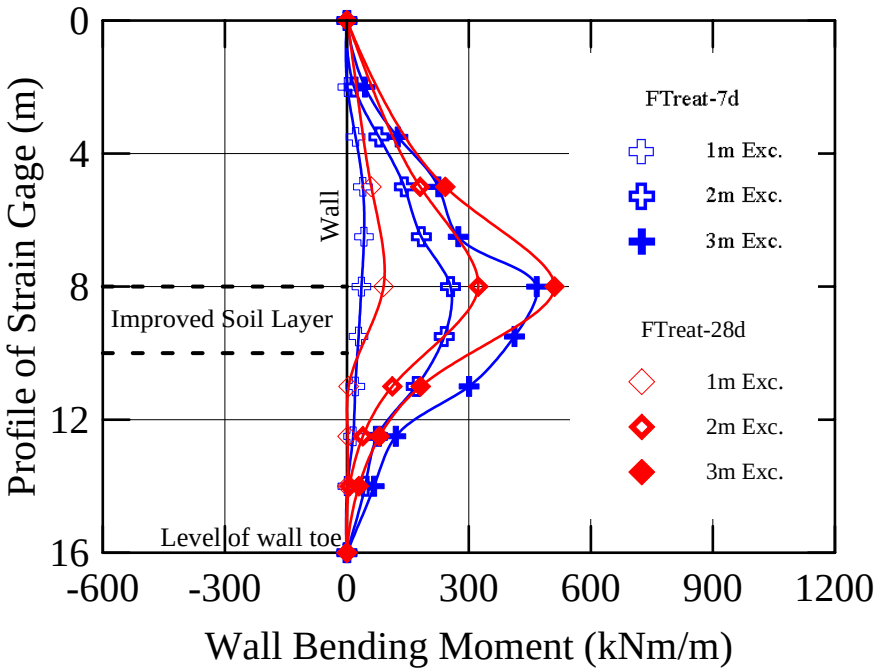

Figure 5.13 Profiles of wall bending moment in Tests FTreat-7d and FTreat-28d

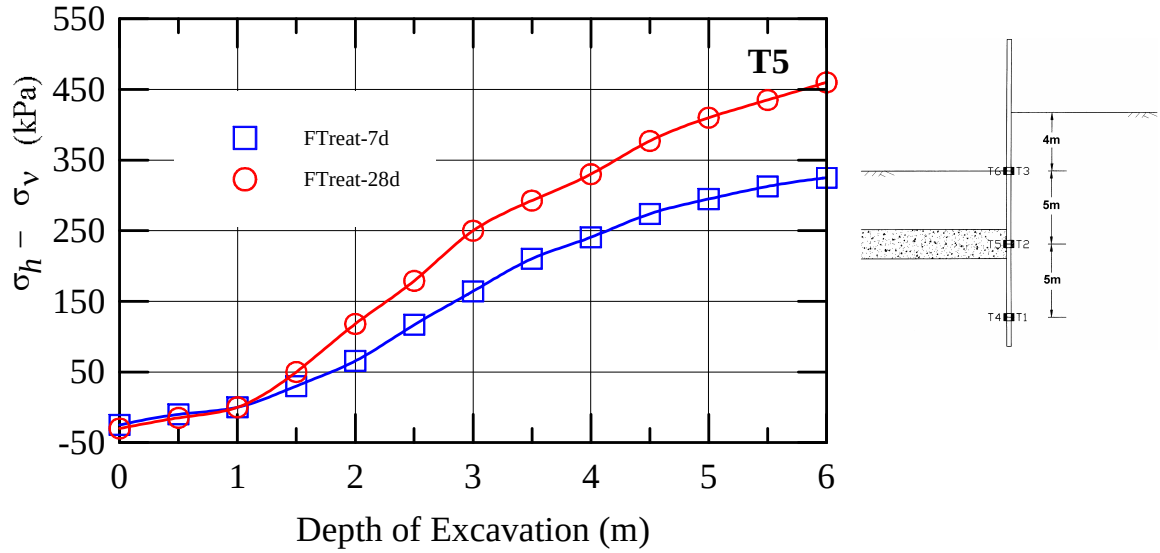

Figure 5.14 Mobilised lateral load resistance in Tests FTreat-7d and FTreat-28d

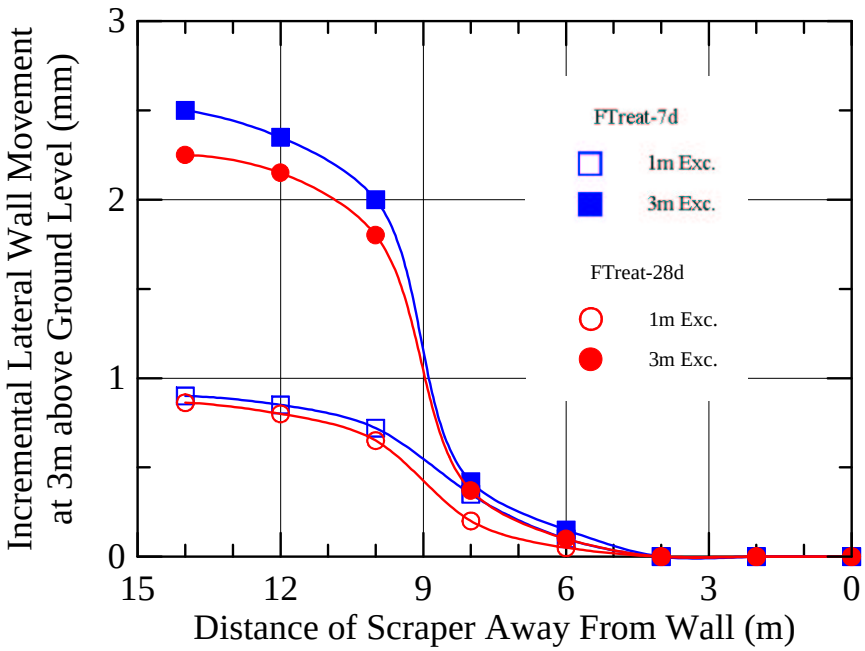

Figure 5.15 Incremental lateral wall movement in Tests FTreat-7d and FTreat-28d

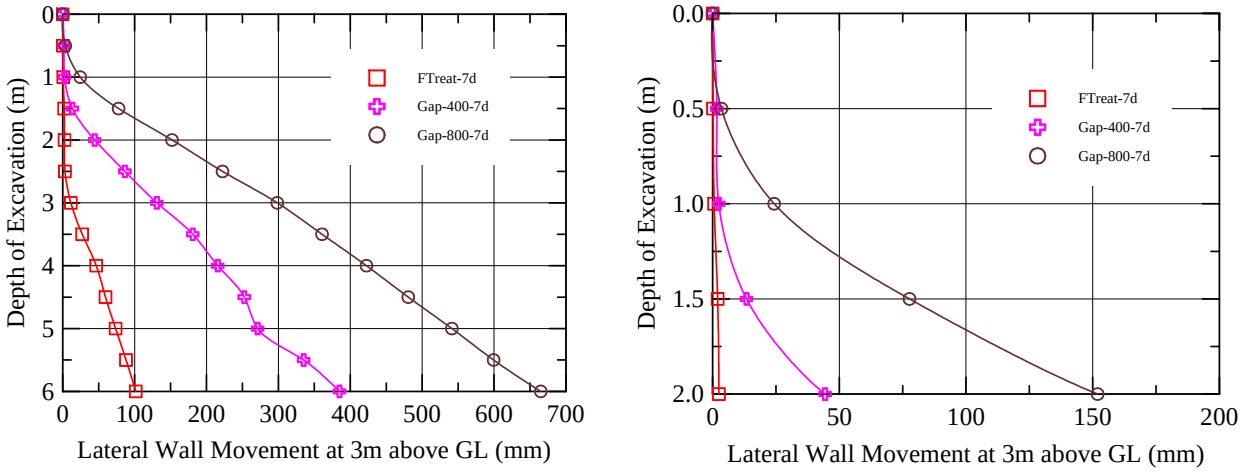

(a) Global (b) Enlarged

Figure 5.16 Lateral wall movement at 3m above ground level in Tests FTreat-7d, Gap-400-7d and Gap-800-7d

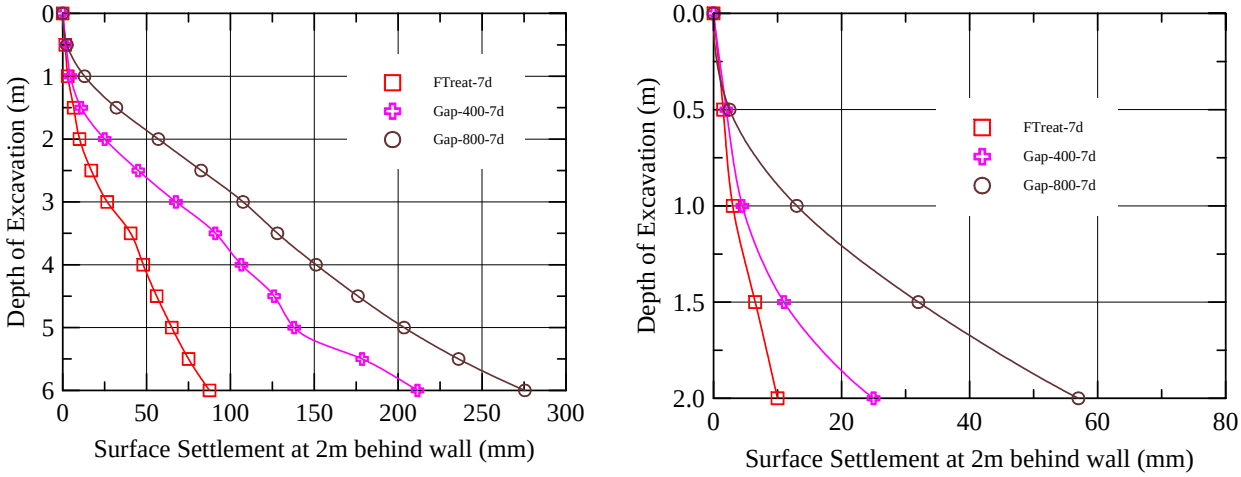

(a) Global (b) Enlarged

Figure 5.17 Surface settlement at 2m behind wall in Tests FTreat-7d, Gap-400-7d and Gap-800-7d

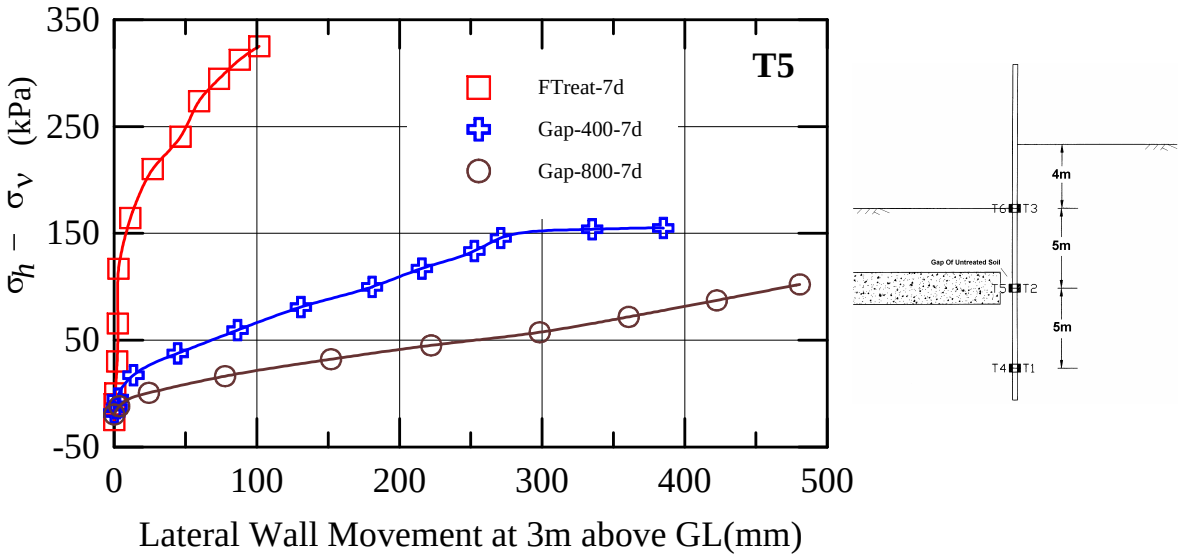

Figure 5.18 Mobilised lateral resistance with lateral wall movement in Tests FTreat-7d, Gap-400-7d and Gap-800-7d

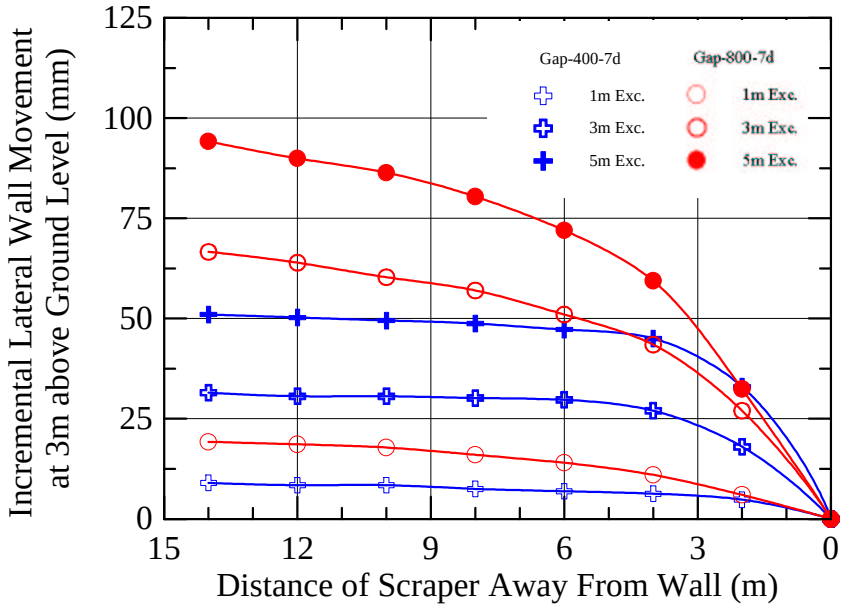

Figure 5.19 Incremental lateral wall movement in Tests Gap-400-7d and Gap-800-7d

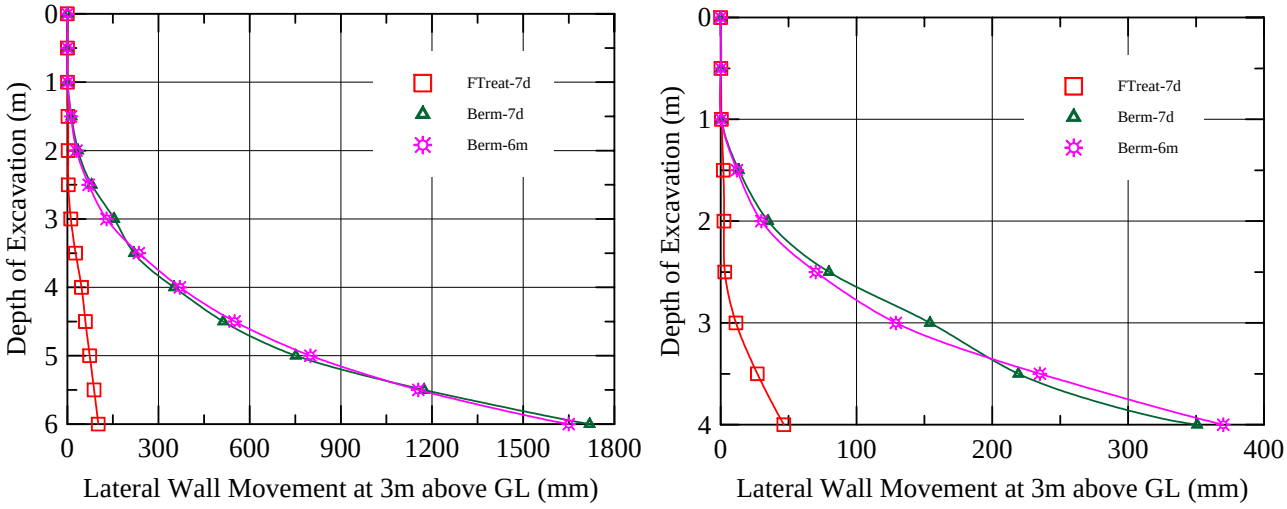

(a) Global (b) Enlarged

Figure 5.20 Lateral wall movement at 3m above ground level in Tests FTreat-7d, Berm-7d and Berm-6m

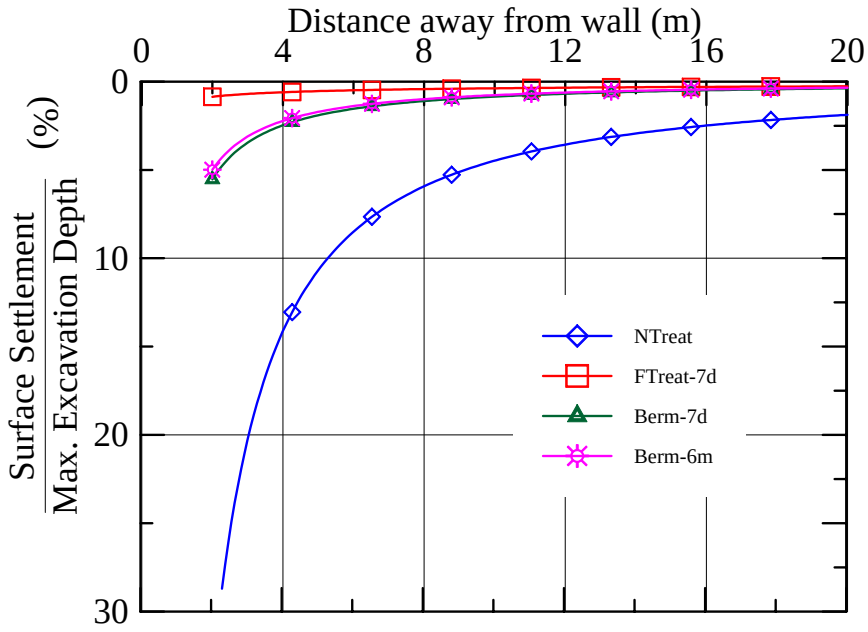

Figure 5.21 Normalised surface settlement behind wall in Tests NTreat, FTreat-7d, Berm-7d and Berm-6m

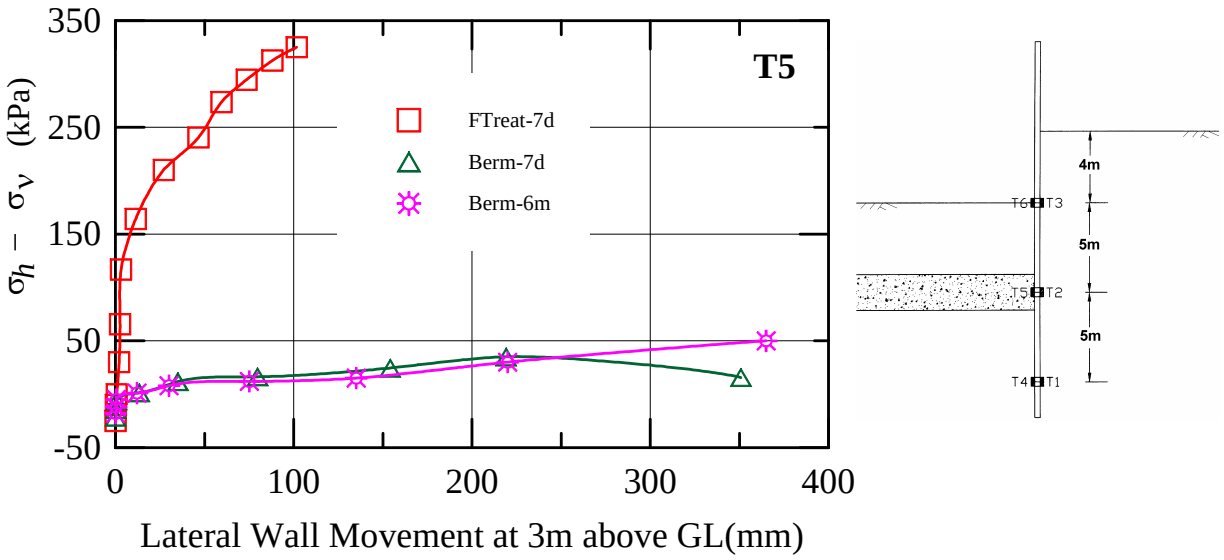

Figure 5.22 Mobilised lateral resistance with lateral wall movement in Tests FTreat-7d, Berm-7d and Berm-6m

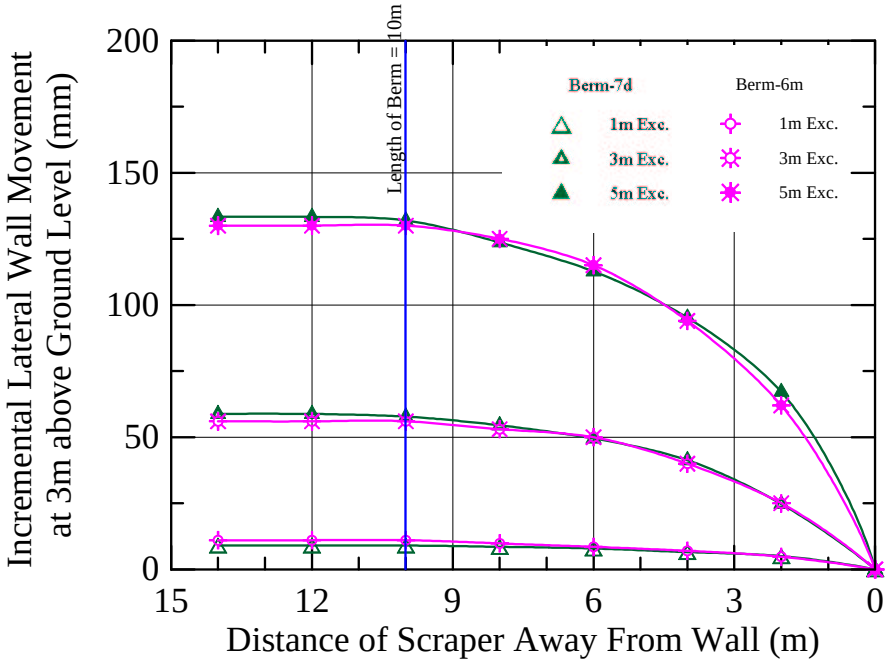

Figure 5.23 Incremental lateral wall movement in Tests Berm-7d and Berm-6m

Chapter 6

BEHAVIOUR OF AN EMBEDDED IMPROVED SOIL LAYER

6.1 Introduction

In the preceding chapter, results from a series of excavation tests performed on the centrifuge were used to distinguish certain behaviour of excavation stabilised with different arrangements of improved soil layer. It was clearly shown that there were distinct differences on how the composite ground on the passive side had mobilised its resistance. Instead of relying solely on the compression of the improved soil as in the case of an improved soil strut, there were other important contributing factors (e.g. gap and berm) that could also affect the performance of the embedded improved soil layer. In effect, these experimental results have provided considerable amount of evidences that the behaviour of a stabilised excavation is much more complicated. The behaviour of the embedded improved soil layer during excavation has not been analysed in detail previously, mainly due to a dearth of quality data, both from field and model tests. As shown in Chapter 5, this has been partly alleviated with the series of centrifuge tests that had been conducted.

As centrifuge tests are complicated and time-consuming, it is impractical in this study that all desired tests are to be conducted using the centrifuge technique. Furthermore, the instrumentation technology and data acquisition system employed during these centrifuge tests (as discussed in Chapter 4) could not allow enough measuring devices to be installed in each test and as a result, only a limited range of data could be captured. Also, installing too many instruments at one time will cause significant disturbance to the soil sample in a small-scaled model. Owing to such constraints, there are insufficient experimental data for providing a detailed

understanding of the mechanisms involved.

Considering the limitation of centrifuge testing, one solution is to use a numerical method to complement the study. The numerical method is an effective approach as it can provide comprehensive outputs at all desired locations. However, the major concern of a numerical study is that the analysis is highly dependent on the input material parameters and selected models, which may not simulate accurately the real behaviour. This is where the centrifuge test results available can be used to complement results from the numerical analysis to ensure the right behaviour is correctly captured. This will facilitate the understanding of mechanisms of the embedded improved soil layer through detailed parametric studies.

6.2 Finite Element Method (FEM)

6.2.1 CRItical State Programme (CRISP)

Two-dimensional numerical analysis was performed using a finite element (FE) program called CRISP (**CRI**ctical **S**tate **P**rogram). This program incorporates a fully coupled consolidation analysis based on Biot's formulation using a number of well-known constitutive models for soils, which have been widely used to study problems related to excavation and earth retaining structures [Powrie and Li (1991 and Yong et al. (1996)]. In this study, numerical analyses were carried out using the commercial version known as SAGE-CRISP [Woods and Rahim (1999)]. Details of the CRISP program will not be given here but can be found in Britto and Gunn (1987).

In the present numerical study, the Finite Element Method (FEM) was preferred over classical empirical and semi-empirical approaches because the retaining structures analysed using these conventional methods could only address the stability issue without offering means to predict the ground deformation directly. It is

particularly crucial in this study to be able to assess the stress and strain behaviours of the embedded improved soil layer so as to understand in greater detail the mechanisms involved. These aspects can be addressed by the FEM, which basically treats the soil as a continuum. The FEM takes relatively longer time to execute but nowadays, it no longer a problem with the availability of powerful desktop computational resources.

6.2.2 Selection of Input Parameters

For an appropriate simulation of the mechanical behaviour of an excavation support system using the FE analysis, it is crucial to realistically model the stress-strain behaviour of the soil. Besides using the basic linear elastic model derived from Hooke's Law, constitutive soil models that are capable of simulating the plastic behaviour of soils have also been used. Currently, there are three main types of soil models that are widely used in geotechnical engineering and excavation analyses especially in engineering practice, namely: -

(a) Hyperbolic stress-strain model such as those used by Clough, Duncan and their colleagues [Duncan and Chang (1970), Tsui and Clough (1974)] as well as other researchers [Balasubramaniam et al. (1976), Wong and Broms (1989), Ou and Chiou (1993)].

(b) Elastic-perfectly-plastic model of Mohr-Coulomb or Druck-Pager criteria [Brown and Booker (1985), Yong et al. (1989), Smith and Ho (1992)].

(c) Cam-Clay models including the Schofield model [Schofield and Wroth (1968)], Critical State model [Zienkiewicz et al (1972)], Cap model [DiMaggio and Sandler (1971)] and modified Cam-Clay model [Simpson (1972), Britto and Kusakabe (1984), Lee et al. (1989)].

In this study, the soil in the model ground was simulated using the modified

Cam-Clay model. The modified Cam-Clay is an isotropic, non-linear, elasto-plastic strain hardening soil model, which has originally been developed at the University of Cambridge in the 1960s. For the model described by Roscoe and Burland (1968), it is usually called the modified Cam-Clay in order to distinguish it from an earlier model described by Schofield and Wroth (1968), known as the original Cam-Clay model. The main soil properties for the modified Cam Clay soil model (λ, κ) used for the FE analyses were obtained from oedometer test results on remoulded soil samples (please refer to Chapter 4). If there was insufficient information available, reported values (M and Poisson's ratio, ν) from other sources were used [e.g. Bolton et al. (1989)]. Typically, the variation of M and ν for similar type of clay is expected to be small and also less sensitive to the overall behaviour of the excavation. The input parameters used are summarised in Table 6.1.

The improved soil layer was modelled using the elastic-perfectly-plastic model following the yield criterion of Mohr-Coulomb. The Mohr-Coulomb yield criterion is also widely used for soils, especially for a stiffer material. The main parameters for the Mohr-Coulomb used for the FE analyses, E (Young's modulus) and C (shear strength), were determined from a series of unconfined compression tests (please refer to Chapter 3), as shown in Table 6.2. In most situations involving stabilised excavation, the failure state will not be reached and therefore, capturing the right E of the improved soil layer is more important as compared to the c value. The model retaining wall has also been modelled using the elastic-perfectly-plastic model of Mohr-Coulomb and its properties are shown in Table 6.3.

6.2.3 Generated Mesh, Boundary Conditions and In-situ Stress States

Meshes used for the FE analyses are shown in Figure 6.1. Eight nodes

quadrilateral elements were used to model the soft ground, diaphragm wall and improved soil layer. The geometry of these meshes followed strictly the dimension of the centrifuge tests in model scale. All vertical boundaries are restrained against horizontal translation but are free to move vertically. The horizontal boundary at the bottom of mesh is restrained both horizontally and vertically while the top horizontal boundary, which represented the ground surface level, is free.

In this study, the soil profile comprised two layers, namely the normally consolidated (NC) clay that underlay a thin layer of over-consolidated (OC) clay. The vertical and horizontal effective stresses were calculated from the bulk unit weight and the K_o values of the two soil layers. Since a single soil model was used, these two layers were distinguished through the initial stress condition by using different over-consolidation ratio and K_o value.

For normally consolidated clay, the coefficient of lateral earth pressure, K_o was determined using Jaky's (1944) relation,

$$K_o = K_{nc} = 1 - \sin \phi' \tag{6.1}$$

where ϕ' is the effective friction angle

For over-consolidated clay, K_o was determined from the empirical relationship proposed by Wroth (1975),

$$K_o = OCR.K_{nc} - \frac{\nu'}{1-\nu'}(OCR-1) \tag{6.2}$$

where OCR is the over consolidation ratio, ν' is the Poisson ratio, and K_{nc} is obtained using Equation (6.1)

6.2.4 Simulation of Construction Sequence

Each stage of excavation was simulated using an increment block in the FE

analysis. In these FE models, the excavation was simulated by removal of elements at the excavated zone from the mesh. An important point to note here is that this simulation by removing elements en-bloc is almost identical to the scrapping of an entire layer of soil in the centrifuge. CRISP uses an incremental non-linear tangential stiffness approach and therefore, it is imperative that the load steps used are adequately small to avoid large cumulative errors. Each increment block simulating the construction sequence was divided into adequate number of sub-increments to resemble the incremental load application over the specified time frame. As the analyses were based on Biot's fully coupled consolidation theory, the increments were also used to simulate the gradual dissipation of pore water pressure with time.

6.2.5 Comparison of FEM and Centrifuge Test Results

A comparison of ground displacement vectors from the FEM and centrifuge results for the excavation test without soil improvement (NTreat) is shown in Figure 6.2. It can be seen that displacement vectors from the FE analysis using the soil parameters in Table 6.1 agree reasonably well with those obtained from the centrifuge test though there are some discrepancies. On the active side next to the wall, the predicted value is smaller than measured values while away from the wall, the predicted value is much bigger. Both aspects are well known. In the present numerical analysis, no slip element is used and thus the model cannot capture the behaviour next to the wall accurately. The use of Modified Cam-Clay model is unable to account for the non-linear elastic behaviour at small strain and this partly explains the deviation some distance away from the wall where the strain is expected to be very small. Nevertheless, the reasonable match of the overall pattern of the displacement especially on the passive side shows that the input parameters used are acceptable.

Though further fine-adjustment was clearly possible to ensure better fit to these results, this was not done, as the main purpose of the numerical analyses was not to develop precise quantitative results, but rather to capture the right trend of behaviour.

A comparison between numerical and experimental results was also made for three stabilised excavation tests, namely Tests FTreat-7d, Gap-800-7d and Berm-7d. As shown in Figure 6.3, the surface settlements at 2m behind the wall predicted by the FE analyses produced results quite consistent with those from the centrifuge tests except for the case when an improved soil berm is used. Nevertheless, this suggests that the input parameters used are reasonable, providing some confidence in the outputs from further FE analyses. Though the current verification was only based on displacement results, attempts were also made to compare other types of measurements. These will be presented intermittently in this chapter.

6.3 Resistance Mechanism of An Embedded Improved Soil Strut

In the preceding chapter, the way resisting forces have been mobilised by an embedded improved soil strut was discussed entirely using results from centrifuge tests. It was shown that an embedded improved soil strut had mobilised its resistance through compression. Thus, the stiffness of an improved soil strut is an important parameter governing its performance during an excavation. However, as mentioned earlier, results from the centrifuge tests were not detailed enough to provide a full picture of the way various stresses were being mobilised in the improved soil strut.

6.3.1 Distribution of Stresses in the Embedded Improved Soil Strut

To better understand how the embedded improved soil strut reacts during the process of excavation, stresses induced in the improved soil layer were examined from

the numerical simulation of Test FTreat-7d. Figures 6.4 present the deviatoric stress of vertical sections across the embedded improved soil layer at various distances away from the retaining wall. Stress profiles at a distance 0.25m away from the wall for excavation depths of 3m and 5m [Figure 6.4 (a)] showed that stresses were concentrated at both corners of the improved soil layer next to the wall, while much lower stresses were registered towards the centre. The stresses are concentrated at both corners because these are sharp corners and in mechanics, a sharp corner is a stress concentrator. In reality, such corner is likely to yield and the over-loading is then reduced by stress spreading.

A comparison of the deviatoric stresses induced in the mid-depth of the embedded improved soil layer was made between results from the FE analysis and the centrifuge test (FTreat-7d) as presented in Figure 6.4 (a). As can be seen, deviatoric stresses predicted by the FE analysis agree reasonably well with measured values, though the values for the deeper excavation of 5m did not match so well. Considering the fact that the soil model is a simplified critical state model and no refinement in soil parameters has been carried out, this level of matching is reasonable. A point to note here is that the vertical stress, σ_v used to derive the deviatoric stress from the experimental centrifuge test results is merely an estimation instead of the actual measured value.

The stress profile of the vertical section across the embedded improved soil layer at a distance 3.5m away from the wall was shown in Figure 6.4 (b). Higher stresses were observed at the top of the improved soil layer, reducing towards the bottom. However, this trend reversed when vertical sections were taken at distances 8m and 12m away from the wall [Figures 6.4 (c) and (d)]. Here, stresses at the bottom of the improved soil layer were higher. Stresses were also assessed at horizontal

sections across the embedded improved soil layer at the top, middle and bottom levels. As shown in Figure 6.5, again, stresses were concentrated at both corners of the improved soil layer next to the retaining wall. Stresses along the top of the improved soil layer were decreasing with distance away from the wall, but an opposite trend was observed when stresses along the bottom of the improved soil layer were evaluated. Stresses along the mid-level of the improved soil layer were rather constant.

From these stress results, it is clear that there are two locations in the embedded improved soil strut where there is a concentration of high deviatoric stresses; these are located at the two corners adjacent to the retaining wall. These are the regions in the embedded improved soil layer that are likely to be subjected to substantial yielding. In the present numerical analysis, no interfacial elements were used at the interface between the wall and the improved soil strut and this could cause some deviation from what is observed. In addition, stresses at regions along the top part closer to the wall and the bottom part further away from the wall are relatively higher. These are indications, which reflect the way the embedded improved soil strut will deform during an excavation.

6.3.2 Deformed Shape of the Embedded Improved Soil Strut

To better understand the deformation of the embedded improved soil strut during an excavation, vertical displacement along the bottom face of the improved soil layer was plotted in Figure 6.6(a). The total vertical stress along the same bottom face of the improved soil strut was also evaluated as shown in Figure 6.6(b) so that the correlation of this parameter to the pattern of deformation could be observed. The trend of the total stresses is highly consistent with the expectation that the presence of an improved soil strut has an important capping effect on the heaving of the soft layer

below the strut.

This series of results suggests that the deformed shape of the embedded improved soil layer during an excavation will look like an upward arch as proposed in Figure 6.7 or one-half of a beam with fixed ends subjected to net pressure acting on the bottom surface. With the kind of curvature from the arch shape, higher stresses will be expected at several locations as shown in this figure. This ties in very well with results put forth earlier on the way stresses are distributed in the embedded improved soil layer. In addition, this arching behaviour of the embedded improved soil layer was postulated in section 5.2.6. During the centrifuge test, it was found that the incremental wall movement would only develop after a certain amount of soil had been removed from the retaining wall, suggesting that bending of the improved soil layer was the main mode of movement. Tanaka (1993) also proposed a similar kind of deformed shape [Figure 2.9 (d)] from field-instrumented results.

6.3.3 Design Consideration at Sharp Corner

In the preceding section, it was shown that stresses were concentrated at both sharp corners of the improved soil layer next to the wall. Considering the fact that these regions have a greater potential for yielding, it is important to ensure that the improved soil has adequate shear strength within its yielding range to be mobilised to avoid any compression failure. This could be done by comparing the strains at yielded zone with that of the actual strain-compatible strength of the improved soil, ensuring that the actual strength remains higher than the mobilised strength at that level of strain.

Figures 6.8 and 6.9 present the deviatoric stress and horizontal strain distributed at all integration points within the improved soil layer. As shown, high

stresses and strains were found at integration points on these sharp corners of the improved soil layer. This is unavoidable because these sharp corners are stress concentrators. Instead of stresses at a sharp corner moving towards infinity as in a case of a perfectly elastic material, in the present case, the material will undergo plastic yielding as the improved soil is assumed to behave like an elasto-plastic material as suggested by the typical test results shown in Figure 3.9. Though this issue seems academic, in reality, it has actual practical implication.

To evaluate this, the results of design analyses on one section of the excavation for the construction of a major expressway in Singapore are used. In this project, the width and depth of the excavation are 50m and 20m respectively. Due to a deep deposit of marine clay (40-50m thick), the contractor of this project decided to terminate the sheet pile wall in the soft deposit of marine clay. A layer of 3.5m thick jet grout slab is to be installed prior to excavation to provide an embedded improved soil strut to support the retaining walls below the final excavation level. The construction method adopted is common, which is based on a sequence usually referred to as the bottom up excavation.

At the design stage, concern was raised on the maximum stresses being developed in the improved soil struts, picked out in the design process. The original concept of design was to provide an improved soil layer with an adequate factor of safety against the maximum expected stress. This concern was investigated and as a result, it was found that these are isolated stress concentration points, located next to the corner adjacent to the retaining wall. To demonstrate that the high stresses were actually due to the presence of a sharp corner, results from similar FE analyses were examined. In the first run, 6-node triangular elements were used and in the second run, 15-node triangular elements were used, which then will have integration points much

closer to the corner. These integration points are shown in Figures 6.10 (a) and (b) respectively.

Figures 6.11 (a) and (b) show the stresses developed respectively in each case. As can be seen, in the first run, the maximum stress developed at the corner is 770kPa and in the second run, the maximum stress developed is 883kPa. This analysis shows that as the mesh becomes more refined, the calculated stress at the closest integration point to the corner increases, because this point is moving closer to the corner. In both cases, the maximum stress is below the failure strength of 1000kPa. However, originally, this was deemed unacceptable, as the factor of safety achieved was inadequate.

6.3.4 Effect of Stiffness of Improved Soil Strut

The preceding chapter has put forth arguments that for an embedded improved soil layer to function as a strut, it needs to be stiff enough to transmit lateral forces from the retaining wall to the other stiff end without inducing excessive compression. The centrifuge results have shown that the effectiveness of an improved soil strut is very much dependent on its stiffness. However, the results also confirm the expectation that when a stiffer improved soil layer is used, though it provides a higher resistance to the retaining wall, it also induces a much higher bending moment in the wall. In retrospect, this is rather obvious. However, to the author's knowledge and experience from actual participation in similar design projects, this is hardly ever considered in design in Singapore. Clearly, engineers need to be aware of the implications.

Considering the fact that the stiffness of field core samples can vary considerably depending on the quality of workmanship and operational conditions on

site, it is difficult to estimate the actual stiffness of improved soil layer in the field. Besides having a large variation in the stiffness of field core samples [Figures 2.5 and 2.6], the fact that with different configurations, the improved soil columns will overlap differently further complicates the assessment of the true mobilised composite stiffness of the entire improved soil layer. At present, it is almost impossible for anyone to know accurately the true mobilised stiffness of the improved soil layer in the field. It is therefore common for geotechnical engineers to adopt a lower Young's modulus, E, in design, which will account for any of these imperfections. This is usually assumed to be a conservative approach. However, what is being recognised in this research is that the choice of a lower E is conservative only as far as the estimate of ground movement in adjacent ground is concerned. It is not conservative as far as the bending moment induced in the retaining wall is to be considered.

Nevertheless, results from material studies reported in Chapter 3 provided evidences that the Young's modulus (E) of cement treated clays could be much higher than anticipated. Due to non-linearity behaviour of the cement treated clays as shown in Figure 3.10, the E value at a lower strain (0.01%) was found to be 5 to 15 times larger than that at a higher strain (1%). The use of conventional LVDTs to measure displacements had also been found to underestimate the E value by as much as 2.3 times [Figure 3.11]. Moreover, it was shown in Figure 3.12 that the E value could increase further by 1.5 times if the curing time exceeded 28 days.

As the selection of E value has design implications, a parametric study was carried out to evaluate the effect of varying the stiffness on the performance of the embedded improved soil strut and its associated influence on the bending moment in the wall. Since centrifuge tests were very tedious and time consuming to conduct, this aspect was studied using the FE analyses. An expected practical range of E values

from 50 to 600 MPa was considered in this numerical simulation, which is based on Test FTreat. In the field, with other complications mentioned earlier, this variation could be even larger. Figure 6.12 (a) shows the impact on the bending moment in the wall with varying stiffness for the improved soil strut. As expected, there is an increase of bending moment in the wall when the stiffness of improved soil strut is higher. This trend is consistent with those observed from the centrifuge tests results.

To provide a quantitative guide on the increase of bending moment in the wall, the maximum bending moments for different E values were normalised by that for the case of E = 100 MPa [Figure 6.12 (b)]. The value of 100 MPa has been chosen because it falls within the typical range of E values (100-150MPa), commonly used in local design as a "rule of thumb" number. As shown in the figure, the increase in the wall bending moment follows a hyperbolic trend. When the E was initially doubled (200MPa), the bending moment increased by about 7%. However, when the E approached 1000MPa, the increase became insignificant. The overall increase in the wall bending moment was about 15-20%. Meanwhile, in the centrifuge tests, the wall bending moment increased from 467kNm/m to 511kNm/m when E values of improved soil of 300MPa and 450MPa were used, which showed an increase in the wall bending moment of about 10%. Since such increase could greatly affect the reinforcement in the wall. Therefore, it is recommended that in the design of retaining wall, the maximum expected stiffness in the improved soil should be used for analysis of the bending moment in the retaining wall while the minimum expected stiffness be used when assessing ground movements in the surrounding area.

To provide an insight on how a stiffer improved soil strut will react during excavation, stresses along the vertical and horizontal sections across embedded improved soil struts with different stiffness were examined. As shown in Figures 6.13

and 6.14, higher stresses were encountered when a stiffer improved soil layer was used. Figure 6.13 (a) illustrated again the stress concentration at both corners of the improved soil layer abutting the retaining wall but more importantly right here, these corners have attracted higher stresses with stiffer improved soil layer. Deviatoric stresses from centrifuge tests (FTreat-7d and FTreat-28d) have also shown a similar increasing trend. Since the main function of retaining wall is to resist the active earth pressure, more forces will be attracted into the wall with a stiffer improved soil strut.

Having said that, it is also important to recognise that the embedded improved soil strut requires certain stiffness above a threshold value. Results from a parametric study [Figure 6.15] shows that there exists a threshold range of between 100-200MPa, below which the strut would be ineffective and above which the increased effectiveness would be marginal.

6.4 Influence of Gap of Untreated Soil in between the Retaining Wall and Improved Soil Layer

In the preceding chapter, it was shown that the presence of a gap of untreated soil in between the retaining wall and improved soil layer has a tremendous effect on the performance of the overall support system. Significant movement was induced at an early stage of excavation when the overburden close to the retaining wall above the gap was removed. Although the embedded improved soil layer still behaved very much like a strut, high compression in the untreated soil in the gap occurred and as a result, the composite stiffness of the improved soil layer has been reduced significantly.

Owing to the small dimension of the gap in a scaled-down model (e.g. 400mm in prototype scale is equivalent to only 4mm in model scale), it is impossible for the

current instrumentation technology in centrifuge to install any miniature transducer to monitor the behaviour of the untreated soil in this tiny gap. Hence, the behaviour of gap captured during the centrifuge tests in the preceding chapter has to rely very much on indirect measurements, providing only an indicator to the performance of the excavation. It is therefore necessary to adopt a numerical approach here so that more detailed outputs can be studied to complement the results from the centrifuge tests.

6.4.1 Behaviour of Gap of Untreated Soil

From the centrifuge tests, results on the lateral wall movement have indirectly showed that the untreated soil in the gap was highly compressed when the lateral force from the wall was exerted onto it. To illustrate this more clearly, stress and strain behaviours of the untreated soil in the gap from FE analysis, simulating Test Gap-800-7d are evaluated first. Figures 6.16 and 6.17 show the deviatoric stress and horizontal strain at all the integration points within the gap including those in the improved soil layer. In addition, FEM results from Test FTreat-7d were superimposed on the same plot so that a direct comparison of the stress and strain behaviours for the stabilised excavations with and without gap could be made together.

As shown in Figure 6.16, there was no stress concentration in the embedded improved soil layer even at both corners when there was no direct contact of the stiff improved soil layer with the wall. This shows that the untreated soil in the gap has functioned to cushion the impact of the sharp corner and thus, no high stresses were induced. This is logical since the embedded improved soil layer is now resting on the untreated soil and not directly onto the stiff retaining wall. Instead, there was substantial yielding on the untreated soil in the gap. As shown in Figure 6.17, some of these integration points within the gap have exceeded a horizontal strain of 10%,

indicating that large yielding of soil has occurred. This is the reason for the large wall movement occurring even at the initial stage of excavation, which ties in well with what has been observed during the centrifuge testing.

To further understand the deformation behaviour of the untreated soil in the gap during the process of excavation, deformed meshes from the FE analysis at 3 different depths of excavation, namely 2m, 3m and 4m are presented. A closer examination of the deformed shape of the gap is shown in Figure 6.18. It was found that the untreated soil in the gap was laterally compressed, followed by some bulging of soil at the top and bottom of the gap. When the excavation was deeper, the untreated soil was further compressed and the shape of the soil bulging became more obvious especially at the top of the gap where there is less confinement. From the deformed shape of the gap, it is clear that the compression in the untreated soil gap and its interaction with the surrounding soil are important. The deformed shape suggests a transition from compression in a 1-D mode to one where it is closer to an unconfined compression mode, which is the key aspect in governing the composite stiffness of the improved soil system.

To illustrate the behaviour of soil as postulated above, the total vertical and horizontal stresses along the passive side at distance 0.5m away from the retaining wall were assessed as shown in Figures 6.19. For comparison, results from FE analysis for the case of an excavation without soil improvement (Test NTreat) were also presented in the same figure. As can be seen, there was a sudden increase in the stress within the untreated soil region where the gap was located. It was further found that there were small regions of soil at the top and bottom of the gap that were experiencing higher stresses. These are indications showing the way the untreated soil in the gap reacts during excavation.

6.4.2 Effect of Width of Gap and Confinement

In the preceding chapter (section 5.4), the behaviour of an improved soil layer with a gap in between it and the retaining wall was examined in relation with that of an improved soil strut. The induced lateral wall movement and surface settlement from centrifuge tests have shown that these movements developed gradually throughout the excavation depth, showing very similar trend to that of an improved soil strut. Thus, it is possible to consider the concept of a composite stiffness for such a configuration of improved soil layer (that is with a gap) to assist the engineers facing with such problems in the field.

The performance of the embedded improved soil layer with a gap is influenced by the amount of deformation of the untreated soil in the gap. Thus, with a wider gap, larger movements can be expected since more lateral deformation of the untreated soil will occur. This is inline with the observed behaviour in the centrifuge tests where gaps of 400mm and 800mm were studied in the previous chapter. However, when the untreated soil in the gap compresses, this soil also bulges out. It is rather obvious, in retrospect that this tendency to bulge must be to a large extent, a function of the overburden remaining after excavating to a particular depth.

To evaluate these effects, a parametric study using the FE analyses was carried out on different widths of gap, extending from the initial numerical simulation of the case with a gap of 800mm, as presented earlier. The normalised lateral wall displacements were evaluated at different depths of excavation. Figures 6.20 show the detrimental effect of increasing the width of gap of untreated soil. A detailed evaluation on the effect of varying the depth of excavation was also carried out in Figure 6.20 (b) for a range of gap encountered in practice. It was shown that instead of a single curve, there were a series of curves, which were differentiated by the

excavation depth. This means that for a particular width of gap, the depth of excavation also governs the performance of the improved soil layer system. As can be seen, the normalised lateral wall displacement was higher when the excavation was deeper. This is due to two likely reasons. First, with greater depth of excavation, the unbalance load is greater and thus, the normalised lateral wall displacement is expected to be higher. Second, with greater depth of excavation, the amount of confinement imposed on the short length of untreated soil decreases and therefore, the stiffness is expected to reduce. To further isolate the contribution from the changing unbalance loads due to different depths of excavation, all the results are now further normalised by that for the case without gap (a full improved strut) for each particular depth of excavation. This is now shown in Figure 6.20(c) and again, it shows that the effect of confinement on the untreated soil clearly plays an important role.

To illustrate this effect more clearly, the curves from Figure 6.20 (b) were plotted together with an earlier curve [Figure 6.15], obtained from a parametric study by varying the stiffness of the full-improved soil strut that is without a gap [Figure 6.21]. This figure provides a means of determining the stiffness of an equivalent fully improved soil strut that will produce the same normalised lateral wall displacement behaviour at the mid-level of the improved soil layer. This stiffness is referred to as the composite stiffness (E_c). Since there were a series of curves differentiated by the depth of excavation, the effect of confining pressure to the composite stiffness can also be assessed. For example, given a particular width of gap (let say 200mm) at 0.5m depth of excavation, the stiffness (E_c) of an equivalent full-improved soil strut would drop from the original stiffness (E_{imp}) of 300MPa to about 134MPa with the presence of the 200mm gap. However, when the excavation goes deeper (6m), E_c of an equivalent strut is now reduced to 94MPa, which is showing a more severe reduction. This

suggests that the confining pressure affects the composite stiffness of the improved soil layer system.

Figure 6.22 shows the direct impact of the overburden on the composite stiffness of an improved soil layer with a gap. It shows that E_c reduces with increasing depth of excavation, where the thickness of overburden above the gap decreases. The rate of reduction based on different widths of gap is also compared. It is found that the drop in E_c is more rapid when the gap is narrower. This shows that for a smaller gap, the effect of confining pressure is more critical during the early stages of excavation and thereafter, when a substantial amount of soil bulging has taken place, the effect of confining pressure becomes less significant. Figure 6.23 summarises the percentage of reduction in E_c due to both effects, the width of untreated soil gap and the confining pressure, on the overall performance of an improved soil layer with an untreated soil gap in between it and the retaining wall.

The distinction between the compression and confining effect is best illustrated by a simple triaxial test model shown in Figure 6.24. The untreated soil in between two rigid ends of the retaining wall and improved soil layer can be represented by a soft soil sample in a triaxial test. In such an analogy, the lateral force exerted by the retaining wall on the untreated soil in the gap can be modelled as the axial force from the loading ram in a triaxial test, while the confining pressure from overburden above the untreated soil in the gap can be simulated as the cell pressure. With this analogy, the effect of confining pressure on the untreated soil in between the retaining wall and improved soil layer can now be idealised. It is clear that the change in the axial stiffness of the untreated soil is quite complex. First, there is the usual effective stress effect. Then, there is a need to consider the state of drainage and finally, there is also a need to consider the amount of confinement, which will be reducing with increasing

depth of excavation. An approximate means of accounting for these different effects can be found.

To understand this better, a simplified dual spring system is used to describe the composite stiffness of the improved soil layer system as shown in Figure 6.24. The amount of deformation, δL that took place in the improved soil layer with the gap was first formulated and the sum of this deformation over the given length, L was then calculated: -

$$\delta L = \int \frac{P}{AE} dL = \frac{P(L_{imp} + L_{gap})}{AE_c} = \frac{PL_{imp}}{AE_{imp}} + \frac{PL_{gap}}{AE_{gap}} \tag{6.3}$$

where A is the sectional area, L_{imp} is the length of improved soil, L_{gap} is the length of untreated soil, E_{imp} and E_{gap} are Young's modulus of the improved soil and untreated soil in the gap respectively. The composite stiffness of the improved soil system can now be obtained: -

$$E_c = \frac{(L_{imp} + L_{gap})E_{imp}E_{gap}}{L_{imp}E_{gap} + L_{gap}E_{imp}} \tag{6.4}$$

In Equation (6.4), all the parameters except E_{gap} are well defined. Clearly, from the discussion above, E_{gap} is a function of the actual lateral load transferred (mainly because compressibility of a soil is non-linear), the amount of confinement (reflecting a transition from nearly 1-D to an unconfined unaxial compression) and drainage condition (reflecting the initially near undrained condition transiting to that of a near drained condition if there is sufficient time). As the main aim of this section is not to obtain a definitive design guide, but to provide a better understanding of the effect of the gap, some approximations will be made to facilitate an examination of the likely behaviour.

If the condition is assumed to be drained, as most of the tests were conducted with kaolin which has a high permeability, then the axial stiffness, is derived from the

e versus log σ'_v relation and is given as:

$$E_{1D} \sim \frac{2.303\,(1+e)\,\sigma'_v}{C_s} \tag{6.5}$$

Under 1-D condition, in particular, the stiffness increases with increasing effective axial stress and increasing compression or axial strain. On the other hand, under uniaxial unconfined compression, the axial stiffness is the equivalent of Young's modulus, and for most soils, this also usually increases with the effective confining stress but more importantly, decreases with increasing deviatoric strain. Nevertheless, it is clear that when the overburden on the top of the untreated soil is high, the axial stiffness is given by Equation (6.5), whereas when the excavation is deep and the resulting overburden remaining is low, the axial stiffness is closer to E_{50} or even lower if the soil is near yielding. In Figure 6.23, Equation (6.5) is used for estimating the composite stiffness using Equation (6.4) when the excavation is 0.5m while E_{50} is used when estimating the value when the excavation is 6.0m. As can be seen, the results are reasonable, suggesting that the arguments presented here on what is going on in the gap is reasonably correct.

6.5 Resistance Mechanism of An Embedded Improved Soil Berm

In the preceding chapter (section 5.5), the mobilisation of resistance by an embedded improved soil berm during an excavation has been investigated in some details during the centrifuge testing. It was shown that the improved soil berm mobilised its resistance mainly through interfacial shear resistance and end bearing, similar like a horizontal floating pile. It was also found that the stiffness of berm does not have a significant effect on its performance during an excavation. Since the way various forces were mobilised in the shear resistance and end bearing are very

complicated, another doctoral student has been employed to carry out further investigation [Thanadol (2003)]. Here, only one numerical analysis has been carried out to simulate Test Berm-7d so as to confirm that observed behaviours in the centrifuge test can be simulated in the FE analysis.

Figures 6.25 show the shear strain contours of improved soil berm on the excavated side during 3 stages of excavation, namely 2m, 4m and 6m. As can be seen, two high shear strain zones as a result of localised yielding was found on the top and underside surfaces of the improved soil berm. As excavation proceeds, this shearing zone spreads inward as shown in Figures 6.25 (b) and (c). This has clearly demonstrated that there is interfacial shear resistance being mobilised along both surfaces of the improved soil berm.

Figures 6.26 show the deviatoric strain contours of improved soil berm on 3 similar stages of excavation. A closer examination of this contour showed that there was a gradual development of localised yield zone behind the improved soil berm, a sign of the mobilisation of end bearing resistance. However, complementary numerical analyses carried out by Thanadol [2003] have shown that there is a threshold value for the stiffness [E ~ 200MPa] of the improved soil to effectively mobilise the interfacial shear resistance and end bearing. The way the interfacial shear resistance and the end bearing are developed will not be given here but can also be found in Thanadol [2003].

Table 6.1 Soil parameters used in CRISP FEM analysis

Soil Type	Kaolin clay
Soil Model	Modified Cam-Clay
λ	0.244
κ (isotropic)	0.079
M	0.9
e_{cs}	2.221
υ	0.33
γ_{bulk} (kN/m^s)	16.39
k_x (m/s)	2.0 x 10^{-8}
k_y (m/s)	2.0 x 10^{-8}

Derivation λ = Cc / 2.303
κ = Cs / 2.303
κ (isotropic) = 1.5 x κ (anisotropic) [Bolton (1991)]

Table 6.2 Improved soil parameters used in CRISP FEM analysis

Improved Soil Type	Cement treated clay
Soil Model	Original Mohr-Coulomb Elastic Perfectly Plastic
E_o (kPa)	3.0 x 10^5
c (kPa)	500
υ	0.33
φ (deg)	32
γ_{bulk} (kN/m^s)	16.4
k_x (m/s)	2.0 x 10^{-9}
k_y (m/s)	2.0 x 10^{-9}

Table 6.3 Retaining wall parameters used in CRISP FEM analysis

Retaining Wall Type	Aluminum Alloy
Soil Model	Original Mohr-Coulomb Elastic Perfectly Plastic
E_o (kPa)	7.2 x 10^7
c (kPa)	2.75 x 10^5
υ	0.33
φ (deg)	0
γ_{bulk} (kN/m^s)	28
k_x (m/s)	1.0 x 10^{-15}
k_y (m/s)	1.0 x 10^{-15}

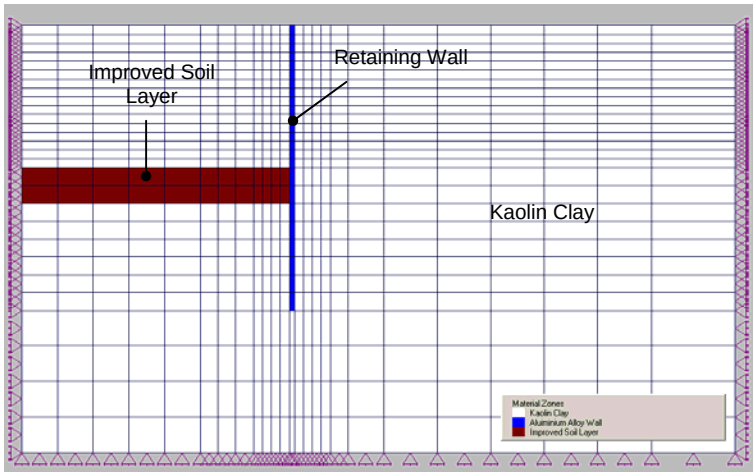

(a) Mesh to simulate Test 'FTreat'

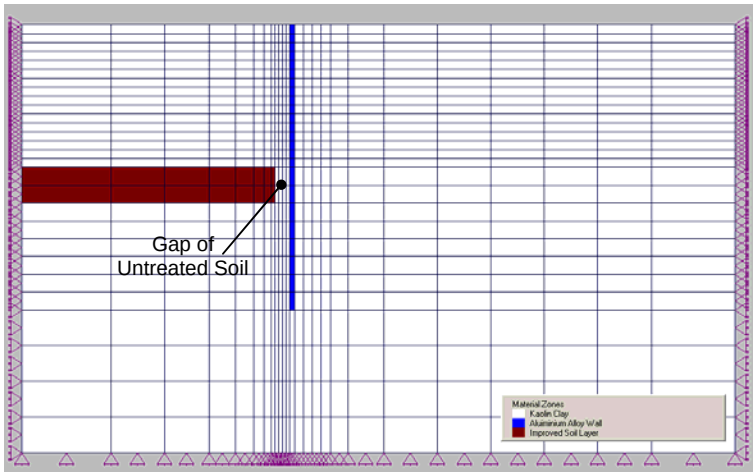

(b) Mesh to simulate Test 'Gap'

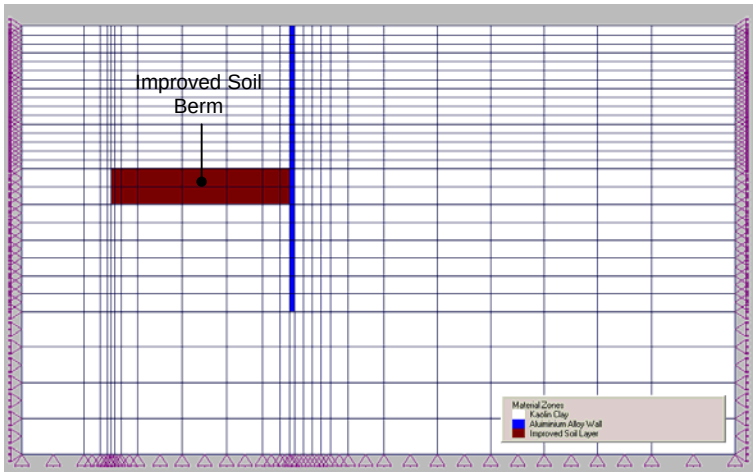

(c) Mesh to simulate Test 'Berm'

Figure 6.1 Typical finite element meshes adopted in current study

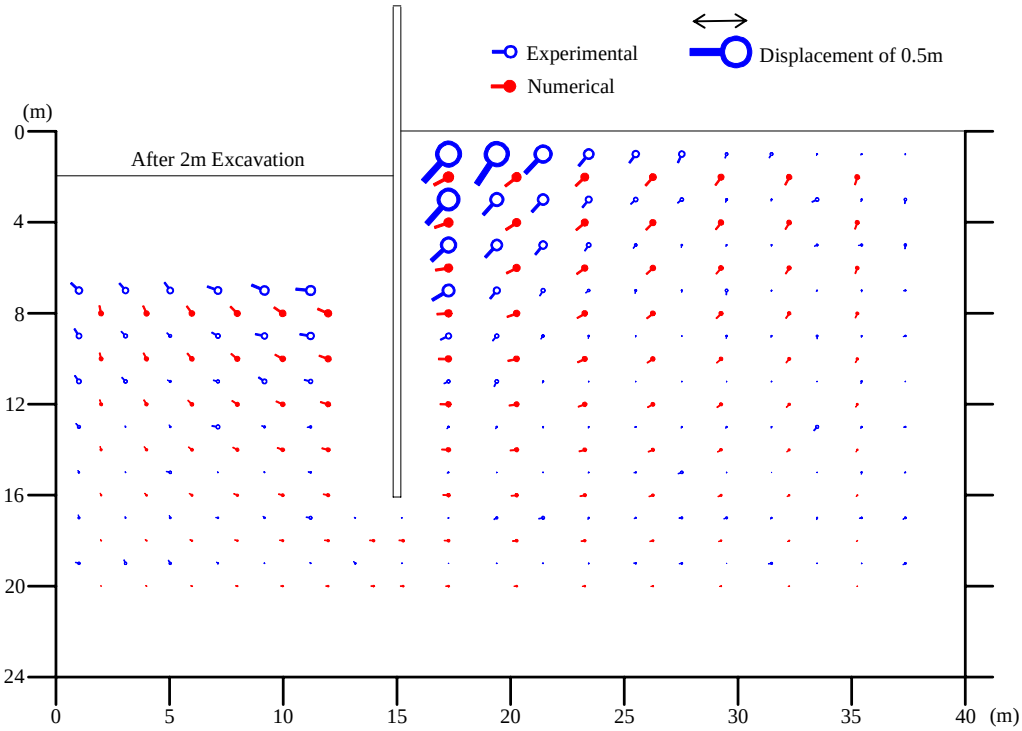

Figure 6.2 Comparison of ground displacement vectors from experimental and numerical (FEM) results for Test NTreat

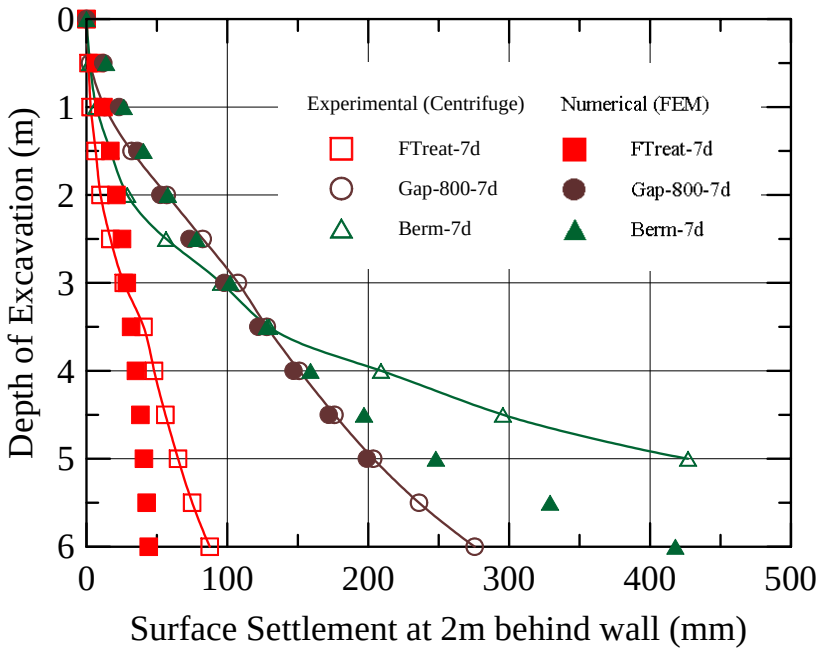

Figure 6.3 Comparison of surface settlement at 2m behind wall from experimental and numerical results for Tests FTreat-7d, Gap-800-7d and Berm-7d

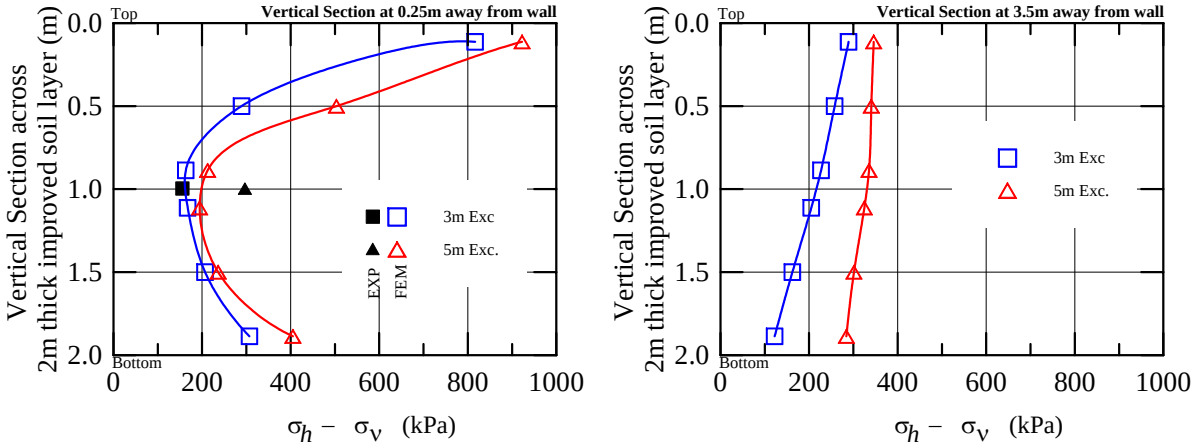

(a) Section at 0.25m from wall

(b) Section at 3.5m from wall

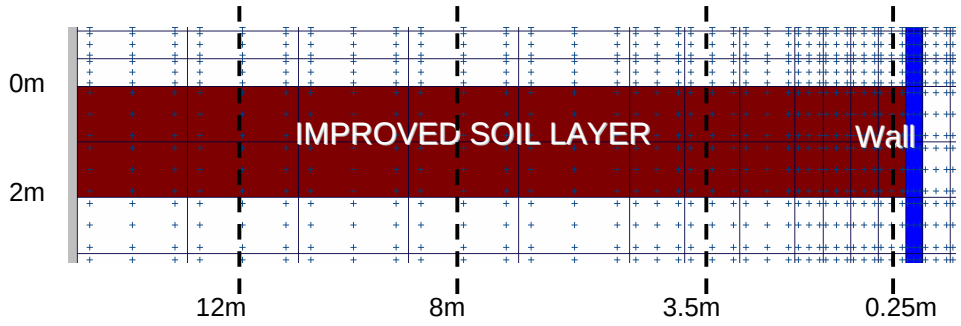

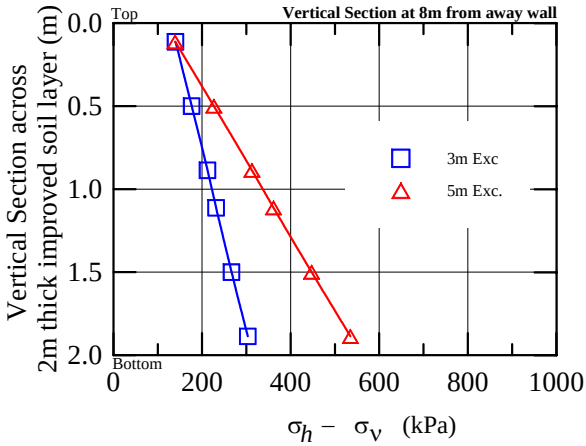

(c) Section at 8m from wall

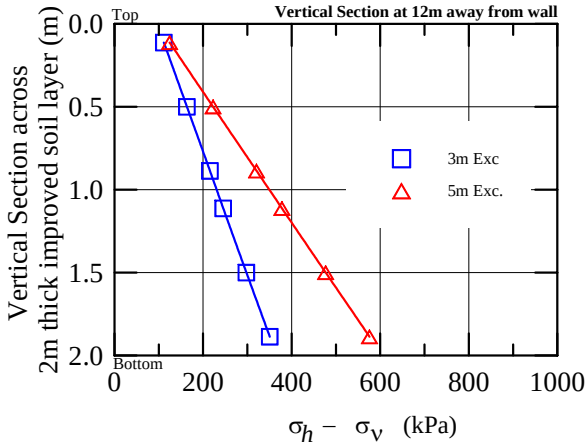

(d) Section at 12m from wall

Figure 6.4 Deviatoric stress (σ_h-σ_v) at vertical section across the improved soil strut (simulation of Test FTreat-7d)

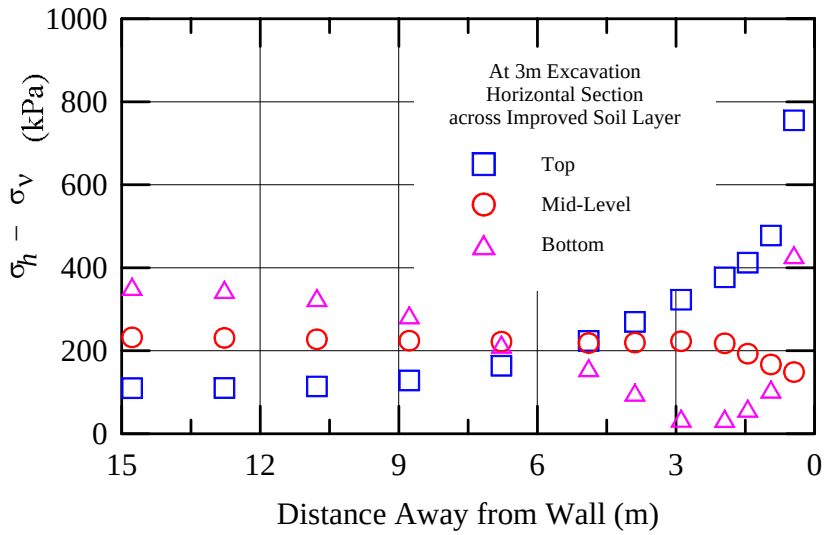

Figure 6.5 Deviatoric stress (σ_h-σ_v) at horizontal section (top, center, bottom levels) across the improved soil strut (simulation of Test FTreat-7d)

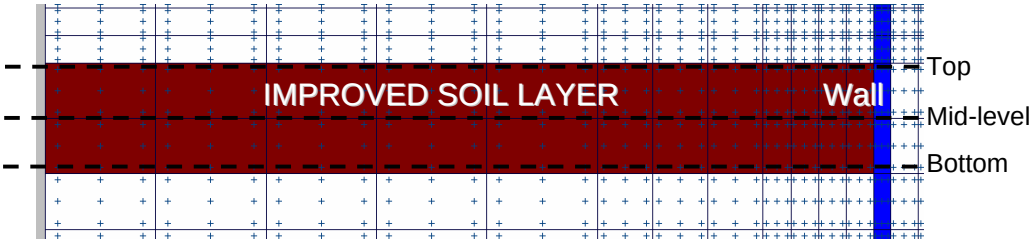

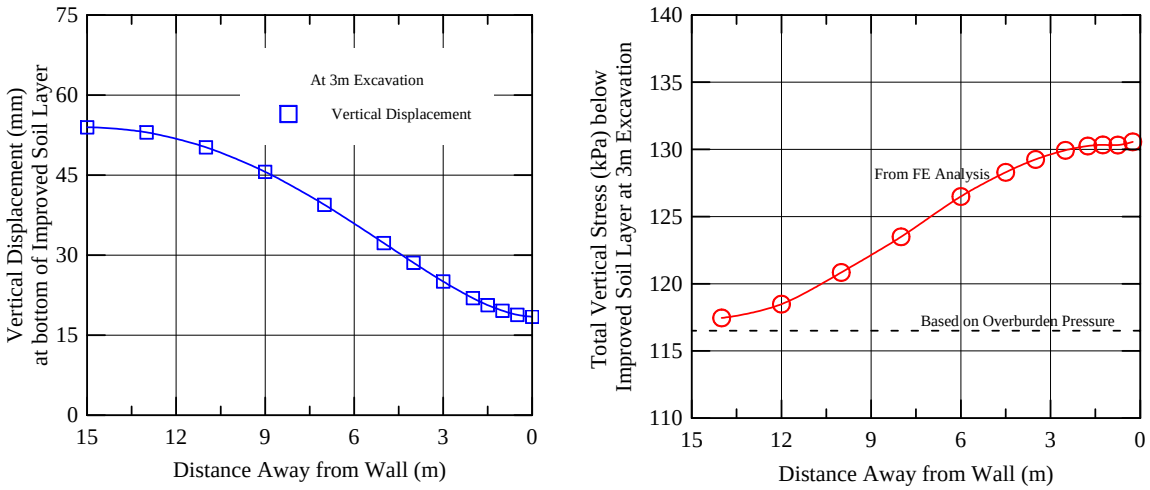

a) Vertical Displacement b) Total Vertical Stress

Figure 6.6 Vertical displacement and total vertical stress below the improved soil strut (simulation of Test FTreat-7d)

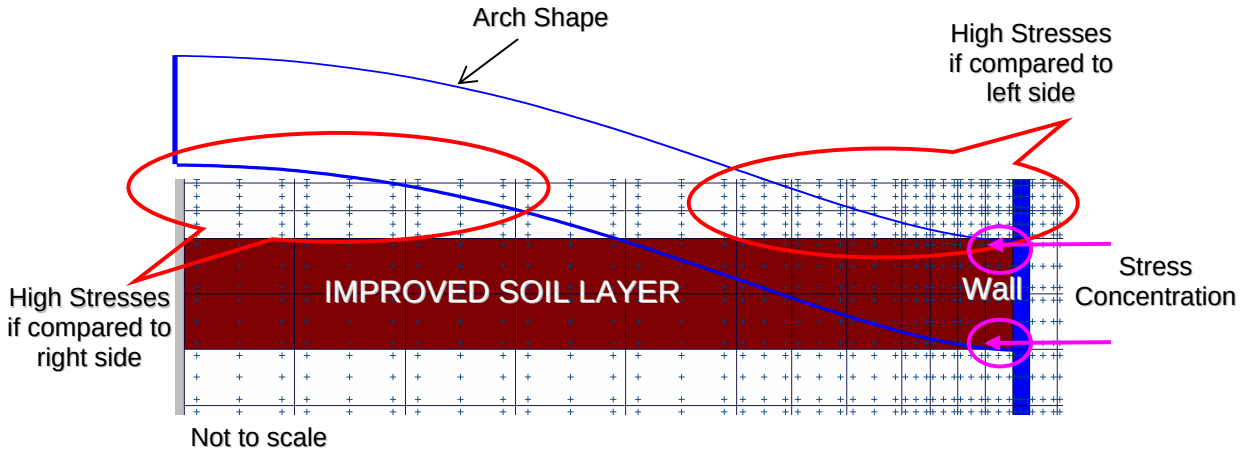

Figure 6.7 Predicted deformed shape of embedded improved soil strut

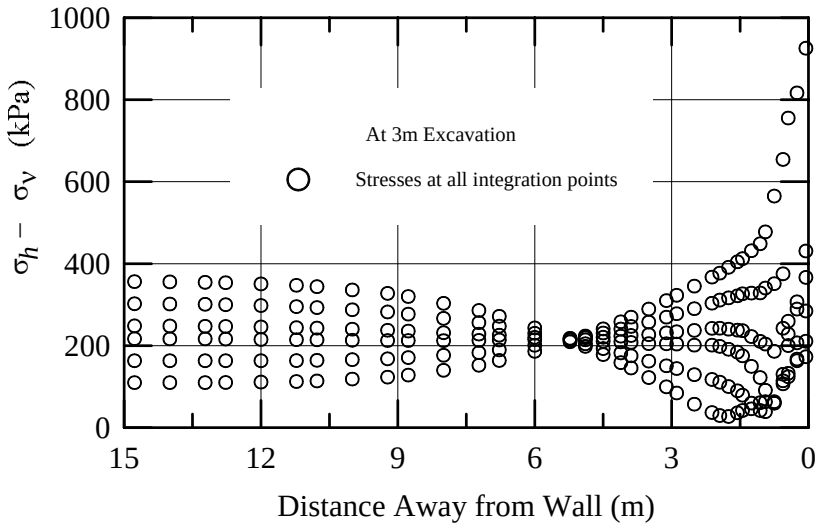

Figure 6.8 Deviatoric stress (σ_h-σ_v) distributed at all integration points in the entire improved soil strut (simulation of Test FTreat-7d)

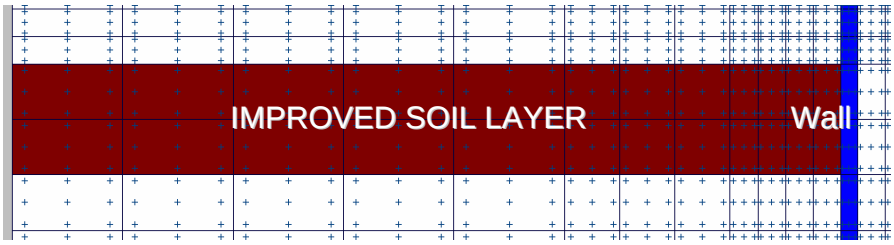

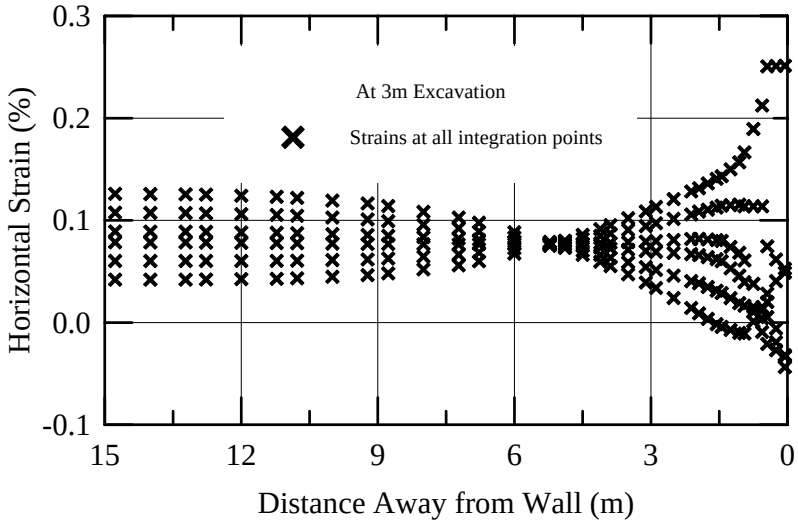

Figure 6.9 Horizontal strain distributed at all integration points in the entire improved soil strut (simulation of Test FTreat-7d)

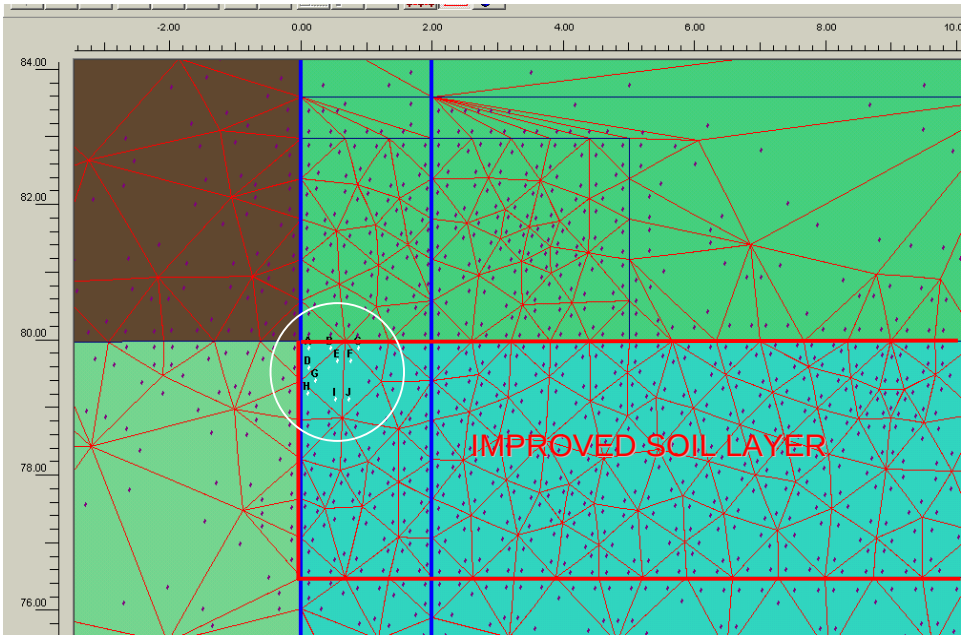

(a) 6-node triangular elements at corner of improved soil layer

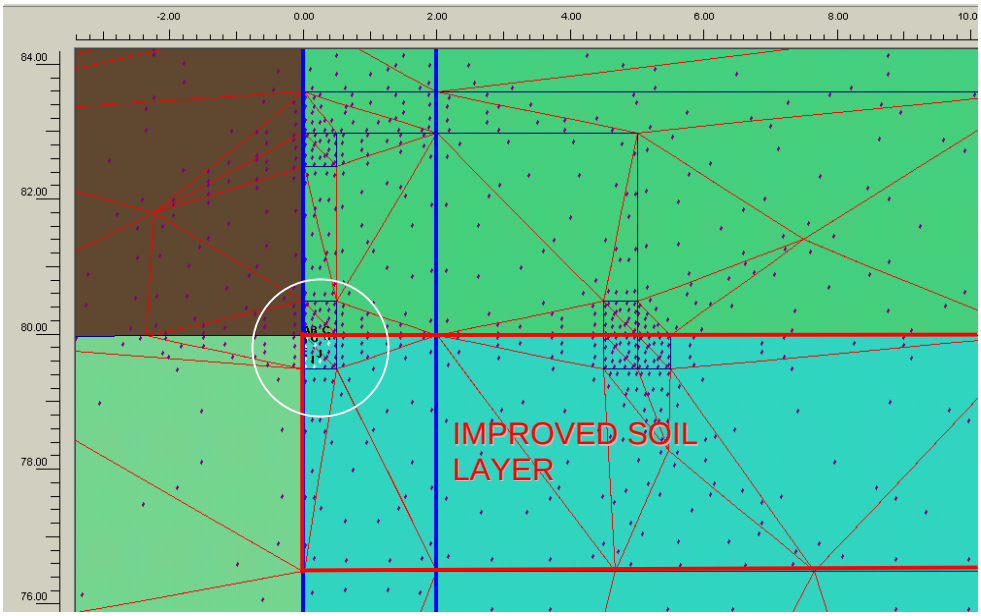

(b) 15-node triangular elements at corner of improved soil layer

Figure 6.10 Mesh generation at corner of improved soil strut

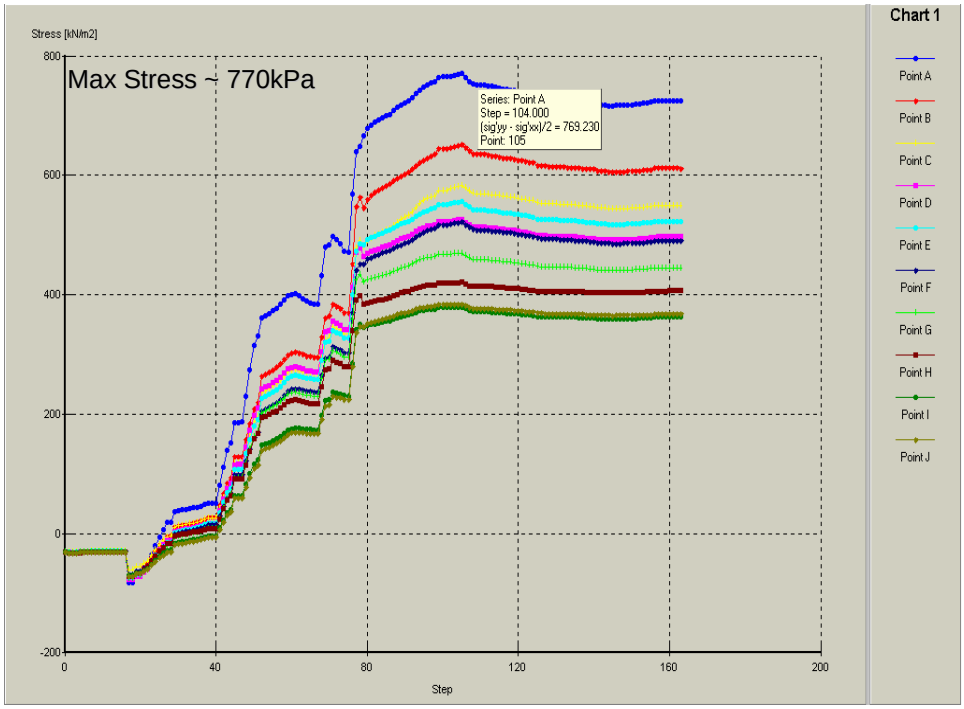

(a) Deviatoric stress $[(\sigma_h-\sigma_v)/2]$ of improved soil layer from 6-node mesh

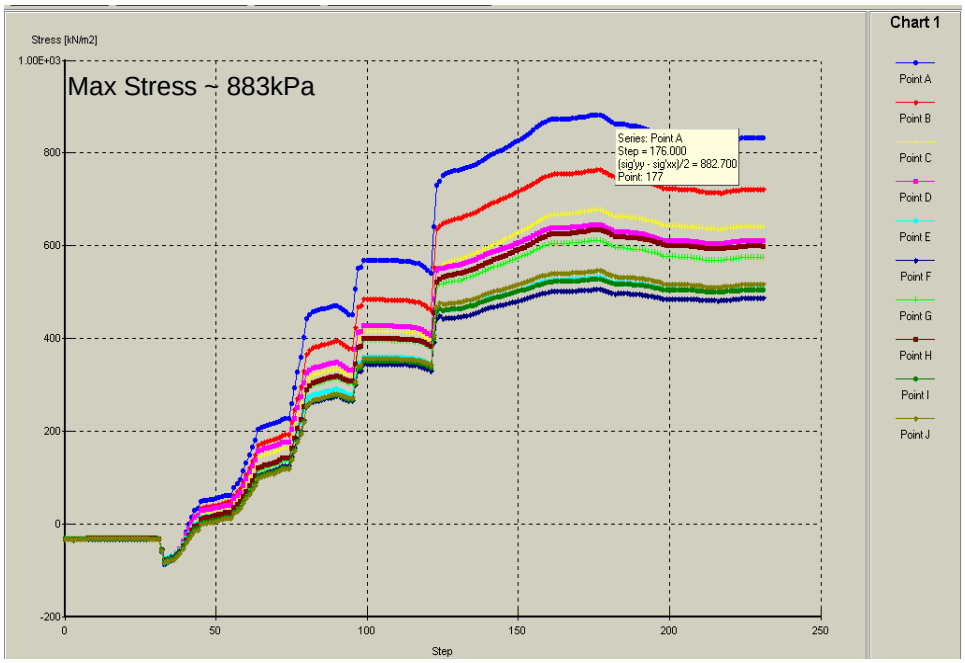

(b) Deviatoric stress $[(\sigma_h-\sigma_v)/2]$ of improved soil layer from 15-node mesh

Figure 6.11 Deviatoric stresses at corner of improved soil strut

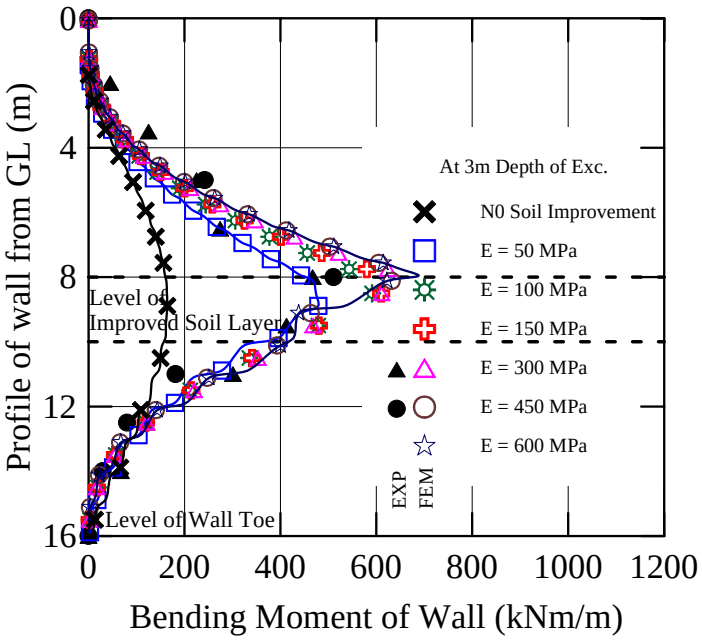

a) Profile of wall bending moment

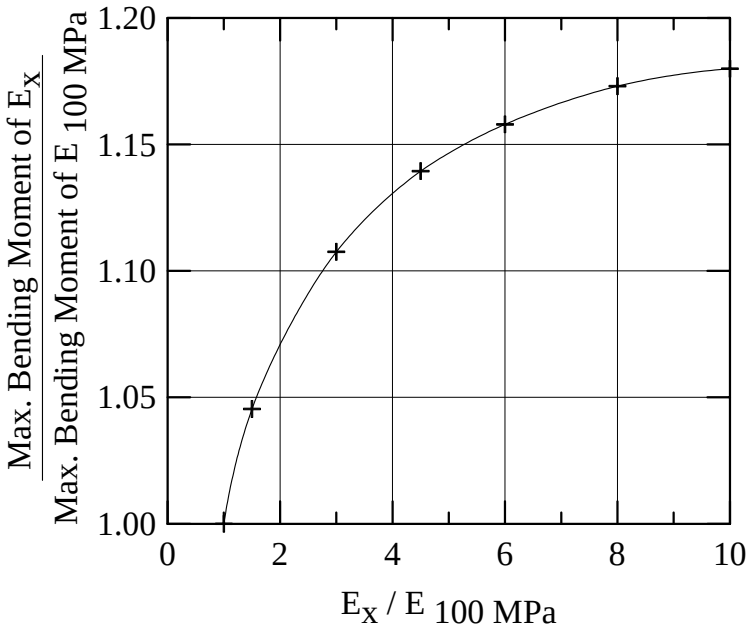

(b) Increase of wall bending moment

Figure 6.12 Wall bending moment with different stiffness of improved soil strut (simulation of Test FTreat)

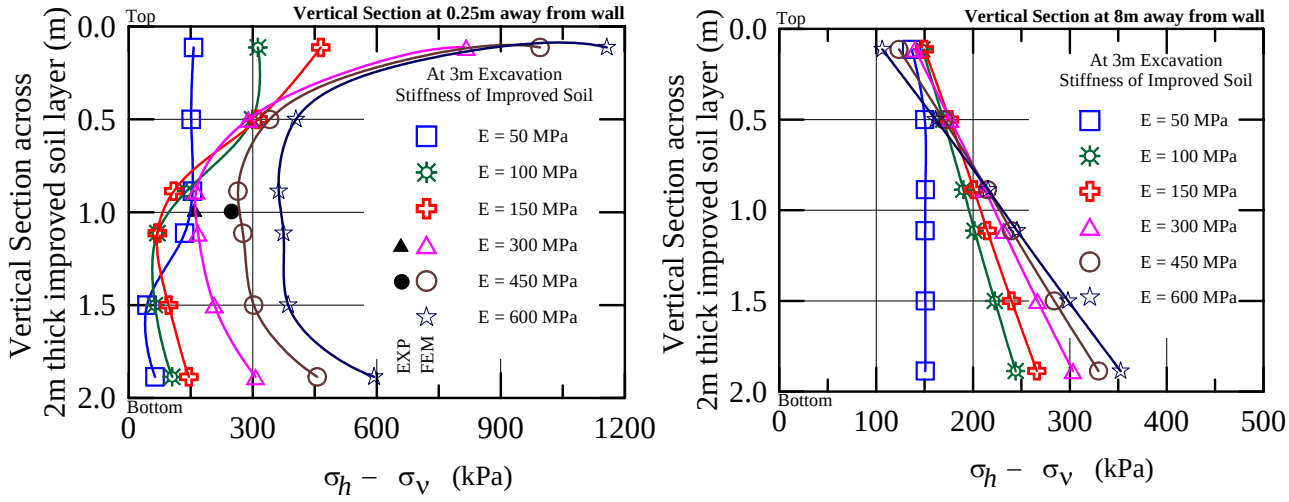

(a) Section at 0.25m from wall (b) Section at 8m from wall

Figure 6.13 Deviatoric stress (σ_h-σ_v) at vertical section across the improved soil strut with different stiffness of improved soil (simulation of Test FTreat)

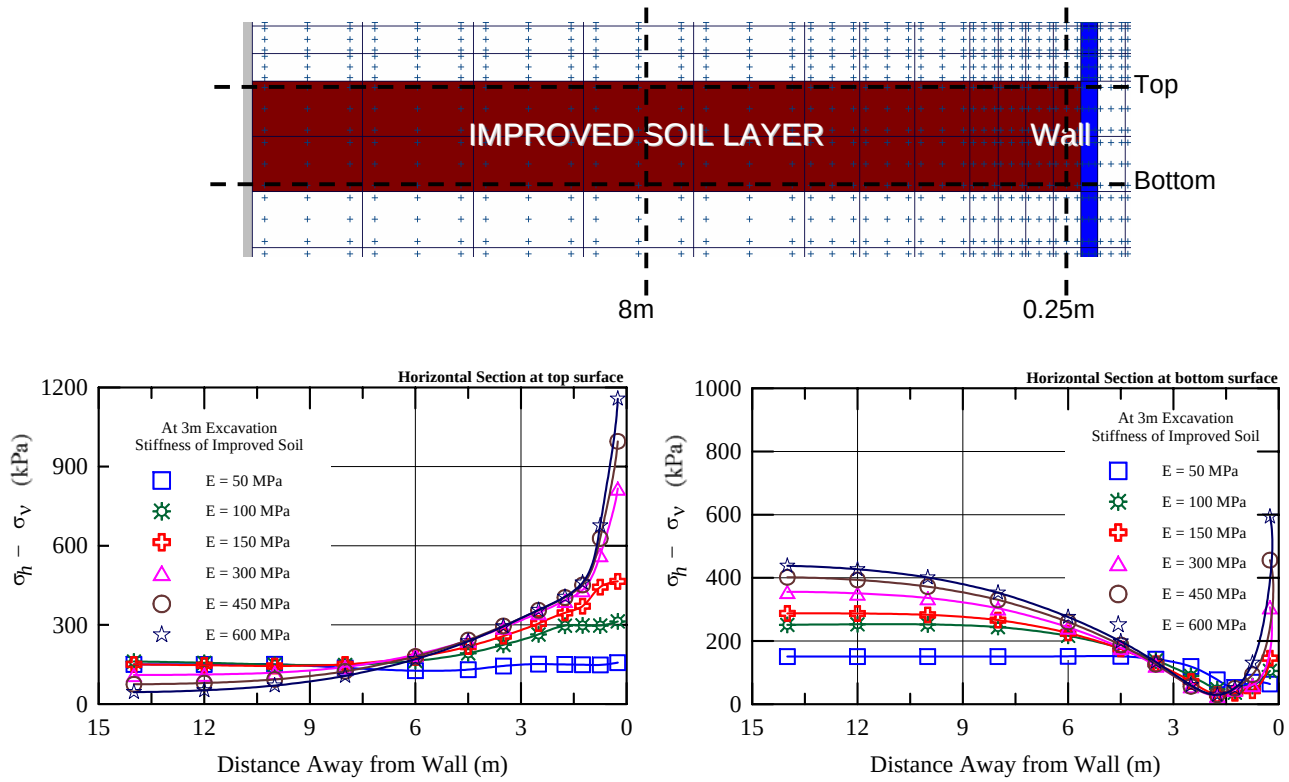

(a) Section at top surface (b) Section at bottom surface

Figure 6.14 Deviatoric stress (σ_h-σ_v) at horizontal section across the improved soil strut with different stiffness of improved soil (simulation of Test FTreat)

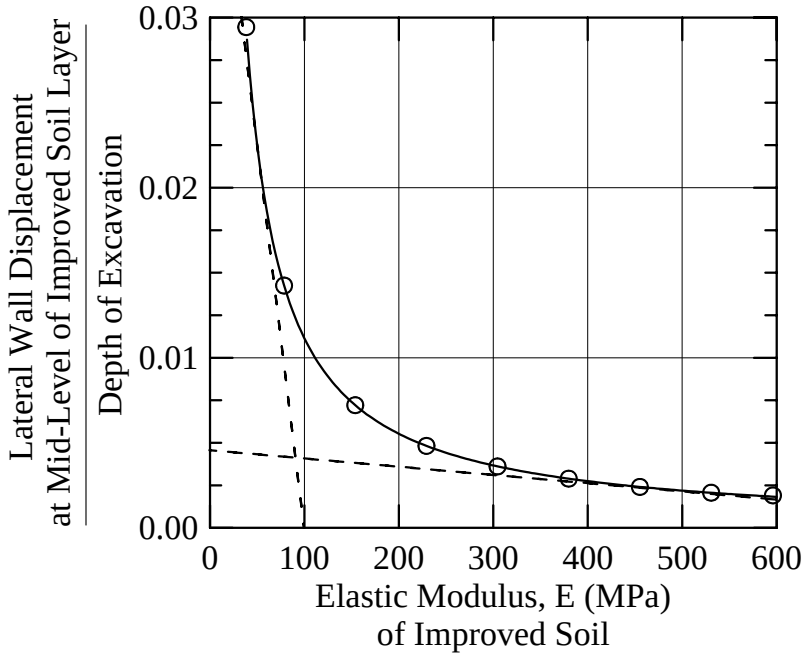

Figure 6.15 Normalised lateral wall displacement with different stiffness of improved soil strut (simulation of Test FTreat)

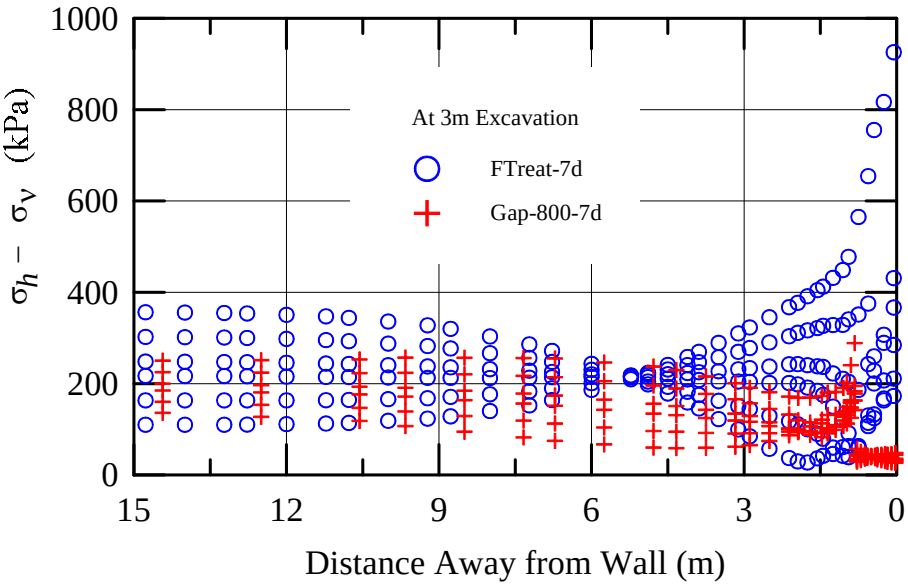

Figure 6.16 Deviatoric stress (σ_h-σ_v) distributed at all integration points at the level where the improved soil layer is located, from simulation of Tests FTreat-7d and Gap-800-7d

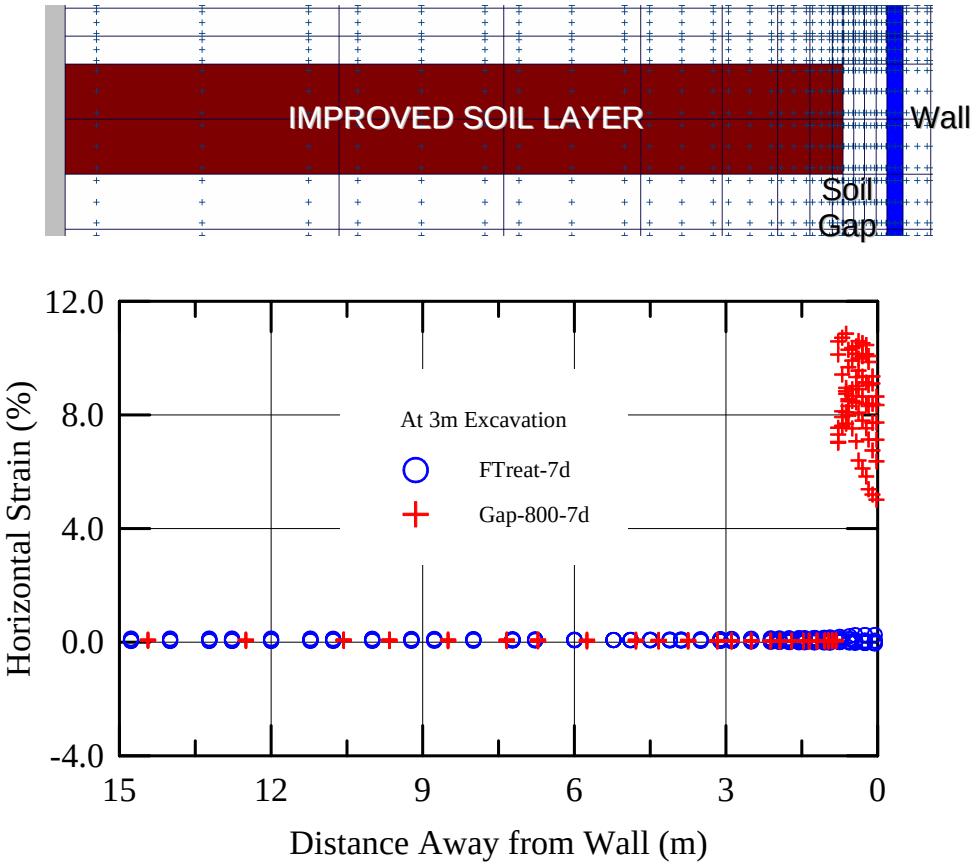

Figure 6.17 Horizontal strain distributed at all integration points at the level where the improved soil layer is located, from simulation of Tests FTreat-7d and Gap-800-7d

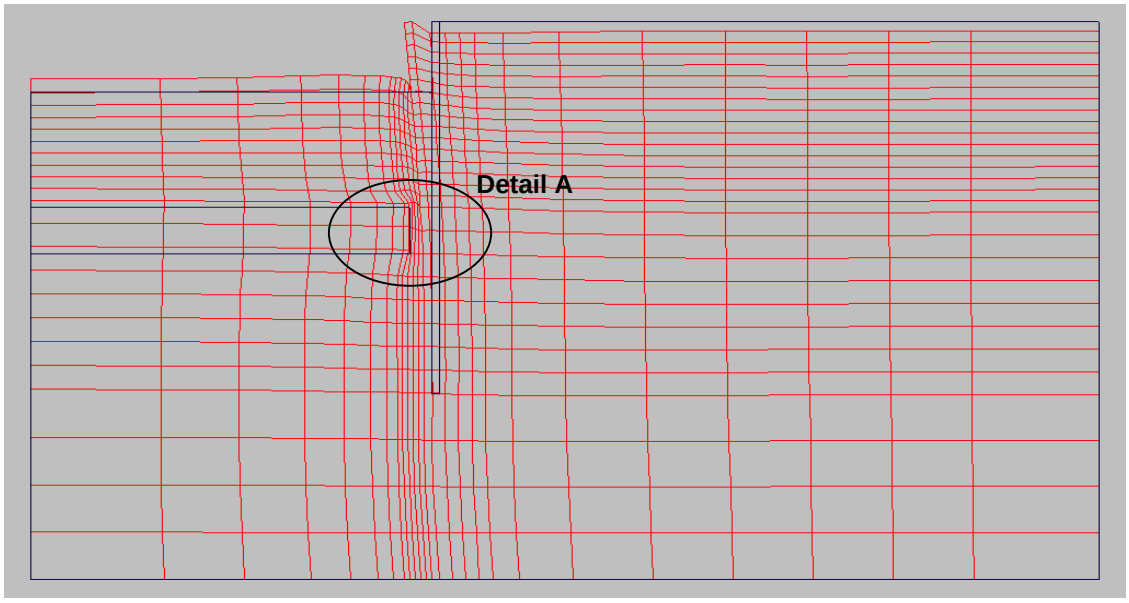

(a) Overall

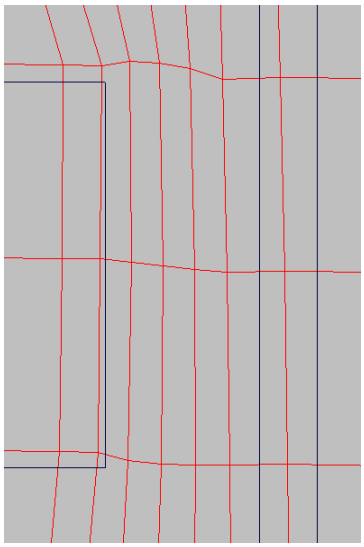

(i) 2m Exc.

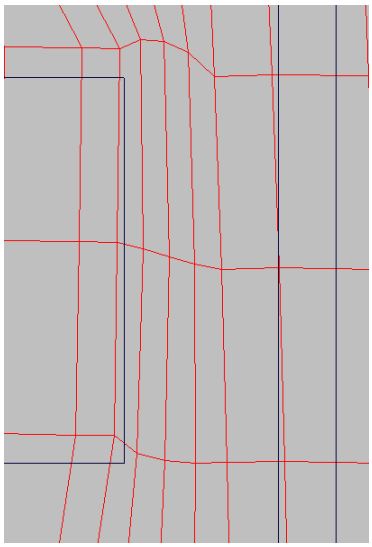

(ii) 3m Exc.

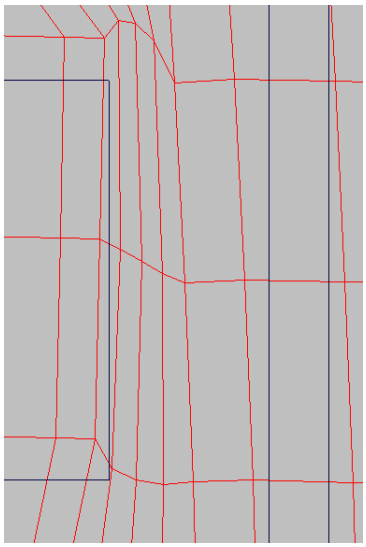

(iii) 4m Exc.

(b) Enlarged – Detail A

Figure 6.18 Deformed mesh of excavation test with 0.8m gap showing the high compression of untreated soil portion in between the retaining wall and improved soil layer (simulation of Test Gap-800-7d)

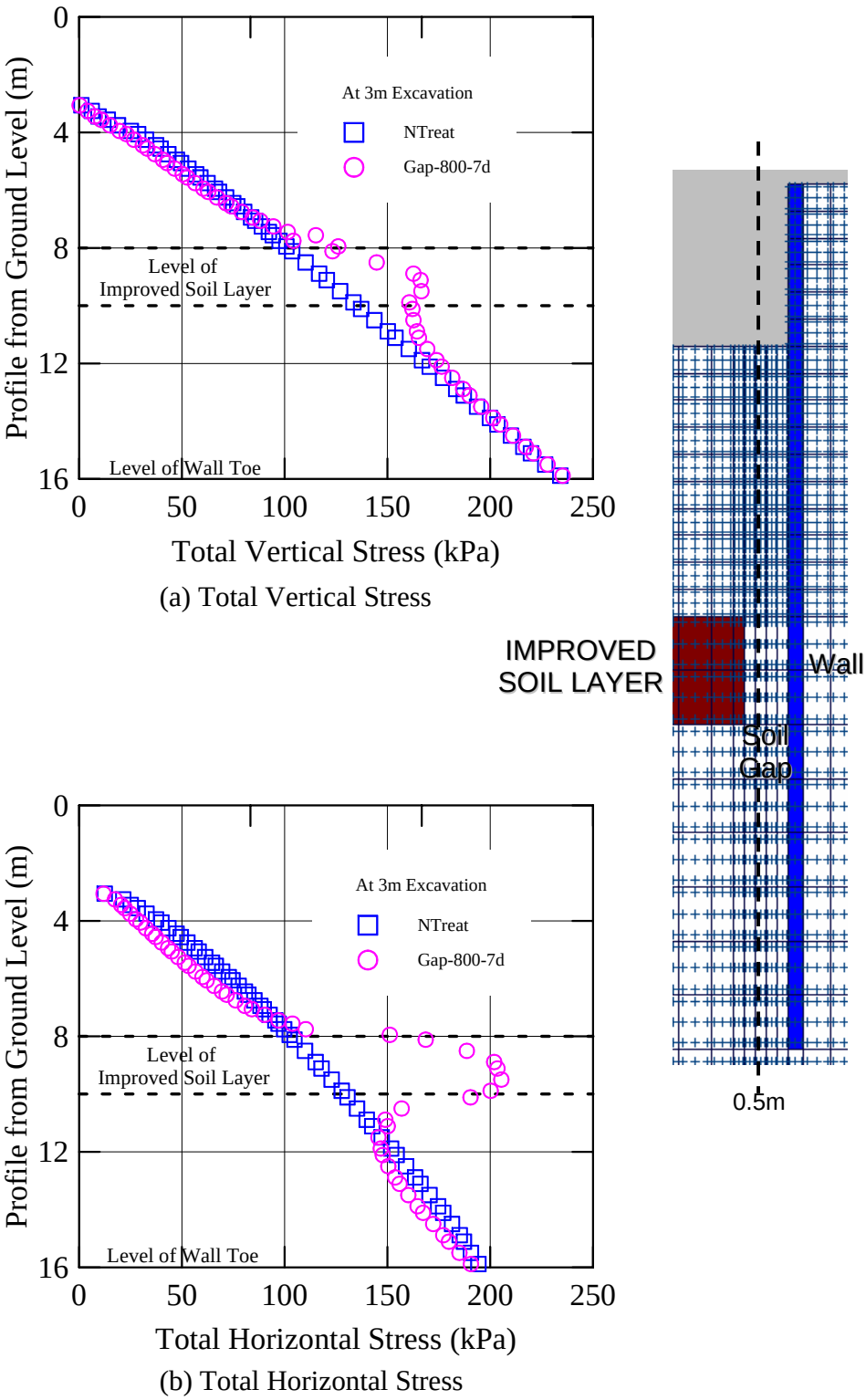

Figure 6.19 Total vertical and horizontal stresses along the excavated side at 0.5m distance away from the retaining wall (simulation of Tests NTreat and Gap-800-7d)

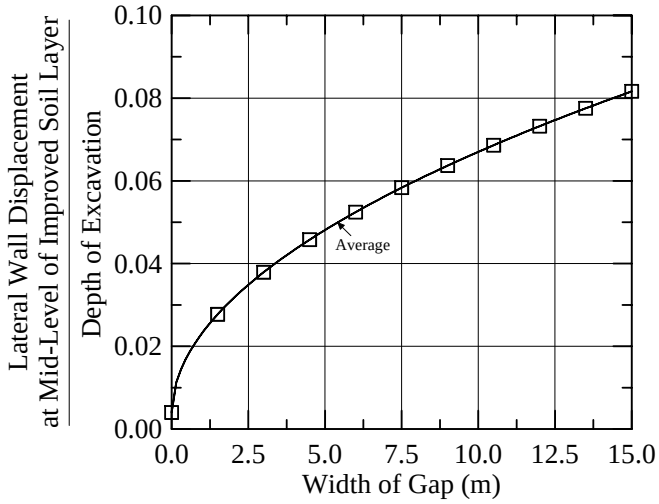

(a) Overall

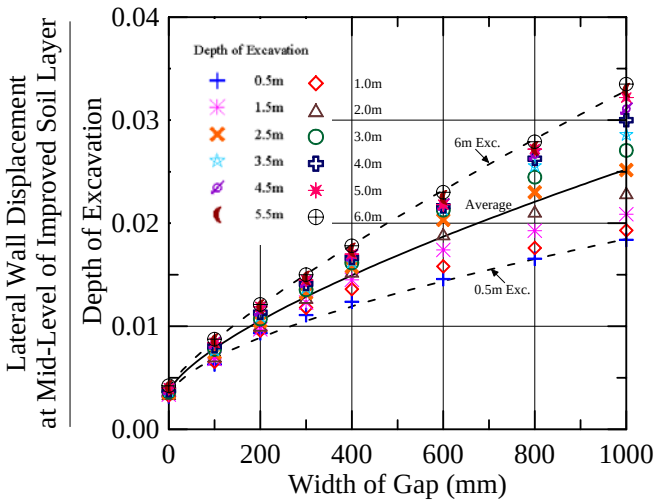

(b) Enlarged

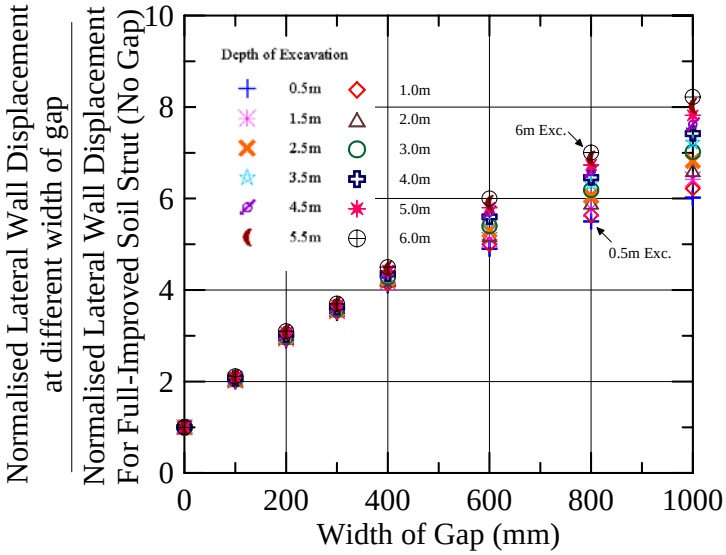

(c) Further normalisation

Figure 6.20 Effect of gap width and confinement on the lateral normalised wall displacement

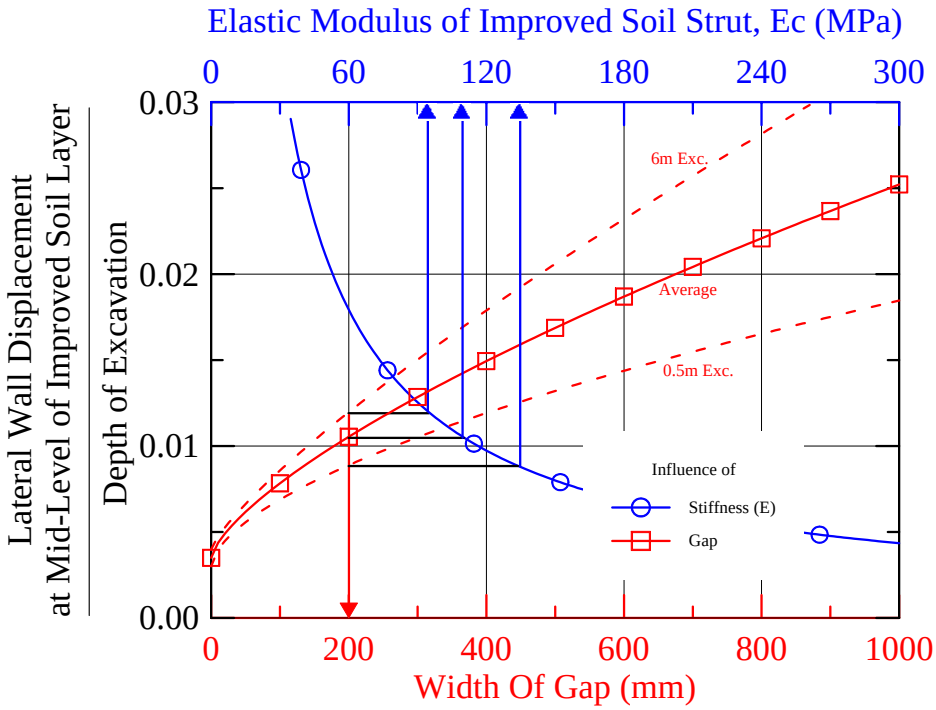

Figure 6.21 Effect of gap width on the composite stiffness of improved soil layer

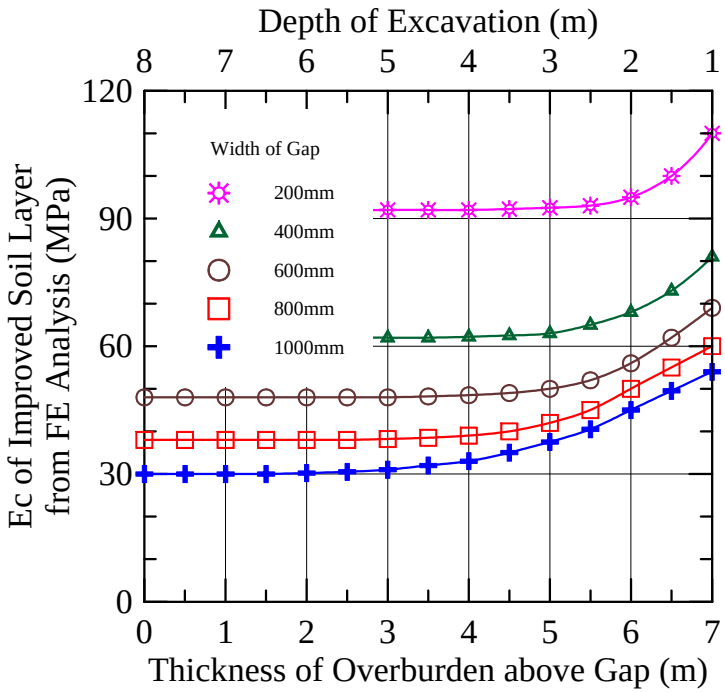

Figure 6.22 Effect of confinement on the composite stiffness of improved soil layer with gap

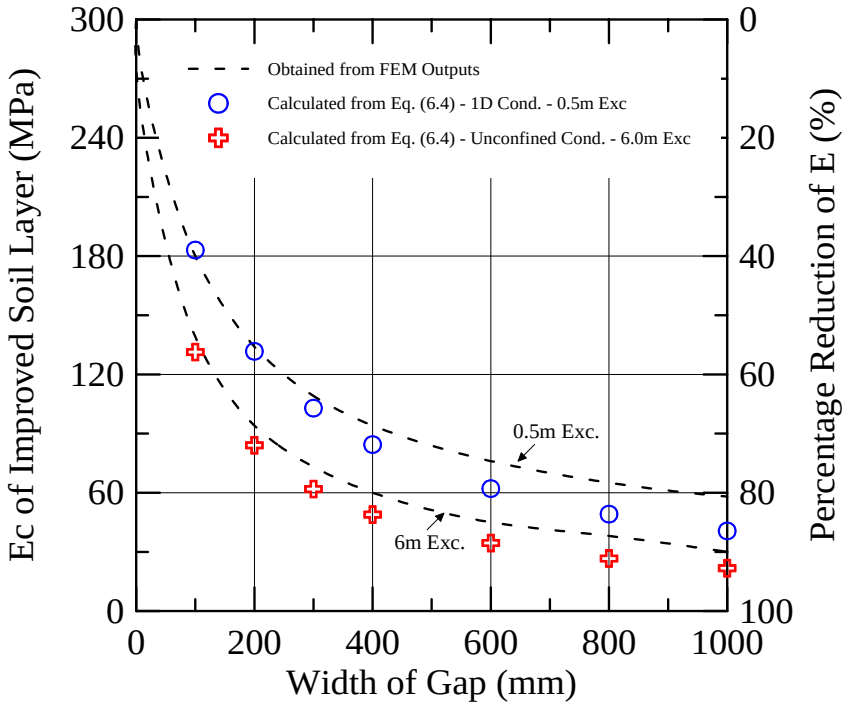

Figure 6.23 Reduction of composite stiffness of improved soil layer obtained from FE analysis and calculated from basic formula

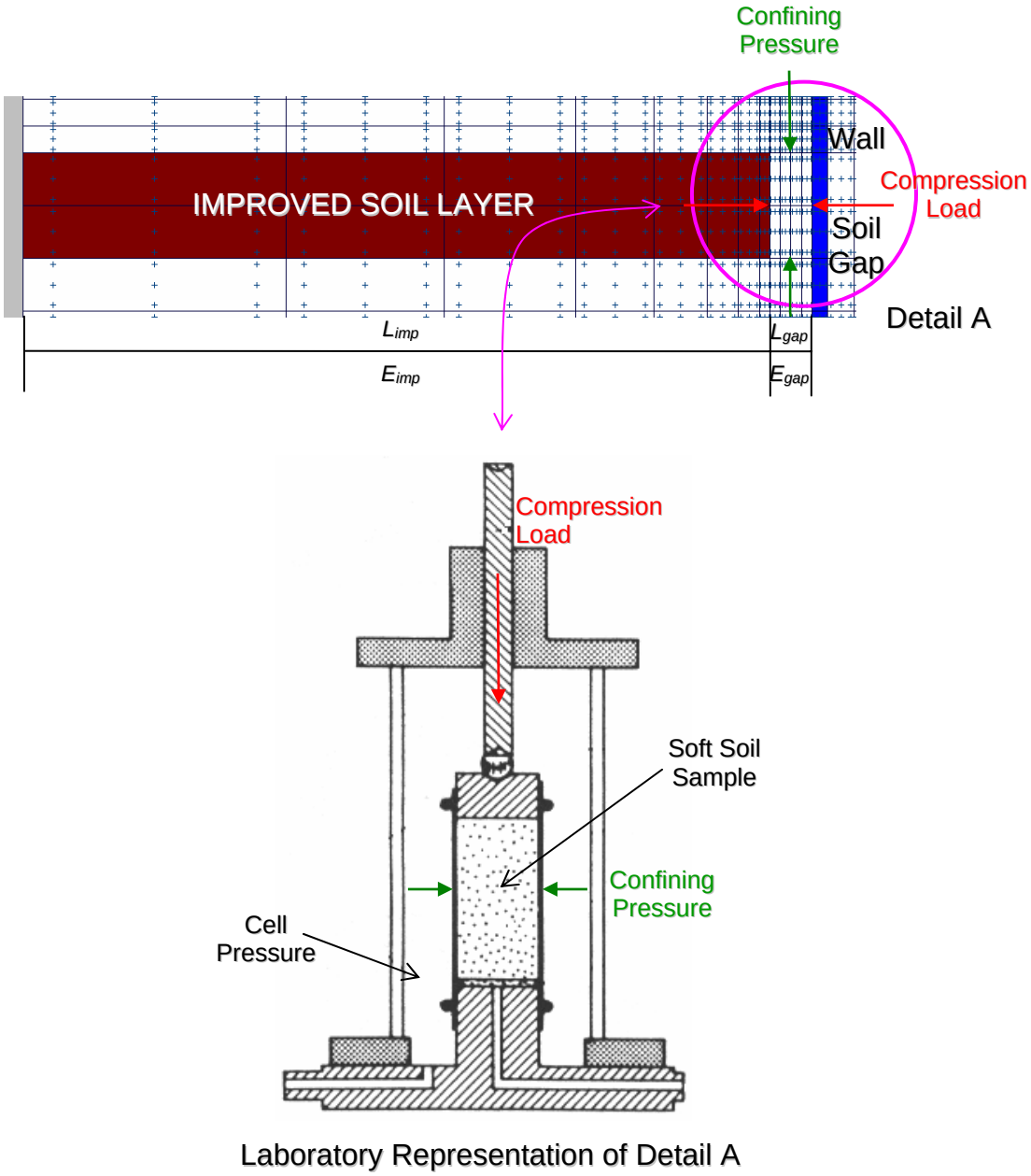

Figure 6.24 Model of untreated soil gap with compression and confining pressure

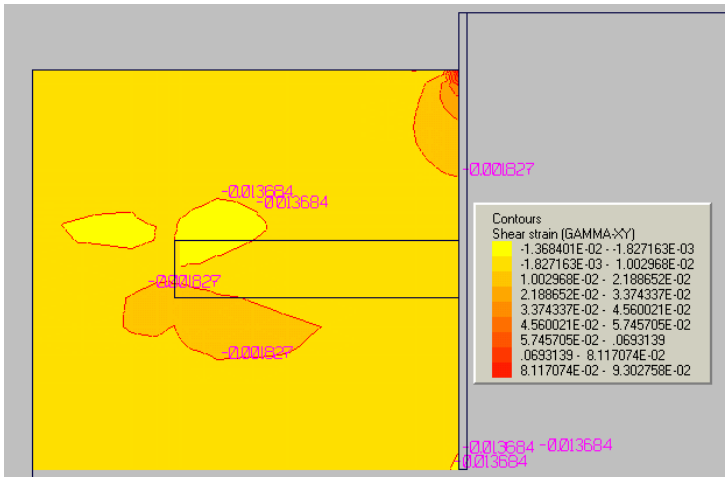

(a) At 2m Excavation

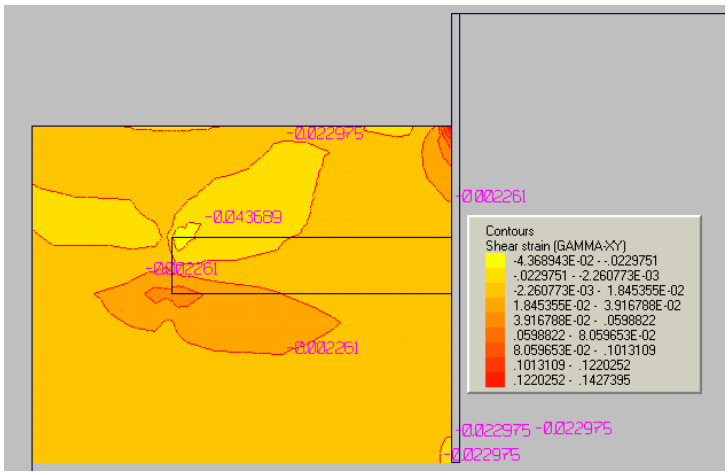

(b) At 4m Excavation

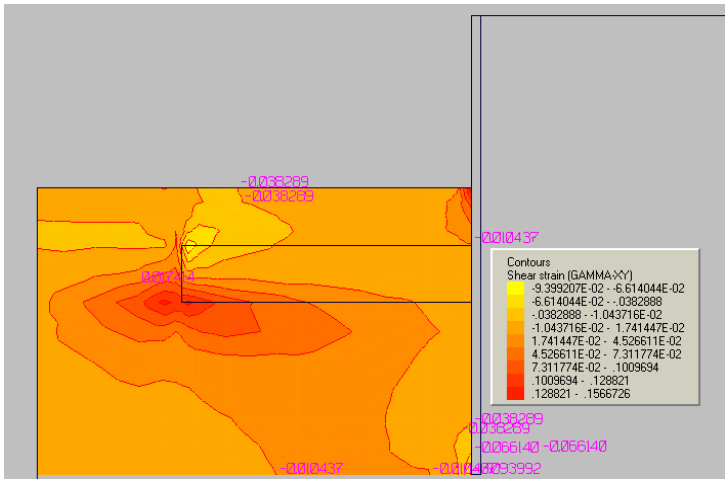

(c) At 6m Excavation

Figure 6.25 Shear strain contours of improved soil berm on excavated side during the excavation process (simulation of Test Berm-7d)

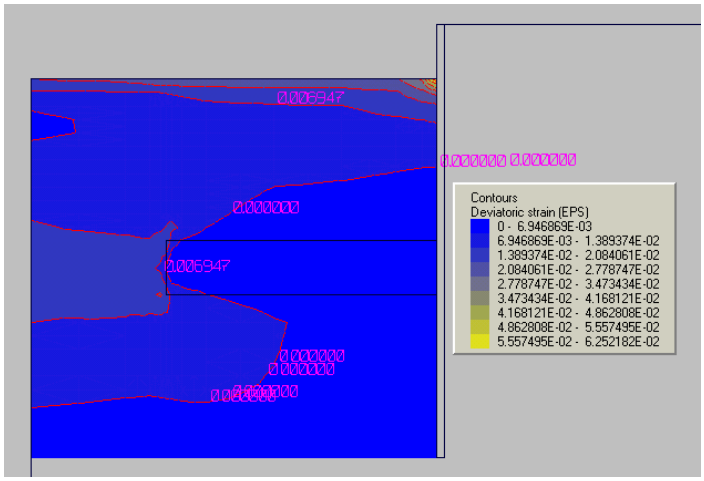

(a) At 2m Excavation

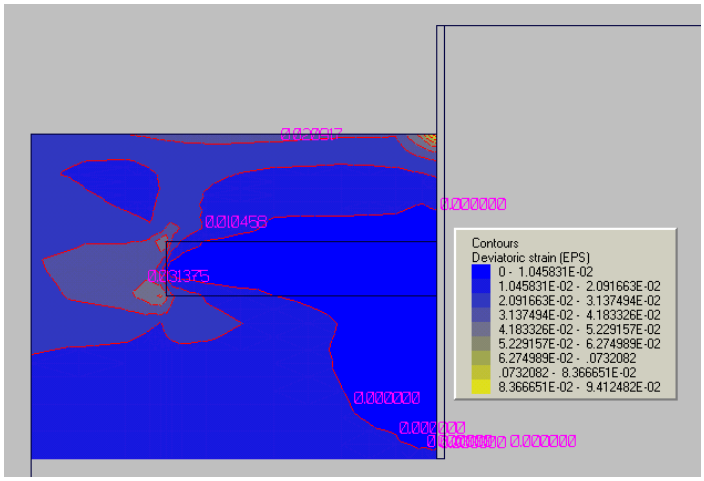

(b) At 4m Excavation

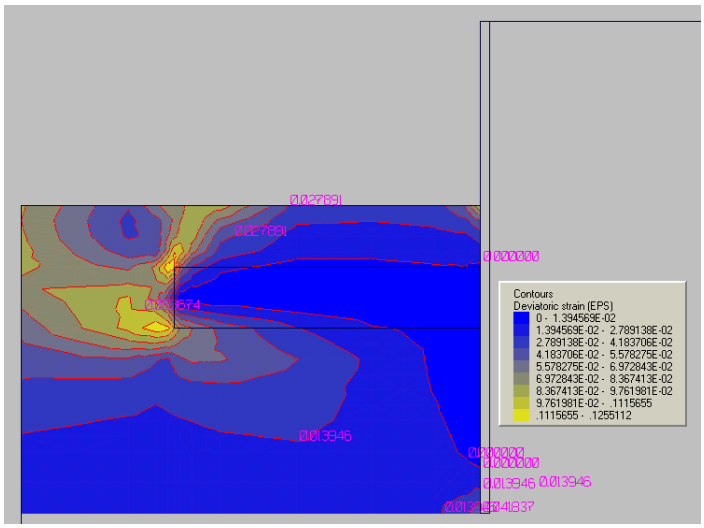

(c) At 6m Excavation

Figure 6.26 Deviator strain contours of improved soil berm on excavated side during the excavation process (simulation of Test Berm-7d)

Chapter 7

CONCLUSIONS

The research presented in preceding chapters is aimed at providing a clearer understanding of the behaviour of an embedded improved soil layer in an excavation in soft ground. In such poor ground condition, the maximum wall deflection usually occurs below the final excavation level where it is impossible to install conventional steel struts. To restrain the wall deflection at the base of excavation, one effective solution is to improve a layer of soft soil around this location. A typical approach is to improve the entire layer within the excavation zone so as to provide full contact between retaining walls. However, in the case of a wide excavation, improvement of a limited region adjacent to the wall has to be considered given the fact that improving the entire area may not be economically viable. In this thesis, when an entire soil layer is improved, the term embedded improved soil strut is used. When only a limited area adjacent to the wall is improved, the term is embedded improved soil berm. The term “embedded” is used to underscore the fact that the improvement is below the final excavation level, as suggested by Dr. David Hight in a discussion. Carrying out improvement works especially close to the retaining wall is difficult and this can lead to a small region of untreated soil between the retaining wall and improved soil layer. Sometimes, this is not detected, while at other times, it may be ignored.

This study investigated these three different scenarios of soil improvement and has provided an insight on the mechanisms involved in mobilising the different configurations of improved grounds to restrain the retaining wall. The investigation has provided substantial evidences that the behaviour of a stabilised excavation is much more complicated and cannot be treated to behave just like a strut all the time with a

composite stiffness assigned to an equivalent strut. Other contributing factors such as the effect of confining pressure, existence of gap of untreated soil, interfacial shear resistance and end bearing of berm have considerable effects on the performance of the embedded improved soil layer. Through an understanding of these resistance mechanisms for different configurations of embedded improved soil layer, the performance of the excavation is established.

7.1 Concluding Remarks

The behaviour of an embedded improved soil layer in an excavation was studied by means of both physical and numerical modelling. Prior to the excavation tests in the centrifuge, material studies were carried out using laboratory mixed samples to determine the strength and stiffness properties of the cement treated clays, which forms part of the present study to understand the behaviour of the monolithic improved soil layer [Tan et al. (2002)]. Subsequently, excavation tests with different configurations of soil improvement were conducted in the centrifuge using the newly developed in-flight excavator. This was then complemented by numerical analyses. From the research works carried out, the following conclusions are drawn: -

a) The strength and stiffness properties of Singapore marine clays improved by cement mixing have been established based on results from a series of unconfined compression tests carried out on laboratory mixed samples. It was found that marine clays from different parts of Singapore yielded different degrees of improvement. A normalisation approach can be used to unify the behaviour of these different improved clays as summarized below: -

$$\frac{q_{u\,Eunos}}{q_{u\,Eunos}(A_w.w.t)} = \frac{q_{u\,CityHall}}{q_{u\,CityHall}(A_w.w.t)} = \frac{q_{u\,SAC}}{q_{u\,SAC}(A_w.w.t)}$$

b) The Young's modulus (E) of cement treated clays was found to be much higher than anticipated. Due to the non-linear stress-strain behaviour of this material, the E value at a small strain (0.01%) was found to be 5 to 15 times higher than that at a larger strain (1%). The use of a local strain measurement technique such as Hall's effect transducer during the test had produced this higher E as compared to that determined using conventional external LVDTs. Correlation between stiffness (E_{sec50}) and unconfined compression strength (q_u) has been obtained for local reference, which is very dependent on how the strain is measured. Using the conventional LVDT method, the E_{sec50} falls within a range of 150 to $400q_u$ [consistent with those reported by Asano et al. (1996) and Futaki et al. (1996)] but a higher correlation of 300 to $800q_u$ can be achieved using the Hall's effect transducer [consistent with those reported by Kawasaki et al. (1984) and Tatsuoka et al. (1996)]. In addition, the stiffness of cement treated clays is expected to increase with curing age. Some empirical relationships were determined to relate the strength at different curing ages with that of 28 days. Considering the fact that the entire process of excavation on site normally takes a longer period than 28 days, the E value of the cement treated clays can be 25-50% larger than that at 28 days.

c) In the centrifuge test, it was shown that to control excessive wall deflection and ground movements, the use of an embedded improved soil strut is highly effective. The centrifuge results showed that the effectiveness of an improved soil strut was very much dependent on its stiffness. The results confirmed that when a stiffer improved soil layer was used, though it provided a higher resistance to the retaining wall, it also induced a much higher bending moment in the wall. Results from a parametric study using the FE analyses clearly demonstrate that there is a considerable increase in the wall bending moment (15-20%) but when the E value

approaches 1000MPa, the increase becomes nominal. In addition, it was shown that there was a threshold value for the stiffness of improved soil in order for an improved soil strut to be effective. In this study, the minimum required stiffness of a monolithic improved soil layer should not fall below 100MPa.

d) In the centrifuge tests, it was clearly difficult to compare the overall behaviours using cumulative parameters such as total wall deflection and surface settlement. Instead, a controlled test using the centrifuge allows the examination of change of more useful parameters, the incremental change of a parameter for the removal of 0.5m of soil at a particular depth. This facilitates the detailed examination of how the system reacts as the layer is slowly excavated. Just as importantly, it also facilitates the examination of the composite stiffness for different configurations of improved soil layer at the same depth.

e) In the case of an embedded improved soil strut at each depth of excavation, only negligible wall movement occurred during the early stage of scrapping where the soil next to the retaining wall is removed. However, after some length of soil has been removed, a more noticeable wall movement was observed. This trend of incremental wall movement strongly suggests that the improved soil layer is behaving like a strut, whereby only after a certain amount of soil has been removed from the retaining wall, the strut will then be allowed to arch and induce a movement.

f) In the design of a retaining wall, the minimum expected stiffness in the improved soil should be used for assessing ground movements in the surrounding area. However, it is recommended in this study that the maximum expected stiffness be used for analysis of the bending moment in the retaining wall.

g) In the numerical study, it was shown that stresses in the improved soil strut were

concentrated at both sharp corners abutting the retaining wall. This was proven by using a more refined mesh where the stresses at the integration points increases as the point moved closer to the corner, a clear indication that the numerical analysis is trying to capture the fact that the corner is a stress concentrator.

h) In the case when the soil improvement has a gap of untreated soil in between the retaining wall and improved soil layer, the overall composite stiffness drops significantly. In the centrifuge study, it was found that significant wall movement was induced even at the early stage of soil scrapping and continued to increase throughout the entire operation. As the gap of untreated soil is located next to the retaining wall, the impact of soil removal will be felt directly once the overburden stress above the untreated soil portion is reduced. From the numerical simulation, it was also found that the untreated soil in the gap was laterally compressed, followed by some bulging of soil at top of the gap. Clearly, the changing boundary conditions on this untreated soil region will have a significant effect.

i) In the centrifuge study, it was shown that the performance of the improved soil layer with a gap of untreated soil was governed by the width of gap and affected directly by the removal of overburden above the gap. The numerical analyses also demonstrate both effects influencing the composite stiffness of the improved soil layer system. Besides demonstrating that a larger gap will lead to a lower composite stiffness (E_c), the results also show the effect of reducing confining pressure due to deeper excavation. The effect of increasing imbalance between the active and passive side is removed by normalising the results with those from an improved soil strut at the same depth of excavation.

j) A simple formula was derived to understand the composite stiffness, based on the idea of two elastic regions joined axially in a series configuration. The formula is:

$$E_c = \frac{(L_{imp} + L_{gap})E_{imp}E_{gap}}{L_{imp}E_{gap} + L_{gap}E_{imp}}$$

For an improved soil layer with a region of untreated soil next to the wall, this means that the width of gap, L_{gap}, has a significant role to play; the bigger is L_{gap}, the smaller the composite stiffness, which is expected. What is more important is the recognition that for a given width of gap of untreated soil, the changes in E_{gap} as excavation proceeds will play an important role. Initially, with the thick overburden acting as confining pressure, the behaviour is close to a 1-D consolidation. Towards the end of excavation when only a small overburden is left, the untreated soil will be subjected to unconfined axial compression, and should be considerably softer with the shearing already induced. The change in E_{gap} from that of a constrained modulus under 1-D condition to that of a tangent stiffness for an unconfined axial compression test will dictate the change in composite stiffness. The effect of this transition was shown in Chapter 6.

k) For a cost-effective design, an embedded improved soil berm is sometimes used in excavations, especially when the excavation area is large. The berm was found to be almost as effective as a strut during the early stages of excavation. Nevertheless, the way the berm transfers the lateral force from the retaining wall to the surrounding soil, which is by a combination of skin friction and end bearing, is different from the behaviour of a strut. The resistance is provided mainly through the contact area of the shear resistance and end bearing, not through compression on the wall at the other end as in the case of an improved soil strut. What is also shown in this case is that the stiffness of the berm does not have a significant effect on the performance during excavation. It is noted that the failure behaviour of a berm is very sudden and therefore, adequate provision in design shall be allowed to avoid such a catastrophic

failure.

7.2 Recommendations for Future Studies

This research has studied several fundamental behaviours of an excavation stabilised by an embedded improved soil layer. However, the present study is limited by the fact that the experimental procedure is highly complex and thus, only few tests can be conducted within the time available for this study. From the insight derived from this study, the following topics are recommended for future study: -

The study has just shown the importance of stiffness of an improved soil layer to the overall behaviour and performance of the excavation. However, these alone are still not enough for establishing guidelines for determining the actual mobilised stiffness, E, to be used for design. In the current centrifuge and numerical studies, the improved layer is assumed to be monolithic but in actual fact, this is not the case in the field. As mentioned earlier, in the field, the soil is improved in the form of short columns vertically, whereas when the improved soil layer is called upon, the compression is applied horizontally. The horizontal stiffness mobilised due to a large number of overlapping vertical columns is not the same as that of a cored element and this needs to be analysed for present studies to be applied directly in design.

REFERENCES

- Asano, J., Ban, K., Azuma, K. and Takahashi, K. (1996), "Deep Mixing Method of soil stabilization using coal ash", Proc. of IS-Tokyo '96 / 2nd Int. Conf. on Ground Improvement Geosystems, Tokyo, vol.1, pp.393-398.
- Assarson, K.G. (1974), "Deep stabilisation of soft cohesive soils", Linden Alimak, Skelleftea.
- Azevedo, R. F. (1983), "Centrifugal and analytical modelling of excavation in sand", PhD Thesis, University of Colorado, Boulder.
- Babasaki, R, Terashi, M., Suzuki, T., Maekawa, A., Kawamura, M. and Fukazawa, E. (1996), "Factors influencing the strength of improved soil", Proc. of IS-Tokyo '96 / 2nd Int. Conf. on Ground Improvement Geosystems, Tokyo, vol.2, pp.913-918.
- Babasaki, R. and Suzuki, K. (1996), "Open cut excavation of soft ground using the DCM Method", Proc. of IS-Tokyo '96 / 2nd Int. Conf. on Ground Improvement Geosystems, Tokyo, vol.1, pp.469-474.
- Balasubramaniam, A.S., Brand, E.W., Sivandran, C. (1976), "Finite element analysis of a full scale test excavation in soft Bangkok clay", Proc. of the 1976 Int. Conf. on FEM in Eng., Adelaide, Australia.
- Bolton M.D., and Powrie, W. (1988), "Behaviour of diaphragm walls in clay prior to collapse', Geotechnique N38, No.2, pp.167-189.
- Bolton, M. (1991), "A guide to soil mechanics", published by Macmillan Education Ltd. in 1979.

- Bolton, M.D., Britto, A.M., Powrie, W. and White, T.P. (1989), “Finite Element Analysis of a centrifuge model of a retaining wall embedded in a heavily over consolidated clay”, Computers Geotechnique 7, pp.289-318.
- Borin, D.L. (1997), “Anchored and Cantilevered Retaining Wall Analysis Program”, WALLAP program user’s manual, Version 4, distributed by Geosolve, UK.
- Britto, A.M. and Gunn, M.J. (1987), “Critical state soil mechanics via finite element”, John Wiley and Sons, New York.
- Britto, A.M. and Kusakabe, O. (1984), “On the stability of supported excavation”, Canadian Geotech. Journal, vol.21, pp338-348.
- Broms, B. B. (1984), “Stabilization of soft clay with lime columns”, Proc. Seminar on Soil Improvement and Construction Techniques in Soft Ground, NTU, Singapore.
- Brown, P.T. and Booker, J.R. (1985), “Finite element analysis of excavation”, Computers and Geotechnics, vol.1, pp.207-220.
- Burland, J. B. (1989), “Small is beautiful –the stiffness of soil at small strains”, 9th Laurits Bjerrum Memorial Lecture, Canadian Geotechnical Journal, vol.26, pp.499-516.
- Chong, P. T., Tan, T. S., Lee, F. H., Yong, K. Y. and Tanaka, H. (1998), “Characterisation of Singapore Lower Marine Clay by In-situ and Laboratory Tests”, Proc. of Int. Symposium on Problematic Soils, IS-Tohoku ‘98, Sendai. pp. 641-644.
- Clayton, C. R. I., Khatrush, S. A., Bica, A. V. D. and Siddique, A. (1989), “The use of Hall effect semiconductors in geotechnical instrumentation”, Geotechnical Testing Journal: vol.12, no.1, pp. 69-76.

- Corte, J-F. (1988), “Centrifuge 88”, Proc. Int. Conf. Centrifuge 1988, Paris, A.A.Balkema, Rotterdam, April 25-27, 1988.
- Craig, W.H. (1984), Proc. Symp. on the application of Centrifuge Modelling to Geotechnical Design, April 16-18, University of Manchester, UK.
- Craig, W.H. and Rowe, P.W. (1981), “Operation of a Geotechnical Centrifuge from 1970-1979”, Geotechnical Testing Journal, GTJODJ, vol.4, No.1, March 1981, pp.19-25.
- DiMaggio, F.L. and Sandler, I.S. (1971), “Material model for granular soils”, Journal of Engineering Mech. Div. ASCE, vol.97, No.3.
- Duncan, J. M. and Chang, C. Y. (1970), “Non-linear Analysis of stress and strain in soils”, JSMFD, ASCE, vol.96, No.SM5, pp.637-659.
- Fam, M. A. and Santamarina, J. C. (1996), “Study of clay-cement slurries with mechanical and electromagnetic waves”, Journal of Geotechnical Engineering, ASCE, pp.365-373.
- Furuya, E., Tsukagoshi, H. and Inoue, H. (1988), “Design of Dry Jet Mixing Method”, Proc. 23rd JSSMFE, pp.2273-2274.
- Futaki, M., Nakano, K. and Hagino, Y. (1996), “Design strength of soil-cement columns as foundation ground for structures”, Proc. of IS-Tokyo ’96 / 2nd Int. Conf. on Ground Improvement Geosystems, Tokyo, vol.1, pp.481-484.
- Gaba, A. R. (1990), “Jet grout at Newton Station, Singapore”, 10th Southeast Asian Geotechnical Conference, Taipei.
- Goh, T.L., Tan, T.S., Yong, K.Y. and Lai, Y. W. (1999), “Stiffness property of Singapore marine clays improved by cement mixing”, Proc. 11th Asian Regional Conf. on Soil Mechanics and Geotechnical Engineering, Seoul. pp.333-336.

- Gotoh, M. (1996), “Study on soil properties affecting the strength of cement treated soils”, Proc. of IS-Tokyo ’96 / 2nd Int. Conf. on Ground Improvement Geosystems, Tokyo, vol.1, pp.399-404.
- Hsi, J.P. and Small, J.C. (1992), “Ground settlements and draw down of the water table around an excavation”, Canadian Geotechnical Journal, vol.29, pp.740-754.
- Hume, TW-Potter, L.A.C. and Shirlaw, J.N. (1989), “Singapore Mass Rapid Transit System Construction”, Proc. Institute of Civil Engineering, Part 1, August, pp.709-770.
- Jaky, J. (1944), “The coefficient of earth pressure at rest”, Journal of Hungarian Architects and Engineers, Budapest, Hungary, Oct., pp.355-358.
- Kado, Y., Ishii, T., Shirlaw, J. N. and Lim, K. (1987), “Chemico lime pile soil improvement”, Case histories in soft clay: Proc. 5th International Geotechnical Seminar, Singapore: pp. 1-12.
- Kawasaki, T., Niina, A., Saitoh, S., Suzuki, Y. and Honjyo, Y. (1981), “Deep Mixing Method using cement hardening agent”, Proc. 10th ICSMFE, Stockholm, vol.12, pp.721-724.
- Kawasaki, T., Saitoh, S., Suzuki, Y. and Babasaki, R. (1984), “Deep Mixing Method using cement slurry as hardening agent”, Seminar on soil improvement and construction techniques in soft ground, Singapore, pp.17-38.
- Khoo, E., Okumara, T. and Lee, F. H. (1994), “Side friction effects in plane strain models”, Proc. Centrifuge 1994, Singapore, pp.649-654.
- Kimura, T. and Saitoh, K. (1982), “The influence of disturbance due to sample preparation on the undrained strength of saturated cohesive soil”, Soils and Foundations, vol.22, No.4, pp.109-120.

- Kimura, T., Kusakabe, O. and Takemura, J. (1998), "Centrifuge 98", Proc. Int. Conf. Centrifuge 1998, Tokyo, Japan, A.A.Balkema, Rotterdam, 23-25 Sept.
- Kimura, T., Takemura, J., Hiro-oka, A., Suemasa, N. and Kouda, N. (1993), "Stability of unsupported and supported vertical cuts in soft clay", 11th SEAGC, Singapore, pp.61-70.
- Kitazume, M., Miyake, M., Omine, K. and Fujisawa, H. (1996), "Japanese design procedures and recent activities of DMM", Proc. of IS-Tokyo '96 / 2nd Int. Conf. on Ground Improvement Geosystems, Tokyo, vol.2, pp.925-930.
- Ko, H.Y. and McLean, F.G. (1991), "Centrifuge 91", Proc. Int. Conf. Centrifuge 1991, Boulder Colorado, A.A.Balkema, Rotterdam, 13-14 June.
- Kohata, Y., Maekawa, H., Muramoto, K., Yajima, J. and Babasaki, R. (1996), "Deformation and strength properties of DM cement treated soils", Proc. of IS-Tokyo '96 / 2nd Int. Conf. on Ground Improvement Geosystems, Tokyo, vol.2, pp.905-911.
- Kusakabe, O. (1996), "Braced excavation and shafts", Geotechnical Aspects of Underground Construction in Soft Ground, Balkema, Rotterdam.
- Ladd, C.C. and Foott, R. (1974), "New design procedure for stability of soft clays", ASCE, Journal of GED, vol.100(GT7), pp.763-786.
- Lee, F. H. (1992), "The National University of Singapore Geotechnical Centrifuge – Users' Manual", Research Report No. CE001. July 1992.
- Lee, F. H., Tan, T. S., Yong, K. Y., Karunaratne, G. P. and Lee, S. L. (1991), "Development of geotechnical centrifuge facility at the National University of Singapore", Proc. Int. Conf. Centrifuge 1991, pp.11-17.

- Lee, S.L. and Yong, K.Y. (1991), “Grouting in Substructure Construction”, Guest Lecture, Proc. 9th Asian Reg. Conf. On SMFE, December, Bangkok, Thailand, vol.2.
- Lee, S.L., Parnploy, U., Yong, K.Y. and Lee, F.H. (1989), “Time-dependent deformation of anchored excavation in soft clay”, Proc. Symp. on Underground Excavations in soils and rocks”, Asian Int. Of Tech., Bangkok, Thailand, pp.377-384.
- Leung, C.F., Lee, F.H. and Tan, T.S. (1991), “Principles and applications of geotechnical centrifuge model testing”, Journal of the Institution of Engineers, Singapore, No.4, vol.31, pp.39-44.
- Leung, C.F., Lee, F.H. and Tan, T.S. (1994), “Centrifuge 94”, Proc. Int. Conf. Centrifuge 1994, Singapore, A.A.Balkema, Rotterdam, 31 Aug. – 2 Sept., 1994.
- Liao, H. J. and Tsai, T. L. (1993), “Passive Resistance of Partially Improved Soft Clayey Soil”, Proc 11th SEAGC, Singapore, pp.751-756.
- Loh, C. K., Tan, T. S. and Lee, F. H. (1998), “Three dimensional excavation tests in the centrifuge”, Centrifuge 1998, Tokyo.
- Lyndon, A. and Schofield, A.N. (1970), “Centrifuge model test of short term failure in London clay”, Geotechnique, (20), No.4, pp.440-442.
- Mair, R.J. (1979), “Centrifugal modelling of tunnel construction in soft clay”, PhD Thesis, Cambridge University, United Kingdom.
- Mihashi, M., Tachibana, T. and Motoyama, S. (1987), “Measure of deformation and effect of large scale excavation on soft ground near the housing situation”, Journal of JSCE, pp.295-302.
- Nagaraj, T.S., Miura, N. Yaligar, P.P. and Yamadera, A. (1996), “Predicting strength development by cement admixture based on water content”, Proc. of

IS-Tokyo ’96 / 2nd Int. Conf. on Ground Improvement Geosystems, Tokyo, vol.1, pp.431-436.

- Neville, A. M. (1996), “Properties of Concrete”, 4th Edition.
- Okumura, T. (1996), “Deep Mixing Method of Japan”, Proc. of IS-Tokyo ’96 / 2nd Int. Conf. on Ground Improvement Geosystems, Tokyo, vol.2, pp.879-887.
- Okumura, T. and Terashi, M. (1975), “Deep Lime Mixing Method of stabilization for marine clays”, Proc. 5th ARC on SMFE, vol.1, pp. 69-75.
- Okumura, T., Mitsumoto, T., Terashi, M., Sakai, M. and Yoshida, T. (1972), “Deep Lime Mixing Method for soil stabilization’, Report of Port and Harbour Research Institute, vol.11, No.1, pp.67-107.
- Ou, C.Y. and Chiou, D.C. (1993), “Three-dimensional finite element analysis of deep excavation”, Proc. of the 11th SEA Geotechnical Conf., 4-8 May, 1993, Singapore, pp.769-774.
- Ou, C.Y. and Wu, T.S. (1996), “Evaluation of material properties for soil improvement in excavation”, Proc. of IS-Tokyo ’96 / 2nd Int. Conf. on Ground Improvement Geosystems, Tokyo, vol.1, pp.545-550.
- Peck, R.B. (1969), “Deep excavations and tunnelling in soft ground”, Proc. 7th Int. Conf. on Soil Mechanics and Foundation Engineering, pp.225-290.
- Powrie, W. (1986), “The Behavior of diaphragm walls in clay”, PhD thesis, Cambridge University, United Kingdom.
- Powrie, W. and Li, E.S.F. (1991), “Finite element analyses of an in situ wall propped at formation level”, Geotechnique, vol.41, No.4, pp.499-514.
- Powrie, W., Richards, D.J. and Kantartzi, C. (1994), “Modelling diaphragm wall installation and excavation processes”, Proc. Int. Conf. Centrifuge 1994, Singapore, A.A.Balkema, Rotterdam, pp.655-661.

- Roscoe, K.H. and Burland, J.B. (1968), "On the generalised stress-strain behaviour of wet clay", Engineering Plasticity, Cambridge University Press.
- Saitoh, S., Nishioka, S., Suzuki, Y. and Okumura, R. (1996), "Required strength of cement improved ground", Proc. of IS-Tokyo '96 / 2nd Int. Conf. on Ground Improvement Geosystems, Tokyo, vol.1, pp.557-562.
- Saitoh, S., Suzuki, Y. and Shirai, K. (1985), "Hardening of soil improved by deep mixing method", Proc. 11th ICSMFE, San Francisco, vol.5, pp.1745-1748.
- Schofield, A.N. (1980), "Cambridge geotechnical centrifuge operation', Geotechnique, vol.30, No.3, pp.227-268.
- Schofield, A.N. and Wroth, C.P. (1968), "Critical state soil mechanics", McGraw-Hill, London.
- Simpson, B. and Wroth, C.P. (1972), "Finite element computation for a model retaining wall in sand", Proc. of the 5th European Conf. on Soil Mechanics and Foundation Engineering, Madrid, 1972, voil.1, pp.85-95.
- Smith, I.M. and Ho, D.K.H. (1992), "Influence of construction technique on the performance of a braced excavation in marine clay", Int. Journal for Numerical and Analytical Methods in Geomech., vol.16, pp.845-867.
- Stewart, D.P. and Randolph, M. F. (1994), "T-Bar penetration testing in soft clay", Journal of Geotechnical Engineering, vol.120, No.12, Dec., 1994.
- Sugawara, S., Shigenawa, S., Gotoh, H. and Hosoi, T. (1996), "Large-scale jet grouting for pre-strutting in soft clay", Proc. of IS-Tokyo '96 / 2nd Int. Conf. on Ground Improvement Geosystems, Tokyo, vol.1, pp.353-356.
- Takada, T., Yamane, Y., Yamamura, M. and Ueki, H. (1998), " Ground Improvement by Jet and Mechanical Mixing Method", Proc. of 2nd Int. Conf. on Ground Improvement Techniques, Singapore.

- Tan, S. L. (1983), “Geotechnical properties and laboratory testing of soft soils in Singapore”, Proc. 1st Int. Seminar on Construction Problems in Soft Soils, Nanyang Technological Institute, Singapore: pp. TSL1-47.
- Tan, T.S., Goh, T.L. and Yong, K.Y. (2002), “Properties of Singapore marine clays improved by cement mixing”, ASTM Geotechnical Testing Journal, Dec 2002, vol.25, pp.422-433.
- Tan, T.S., Ng, T.G., French, D., Wong, F.H. and Takeda, T. (2001), “Use of an Improved Soil Berm for Stabilisation in Deep Excavation”, Proc. of Underground Singapore 2001, Singapore.
- Tan, T.S., Yong, K.Y., Lee, F.H. and Leung, C.F. (1995), “Deep Excavation Problem in Singapore”, Proc. of The Regional Symposium on Infrastructure Development in Civil Engineering, Bangkok, Thailand.
- Tanaka, H. (1993), “Behavior of braced excavations stabilized by Deep Mixing Method”, Soil and Foundations, JSSMFE, vol.33, No.2, pp.105-115.
- Tanaka, H. (1994), “Behavior of a braced excavation in soft clay and the undrained shear strength for passive earth pressure”, Japanese Society of Soil Mechanics and Foundation Engineering, Soil and Foundations, vol.34, No.1, pp.53-64.
- Tatsuoka, F. and Shibuya, S. (1992), “Deformation characteristics of soils and rocks from field and laboratory tests”, Report of the Institute of Industrial Science, The University of Tokyo, vol.37, No.1.
- Tatsuoka, F., Kohata, Y., Uchida, K. and Imai, K. (1996), “Deformation and strength characteristics of cement treated soils in Trans-Tokyo Bay Highway Project”, Proc. of IS-Tokyo ’96 / 2nd Int. Conf. on Ground Improvement Geosystems, Tokyo, vol.1, pp.453-460.

- Taylor, R.N. (1995), “Centrifuge in modelling: Principles and Scale Effects”, Geotechnical Centrifuge Technology, Blackie Academic and Professional.
- Terashi, M., Tanaka, H. and Okumura, T. (1979), “Engineering properties of lime treated marine soils and D.M. Method”, Proc. 6th ARC on SMFE, vol.1, pp.191-194.
- Thanadol, K. (2003), “Behaviour of an embedded improved soil berm in an excavation”, PhD thesis, National University of Singapore.
- Tornaghi, R. and Perelli Cippo, A. (1985), “Soil improvement by jet grouting for the solution of tunnelling problems”, Proc. of Tunneling ’85, Institute of Mining and Metallurgy, ed. by M1 Jones, pp.265-283.
- Trak, B., La Rochelle, P., Tavenas, F., Leroueil, S. and Roy, M. (1980), “A new approach to the stability analysis of embankments on sensitive clays”, Canadian Geotechnical Journal, vol.17(4), pp.526-544.
- Tsui, Y. and Clough, G.W. (1974), “Performance of tie-back walls in clay”, Journal of Geotech. Eng. Div. ASCE, vol.100(GT12), pp.1259-1274.
- Uchiyama, N. and Kamon, M. (1998), “Deformations of buttress type ground improvement and untreated soil during strutted excavation in clay”, 2nd Int. Conf. on Ground Improvement Techniques, 8-9 Oct. 1998, Singapore.
- Uddin, K. (1995), “Strength and Deformation Behavior of Cement Treated Bangkok Clay”, D.Eng Thesis, AIT, Bangkok.
- Whittle, A.J. (1997) ”Prediction of excavation performance in clays”, Civil Engineering Practice, pp.65-88.
- Wong, K.S. and Broms, B.B. (1989), “Lateral wall deflection of braced excavation in clay”, Journal of Geotech. Eng. Div. ASCE, vol.115, No.6, pp.853-870.

- Wong, K.S., Goh, A.T.C., Jaritngam, S. and Chang, L.J.D. (1998), "Optimisation of jet grout configuration for braced excavation in soft clay", Proc. 2nd Int. Conf. on Ground Improvement Techniques, Singapore.
- Wong, K.S., Li, J.C. Goh, A.T.C., Poh, K.B. and Oishi, E. (1999), "Effect of jet grouting on performance of a deep excavation in soft clay", Proc. of the 5th Int. Symposium on Field Measurements in Geomechanics-FMGM99, Singapore.
- Wong, L.W. and Patron, B.C. (1993), "Settlement induced by deep excavations in Taipei", 11th Southeast Asian Geotechnical Conference, 4-8 May, Singapore.
- Woods, R. and Rahim, A. (1999), "Sage Crisp Technical Reference Manual for SAGE-CRISP version 4", The Crisp Consortium Ltd and SAGE Engineering Ltd.
- Wroth, C.P. (1975), "In-situ measurement of initial stress and deformation characteristics", Proc. of the Speciality Conf. in In-situ Measurement of Soil Properties, ASCE, Raleigh, North Carolina, June, pp.181-230.
- Yong, K.Y. and Karunaratne, G.P. (1983), "Geological considerations in excavation and foundation design", Journal of Institute of Engineers, Singapore, vol.23, No.1, pp.9-15.
- Yong, K.Y. and Lee, S.L. (1995), "Time dependent behaviour and grouting of deep excavation in soft clay", The Infrastructure Development in Civil Engineering Conference, Dec 19-20, Bangkok, Thailand.
- Yong, K.Y., Lee, F.H. and Liu, K.X. (1996), "Three dimensional finite element analysis of deep excavation in marine clay", Proc. of the 12th Southeast Asian Geotechnical Conference, 6-10 May, 1996, Kuala Lumpur, pp.435-440.

- Yong, K.Y., Lee, F.H., Tan, T.S. and Lee, S.L. (1998), "Excavation near Critical Structures – Bridging Research and Practice", Special Lecture, 13th Southeast Asian Geotechnical Conference, Taipei, Taiwan.
- Yong, K.Y., Lee. F.H., Parnploy, U. and Lee, S.L. (1990), "Elasto-plastic consolidation analysis for strutted excavation in clay", Computer and Geotechnics, vol.8, pp.311-328.
- Yoshizawa, H., Okumura, R., Hosoya, Y., Sumi, M. and Yamada, T. (1997), "JGS TC Report: Factors affecting the quality of treated soil during execution of DMM", Proc. of IS-Tokyo '96 / 2nd Int. Conf. on Ground Improvement Geosystems, Tokyo: vol.2, pp. 931-937.
- Zienkiewics, O.C. (1972), "The finite element method", McGraw-Hill, London.